


For Reference

NOT TO BE TAKEN FROM THIS ROOM

Ex LIBRIS
UNIVERSITATIS
ALBERTAENSIS





Digitized by the Internet Archive
in 2023 with funding from
University of Alberta Library

<https://archive.org/details/Koppula1970>

THE UNIVERSITY OF ALBERTA

THE CONSOLIDATION OF SOIL IN TWO DIMENSIONS
AND WITH MOVING BOUNDARIES

by



SIVAJOGI DORA KOPPULA

A THESIS

SUBMITTED TO THE FACULTY OF GRADUATE STUDIES
IN PARTIAL FULFILMENT OF THE REQUIREMENTS FOR THE DEGREE OF
DOCTOR OF PHILOSOPHY

DEPARTMENT OF CIVIL ENGINEERING

EDMONTON, ALBERTA

FALL, 1970

ABSTRACT

This dissertation deals with theoretical aspects of the determination of the magnitude and the rate of decay of hydrostatic excess pore pressures caused by applied external stresses in a mass of soil. Numerical methods for the solution of the problems are developed.

The existing theories of primary consolidation used to obtain the compression characteristics of clay are critically reviewed. The techniques of solution are mentioned briefly and the types of boundary value problems that may be encountered are summarized.

A general theory of one-dimensional primary consolidation accounting for the self weight of the soil grains is presented. This general theory is based on nonlinear relationships between the coefficient of permeability, the coefficient of compressibility and the effective stress. Terzaghi's linear theory of consolidation can be considered a special case of this general theory. The general theory evolved can be applied to the case of a sedimenting soil. The data recorded from the Mississippi Continental Shelf is recoverable with appropriate input data.

This dissertation further develops a numerical method in two dimensions for determining the construction pore pressures in embankment sections as a function of their construction history. The numerical algorithm developed is versatile. Problems involving complex boundary conditions,

stratified soils and gradual loading can be solved. The coefficient of consolidation can also be varied as a function of position and time. Case records of six embankments have been analyzed and results compared with field observation. Generally good agreements were obtained.

The numerical algorithm developed is extended to treat the cases of impeded drainage (retarded consolidation) at the junctions of inner cores and outer shells of earth embankments. The impedance to drainage is measured by a parameter called the Impedance Factor. The impedance factor depends on the relative lengths of the drainage paths and the relative permeabilities of the inner cores and the outer shells of the embankment. Results are presented for a hypothetical dam whose dimensions are varied and for different values of the impedance factor.

Terzaghi's classical theory of one-dimensional consolidation is extended to develop a second-order weakly non-linear partial differential equation governing the pore pressure equalization arising out of the erosion of a fully saturated sediment at a prescribed rate. This part of the study aims at correlating some of the geological and physical parameters involved in valley formation.

ACKNOWLEDGEMENTS

The author wishes to express his deep-felt gratitude to Professor N.R. Morgenstern for suggesting the topic for research and for continued stimulating guidance throughout the study of the project.

The author is grateful to Professor S. Thomson who carefully checked the manuscript.

The computer center of the University of Alberta, Edmonton provided the computational facilities on the IBM 360/67 computer. This assistance is appreciated.

Acknowledgement is due to Miss Susan Schultz for typing the thesis in its present form.

The author is grateful to the Department of Civil Engineering, University of Alberta, Edmonton for the award of a Graduate Service Assistantship for the first year of the work and to the National Research Council of Canada during the remaining period.

TABLE OF CONTENTS

	Page
Title Page	
Approval Sheet	
Abstract	i
Acknowledgements	iii
Table of Contents	iv
List of Tables	viii
List of Figures	ix
CHAPTER I - INTRODUCTION	
1.1 Purpose of the Research	1
1.2 Scope of the Study	2
1.3 Organization of the Thesis	4
CHAPTER II - REVIEW OF CONSOLIDATION THEORIES	
2.1 General	6
2.2 Biot's Theory of Three-Dimensional Consolidation	7
2.3 Rendulic's Theory of Three-Dimensional Consolidation	12
2.4 Comparison of Theories of Biot and Rendulic	13
2.5 Terzaghi's Classical One-Dimensional Theory	16
2.6 Modifications to Terzaghi's Theory	18
CHAPTER III - BOUNDARY CONDITIONS - A BRIEF TREATMENT	
3.1 General	20
3.2 Boundary Value Problem	21
3.3 Moving Boundary Conditions	27

CHAPTER IV - TECHNIQUES OF SOLUTION - A BRIEF SUMMARY

4.1	General	30
4.2	Fundamental Concepts in Finite Difference Approximations	31
4.3	Forms of Finite Difference Approximation	32
4.4	General Form of Finite Difference Scheme	33
4.5	Explicit and Implicit Schemes	35
4.6	Alternating - Direction Implicit Method	37
4.7	Barakat and Clark Method	42

CHAPTER V - TWO DIMENSIONAL CONSOLIDATION

A.	General	50
5.A.1	Terzaghi-Rendulic's Two-Dimensional Theory	51
5.A.2	Extension of Davis-Raymond's Theory to Two Dimensions	52
5.A.3	Solution of the Two-Dimensional Equation	61
5.A.4	Comparison of Numerical Solution with Closed Form Solution	63
5.A.5	Comparison with Bernell's Values	66
B.	Impeded Drainage	70
5.B.1	Introduction	70
5.B.2	Analysis and Technique of Solution	74
5.B.3	Results and Discussion	82

CHAPTER VI - INFLUENCE OF DISSIPATION ON CONSTRUCTION PORE PRESSURES

6.1	General	111
6.2	Summary of the Theoretical Methods for Predicting Construction Pore Pressures	111

Page

6.3	Analysis and Technique of Solution	120
6.4	Case Histories	127
6.4.A	Otter Brook Dam	127
6.4.B	Tooma Dam	131
6.4.C	Seitenoikea Dam	135
6.4.D	Miraflores Dam	139
6.4.E	Jari Dam	142
6.4.F	Usk Dam	146
6.5	Discussion	150

CHAPTER VII - FINITE STRAIN ONE-DIMENSIONAL CONSOLIDATION SEDIMENTATION

7.1	General	197
7.2	Mathematical Formulation	200
7.3	Permeability, Compressibility, Void Ratio, and Effective Stress Relationships	214
7.4	One-Dimensional Consolidation Equation	217
7.5	Thickness of the Sediment	221
7.6	Density of the Sediment	222
7.7	Finite Difference Representation	223
7.8	Summary	226
7.9	A Case History	227
7.10	Discussion	235

CHAPTER VIII - EROSION AND SWELLING IN VALLEY FORMATION

8.1	General	255
8.2	Formulation	255
8.3	Discussion of Numerical Results	260

	Page
LIST OF REFERENCES	273
APPENDIX A - COMPUTER PROGRAM AND USAGE FOR TWO-DIMENSIONAL IMPEDED DRAINAGE	A-1
APPENDIX B - COMPUTER PROGRAM AND USAGE FOR PREDICTION OF CONSTRUCTION PORE PRESSURES	B-1
APPENDIX C - COMPUTER PROGRAM AND USAGE FOR ONE-DIMENSIONAL FINITE STRAIN CONSOLIDATION	C-1
APPENDIX D - COMPUTER PROGRAM AND USAGE FOR EROSION AND SWELLING IN VALLEY FORMATION	D-1

LIST OF TABLES

Table		Page
4.1(a)	Percentage pore pressure values at the impervious boundary on the centre line	46
4.1(b)	Values of average degree of consolidation in percentage	46
4.2	Comparison between ADI and Barakat and Clark Methods	47
5.1	Values of pore pressure for a rectangular section of side ratio 2.4	91
5.2	Values of pore pressure for a rectangular section of side ratio 1.5	92
5.3	Values of λ for a hypothetical dam	93
6.1	Observational data for impervious core zones, dams	156
6.2	Calculation of a representative value of coefficient of consolidation, Otter Brook Dam	157
6.3	Values of pore pressure at cell no. 5, Seitenoikea Dam	158
6.4	Observed values of r_u , Seitenoikea Dam	158
6.5	Representative value for c_v , Seitenoikea Dam	159
6.6	Representative value for c_v , Miraflores Dam	160
6.7	Representative value for c_v , Jari Dam	161
7.1	Deltaic deposits off Louisiana	239

LIST OF FIGURES

Figure		Page
3.1	Surface Boundary Conditions	29
4.1	Finite Difference Schemes	48
4.2	Soil Sample	49
5.1	A Rectangle with Nonhomogeneous Boundary Conditions of the Third Kind	94
5.2	A Rectangle with Mixed Boundary Conditions of First and Third Kind	94
5.3a	Variation of Pore Pressure with Time	95
5.3b	Variation of Pore Pressure with Time	96
5.3c	Percentage of Maximum Pore Pressure with Time	97
5.3d	Percentage of Maximum Pore Pressure with Time	98
5.4	Idealized Dam Cross-Section	99
5.5a	Percentage of Maximum Pore Pressure with Time	100
5.5b	Percentage of Maximum Pore Pressure with Time	101
5.6a	Rectangular Section with Side Drains	102
5.6b	Rectangular Section with Side Drains	102
5.7a	Space Grid for Materials for A and B	103
5.7b	Space Grid for Material A Only	103
5.8	Relationship between Average Degree of Consolidation and Time Factor	104
5.9	Relationship between Average Degree of Consolidation and Time Factor	105
5.10	Relationship between Average Degree of Consolidation and Time Factor	106
5.11	Relationship between Average Degree of Consolidation and Time Factor	107

Figure	Page
5.12 Relationship between Average Degree of Consolidation and Time Factor	108
5.13 Relationship between Average Degree of Consolidation and Time Factor	109
5.14 Relationship between Average Degree of Consolidation and Time Factor	110
6.1 Computation of Pore Pressure Allowing Drainage	162
6.2 Cross-Section of Otter Brook Dam	163
6.3 Rate of Construction: Otter Brook Dam	164
6.4a Assumed Cross-Section of Otter Brook Dam	165
6.4b Idealized Cross-Section of Otter Brook Dam	166
6.5 Development of Construction Pore Pressures, Otter Brook Dam	167
6.6 Pore Pressure Ratio with Time	168
6.7 Cross-Section of Tooma Dam	169
6.8a Cross-Section of Core of Tooma Dam	170
6.8b Idealized Cross-Section of Core of Tooma Dam	170
6.9 Rate of Construction: Tooma Dam	171
6.10 Values of Pore Pressure Ratio, Tooma Dam	172
6.11 Values of Pore Pressure Ratio, Tooma Dam	173
6.12 Cross-Section of Seitenoikea Dam	174
6.13 Rate of Construction: Seitenoikea Dam	175
6.14a Assumed Cross-Section of Seitenoikea Dam	176
6.14b Idealized Cross-Section	177
6.14c Alternate Idealized Cross-Section	177
6.15 Values of Pore Pressure Ratio, Seitenoikea Dam	178

Figure	Page
6.16	Cross-Section of Miraflores Dam 179
6.17	Rate of Construction: Miraflores Dam 180
6.18a	Assumed Cross-Section of Miraflores Dam 181
6.18b	Idealized Section of Miraflores 181
6.19	Pore Pressures Immediately after Construction 182
6.20	Summary of Pore Pressures 183
6.21	Cross-Section of Jari Dam 184
6.22a	Assumed Cross-Section of Jari Dam 185
6.22b	Idealized Section of Jari Dam 186
6.23	Rate of Construction: Jari Dam 187
6.24a	Construction Pore Pressures, Jari Dam 188
6.24b	Construction Pore Pressures, Jari Dam 189
6.24c	Construction Pore Pressures, Jari Dam 190
6.24d	Construction Pore Pressures, Jari Dam 191
6.25	Cross-Section of Usk Dam 192
6.26	Rate of Construction: Usk Dam 193
6.27	Assumed Cross-Section of Usk Dam 194
6.28a	Pore Water Pressures in October, 1953 Usk Dam 195
6.28b	Pore Water Pressures at end of Construction, Usk Dam 196
7.1	Configuration of Soil Element 240
7.2	Permeability - Effective Stress Relationship for N.C. Clays 241
7.3	Sediment Layer Growth 242
7.4	Relationship between Void Ratio and Effective Stress 243
7.5	Relationship between Compressibility and Effective Stress 244

Figure		Page
7.6	Relationship between c_v and q	245
7.7	Relationship between Void Ratio and Depth, Eugene Island Block, 188	246
7.8	Relationship between Void Ratio and Depth, Grand Isle Block, 23	247
7.9	Relationship between Void Ratio and Depth, South Pass Block, 20	248
7.10	Variation of Permeability with Depth, Eugene Island Block, 188	249
7.11	Variation of Permeability with Depth, Grand Isle Block, 23	250
7.12	Variation of Permeability with Depth, South Pass Block, 20	251
7.13	Variation of Coefficient of Consolidation with Depth, Eugene Island Block, 188	252
7.14	Variation of Coefficient of Consolidation with Depth, Grand Isle Block, 23	253
7.15	Variation of Coefficient of Consolidation with Depth, South Pass Block, 20	254
8.1	Pore Pressure Isochrones	265
8.2	Pore Pressure Isochrones	266
8.3	Pore Pressure Isochrones	267
8.4	Pore Pressure Isochrones	268
8.5	Percent of Hydrostatic Pressure vs. Depth	269
8.6	Percent of Hydrostatic Pressure vs. Depth	270
8.7	Percent of Hydrostatic Pressure vs. Depth	271
8.8	Percent of Hydrostatic Pressure vs. Depth	272

CHAPTER I

INTRODUCTION

1.1 PURPOSE OF THE RESEARCH

The study comprising this thesis is based on the well-known classical Terzaghi theory. In deriving the differential equation governing one-dimensional consolidation, Terzaghi assumed constant coefficients of permeability and compressibility for the soil together with infinitesimal strains to realize a linear theory. Such assumptions characterized early studies in mathematical physics for two very important reasons. First, a linear theory yields governing equations which are amenable to closed form solution. This requirement was almost essential prior to the advent of high speed computers. Second, a linear theory enables one to apply the principle of superposition. However, the idealizations assumed by Terzaghi obviously are at variance with reality.

Differences in observed and predicted results have stimulated a series of modifications to the theory. Non-homogeneous soils whose properties vary with depth have been treated by Schiffman and Gibson (1964) and Raymond (1965). Small strain theories for compressible, normally consolidated clay incorporating stress-dependent coefficients of compressibility and permeability have been presented by Davis and Raymond (1965) and Barden and Berry (1965). Large

strains have been considered by Mikasa (1965) and by Gibson et al. (1967). Gibson et al. (op. cit.) have incorporated the relative velocity between water and soil in applying Darcy's law. Many of the above treatments lead to non-linear partial differential equations which cannot be solved rigorously. Recourse is usually made to numerical methods.

Under three-dimensional conditions, three-dimensional strains as well as three-dimensional flow of water take place. The three-dimensional treatments have all assumed linear elastic characteristics, as anything more realistic leads to extreme mathematical complexity. Pseudo three-dimensional cases which involve three-dimensional flow of water but only one-dimensional vertical strain are comparatively simple to treat if the bulk stress remains constant. The solutions for sand drain design (Barron, 1948) are of this type, as also is the more complex analysis for sand drains in layered clays (Horne, 1964).

All of the studies mentioned above neglect the true self-weight of the soil.

1.2 SCOPE OF THE STUDY

The scope of this study includes a summary of all of the existing theories of one- and three-dimensional consolidation. The assumptions involved in each theory are examined and criticized. A general, nonlinear theory of

one-dimensional consolidation is developed incorporating the self weight of the soil, the relative velocity of soil and water in Darcy's law, and a variation of the coefficients of permeability and compressibility with effective stress which in turn is a function of depth and time.

A two-dimensional plane strain case for consolidation is developed on the basis of Terzaghi's assumptions, which involves two-dimensional dissipation of water and one-dimensional vertical compression. The development of the equation is general and incorporates a moving boundary involving the thickness of the clay layer increasing with time. This equation is used to predict the construction pore pressures and the effect of dissipation during construction shutdown. Six case histories have been studied and the calculated and recorded pore pressures are compared.

Arising out of the solution of the two-dimensional equation, rectangular clay cores having side drains are examined. The impedance of the side drains to the normal flow of water due to dissipation is studied.

As part of an investigation into processes associated with valley formation the erosion of a fully saturated soil mass at a specified rate has been studied and the resulting pore pressure isochrones have been computed. This is a corollary to the one-dimensional sedimentation case (Gibson, 1958). The equation governing one-dimensional erosion is developed and results are obtained for typical cases.

1.3 ORGANIZATION OF THE THESIS

This study can be divided into the following main parts.

Chapter II deals with a brief critical review of the existing theories of consolidation of clay layers.

Chapter III comprises a brief treatment of the boundary conditions that may arise in consolidation problems.

Chapter IV includes a summary of the numerical techniques involved and a detailed discussion of the methods employed.

Chapter V is a discussion of the Terzaghi two-dimensional consolidation case. Also an extension of the Davis-Raymond theory to two dimensions is included. A complete section is devoted to the development and discussion of impeded drainage in two-dimensional dissipation.

Chapter VI deals with the analysis and techniques of solution of a two-dimensional consolidation equation which yields the construction pore pressures in a growing wedge. A summary of the theoretical methods for predicting construction pore pressures is provided. Six case histories are presented and comparisons are made between the numerical and recorded pore pressure results.

Chapter VII is the development of analysis and solution of a general, nonlinear, finite strain, one-dimensional consolidation theory for clay layers increasing in thickness with time. The development accounts for the

self weight of the soil grains. The material property behavior is based on observed data. A case history is cited.

Chapter VIII refers to the analysis of the one-dimensional equation governing the deficient pore pressure dissipation arising out of the depositional and erosional balance in valley formation. Results are provided for few general cases.

CHAPTER II

REVIEW OF CONSOLIDATION THEORIES

2.1 GENERAL

When a load is applied to a saturated soil mass, initially the entire load is taken up by the water in the pores of the soil skeleton. The pore water thus develops a pressure excess (in excess of the equilibrium pore water pressure) equal to the applied load at the instant of loading. If the duration of load application to the saturated soil mass is short, i.e., short compared to the dissipation time of excess pore pressure, water begins to flow due to the hydraulic gradient caused by the excess pore pressure, and the soil changes in volume. The process involving a decrease of the water content of a saturated soil without replacement by air is called the 'Process of Consolidation'. The mathematical theory describing the dissipation of excess pore pressures and associated deformation of the soil is called 'Consolidation Theory'. The amount of compression that has occurred in the soil skeleton at any time is related not only to the applied load but also to the amount of stress transmitted at the soil particle contacts, i.e., to the difference between the applied stress and the pore pressure. This difference is called the 'Effective Stress'.

2.2 BIOT'S THEORY OF THREE-DIMENSIONAL CONSOLIDATION

Biot (1941) has presented a rigorous and complete treatment of the theory of consolidation. The following basic properties of the saturated soil were assumed:

- (a) isotropy of the material
- (b) reversibility of stress-strain relations under final equilibrium conditions
- (c) linearity of stress-strain relations
- (d) small strains
- (e) the water contained in the pores is incompressible
- and (f) the water flows through the porous soil skeleton according to Darcy's law.

The strains are assumed to be related to the effective stress changes by equations such as

$$\epsilon_{xx} = \frac{1 + \mu}{E} \sigma'_{xx} - \frac{\mu}{E} \theta' \quad 2.1a$$

where ϵ_{xx} denotes strain in the x-direction

σ'_{xx} denotes effective stress in the x-direction
 $= (\sigma_{xx} - u)$

σ_{xx} denotes total stress in the x-direction

u denotes pore water pressure

μ denotes Poisson's ratio of the soil skeleton

E denotes Young's Modulus of Elasticity for the soil skeleton

$$\theta' \quad \text{denotes } (\sigma'_{xx} + \sigma'_{yy} + \sigma'_{zz}) = (\sigma_{xx} + \sigma_{yy} + \sigma_{zz}) - 3u \quad 2.1b$$

$$\text{i.e., } \theta' = \theta - 3u \quad 2.1c$$

where θ' is called the first effective stress invariant, and θ the first total stress invariant. Similar relations such as 2.1a can be written for strains in the y - and z -directions. They are

$$\epsilon_{yy} = \frac{1 + \mu}{E} \sigma'_{yy} - \frac{\mu}{E} \theta' \quad 2.2$$

$$\epsilon_{zz} = \frac{1 + \mu}{E} \sigma'_{zz} - \frac{\mu}{E} \theta' \quad 2.3$$

Adding equations 2.1a, 2.2, and 2.3, we have

$$\epsilon_{xx} + \epsilon_{yy} + \epsilon_{zz} = \frac{1 - 2\mu}{E} \theta'$$

$$\text{or} \quad \Delta = \frac{1 - 2\mu}{E} \theta' \quad 2.4$$

where

$$\Delta = \epsilon_{xx} + \epsilon_{yy} + \epsilon_{zz}$$

Equation 2.4 yields

$$\theta' = \frac{E\Delta}{(1 - 2\mu)}$$

Substituting 2.1c in the above equation leads to

$$\theta - 3u = \frac{E\Delta}{(1 - 2\mu)}$$

2.5

or

$$\frac{1}{3} \theta - u = \frac{E\Delta}{3(1 - 2\mu)}$$

Further, Darcy's law is assumed valid for the flow of pore water through the porous soil skeleton. Therefore,

$$v_x = -k i_x = -\frac{k}{\gamma_w} \frac{\partial u}{\partial x} \quad 2.6$$

where v_x denotes the velocity of fluid flow in the x-direction

i_x denotes the hydraulic gradient in the x-direction

k denotes the coefficient of permeability of the soil.

On differentiation, equation 2.6 becomes

$$\frac{\partial}{\partial x} (v_x) = -\frac{k}{\gamma_w} \frac{\partial}{\partial x} \left(\frac{\partial u}{\partial x} \right)$$

or
$$\frac{\partial}{\partial x} (\delta x / dt) = - \frac{k}{\gamma_w} \frac{\partial^2 u}{\partial x^2}$$

i.e.,
$$\frac{\partial}{\partial t} (\delta x / dx) = - \frac{k}{\gamma_w} \frac{\partial^2 u}{\partial x^2}$$

where
$$\delta x / dx = \epsilon_{xx}$$

Therefore equation 2.6 transforms to

$$\frac{\partial}{\partial t} (\epsilon_{xx}) = - \frac{k}{\gamma_w} \frac{\partial^2 u}{\partial x^2} \quad 2.7a$$

Similar equations for strains in y- and z-directions are

$$\frac{\partial}{\partial t} (\epsilon_{yy}) = - \frac{k}{\gamma_w} \frac{\partial^2 u}{\partial y^2} \quad 2.7b$$

and
$$\frac{\partial}{\partial t} (\epsilon_{zz}) = - \frac{k}{\gamma_w} \frac{\partial^2 u}{\partial z^2} \quad 2.7c$$

Adding equations 2.7, we have

$$\frac{\partial \Delta}{\partial t} = - \frac{k}{\gamma_w} \nabla^2 u \quad 2.8a$$

where
$$\nabla^2 = \frac{\partial^2}{\partial x^2} + \frac{\partial^2}{\partial y^2} + \frac{\partial^2}{\partial z^2} \quad 2.8b$$

Substituting 2.5 in 2.8 yields

$$\frac{\partial}{\partial t} \left\{ \frac{3(1 - 2\mu)}{E} \left(\frac{1}{3} \theta - u \right) \right\} = - \frac{k}{\gamma_w} \nabla^2 u \quad 2.9$$

The above equation may be written as

$$\nabla^2 u = \frac{3(1 - 2\mu)\gamma_w}{kE} \left(\frac{\partial u}{\partial t} - \frac{1}{3} \frac{\partial \theta}{\partial t} \right)$$

$$\text{i.e.,} \quad c \nabla^2 u = \frac{\partial u}{\partial t} - \frac{1}{3} \frac{\partial \theta}{\partial t} \quad 2.10$$

$$\text{where} \quad c = \frac{kE}{3(1 - 2\mu)\gamma_w}$$

Equation 2.10 is the general equation for consolidation in three-dimensions. An unique solution to equation 2.10 depends on the specified boundary and initial conditions. Boundary and initial conditions are discussed in a subsequent section.

Of the basic assumptions made, (b) and (c) are most subject to criticism. Biot (1941) contends that it can be imagined that the grains comprising the soil are held together by surface tension forces and tend to assume a configuration of minimum potential energy; this Biot believes is essentially true for the colloidal particles constituting clay. Biot (op. cit.) assumed that for small strains,

when the soil grain pattern is not too much disturbed, the assumption of reversibility will be applicable. The assumption (a) of isotropy is not essential and anisotropy can easily be introduced as a refinement.

In Biot's presentation it is emphasized that all equilibrium, compatibility and stress-strain relationships have been satisfied. It is evident that the formal solution of the equation 2.10a is rather complex; only few special cases have been solved. For example, De Jong (1957) presented the solution for a circular uniformly loaded area supported on a compressible soil of infinite extent and Gibson and McNamee (1957) solved the case of a rectangular uniformly loaded area on the surface of a semi infinite, isotropic, homogeneous, and fully saturated porous elastic medium with a fully permeable upper surface. The analysis was restricted to a medium with a Poisson's Ratio equal to zero.

2.3 RENDULIC'S THEORY OF THREE-DIMENSIONAL CONSOLIDATION

Rendulic (1936) presented a theory for three-dimensional consolidation. Assuming that the soil is isotropic and homogeneous, the three-dimensional consolidation equation may be written as

$$c\nabla^2 u + \frac{1}{3} \frac{\partial \theta}{\partial t} = \frac{\partial u}{\partial t} \quad 2.11$$

where $\theta_1 = \sigma_1 + \sigma_2 + \sigma_3 = \sigma_{xx} + \sigma_{yy} + \sigma_{zz}$

and
$$c = \frac{kE}{3(1 - 2\mu)\gamma_w}$$

This equation was obtained by assuming a linear elastic stress-strain law, and no attempt was made to refer to strain compatibility. This theory is called the pseudo-three-dimensional theory of consolidation.

Equation 2.11 is identical with 2.10 for an elastic skeleton; but it is important to realise that θ_1 in 2.11 is the sum of the externally applied total stresses, whereas θ in 2.10a is the sum of the total stresses at the point under consideration. The value of $\frac{\partial \theta}{\partial t}$ is determined not only by the time rate of change of external stresses (as is $\frac{\partial \theta_1}{\partial t}$), but also by the change in volume as the consolidation process progresses (Schiffman, 1967).

2.4 COMPARISON OF THEORIES OF BIOT AND RENDULIC

Generally the term $\frac{\partial \theta}{\partial t}$ is non-zero, since stress redistribution does take place within the soil mass during consolidation, even when the applied load is maintained constant. The term $\frac{\partial \theta_1}{\partial t}$ will be zero when the externally applied load is constant. When, as a first approximation $\frac{\partial \theta}{\partial t}$ is taken equal to zero (as in Terzaghi theory, to be followed), then the governing equation for consolidation is

$$c \nabla^2 u = \frac{\partial u}{\partial t} \quad 2.12$$

As pointed out earlier, under three-dimensional strain conditions, 2.12 assumes the form

$$c_3 \left(\frac{\partial^2 u}{\partial x^2} + \frac{\partial^2 u}{\partial y^2} + \frac{\partial^2 u}{\partial z^2} \right) = \frac{\partial u}{\partial t} \quad 2.13$$

where

$$c_3 = \frac{kE}{3(1 - 2\mu)\gamma_w}$$

Under two-dimensional strain conditions, the strain in one of the directions (say y-direction) is considered to be zero (plane strain case) and it can be shown that equation 2.12 assumes the form

$$c_2 \left(\frac{\partial^2 u}{\partial x^2} + \frac{\partial^2 u}{\partial z^2} \right) = \frac{\partial u}{\partial t} \quad 2.14$$

where

$$c_2 = \frac{kE}{2(1 - 2\mu)(1 + \mu)\gamma_w}$$

and is the coefficient of consolidation under two-dimensional strain.

For one-dimensional strain condition, the equation becomes

$$c_1 \left(\frac{\partial^2 u}{\partial x^2} \right) = \frac{\partial u}{\partial t} \quad 2.15$$

where

$$c_1 = \frac{kE(1 - \mu)}{(1 - 2\mu)(1 + \mu)\gamma_w}$$

and is the coefficient of consolidation under one-dimensional strain.

Thus it may be seen that the form of the equation 2.12 depends on the flow (or drainage) conditions, while the value of the coefficient of consolidation depends on the strain conditions. It will be noted that

$$c_1 = 2(1 - \mu)c_2 = 3\left(\frac{1 - \mu}{1 + \mu}\right)c_3$$

For a value of $\mu = 0.5$ $c_1 = c_2 = c_3$

For a value of $\mu = 0.0$ $c_1 = 2c_2 = 3c_3$

The difference between these values of c can be important. The value of c in the definition of time factor for a tri-axial test is c_3 , whereas that for the oedometer test is c_1 .

The three-dimensional theory of primary consolidation (poroelasticity) due to Biot makes no assumptions as to the time-dependent variables. The state of total stress is a function of the excess pore pressure and the compatibility relationships for the soil skeleton. This theory is completely self-consistent and does not call for a separation of the magnitude and progress of consolidation. The pseudo-three-dimensional theory maintains a lack of coupling between magnitude and progress of consolidation.

Comparing these two theories, Schiffman (1967) considered the problem of a strip load (plane strain) on the surface of a semi infinite body. It was found that the total stress is not constant with time. Furthermore, excessive pore pressures, instead of decreasing with time, increase at first, and then decrease. This effect, called the Mandel-Cryer effect, appears only in the three-dimensional theory, and is absent from the pseudo-three-dimensional theory.

The solution of three-dimensional problems and subsequent application to practical cases is seriously limited because of the lack of techniques of solution and also because accurate values of E and μ are difficult to obtain.

2.5 TERZAGHI'S CLASSICAL ONE-DIMENSIONAL THEORY

The one-dimensional consolidation theory (Terzaghi, 1923) has been applied widely to many field problems. The results obtained are usually acceptable and, within practical limits, quite reliable. The assumptions involved in the Terzaghi theory are:

- (i) homogeneous soil
- (ii) incompressible soil grains and the voids fully saturated by an incompressible fluid
- (iii) small strains
- (iv) void ratio is linearly related to the effective stress

(v) the fluid flow through the soil skeleton is governed by Darcy's law.

and (vi) permeability and compressibility are constant throughout the process of consolidation.

This theory considers only the diffusion of water through a porous medium. For an isotropic soil in which water flows only in one direction and compression occurs only in the same direction, the governing equation may be written as

$$c \left(\frac{\partial^2 u}{\partial x^2} \right) = \frac{\partial u}{\partial t} \quad 2.16$$

The one-dimensionality of consolidation may be due either to a surface loading of uniform magnitude infinitely extended in all directions or due to a lateral physical restraint as in the oedometer test .

The application of one-dimensional theory, which depends on unreal assumptions as to the direction of compression and material properties, paradoxically, yields acceptable results and permits a large variety of solutions to be obtained. Recent developments in numerical analysis and in computer technology provide improved capability in handling one-dimensional consolidation equation for an arbitrary loading history and for variations in soil properties.

2.6 MODIFICATIONS TO TERZAGHI'S THEORY

From time to time, many of the assumptions made in Terzaghi's theory have been modified.

It is known that the Terzaghi theory does not hold good for the case of soft clay whose permeability k and compressibility m_v change their values during the consolidation process. Small strain theories for compressible normally consolidated clay incorporating a decreasing m_v and k have been presented by Davis and Raymond (1965). Non-homogeneous soils whose properties vary spatially and with time have been treated by Schiffman and Gibson (1964) and Raymond (1965). Layered soils can also be considered.

The assumption of the validity of Darcy's law is generally acceptable but a modification may be introduced. The seepage velocity of flow is replaced by the relative velocity of flow of fluid with respect to that of the solid grains (Scheidegger, 1960). This extends Darcy's law to a more presentable and accurate form.

The limitation of small strains has been overcome by making use of Lagrangian coordinates (Gibson et al., 1967). Also Mikasa (1965) considers large strains.

Many of the above modifications in combination or singly lead invariably to nonlinear partial differential equations governing the process of consolidation, for which analytical (closed form) solutions are difficult to obtain.

In actual practice, the total load on a clay layer

is usually applied over a period of time, t_c . If t_c is such that only a small proportion of the total consolidation occurs during this period then the load may be considered to be applied instantaneously. On the other hand, if a sufficiently large proportion of the excess pore pressure has been dissipated during the period t_c , then the problem may be treated in either of the following ways:

(i) The time-dependency of loading may be considered to be the variation in loading with time, i.e., the rate of load application is arbitrary, e.g., construction rate of loading.

(ii) The total load on the element of soil under consideration may also change because of the addition of subsequent layers of soil on top of the element. Such a case is also one of time-dependent loading except that this case involves the physical movement of the top boundary. This is a moving boundary problem.

CHAPTER III

BOUNDARY CONDITIONS - A BRIEF TREATMENT

3.1 GENERAL

The basic governing equation for the dissipation of excess pore pressure in an ideal soil according to Terzaghi's theory is

$$c_v \nabla^2 u = \frac{\partial u}{\partial t} \quad 3.1$$

The solution of this differential equation for various geometrical configurations and boundary conditions* has been attempted by many since the advent of Fourier mathematics. Equation 3.1 will have numerous solutions unless a set of boundary conditions and an initial condition are prescribed. The conditions prescribed at the boundary surfaces of the region may be linear or non-linear.

The general problem may be formulated as follows:

It is required to determine the distribution of excess pore pressure in a homogeneous and isotropic (soil) body

* The term 'boundary condition', sometimes, may include the so called 'initial conditions'. This means, according to some schools of thought, that 'bounds' are considered to be limitations in time as well as in space.

at any given instant when the following is given.

(a) The pore pressure excess distribution at any other instance, mostly at an earlier instance (e.g., at time $t = 0$, i.e., initial pore pressure distribution).

(b) The influence of the surroundings of the body on its surface. For example, it may be assumed that by some means a definite excess pore pressure distribution can be imposed on the surface of the body by external forces; this distribution may be constant or time-dependent.

The conditions under (a) and (b) above are called the boundary conditions, the first being with respect to time and the second with space.

3.2 BOUNDARY VALUE PROBLEM

In the equation

$$u = f(x,y,z,t) \quad 3.2$$

u may be interpreted as given by a function f within a domain of a four dimensional space - time region and to solve for u uniquely mathematics demand certain values (called conditions) at the boundary of this domain. In mathematical terminology, these conditions which must be satisfied in addition to the governing differential equation, are known as boundary conditions. And the problem(s) thus posed are called BOUNDARY VALUE PROBLEM(S).

A. BOUNDARY CONDITION FOR TIME

The boundary condition for time may be given by a function

$$u = F(x,y,z) \quad 3.3$$

which represents the distribution of excess pore pressure at any given instant. This distribution can be chosen, arbitrarily, to be continuous or discontinuous. In most problems, excess pore pressure at a later instant is of interest. This is obtained using the governing equation in conjunction with the boundary conditions for space.

B. BOUNDARY CONDITIONS IN SPACE

In the study of boundary value problems of heat conduction in mathematical physics, the conditions at the boundary surfaces of the region may be linear or nonlinear. The same holds good for excess pore pressure dissipation in a (soil) body as the similarity between pore pressure dissipation and temperature transmission has been well established (Terzaghi, 1923). In the following pages, only linear boundary conditions are considered.

For convenience the linear boundary conditions may be presented as follows:

(i) BOUNDARY CONDITION OF THE FIRST KIND

Excess pore pressure is prescribed at every point on the boundary surface and for the general case it is a function of both time and position, i.e.,

$$u = f_1(x, y, z, t) \quad 3.4a$$

The function itself may be arbitrary, continuous or discontinuous with respect to time and position.

Special cases include excess pore pressure at the boundary surface as a function of position only, or a function of time only, or a constant. If the excess pore pressure u at the boundary surface vanishes, then

$$u = 0 \quad 3.4b$$

This special case is called the homogeneous boundary condition of the first kind. A boundary surface which is kept at a constant pore pressure U , also satisfies the homogeneous boundary condition of the first kind if the excess pore pressure is measured in excess of U .

(ii) BOUNDARY CONDITION OF THE SECOND KIND

The second kind of boundary condition consists in expressing the amount of water exchanged (in case of thermodynamics, it is the quantity of heat exchange at the surface,

again as a function of time and position. This function may be quite arbitrary.

The normal derivative of excess pore pressure is prescribed at the boundary surface, e.g., in an orthogonal coordinate system it is expressed in the form

$$\frac{\partial u}{\partial n} = f_2(x, y, z, t) \quad 3.5a$$

where $\partial/\partial n$ denotes the differentiation along the outward drawn normal at the boundary surface. This boundary condition is equivalent to that of prescribing the magnitude of the quantity of water exchanged along the boundary surface.

Special cases of the above equation include the normal derivative of excess pore pressure at the boundary surface to be a function of position only, or a function of time only, or a constant. If the normal derivative of excess pore pressure at the boundary surface vanishes, then

$$\frac{\partial u}{\partial n} = 0 \quad 3.5b$$

This special case is called the homogeneous boundary condition of the second kind. An impervious boundary (an insulated boundary, in thermodynamics) satisfies this condition.

(iii) BOUNDARY CONDITION OF THE THIRD KIND

The third kind of boundary condition gives a linear combination of the excess pore pressure and its normal derivative at the boundary surface. In other words, this type consists in defining the excess pore pressure at the surface together with a law for the water exchange between the surface of the (soil) body and its surroundings.

In mathematical terms this may be expressed as,

$$A_1 \frac{\partial u}{\partial n} + A_2 u = f_3(x, y, z, t) \quad 3.6a$$

Thus this type is a combination of the first two types of boundary conditions and each of the first two boundary conditions can be obtained by appropriately choosing A_1 or A_2 to vanish.

A special case of the above equation is,

$$A_1 \frac{\partial u}{\partial n} + A_2 u = 0 \quad 3.6b$$

which is called the homogeneous boundary condition of the third kind. Such a situation can be realized in reality through the dissipation of water into a surrounding which impedes drainage for example, the core of a dam dissipating excess pore pressure into a side drain whose efficiency is not unity .

A graphical representation may be useful to illustrate the nature of the three types of boundary conditions discussed above. In Figure 3.1 ds represents an element on the surface of a (soil) body and n the outward drawn (positive direction) normal.

In the first type of boundary value problem the excess pore pressure U_0 at the surface is known. The hydraulic gradient and the amount of water exchanged at the boundary surface are the unknowns to be determined (Figure 3.1a).

In the second type of boundary condition problem, the conditions are opposite to those of the first type. In this type, the value of the excess pore pressure at the surface is the unknown, while the hydraulic gradient and/or the amount of water exchanged at the boundary surface is known (Figure 3.1b).

In the third type of boundary value problem a point on the outward drawn normal is given through which all the possible tangents to the excess pore pressure curve at the surface must pass. This point known as 'POLE' lies at a distance $k/\alpha = h$ from the surface. (k is the coefficient of permeability and α is the 'water exchange coefficient'). The unknowns in this type are the excess pore pressure at surface and the quantity of water exchanged. (The proof is given by Gröber et al., 1963).

The three types of boundary conditions described above cover most cases of practical interest. Boundary conditions associated with powers of excess pore pressure

other than unity are nonlinear. Also boundary conditions associated with changes in material content of the (soil) body (e.g., erosion or deposition) are nonlinear boundary conditions in that the boundary conditions are moving with respect to time.

3.3 MOVING BOUNDARY CONDITIONS

As mentioned in the previous paragraph, an important class of problems in pore pressure dissipation (as in heat conduction) deals with the determination of pore pressure (temperature) in a body whose boundaries are not fixed in space. Two types of problems may possibly be distinguished:

(a) those in which the motion of the boundary is due to rigid body motion of the entire body, and

(b) those in which the motion of the boundary is due to local conditions near the boundary.

Case (a) is usually referred to as moving body problem(s). Solutions for several problems of this type for bodies moving with a constant velocity are given by Carslaw and Jaeger (1959).

Case (b) may be divided into two cases, namely those in which the motion of the boundary is prescribed, and those in which it must be determined as part of the solution of the problem. The first of these cases is simpler than the second, since it is a linear problem although with variable coefficients. An example of this is the problem solved by

Gibson (1958). The latter case is sometimes referred to as 'floating - boundary' problem.

However, very few exact (closed form) solutions are available for such problems, and these problems indeed tend to become rather difficult except in few cases. As a consequence approximate and/or numerical methods of solution are very important.

The importance of floating-boundary problems in pore pressure dissipation arises primarily from the problems of deposition and erosion, in which the position of the interface between the deposit and the freshly deposited material is not known beforehand and must be determined in the solution. In a typical problem, the conditions to be satisfied on the moving front are that the pore pressure should be the same at the interface in both media and the continuity of flow must be maintained.

To simplify the analysis of problems such as erosion, it is assumed that the eroded material is completely removed from the surface as soon as it is eroded. There will therefore be no eroded phase on the surface of erosion. In reality a certain thickness of eroded material will always be in contact with the surface of erosion. Such cases are very difficult to treat.

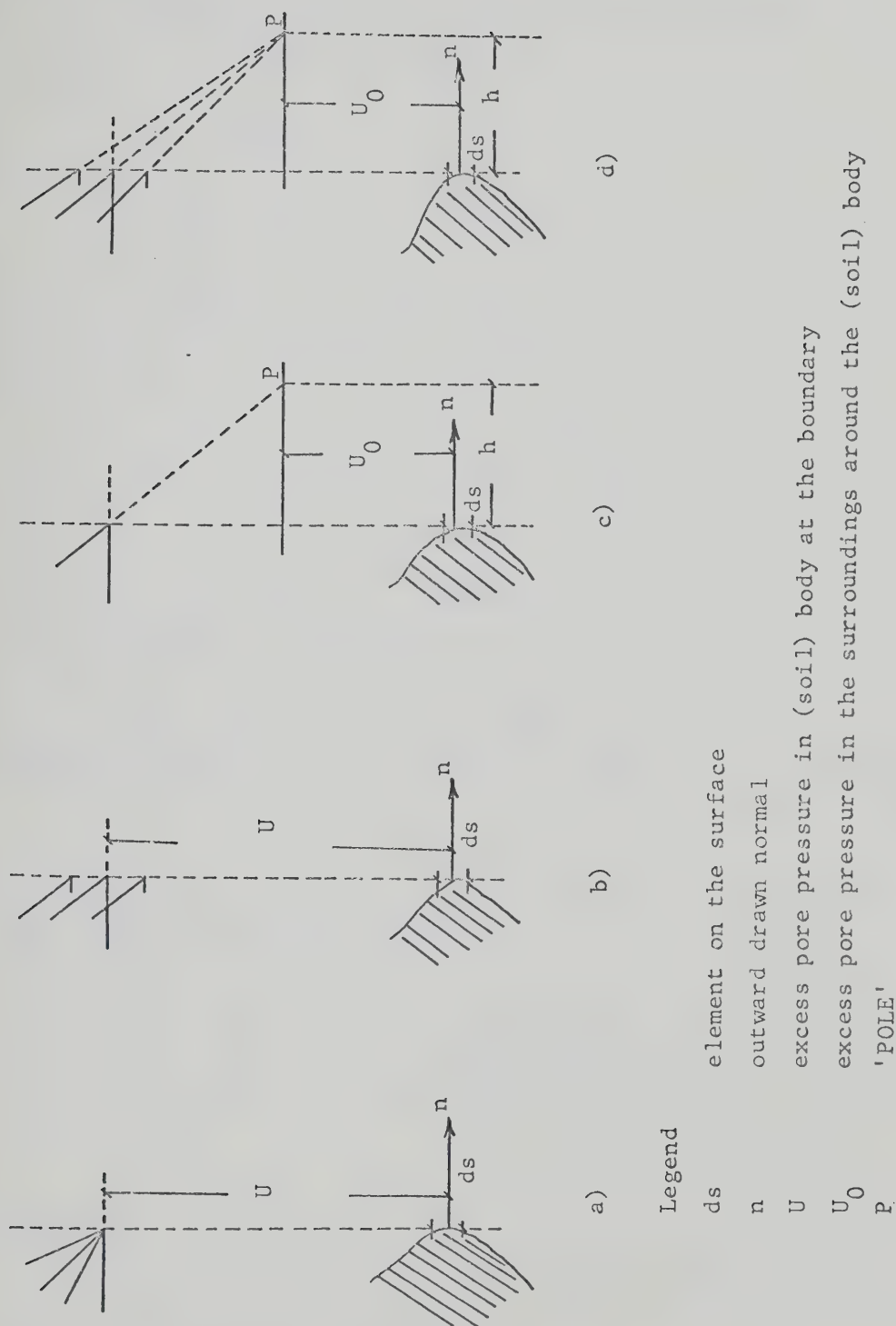


FIGURE 3.1 SURFACE BOUNDARY CONDITIONS

CHAPTER IV

TECHNIQUES OF SOLUTION - A BRIEF SUMMARY

4.1 GENERAL

In this chapter an examination of the finite difference approximation of the boundary value problems of excess pore pressure dissipation (similar to problems of heat conduction) is presented. Digital and analog computers are of great value for solving problems that cannot ordinarily be handled analytically because of complicated geometry and/or boundary conditions, or because the numerical evaluation of the analytical solution becomes too laborious. Digital computers are frequently put to use because of the fact that high-speed precise and versatile computers are available.

By analogy with heat conduction theory it is possible to distinguish three analytical methods for the solution of the equation (Abbott, 1960),

$$c_v \quad \frac{\partial^2 u}{\partial x^2} = \frac{\partial u}{\partial t} \quad 4.1$$

These are:

- (a) Classical methods based on Fourier mathematics,
- (b) Green's function,
- (c) Integral transformation, such as Laplace's.

The classical methods are useful for calculations of

pore pressure distribution in homogeneous soils and implicit in these is the underlying assumption of linearity, whereby the principle of superposition may be employed. However, most soils exhibit a nonlinear behavior, hence the principle of superposition is no longer applicable. There are thus considerable objections to further employment of classical methods of Fourier mathematics. The same objections limit the application of Green's function.

Integral transformations offer excellent means for the solution of the above equation except that computation of a set of results presents considerable algebraic and arithmetical problems. Generally, integral transformations are limited to solutions of linear differential equations.

Thus closed-form solutions of the above equation for consolidation problems of non-homogeneous and nonlinear soils are difficult to obtain and alternate methods must often be employed.

An alternative to analytical methods is numerical analysis, wherein the operation of solving the equation is reduced to solving a series of algebraic equations.

4.2 FUNDAMENTAL CONCEPTS IN FINITE DIFFERENCE APPROXIMATIONS

A fundamental concept in the finite difference approximation of a differential equation is the expansion of the

function by Taylor's series. Once the finite difference approximation is obtained, the problem reduces to the solution of a set of algebraic equations. These equations may be translated into a set of commands understood and performed by a digital computer.

In the process of solution of differential equations, errors are introduced at each step of the calculation due to approximations involved in finite difference and numerical calculations. Cumulative effects of such errors on the final result and stability of the solution are very important. An exhaustive treatment of the above aspects can be found in Fox (1962), Richtmeyer (1957), and others.

4.3 FORMS OF FINITE DIFFERENCE APPROXIMATION

Various schemes are available to express the differential equation in a finite difference form. Richtmeyer (1957) lists thirteen different schemes, ranging from the explicit form to a fully implicit form for finite differencing of the one-dimensional time-dependent heat conduction equation.

An explicit scheme provides a noniterative 'marching' process for obtaining the solution at each present nodal point in terms of known preceding and boundary points. Questions of stability are most critical for explicit schemes. Implicit procedures are usually iterative simultaneous calculations of many known present values together with preceding values and boundary conditions.

Each of these difference schemes has its merits and limitations as explained in 4.5. When the boundary conditions involve derivatives, a forward, backward, or central differencing scheme may be used in expressing the boundary condition in finite difference form.

4.4 GENERAL FORM OF FINITE DIFFERENCE SCHEME

The differential equation

$$\frac{\partial^2 u}{\partial x^2} + B(x) \frac{\partial u}{\partial x} + c(x, T) = \frac{\partial u}{\partial T} \quad 4.2$$

in the region $0 \leq x \leq 1$ for $0 \leq T \leq \infty$ can be put in finite difference form by expanding the derivatives. The space derivatives may be expanded in terms of first order central differences, and the time derivative as a first order forward difference (Figure 4.1).

$$\frac{\partial u}{\partial x} (i, k + \lambda \Delta T) = \frac{1}{2\Delta x} \{u(i+1, k+\lambda) - u(i-1, k+\lambda)\} \quad 4.3a$$

$$\begin{aligned} \frac{\partial^2 u}{\partial x^2} (i, k + \lambda \Delta T) = & \frac{1}{(\Delta x)^2} \{u(i-1, k+\lambda) - 2u(i, k+\lambda) \\ & + u(i+1, k+\lambda)\} \end{aligned} \quad 4.3b$$

$$\frac{\partial u}{\partial T} (i, k + \lambda \Delta T) = \frac{1}{\Delta T} \{u(i, k+1) - u(i, k)\} \quad 4.3c$$

The factor λ may take an arbitrary value between zero and unity.

The value of $u(i, k+\lambda)$ can be found in terms of $u(i, k)$ and $u(i, k+1)$, by a linear interpolation over T , as

$$u(i, k+\lambda) = \lambda u(i, k+1) + (1-\lambda) u(i, k) \quad 4.3d$$

The boundary and initial conditions can also be expressed in finite difference notation.

From equations 4.3, equation 4.2 may be obtained in a general form as

$$\lambda \{A u(i-1, k+1) - B u(i, k+1)\} \quad 4.4$$

$$= (\lambda-1) \{A_1 u(i-1, k) + B_1 u(i, k) + C_1\} - \lambda C_2$$

where A , B , A_1 , B_1 , C_1 , and C_2 are quantities involving Δz and ΔT and as such are constants.

Choosing a value for λ will yield a particular method of computation.

4.5 EXPLICIT AND IMPLICIT SCHEMES

A. EXPLICIT SCHEME

Let λ be chosen equal to zero.

Equation 4.4 becomes

$$u(i, k+1) = C_1 u(i-1, k) + C_2 u(i, k) + C_3 u(i+1, k) + D(i, k) \quad 4.5$$

where C_1 , C_2 , C_3 , and D are constants involving Δx and ΔT .

Thus this scheme calculates u at point i in space and $(k+1)$ in time, in terms of the values of u at points $(i-1)$, i , $(i+1)$ at the preceding time step k . Hence this method 'marches forward' in time.

B. IMPLICIT SCHEME

Let λ be equal to unity.

Equation 4.4 yields

$$\begin{aligned} C_1' u(i-1, k+1) + C_2' u(i, k+1) + C_3' u(i+1, k+1) \\ + D'(i, k+1) = u(i, k) \end{aligned} \quad 4.6$$

This scheme involves the unknown values of u at time $(k+1)$ for points $(i-1)$, i , $(i+1)$ to calculate the value of u at time k for space point i . In other words, the value of

u at any time is implicitly expressed in terms of unknown values of u at a following time step hence the name implicit.

The iterative solution for this scheme may be obtained by solving a set of $(n+1)$ linear simultaneous equations for $(n+1)$ unknowns $u(i, k+1)$ for $i=0, 1, 2, \dots, n$.

C. CRANK - NICHOLSON SCHEME

Let λ be set equal to one-half.

Another implicit scheme results and is given by

$$\begin{aligned} B_1 u(i-1, k+1) + B_2 u(i, k+1) + B_3 u(i+1, k+1) + B_4 u(i, k+1) \\ = A_1 u(i-1, k) + A_2 u(i, k) + A_3 u(i+1, k) + A_4 u(i, k) \end{aligned}$$

where $B_1, B_2, B_3, B_4, A_1, A_2, A_3, A_4$ involve Δx and ΔT and hence constants.

The right-hand side of equation 4.7 contains only quantities at time k and hence it is similar to equation 4.6.

Solution of equation 4.7 is similar to that of equation 4.6.

D. COMPARISON OF METHODS

An explicit method of finite difference representation of the differential equation 4.2 results in a set of simple algebraic relations which could easily be solved with a digi-

tal computer. However, stability considerations restrict the size of the time step ΔT for a given value of Δx . If the space step Δx is to be chosen small for improved accuracy, then ΔT correspondingly also has to be chosen small. This results in a large number of time steps and computation becomes unwieldy. In such cases an implicit method is usually employed.

The implicit method does not restrict the value of ΔT and has no restriction on iteration rate. The time taken for each iteration may be high, but total time taken for all iterations is small; smaller than the time taken for the explicit method. However, it is more difficult to set up the calculation procedure for an implicit method than for the explicit method.

4.6 ALTERNATING - DIRECTION IMPLICIT METHOD

As noted in a previous paragraph, the implicit method has the advantage that it is unconditionally stable for all values of time step ΔT . On the other hand, the computational problems become enormous when two- or three-dimensional pore pressure dissipation (heat conduction) equations are to be solved over a region requiring a large number of subdivisions. For example, for a three-dimensional problem with N interior points in each direction there is a total of N^3 interior points, hence an $N^3 \times N^3$ matrix must be solved for each time increment. The procedure becomes obviously

impractical if N exceeds, say, about 10.

Peaceman and Rachford (1955) introduced an alternating-direction implicit (ADI) method for use in problems involving a large number of internal nodal points. In this method the size of the matrix to be solved at each time step is reduced at the expense of solving the reduced matrix many times for each time step. For example, referring to the above problem of a three-dimensional region the ADI method transforms the problem to solving an $N \times N$ matrix N^2 times for each time step, which is easier than solving an $N^3 \times N^3$ matrix at a time.

An alternating-direction implicit procedure requires a line-by-line solution of small sets of simultaneous equations that can be solved by a direct, non-iterative method. Analysis of the procedure shows it to be stable for any size time step and to require much less work than other methods that have been studied. As a practical test, the new procedure was used (Peaceman and Rachford, 1955) to solve the heat flow equation with boundary conditions for which a formal solution is known. The two solutions were in good agreement. Also a rapid convergence for the solution of Laplace's equation in a square was obtained using a suitable set of iteration parameters which were easily calculated. An analysis was presented (Peaceman and Rachford, op. cit.) that showed the method to require about $(2 \log N)/N$ as many calculations as the best previously known iterative procedure for solving Laplace's equation, where N^2 is the number of

points for which the solution is computed.

In obtaining the usual implicit difference equation for

$$\frac{\partial^2 u}{\partial x^2} + \frac{\partial^2 u}{\partial z^2} = \frac{\partial u}{\partial T} \quad 4.8$$

both the second derivatives are replaced by second differences evaluated in terms of the unknown values of u .

$$\begin{aligned} & \{u(i-1, j, k+1) - 2u(i, j, k+1) + u(i+1, j, k+1)\}/(\Delta x)^2 \\ & + \{u(i, j-1, k+1) - 2u(i, j, k+1) + u(i, j+1, k+1)\}/(\Delta z)^2 \\ & = \{u(i, j, k+1) - u(i, j, k)\}/\Delta T \end{aligned} \quad 4.9a$$

which can be written as

$$\begin{aligned} & u(i-1, j, k+1) + u(i+1, j, k+1) + u(i, j-1, k+1) \\ & + u(i, j+1, k+1) - (4 + R) u(i, j, k+1) \\ & = -Ru(i, j, k) \end{aligned} \quad 4.9b$$

where

$$R = \frac{(\Delta x)^2}{\Delta T} = \frac{(\Delta z)^2}{\Delta T} \quad 4.9c$$

if a mesh is chosen such that $\Delta x = \Delta z$.

Thus the unknown excess pore pressure at the time step k may be solved for implicitly by the above equation, provided the excess pore pressure at the time step $(k+1)$ is known.

Large sets of simultaneous equations are formed, which can be solved practically, only by iteration. If, however, only one of the second derivatives, say $\frac{\partial^2 u}{\partial z^2}$, is replaced by a second difference evaluated in terms of the unknown values of u , while the other derivative $\frac{\partial^2 u}{\partial x^2}$, is replaced by a second difference evaluated in terms of the known values of u , sets of simultaneous equations are formed that can be solved easily without iteration. These equations are implicit in the z -direction. If the procedure is then repeated for a second time step of equal size, with difference equations implicit in the x -direction, the overall procedure for the two time steps is proved to be stable for any size time step. Thus two difference equations are used, one for the first time step, the other for the second time step.

$$\begin{aligned}
 & \{u(i-1,j,k+1) - 2u(i,j,k+1) + u(i+1,j,k+1)\}/(\Delta z)^2 \\
 & + \{u(i,j-1,k) - 2u(i,j,k) + u(i,j+1,k)\}/(\Delta x)^2 \\
 & = \{u(i,j,k+1) - u(i,j,k)\}/\Delta T
 \end{aligned}
 \tag{4.10a}$$

and

$$\begin{aligned}
& \{u(i-1,j,k+1) - 2u(i,j,k+1) + u(i+1,j,k+1)\}/(\Delta z)^2 \\
& + \{u(i,j-1,k+2) - 2u(i,j,k+2) + u(i,j+1,k+2)\}/(\Delta x)^2 \\
& = \{u(i,j,k+2) - u(i,j,k+1)\}/\Delta T
\end{aligned}
\tag{4.10b}$$

These equations may be arranged in the following form suitable for calculation.

$$\begin{aligned}
& u(i-1,j,k+1) - (R + 2) u(i,j,k+1) + u(i+1,j,k+1) \\
& = - u(i,j-1,k) + (2 - R) u(i,j,k) - u(i,j+1,k)
\end{aligned}
\tag{4.11a}$$

and

$$\begin{aligned}
& u(i,j-1,k+2) - (2 + R) u(i,j,k+2) + u(i,j+1,k+2) \\
& = - u(i-1,j,k+1) + (2 - R) u(i,j,k+1) - u(i+1,j,k+1)
\end{aligned}
\tag{4.11b}$$

Use of each of the above equations at each time step leads to N sets of N simultaneous equations. The general procedure for solving these equations, the criteria for stability and convergence and related phenomena are fully discussed by Peaceman and Rachford (op. cit.) and Douglas (1955).

4.7 BARAKAT AND CLARK METHOD

Barakat and Clark (1966) described an explicit difference scheme which is unconditionally stable for the solution of the multi-dimensional, time-dependent heat-conduction equation. The method possesses the advantages of the implicit scheme (i.e., there is no severe limitation on the size of time increment), and the simplicity of the explicit scheme.

Barakat and Clark (op. cit.) examined the finite difference representation of the following boundary value problem of heat conduction,

$$\frac{\partial^2 u}{\partial x^2} + \frac{\partial^2 u}{\partial z^2} = \frac{\partial u}{\partial T} \quad \text{in} \quad \begin{matrix} 0 \leq x \leq 1 \\ 0 \leq z \leq 1 \end{matrix} \quad 4.12$$

subjected to prescribed temperature at the boundaries and to a prescribed initial condition.

To solve the above problem with finite difference, they considered two auxiliary functions $V(i,j,k)$ and $W(i,j,k)$ satisfying the following difference equations,

$$\begin{aligned} & \{V(i+1,j,k) - V(i,j,k) - V(i,j,k+1) + V(i-1,j,k+1)\}/(\Delta x)^2 \\ & + \{V(i,j+1,k) - V(i,j,k) - V(i,j,k+1) + V(i,j-1,k+1)\} \\ & /(\Delta z)^2 = \{V(i,j,k+1) - V(i,j,k)\}/\Delta T \end{aligned} \quad 4.13$$

and a similar expression for $W(i,j,k)$ with subscripts k and $(k+1)$ interchanged on the left hand side of equation 4.13.

Assuming $V(i,j,k)$ and $W(i,j,k)$ functions also satisfy the boundary and initial conditions for the heat conduction problem, the temperature $U(i,j,k)$ at any time level k may be taken as the arithmetic average of $V(i,j,k)$ and $W(i,j,k)$, i.e.,

$$U(i,j,k) = 1/2 [V(i,j,k) + W(i,j,k)] \quad 4.14$$

If finite difference equations for $V(i,j,k)$ and $W(i,j,k)$ functions are stable the solution of the equation 4.12 will be stable. It has been found that the finite difference solution for 4.12 is unconditionally stable for all values of Δt , Δx , Δz .

Equation 4.12 was solved for the following boundary and initial conditions employing both the present method and the ADI method to study the effect of the form of the difference equation on the relative accuracy. The initial and boundary conditions are:

$$U(x,z,0) = 100. \text{ units}$$

$$\frac{\partial U}{\partial x}(x,z,t) = 0.$$

$$U(1,z,t) = 0.$$

$$U(x,0,t) = 0.$$

and $U(x,1,t) = 0. \quad (\text{Fig. 4.2}).$

The results are given in Table 4.1. Both the numerical methods give results of comparable accuracy. Both the methods are unconditionally stable for any time step interval. ADI method requires the solution of a tridiagonal matrix whose solution can be obtained by an algorithm derived from the Gaussian elimination technique. The present method possesses the simplicity of an explicit method and employs the same "marching" type technique of solution. Thus the present method is simpler to formulate and easier to program. Table 4.2 gives a summary of the comparison between the two methods.

It is interesting to compare the machine time required by the present and the ADI methods for two dimensional problems. The ADI method needs to solve N sets of N simultaneous equations for $N \times N$ nodal points at each time step. And the present method requires the solution of N explicit equations N times for the same number of nodal points at each time step. As illustrated in Table 4.2, the present method takes less time than that taken by ADI.

The one serious drawback of the present method is that it requires at least twice the storage requirement of the ADI (Table 4.2). This is inherent in the method of solution since a single function $U(i,j,k)$ is split into two components $V(i,j,k)$ and $W(i,j,k)$ and both components are to be stored in memory in order to evaluate $U(i,j,k)$ by equation 4.14. For many of the problems considered in determining the excess pore pressure distribution the storage

requirement by the present method will be excessive for a large number of time steps.

It may be mentioned here that the present method can be extended to handle problems having three dimensions which is not convenient for the ADI method (Barakat and Clark, op. cit.).

Table 4.1a Comparison between ADI and Barakat and Clark Methods: Percentage pore pressure values at the impervious boundary on the centre line.

$$\Delta t = 0.1$$

$$\Delta x = 2.$$

$$\Delta z = 2.$$

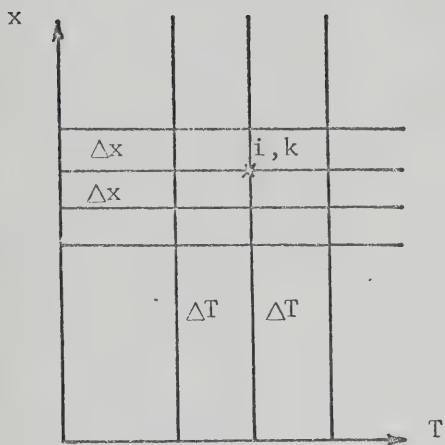
Time Factor	ADI	Barakat & Clark
0.	100.0	100.0
0.01	98.1	99.8
0.02	93.7	92.9
0.03	88.6	87.8
0.04	83.7	83.0
0.05	79.2	78.6
0.06	75.2	74.7
0.07	71.7	71.2
0.08	68.5	68.0
0.09	65.7	65.3
0.10	63.1	62.7

Table 4.1b Comparison between ADI and Barakat and Clark Methods: Values of average degree of consolidation in percentage.

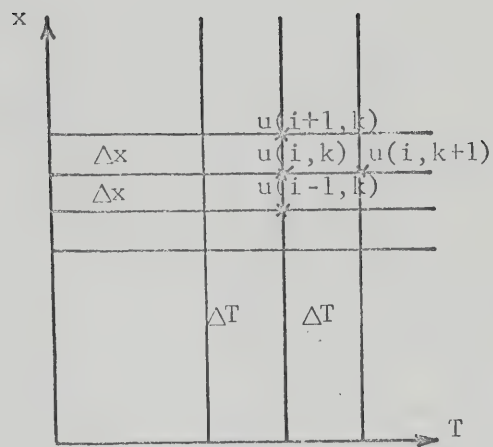
Time Factor	ADI	Barakat & Clark
0.0	0.0	0.0
0.001	11.645	11.791
0.002	12.194	12.340
0.005	13.777	13.926
0.010	16.229	16.377
0.020	20.541	20.683
0.030	24.238	24.375
0.040	27.477	27.610
0.050	30.366	30.498
0.060	32.366	33.117
0.080	37.604	37.746
0.100	41.627	41.778

Table 4.2 Comparison between ADI and Barakat and Clark Methods

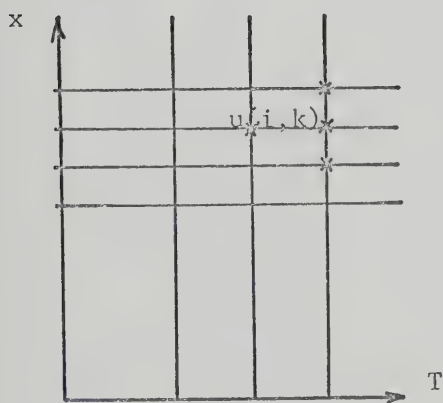
	ADI	Barakat & Clark
1. Time	0.44 min.	0.40 min.
2. Core Storage	90 K	150 K
3. Accuracy	Both methods are accurate to the same degree	
4. Programming	Quite difficult Complicated	Easier and Straight forward



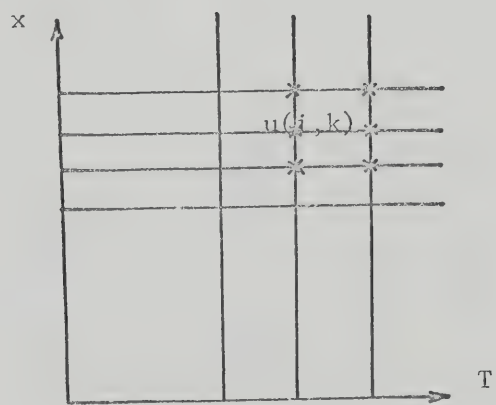
Space Time Mesh



Explicit Scheme



Implicit Scheme



Crank-Nicholson Scheme

FIG. 4.1 FINITE DIFFERENCE SCHEMES

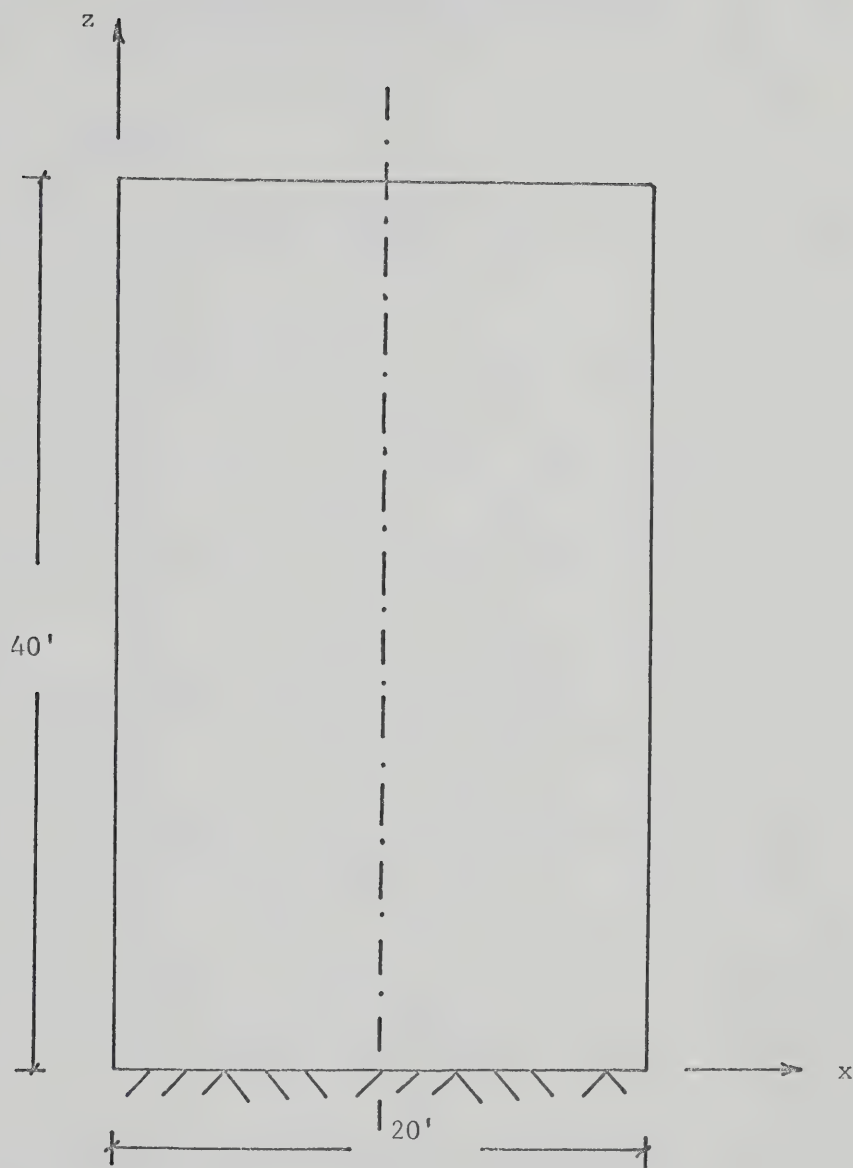


FIG. 4.2 SOIL SAMPLE USED FOR COMPARISON OF
ADI AND BARAKAT AND CLARK METHODS

CHAPTER V

TWO-DIMENSIONAL CONSOLIDATION

A. GENERAL

When a soil consolidates under an applied load drainage and compression frequently take place in three dimensions (as opposed to the assumption of one-dimensional drainage and compression in the classical theory of one-dimensional consolidation due to Terzaghi). The present state of knowledge of the compression characteristics of soil in three dimensions, however, is meagre; and the displacement of principal importance in structural applications is the vertical compression. With due recognition of this fact, the effect of compression in directions other than the vertical may often be neglected. However, the process of drainage of water in three dimensions does have a considerable effect on the rate of settlement of a soil loaded at the surface.

The actual rates at which foundations on clay settle (published evidence) are generally faster than those predicted by the one-dimensional Terzaghi consolidation theory. In some instances the differences are very large. In many practical cases, it is obvious that the geometric conditions are far from being one-dimensional and that horizontal dissipation of pore pressure (not accounted for in the classical theory) must make the actual rate of settlement (i.e., rate

of dissipation of pore pressure) more rapid. Rowe (1968) has demonstrated that the real drainage behavior (and hence the pore pressure dissipation) of a deposit as a whole depends on the geological details of its formation. Veins of silt along fissures, or organic inclusions can affect the permeability of the mass to a large extent and hence the drainage characteristics.

5.A.1 TERZAGHI - RENDULIC - TWO-DIMENSIONAL THEORY

The simple consolidation theory generally attributed to Terzaghi (1925) and Rendulic (1937) considers the three-dimensional diffusion of water through a porous medium. For an isotropic soil in which water flows in all three coordinate directions, such a consideration leads to a single equation 2.12 which is reproduced as

$$c \nabla^2 u = \frac{\partial u}{\partial t} \quad 5.1$$

Equation 5.1 is a half-way solution between the classical one-dimensional theory and a true three-dimensional theory. This equation retains all the characteristics of one-dimensional theory and is based exactly on the same assumptions, except that it is more complex than the classical one-dimensional theory. Equation 5.1 provides a means for dissipation of excess pore pressure in all directions

though the compression is restricted only to the vertical direction.

Under plane strain conditions, equation 5.1 reduces to equation 2.14 which is

$$c\left(\frac{\partial^2 u}{\partial x^2} + \frac{\partial^2 u}{\partial z^2}\right) = \frac{\partial u}{\partial t} \quad 5.2$$

This equation has all the characteristics of the classical one-dimensional theory and yet provides a means for accounting the dissipation of excess pore pressure in the horizontal direction.

Though equation 5.2 is more complex than the one-dimensional consolidation equation 2.15 and less complex than equation 5.1, it has not lost its versatility and may be put to use for all types of problems solved using classical one-dimensional theory. Equation 5.2 is called the Terzaghi equation for consolidation in two dimensions. The solution of this equation for given boundary and initial conditions is presented in a subsequent section.

5.A.2 EXTENSION OF DAVIS - RAYMOND THEORY TO TWO DIMENSIONS

Davis and Raymond (1965) proposed a modification to the classical Terzaghi theory for overcoming the inaccuracies of the following assumptions:

- (a) the coefficient of permeability k is a constant during consolidation under a given stress increment; and
- (b) the coefficient of compressibility m_v is also a constant during consolidation under a given stress increment.

For a normally consolidated clay, Davis and Raymond have pointed out that, during a stress increment the coefficient of consolidation c_v is usually observed to change much less than the coefficient of compressibility. They assumed c_v to be a constant, i.e.,

$$c_v = \frac{k}{\gamma_w m_v} = \text{constant.} \quad 5.3a$$

This is seen to be equivalent to assuming that, as the soil particles move closer together, the decrease in coefficient of permeability k is proportional to the decrease in volume compressibility m_v .

Further, instead of assuming that a_v is a constant, they adopted an empirical relationship between the void ratio e and the effective stress σ' as

$$e = e_0 - c_c \log_{10}(\theta'_1/\theta'_0) \quad 5.3b$$

where $\theta'_0 = (\sigma'_{x0} + \sigma'_{y0} + \sigma'_{z0})/3$

so that m_v is given by

$$m_v = A/\theta_1' \quad 5.3c$$

where A is a constant which depends on the initial void ratio e_0 and the compressibility index c_c .

With these modifications, Davis and Raymond (op. cit.) have developed a nonlinear theory of one-dimensional consolidation. In the following section a three-dimensional theory is developed on the basis of the Terzaghi-Rendulic assumption with the modifications suggested by Davis and Raymond (op. cit.). The development is exactly on the lines adopted by Davis and Raymond (op. cit.).

The coefficient of compressibility m_v is given by

$$m_v = - \frac{1}{1+e} \frac{\partial e}{\partial \theta_1'} \quad 5.4a$$

where

$$\theta_1' = \frac{\sigma_{xx}' + \sigma_{yy}' + \sigma_{zz}'}{3} \quad 5.4b$$

since all round compression is considered.

Substituting equation 5.3b in equation 5.4a yields

$$m_v = \frac{0.434 c_c}{(1+e)\theta_1'} = \frac{A}{\theta_1'} \quad 5.5a$$

where

$$A = \frac{0.434 c_c}{(1+e)} \quad 5.5b$$

In the equation 5.5b the term $(1+e)$ is assumed constant. Thus the change in void ratio e is considered too small to affect the total volume $(1+e)$.

Darcy's law is assumed to be applicable and hence in general

$$v_x = -k_x i_x = -\frac{k_x}{\gamma_w} \frac{\partial u}{\partial x} \quad 5.6$$

where v_x denotes the velocity of flow in the x-direction

k_x denotes the coefficient of permeability in the x-direction

i_x denotes the hydraulic gradient in the x-direction

u denotes the excess pore pressure

and γ_w denotes the unit weight of water.

Substituting equation 5.3a in equation 5.6 and differentiating the resulting equation with respect to x yields

$$\frac{\partial v_x}{\partial x} = -\frac{\partial}{\partial x} (c_v m_v \frac{\partial u}{\partial x}) \quad 5.7a$$

Similar expressions such as 5.7a can be written in the y- and z-directions. They are

$$\frac{\partial v_y}{\partial y} = - \frac{\partial}{\partial y} (c_v m_v \frac{\partial u}{\partial y}) \quad 5.7b$$

and

$$\frac{\partial v_z}{\partial z} = - \frac{\partial}{\partial z} (c_v m_v \frac{\partial u}{\partial z}) \quad 5.7c$$

The soil is assumed to be completely saturated and the pore water and soil particles are incompressible relative to the soil skeleton. Therefore the effective stress at any point may be written as

$$\sigma'_{xx} + \sigma'_{yy} + \sigma'_{zz} = \sigma_{xx} + \sigma_{yy} + \sigma_{zz} - 3u$$

The vertical strain developed in the soil skeleton is ϵ which may be expressed as

$$\epsilon = \frac{(e_0 - e)}{(1 + e)} \quad 5.8a$$

where e_0 denotes the void ratio corresponding to zero strain and effective stress σ_0 .

Using equation 5.3b, the above equation may be written as

$$\epsilon = \frac{c_c}{(1 + e_0)} \log_{10} \left(\frac{\sigma'_1}{\sigma'_0} \right) \quad 5.8b$$

Differentiating equation 5.8b with respect to time and making use of equation 5.5a yields

$$\frac{\partial \varepsilon}{\partial t} = \frac{A}{\theta_1'} \frac{\partial \theta_1'}{\partial t} \quad 5.8c$$

The equation of continuity of flow demands that the rate of water lost through an element $dx dy dz$ should equal the rate of volume decrease within that element. Therefore,

$$\left(\frac{\partial v_x}{\partial x} + \frac{\partial v_y}{\partial y} + \frac{\partial v_z}{\partial z} \right) dx dy dz = \frac{\partial \varepsilon}{\partial t} dx dy dz$$

Making use of equations 5.7 and 5.8c, the above equation may be reduced to

$$\begin{aligned} - c_v \left\{ \frac{1}{\theta_1'} \nabla^2 u - \frac{1}{3} \left(\frac{1}{\theta_1'} \right)^2 \left[\frac{\partial \sigma_{zz}'}{\partial z} \cdot \frac{\partial u}{\partial z} + \frac{\partial \sigma_{yy}'}{\partial y} \cdot \frac{\partial u}{\partial y} + \frac{\partial \sigma_{xx}'}{\partial x} \cdot \frac{\partial u}{\partial x} \right] \right\} \\ = \frac{1}{\theta_1'} \frac{\partial \theta_1'}{\partial t} \end{aligned} \quad 5.9$$

where

$$\nabla^2 = \frac{\partial^2}{\partial x^2} + \frac{\partial^2}{\partial y^2} + \frac{\partial^2}{\partial z^2}$$

Equation 5.9 is the general three-dimensional consolidation equation for the assumptions made in Davis and

Raymond theory. As in their original theory, no assumptions have been made as to the type or rate of loading.

Special Cases

CASE 1

To derive the form of the original Davis-Raymond one-dimensional theory, we may put $\frac{\partial^2 u}{\partial x^2} = 0 = \frac{\partial^2 u}{\partial y^2}$, for the flow in the x- and y-directions is assumed to be absent (and hence $\frac{\partial u}{\partial x} = 0 = \frac{\partial u}{\partial y}$). Then the equation 5.9b reduces to

$$-c_v \left\{ \frac{1}{\sigma_{zz}'} \frac{\partial^2 u}{\partial z^2} - \left(\frac{1}{\sigma_{zz}'} \right)^2 \frac{\partial \sigma_{zz}'}{\partial z} \frac{\partial u}{\partial z} \right\} = \frac{1}{\sigma_{zz}'} \frac{\partial \sigma_{zz}'}{\partial t}$$

which is same as given by Davis and Raymond (1965).

CASE 2 CONSTANT LOAD

Let the applied load be constant with depth and as well with time (as in case of oedometer or thin clay deposits when load is maintained the same). Hence $(\sigma_{xx} + \sigma_{yy} + \sigma_{zz})$ is constant in the following term

$$\sigma_{xx}' + \sigma_{yy}' + \sigma_{zz}' = \sigma_{xx} + \sigma_{yy} + \sigma_{zz} - 3u$$

which on differentiation yields

$$\frac{\partial \sigma'_{xx}}{\partial x} = -3 \frac{\partial u}{\partial x}, \quad \frac{\partial \sigma'_{yy}}{\partial y} = -3 \frac{\partial u}{\partial y} \quad \text{and} \quad \frac{\partial \sigma'_{zz}}{\partial z} = -3 \frac{\partial u}{\partial z} \quad 5.10$$

Substituting 5.10 in equation 5.9 yields

$$-c_v \left\{ \frac{1}{\theta'_1} \nabla^2 u + \left(\frac{1}{\theta'_1} \right)^2 \left[\left(\frac{\partial u}{\partial x} \right)^2 + \left(\frac{\partial u}{\partial y} \right)^2 + \left(\frac{\partial u}{\partial z} \right)^2 \right] \right\} = \frac{1}{\theta'_1} \frac{\partial \theta'_1}{\partial t} \quad 5.11$$

which is the governing equation for a normally consolidated soil under a constant-load.

For the plane strain case (the strain in the y -direction may be assumed zero), equation 5.11 becomes

$$\begin{aligned} -c_v \left\{ \frac{1}{\theta'_1} \left(\frac{\partial^2 u}{\partial x^2} + \frac{\partial^2 u}{\partial z^2} \right) + \left(\frac{1}{\theta'_1} \right)^2 \left[\left(\frac{\partial u}{\partial x} \right)^2 + \left(\frac{\partial u}{\partial z} \right)^2 \right] \right\} \\ = \frac{1}{\theta'_1} \frac{\partial \theta'_1}{\partial t} \end{aligned} \quad 5.12$$

A solution to the equation 5.11 or 5.12 will be unique depending on the specified boundary and initial conditions.

Using the substitution:

$$W = \log_{10} \frac{\theta'_1}{\theta'_f} \quad 5.13a$$

$$\text{where} \quad \theta'_f = (\sigma'_{xf} + \sigma'_{yf} + \sigma'_{zf})/3 \quad 5.13b$$

and f denotes final stress

Also
$$\sigma_{xx}' = \sigma_{xf}' - u \quad 5.13c$$

$$\sigma_{yy}' = \sigma_{yf}' - u \quad 5.13d$$

and
$$\sigma_{zz}' = \sigma_{zf}' - u \quad 5.13e$$

Adding 5.13c, 5.13d and 5.13e yields

$$\sigma_{xx}' + \sigma_{yy}' + \sigma_{zz}' = \sigma_{xf}' + \sigma_{yf}' + \sigma_{zf}' - 3u$$

or
$$\theta_l' = \theta_f' - u \quad 5.13f$$

Using equation 5.13f, equation 5.13a may be expressed as

$$w = \log_{10} \frac{\theta_f' - u}{\theta_f'}$$

Substituting this expression in equation 5.11, yields

$$c_v \nabla^2 w = \frac{\partial w}{\partial t} \quad 5.14$$

which when expressed in two dimensions is

$$c_v \left(\frac{\partial^2 w}{\partial x^2} + \frac{\partial^2 w}{\partial z^2} \right) = \frac{\partial w}{\partial t}$$

The above equation is identical in form to that of the Terzaghi two-dimensional equation (5.2) and can be solved using the ADI method described in Chapter IV.

5.A.3 SOLUTION OF THE TWO-DIMENSIONAL EQUATION

Equation 5.2 may be solved by any of the following means:

- (a) closed form (analytical) method
- (b) electric analogue method, and
- (c) numerical analysis method.

The solution obtained depends primarily on the boundary conditions specified.

Rigorous analytical solutions obtained for one-dimensional classical theory (equation 2.15) may be extended to this equation. Equation 5.2 is identical with the differential equation of heat flow (Carslaw and Jaeger, 1959). If u is interpreted as temperature and c as the diffusivity constant, the solutions of the equation of heat conduction can be utilized in the theory of consolidation. Several solutions of heat conduction problems have in fact provided immediate answers to problems in consolidation.

Carillo (1942) has demonstrated how the familiar one-dimensional solutions of the differential equation of consoli-

dation (of the analogous heat flow) can easily be combined to furnish simple solutions for several important two- and three-dimensional problems. In finding the solution for equation 5.2, Carillo (op. cit.) made use of the following theorem:

'If $u_1 = f_1(x,t)$ is a solution of the linear flow equation

$$c \frac{\partial^2 u}{\partial x^2} = \frac{\partial u}{\partial t}$$

and $u_2 = f_2(y,t)$ is a solution of linear flow equation

$$c \frac{\partial^2 u}{\partial y^2} = \frac{\partial u}{\partial t}$$

then $u = u_1 u_2$ is necessarily a solution of the two-dimensional flow equation

$$c \left(\frac{\partial^2 u}{\partial x^2} + \frac{\partial^2 u}{\partial y^2} \right) = \frac{\partial u}{\partial t} ,$$

A variety of other analytical techniques such as integral transforms, Green's functions may be used to obtain desired results. Integral transformation offers, in principle, a means for the solution of the equation 5.2. However, the mere computation of a set of results presents considerable algebraic and arithmetical problems (Abbott, 1960).

Another technique that may be employed to obtain numerical results for the equation 5.2 is the analogue technique. Bernell and Nilsson (1957) have described an electric analogue method to solve the equation 5.2. However, it will be shown that the results furnished (Bernell, 1958) are incorrect in section 5.A.5.

An alternative to analytical and analogue methods just described is numerical analysis (Gibson and Lumb, 1953). By this the process of integrating the differential equations is reduced to solving a series of simultaneous algebraic equations. The Alternating Direction Implicit method (ADI, as described in Chapter IV) can be made use of for the advantages cited herein.

5.A.4 COMPARISON OF NUMERICAL SOLUTION WITH CLOSED FORM SOLUTION

For a chosen rectangular soil mass and prescribed boundary and initial conditions, equation 5.2 was solved both analytically and by the ADI method.

For the analytical technique the solution (Art. 2-8, p. 84, Özisik, 1968) for a finite rectangle (Figure 5.1) is made use of. For the boundary conditions of the third kind specified therein, the solution for equation 5.2 in the region $0 \leq x \leq a$, $0 \leq z \leq b$, $t > 0$ is

$$u(x, z, t) = \sum_{m=1}^{\infty} \sum_{n=1}^{\infty} e^{-c(\beta_m^2 + v_n^2)t} K(\beta_m, x) K(v_n, z) \left\{ \bar{F}(\beta_m, v_n) + \int_{t'=0}^t e^{c(\beta_m^2 + v_n^2)t'} A(\beta_m, v_n, t') dt' \right\} \quad 5.15$$

where

$$\begin{aligned} A(\beta_m, v_n, t') = & c \left\{ \frac{K(\beta_m, x)}{k_1} \Big|_{x=0} \int_{z'=0}^b K(v_n, z') f_1(z', t') dz' \right. \\ & + \frac{K(\beta_m, x)}{k_2} \Big|_{x=a} \int_{z'=0}^b K(v_n, z') f_2(z', t') dz' \\ & + \frac{K(v_n, z)}{k_3} \Big|_{z=0} \int_{x'=0}^a K(\beta_m, x') f_3(x', t') dx' \\ & \left. + \frac{K(v_n, z)}{k_4} \Big|_{z=b} \int_{x'=0}^a K(\beta_m, x') f_4(x', t') dx' \right\} \end{aligned}$$

and

$$\bar{F}(\beta_m, v_n) = \int_{x'=0}^a \int_{z'=0}^b k(\beta_m, x') K(v_n, z') F(x', z') dx' dz'$$

where summation is taken over all eigenvalues β_m and v_n . The kernels $K(\beta_m, x)$ and $K(v_n, z)$ and the corresponding eigenvalues

β_m and v_n are obtained from Table 2.1, pp. 50-51, cf. (Özsisik, 1968) for various combinations of boundary conditions.

Figure 5.2 represents a rectangular section with the boundary conditions specified thereon. For these conditions equation 5.15 reduces to

$$u(x,z,t) = \sum_{m=1}^{\infty} \sum_{n=1}^{\infty} e^{c\left(\frac{m^2\pi^2}{a^2} + \frac{n^2\pi^2}{b^2}\right)t} \frac{4U_0}{mn\pi^2} \sin(\beta_m x) \sin(v_n z) \cos(m\pi-1) \cos(n\pi-1) \quad 5.16$$

Equation 5.16 yields the excess pore pressure u at a point (x,z) at a given time t , provided the value U_0 , the excess pore pressure at initial time ($t=0$) is specified. Equation 5.16 has been made use of to calculate the values of excess pore pressure at points $(a/2, b/2)$ and $(a/2, 3b/4)$ for rectangular sections of height to width ratio of 1.5 and 2.4. The values are plotted in Figure 5.3.

Equation 5.2 has also been solved by numerical analysis using ADI method for the boundary conditions specified in Figure 5.2. The initial condition is the same as that used for the analytical solution. Results have been obtained for the same points K and P (Figure 5.3). The results obtained by both techniques are in very close agreement with each other as is evident from Tables 5.1 and 5.2. Thus either of the methods, analytical or numerical, may be employed in

the solution of equation 5.2.

The analytical method yields a rigorous and complete solution, while the numerical method only approximates, to a large degree, the actual values. But then the analytical method is limited in its versatility, because of the considerable algebraic and arithmetical complexities which arise. On the other hand, the numerical method is applicable to all sorts of problems and can theoretically handle any number of variations in the parameters of the continuum, limited only by the capacity of the computer which is used. Also with the advances in computer science the numerical solutions are obtained at a faster and cheaper rate. Thus the numerical technique has a decided advantage over the analytical (closed form) method. This clearly demonstrates the reliability of the numerical technique that can be employed in the solution of such equations as 5.2.

5.A.5 COMPARISON WITH BERNELL'S VALUES

Equation 5.2 was also solved using an electric analogue method described by Bernell and Nilsson (1957). Bernell (1958) made use of an idealized dam cross-section (Figure 5.4) and developed a series of pore pressure time curves. By these results, Bernell (op. cit.) demonstrated the dissipation of initial construction pore pressures as a function of the slope of the core of the dam. The idealized dam had an impervious core with varying side slopes. The core was

surrounded by a pervious fill with side slopes of 1 on 2. The dam was founded on an impermeable base and had a height of 20 meters with a crest width of 4 meters. The coefficient of consolidation of the core material was assumed equal to $0.1 \text{ cm}^2/\text{sec}$. The core was assigned side slopes of 10 on 1, 5 on 1, 2 on 1, and 1 on 2. Two cases were considered:

- (a) the dam half completed, i.e., a fill height of 10 meters, and
- (b) the dam raised to the full height of 20 meters.

The initial pore pressure was assumed equal to 100 per cent, which is often the condition experienced with the wet fill technique of dam construction (especially in Sweden). The effect of core thickness is easily discernible (Figure 5.5).

The same hypothetical dam with the prescribed boundary and initial conditions was considered for solution by the ADI numerical technique. Both the cases (a) and (b) mentioned in the previous paragraph were solved and the pore pressure-time curves were drawn for the same assumptions of material properties. As is evident from Figure 5.5, the respective pore pressure time curves do not have any agreement at all. Bernell's curves are flat and are almost straight on a semi-logarithmic plot. This is never the case in practice. In almost all cases, the dissipation of pore pressure is rapid at the initial stages because of the development of enormously high hydraulic gradients. As dissipation continues, the value of the hydraulic gradient decreases,

and hence the rate of pore pressure dissipation decreases and ultimately when the excess pore pressures are very small the rate of dissipation also will be small, or in other words, the time taken will be large. Thus the shape for pore pressure-time plots anticipated are of inverted S-type, the familiar consolidation curves. Such S-type plots have been obtained by the numerical technique employed.

The Bernell's curves are almost straight lines and depict that the hydraulic gradient is almost constant throughout the dissipation of excess hydrostatic pressure over the days. This indicates that at earlier stages Bernell's curves yield a lower excess pore pressure than those which actually exist in the dam while at later stages the pore pressure excess values are higher. This is particularly true when the full height of 20 meters is built up (Figure 5.5b). Thus the greater the height of the dam, larger will be the error involved in the Bernell's values. This is amplified all the more in the case of thick cores (side slopes 5 on 1, or more) for shorter times and for longer times in case of thinner cores. Thus, the pore pressure time curves obtained by Bernell through electric analogue method are misleading and yield erroneous results.

The ADI method used has been tested for its reliability in the previous section. And as such the results obtained are trustworthy. At this stage it may be pointed that this technique is versatile and can handle any set of geometric configurations and boundary conditions. Also it

is capable of handling any type of initial excess pore pressure distribution in the soil mass. It may be mentioned, further, that the algorithm developed can handle any non-homogeneity within the soil mass and also any arbitrary soil behavior with time. That is to say any variation in the coefficient of consolidation c_v (to mention only one soil property) with space and/or time can very easily be handled by the program. This ADI technique is the basis for all the numerical work discussed in the following sections and chapters dealing with two-dimensional problems.

B. IMPEDED DRAINAGE

5.B.1 INTRODUCTION

Embankments of granular or noncohesive materials are more stable than those made of cohesive soils because granular materials have a higher frictional resistance and because their greater permeability permits rapid dissipation of pore water pressures. Embankments of homogeneous materials of relatively low permeability generally have flat slopes. Zoned embankments, which have free-draining outer zones supporting inner zones of relatively impervious materials, are made use of where

- (a) homogeneous materials are not available in large measure;
- (b) sufficient pervious material is available; and
- (c) the section of the dam cannot be made too large because of cost considerations.

The two principal requirements for a satisfactory free-draining outer zone are that it must be more pervious than the protected soil in order to act as a drain and that it must be fine enough to prevent particles of the protected soil from washing into its voids. Where the difference in coarseness between the fine and coarse embankment zones is too great to meet filter criteria, zones of intermediate gradation must be provided. These are constructed of sands and gravels with special gradation characteristics and are called filters.

The purpose of a filter is to provide an easy path for the excess water to flow as it is squeezed out of a soil layer during consolidation and during steady seepage. Thus an effective filter will accelerate the process of consolidation. In practice, however, such installations of filters have met with varied success. Two case histories will be cited in support of this statement.

Valajoskoski Dam (Arhippainen, 1964) is a composite earthfill section with a central rolled earthfill of glacial moraine surrounded by transition zones of graded filter material and supported by pervious earthfill zones. It has been observed that the pore water pressures measured in central morainic fill and the outer pervious earthfill are comparable in magnitude.

Nanak Sagar Dam (Gupta and Sharma, 1964) is a symmetrical rolled fill zoned section constructed with silty clay material in the core and sandy material with traces of fines in the outer casing. Here again the measured pore water pressures long after the construction has been completed in the core and the outer shell are of comparable magnitude.

These two field examples clearly indicate the inadequacy of the performance of some outer shells as efficient filters.

To evaluate pore water pressures in the core of a zoned embankment after it has been constructed, generally it is believed that the filter zones act with full efficiency. This implies that the pore fluid at the interface of the

core and outer shells remains at atmospheric pressure, although for this to be strictly true the filter should be infinitely pervious. In other words, the degree of dissipation of pore pressure at any given time depends on the relative permeabilities and dimensions of the core and the filter zones in contact with it. This problem of retarded consolidation is similar mathematically to the heat conduction problem of a slab initially at a temperature, and cooling at its surfaces according to Newton's law of radiation. analogous to condition 5.19a (Carslaw and Jaeger, 1959).

The problem of retarded consolidation (or otherwise called as Impeded Drainage) is also experienced in laboratory testing. Impeded drainage in testing is concerned with the effects of porous stones and filter drains on the degree of dissipation. In an oedometer test, the effect of fine porous stone can affect the test results and the coefficients derived on the basis of test results. In a triaxial test, the effect of fine porous end caps and of filter drains with finite permeability can affect the coefficient, the shear strength, and the duration of testing in a drained test. Newland and Allely (1960) have investigated the effect of various types of filter disk and different specimen thickness on the observed time-settlement behaviour of undisturbed and remoulded specimens of Whangamarino clay. Their results not only emphasize the importance of adequate permeability but also suggest that overall disk permeability alone may be an insufficient criterion, and that special precautions may be necessary to

avoid

- (a) the formation of a thin boundary layer of the disk becoming clogged with clay, and
- (b) the head drop at the specimen-disk interface due to convergence of flow into the pores of the disk.

Schiffman (unpublished work) recommends the following to have effective drainage in oedometer and triaxial tests:

- (i) for soft clays: coarse stones with filter paper,
- (ii) for stiff clays: fine stones to avoid clogging and make necessary corrections thereafter.

Bishop and Gibson (1963) considered the effects of disk permeability on the progress of one-dimensional consolidation of a clay layer, assuming that the clay is fully saturated and behaves in accordance with the simplifying assumptions adopted by Terzaghi.

In many cases, the field evidence shows that the drainage is far from being one-dimensional. For example, Gibson (1958) while comparing the calculated and observed pore pressures for Usk Dam remarked that towards the end of construction the lateral flow of pore water became important in spite of the fact that all the internal drainage provided is by horizontal filters at various levels. In this chapter, the dissipation is considered to be two-dimensional and an assessment of the influence of impedance of actual drains on dissipation is made.

5.B.2 ANALYSIS AND TECHNIQUE OF SOLUTION

Consider the general problem of two-dimensional (horizontal and vertical) drainage. The pore pressure dissipation is governed by equation 5.2 which is

$$c \left(\frac{\partial^2 u}{\partial x^2} + \frac{\partial^2 u}{\partial z^2} \right) = \frac{\partial u}{\partial t} \quad 5.2$$

and the pore pressure is defined in the region $0 \leq x \leq 2H$ and $0 \leq z \leq L$. The general boundary conditions are,

$$A_1 \frac{\partial u}{\partial z} (x, 0, t) + B_1 u(x, 0, t) = 0$$

$$A_2 \frac{\partial u}{\partial z} (x, L, t) + B_2 u(x, L, t) = 0$$

$$A_3 \frac{\partial u}{\partial x} (0, z, t) + B_3 u(0, z, t) = 0$$

$$A_4 \frac{\partial u}{\partial x} (2H, z, t) + B_4 u(2H, z, t) = 0$$

These boundary conditions can be

free draining, if $A_i = 0$

impervious, if $B_i = 0$

impeded, as they are.

The equation 5.2 yields the progress of consolidation in two dimensions of a clay layer, assuming that the clay is fully saturated and behaves in accordance with the simplifying assumptions due to Terzaghi. Equation 5.2 may be solved for a given set of boundary conditions either analytically (Carillo, 1942) or by numerical methods (ADI).

As mentioned earlier, the filters are usually not fully effective. To assess the effectiveness of a filter, consider a rectangular section with vertical side drains of the same thickness on either side (Figure 5.6a). The height to breadth ratio of the section may be varied.

The rectangular (core) section of the clay is of height L and width $2H$; the drain on each side is of height L and thickness d . The base of the section is assumed impervious. The core has a permeability k_1 and its coefficient of two-dimensional consolidation is c_v . The drain material is assumed to be ideally non-consolidating, i.e., the drain material is an incompressible layer. In addition, it is assumed to be fully saturated. As the drain material is incompressible, its two-dimensional compressibility may be taken as equal to zero; therefore, its coefficient of two-dimensional consolidation is infinite.

The clay is assumed to have uniform excess pore pressure due to suddenly applied load at time $t = 0$, and thereafter the excess pore pressure $u(x,z,t)$ in the clay layer is governed by the equation 5.2. The initial condition ($t = 0$) is $u(x,z,0) = \Delta\sigma$, a constant within the entire clay region.

Only half the section (Figure 5.6b) need be considered for analysis, because of symmetry. The boundary conditions for the clay layer then, at any instant $t > 0$, are

$$\frac{\partial u}{\partial x} = 0 \quad \text{at} \quad z = 0 \quad 5.17a$$

$$u = 0 \quad \text{at} \quad z = L \quad 5.17b$$

and
$$\frac{\partial u}{\partial z} = 0 \quad \text{at} \quad x = 0. \quad 5.17c$$

The boundary condition at the internal boundary ($x = H$) between the two materials is to be determined.

The equation governing the dissipation of excess pore pressure in the drain material is

$$\frac{\partial^2 u_1}{\partial x^2} + \frac{\partial^2 u_1}{\partial y^2} = 0 \quad 5.18$$

since $c_v = \infty$.^{*} Equation 5.18 is the Laplacian equation for steady state condition of flow of water through the drain material.

If the drain is efficient, it is evident that the con-

* $c_v = \infty$ since the drain material is assumed incompressible. The assumption of incompressibility leads to the condition that the hydraulic gradient in the drain thickness is linear with hydrostatic pressure equalling atmosphere at the outer boundary of drain.

solidation of the compressible core material will take place as a result of the flow of the pore water from the core into the drains in the horizontal direction; depending on the ratio of the height to the breadth of the core some pore water will get dissipated from the top since the base is assumed completely impervious .

From Figure 5.6b, it is seen that there exists an interface between the two materials A and B. At this internal boundary the conditions to be satisfied are:

- (a) continuity of flow be maintained; and
- (b) the pore pressure be the same between the core and the drain.

Water squeezed out from the consolidating material (core), in the horizontal direction, enters the drain through the interface. Thus to maintain full continuity at the interface the amount of water expelled from the core material should equal the amount of water entering the drain. In other words, the velocities of flow in both the materials should be same on either side of the interface. Therefore,

$$k_1 \frac{\partial u}{\partial x} (H, z, t) = k_2 \frac{\partial u_1}{\partial x} (H, z, t) \quad 5.19a$$

where k_1 and k_2 respectively are the permeabilities of consolidating core material A and drain material B.

$$\frac{\partial u_1}{\partial x} (H, z, t) = \frac{u_1(H, z, t)}{d} \quad 5.19b$$

In deriving equation 5.18, the material B is assumed to be incompressible and also that the excess water pressure is zero at the outer boundary ($x = H+d$) of the drain.

When consolidation takes place in the vertical direction, the water (of dissipation) travels in that direction. As such the water expelled during this dissipation does not enter the drain; hence during vertical dissipation the condition of continuity of flow (at the interface) need not be considered.

The value of the pore pressure shall be the same at the interface ($x = H$). This is accomplished by choosing a single value at the internal boundary, for horizontal dissipation, for both the materials, i.e., $u(H,z,t) = u_1(H,z,t)$ and then satisfying the equation 5.17. Thus

$$k_1 \frac{\partial u}{\partial x} (H,z,t) = k_2 \frac{u(H,z,t)}{d} \quad 5.19c$$

for horizontal dissipation.

During vertical dissipation, it is assumed that the value of pore pressure at the interface remains at the same value as that obtained during previous horizontal dissipation. This is justified by the fact that the equation 5.16 governing the flow of water in the drain is in a steady state condition. Also, during vertical dissipation water squeezed out of the consolidating material does not enter the drain and hence does in no way disturb the equilibrium attained

during and after horizontal dissipation. Thus this condition helps in determining the value of pore pressure at the interface as,

$$u(H,z,t)_H = u(H,z,t + \Delta t)_V \quad 5.19d$$

for vertical dissipation, where

$u(H,z,t)_H$ is the pore pressure value at time t during horizontal dissipation; and $u(H,z,t + \Delta t)_V$ is the pore pressure value at time $t + \Delta t$ during vertical dissipation.

Thus equations 5.19 yield the boundary condition at the interface ($x = H$) between the two materials. Equation 5.2 may now be solved for the boundary conditions given by equations 5.17a, 5.17b, 5.17c, and 5.19c (for 5.19d) together with the prescribed initial condition.

The solution to equation 5.2 for the conditions mentioned above may be obtained by numerical methods using ADI. Equation 5.2 may be expressed in a dimensionless form as

$$\frac{\partial^2 u}{\partial X^2} + \frac{\partial^2 u}{\partial Z^2} = \frac{\partial u}{\partial T} \quad 5.20$$

where $X = \frac{x}{H}$, $Y = \frac{y}{H}$ and $T = \frac{c_v t}{H^2}$

Equation 5.20 may be expressed in finite difference form for any general nodal point of the finite difference

mesh. During the operation by ADI, the dissipation is allowed to take place in either direction at each time step alternatively. An impermeable boundary, signifying no flow across the boundary, is denoted by $\frac{\partial u}{\partial x}$ (or $\frac{\partial u}{\partial z}$) = 0. To maintain a truncation error of $O(\Delta x)^2$ or $O(\Delta z)^2$, fictitious points are introduced in the grid system and the impermeable boundary condition (at $i = 1$) is satisfied by setting

$$u(1, j, t) = u(-1, j, t)$$

Permeable boundaries (at $i = I$) are represented by setting

$$u(I, j, t) = 0$$

The boundary condition given by the equation 5.19c may be expressed in finite difference form as

$$(u(I-1, z, t) - u(I, z, t))/\Delta x = ((k_2/k_1) u(I, z, t))/d$$

$$\text{or } (u(I-1, z, t) - u(I, z, t)) = (k_2/k_1) (H/d) \Delta x u(I, z, t)$$

$$\text{i.e., } u(I, z, t) = (1/(1+\lambda \Delta x)) u(I-1, z, t) \quad 5.21$$

where $\lambda = (k_2/k_1) (H/d)$, is called the impedance factor.

Hence knowing the value of excess pore pressure $u(I-1, z, t)$ at the nodal point just previous to the interface, the value

of excess pore pressure $u(I, z, t)$ at the interface can be determined. Thus the interface condition is satisfied.

The impedance factor λ , involves the ratio of the permeabilities of the two materials A and B, and also the ratio of the relative lengths of flow of water in both the materials. Thus λ may be said to be a true indicator of the effectiveness of the filter drain. The greater the value of λ : either the permeability of the drain material is large compared to that of clay material or the thickness of the drain is very small compared to the half width of the compressible clay layer. In either case the drain is quite efficient. And in the case $\lambda \rightarrow \infty$, the pore pressure excess at the interface is zero, the drain is termed perfectly efficient. The smaller the value of λ : either the relative permeability is low (i.e., the drain permeability is comparable to that of the core material) or the length of the seepage path in the drain material is quite large compared to half width of the consolidating material; and for such small values of λ the drain is impeding and it is not fully efficient. The major effect of the impedance to drainage is on the excess pore pressure dissipation. Impeded drainage retards the dissipation of excess pore pressures, which may be detrimental to the safety of the embankment and extend the duration of settlement.

5.B.3 RESULTS AND DISCUSSION

In this study, the common case considered is a rectangular section of height L and width $2H$ provided with side drains of thickness d each on either side. The entire section is founded on an impermeable base. The drains are considered to be fully effective (i.e., the impedance factor $\lambda \rightarrow \infty$) to fully impeded (i.e., $\lambda \rightarrow 0$). The impedance factor λ is varied over a wide range of values differing mainly by an order of magnitude, e.g., 0.0, 0.01, 0.1, 1.0, 10.0 and ∞ for given rectangular sections. The cases considered are for various values of height/width ratio of the consolidating layer; e.g., 5.0, 2.0, 1.0, 0.5, and 0.25. The results are presented in Figures 5.8 to 5.14. The average degree of consolidation is calculated for the x - z plane at each time step. This is accomplished by first integrating the values of pore pressure along one axis (say z -axis) and obtaining ordinates at nodal points along the other axis (x -axis). These values are then again integrated. Thus this double integration at any time step compared to the double integration over the entire plane at the initial time yields the average degree of consolidation at that time step. The integration in either direction is carried out making use of the Simpson's rule for the largest even number of consecutive complete subintervals in the range of integration; the remaining subintervals, if any, are evaluated according to the trapezoidal rule. This may be termed as the 'two-dimen-

sional integration'.

In one-dimensional consolidation problems, the dissipation is allowed to take place only in one direction along a chosen axis. At any time step the average degree of consolidation along that axis is calculated. This may be termed as 'one-dimensional integration'. But usually in plane strain cases, the pore pressure dissipation is in two directions. One way to calculate the average degree of consolidation in such cases is by two-dimensional integration. Another is to obtain the values of pore pressure (after two-dimensional dissipation) along a chosen axis and calculate the average degree of consolidation by one-dimensional integration. By the latter means the results could be compared with the published results of one-dimensional consolidation.

For a height to width ratio of 0.25 (Figure 5.8) the effect of λ , the impedance factor, is almost negligible. This is mainly because of one-dimensional drainage taking place in the vertical direction and the impedance at the sides does not have any influence on the rate (or amount) of dissipation. Also because of the small height, there are relatively high rates of drainage occurring in the early stages of the process of consolidation. To fully ascertain the effect of impedance, the drainage is allowed to take place in two dimensions (horizontal and vertical) while the average degree of consolidation is calculated

- (a) only along a vertical section passing through the center line; and

- (b) for the entire region by two-dimensional integration.

Figure 5.9 shows that λ does not have any effect on the average degree of consolidation calculated at the center line by one-dimensional integration. It is obvious from Figure 5.8 that the effect of λ on the average degree of consolidation through two-dimensional integration is small.

Figure 5.10 gives the average degree of consolidation versus the time factor for a height to width ratio of 0.5. For this ratio of 0.5, the drainage may be considered two-dimensional - horizontal and vertical. The horizontal drainage is impeded because of the presence of an inefficient drain. In these curves, given by Figure 5.10, the effect of λ is clearly discernible. The smaller the value of λ , greater the impedance and consequently the smaller is the degree of dissipation. However, as the consolidation proceeds, the average degree of consolidation almost equals the same value irrespective of the value of λ at very large time factor. This is because, at very large values of time the hydraulic gradient is small; the dissipation is almost complete and hence the same value of the degree of consolidation is obtained.

A height to width ratio of 1.0 yields a family of curves (Figure 5.11) for the degree of consolidation against time factor. The rectangular section is square, and the drainage definitely is two-dimensional. As such it is expected that the impedance (due to the drain) to horizontal drainage does have a profound influence on the amount of con-

solidation. This is amply evident from Figure 5.11. For small values of λ , the rate of dissipation is very slow to start with compared to that for higher values of λ . Similar trends may be observed in the cases of height to width ratio of 2.0 and 5.0.

For a height to width ratio of 10.0, the dissipation may be expected to be mainly one-dimensional in the horizontal direction. To ascertain, if it is so, the drains are maintained effectively non-impeding ($\lambda \rightarrow \infty$) and the values of the average degree of consolidation (two-dimensional integration) are obtained for various values of time factor. These values are compared against the classical one-dimensional results for the same drainage conditions (Figure 5.14). The results agree very closely. Further to make sure that the dissipation is mainly one-dimensional, one-dimensional integration is carried out at the centre line in the horizontal direction and the average degree of consolidation is calculated. These values coincide with those of the classical one-dimensional theory (Figure 5.14). Since it is established that the dissipation is mostly one-dimensional, the effect of an impeded drain in the horizontal direction is very high (Figure 5.13).

From the Figures 5.8 to 5.14 it may be seen that a value of $\lambda = 0.0$ or a value of $\lambda = 0.01$ or for that matter a value of $\lambda = 0.1$ has the same effect on the average degree of consolidation. For all these values, the average degree of consolidation versus the time factor curves are almost

the same for any value of height to width ratio. This shows that for this range an order of variation in the relative permeabilities of the drain and the consolidating material does not have much influence on the degree of dissipation, i.e., they effectively impede the drainage to the same extent. Then again, there is a wide variation in the values of the average degree of consolidation for a value of $\lambda = 0.1$ to a value of $\lambda = 1.0$ to 10.0 . The values of the average degree of consolidation obtained for $\lambda = 10.0$ and those obtained for $\lambda \rightarrow \infty$ are almost identical, which again indicates that an order of variation in the relative permeabilities after a certain value, say $\lambda = 10.0$, in the increasing direction does not really add to the effectiveness of the filter drain. In other words, whether the drain is infinitely permeable or permeable to an extent such that $\lambda = 10.0$, the average degree of consolidation is not affected to any appreciable degree.

It is of interest to investigate the value of λ which obtain in some of the existing dam sections.

McNary Dam in Oregon, U.S.A. (Sherad et al., 1963) has a vertical core of total width 50 feet with vertical side drains 8 feet wide on either side. The central core is made up of fine silt while the side drains are built of sand and gravel. Terzaghi and Peck (1967, p. 55) quote the following values for the coefficient of permeability of the above materials:

k for fine silt $- 10^{-4}$ to 10^{-6} cm/sec.

k for sand and gravel mix $- 1$ to 10^{-3} cm/sec.

Taking average values of 10^{-5} cm/sec for fine silt and 10^{-2} cm/sec for sandy gravel mixture, a value for λ , the impedance factor is obtained.

$$\lambda = \frac{50/2}{8} \times \frac{10^{-2}}{10^{-5}} = 3.12 \times 10^3 = 3120$$

From the order of magnitude of λ calculated no impedance to drainage should exist and the side drain may be termed as an effective filter.

Nanak Sagar Dam (Gupta and Sharma, 1964) has a central core (trapezoidal section) of 20 meters at the base and is provided with casing (on either side) having a width of 24 meters. The values for the coefficient of permeability are given

$$k \text{ for core} = 2 \times 10^{-6} \text{ cm/sec}$$

$$k \text{ for casing} = 2 \times 10^{-5} \text{ cm/sec}$$

Therefore,
$$\lambda = \frac{20/2}{24} \times \frac{2 \times 10^{-5}}{2 \times 10^{-6}} = 4.17 .$$

From this value of λ , it may be inferred that the flow of the pore water in the horizontal direction is impeded. The

observations from the piezometers located in the casing indicate that the pore water pressure values in the casing are substantial and are of the order of 20% to 25% of the pore water pressures in the core. Thus this shows that the parameter λ correctly indicates the efficiency of the drain within practical limits.

Sherard et al. (1963) state that theoretically a filter can be very thin. However, from the practical standpoint, a minimum thickness exists depending on the filter material available and the method of construction adopted. Also the thickness is governed by the fact that there should exist no gaps or incorporation of segregated material. Horizontal layers can be as thin as possible because they can be easily placed. Minimum thickness for horizontal layers are about 6 inches for sand and 12 inches for gravel, although thicker layers are generally specified. For vertical or inclined filters, a minimum width of 8 feet to 10 feet is suggested for ease of construction while 12 feet to 15 feet is preferable.

Sherard et al. (op. cit.) have noted that the determination of a minimum thickness for the central core of an earth dam is not amenable to theoretical treatment. It is governed for practical purposes by the following factors:

- (a) the tolerable seepage loss;
- (b) the minimum width which will permit proper construction;
- (c) the type of material available for core and shells;

and (d) the design of proposed filter layers.

The following criteria represent current field practice:

- (1) Cores with a width of 30% to 50% of the water head have proved satisfactory on many dams under diverse conditions. Probably a core of this width is adequate for any soil type and dam height.
- (2) Cores with a width of 15% to 20% of the water head are considered thin but, if adequately designed and constructed filter layers are used, they are satisfactory under most circumstances.

If now, to get an idea of what should be the ratios of permeabilities of the filter and the core materials, let us choose the following:

- (a) a minimum width of 12 feet for a vertical filter;
- (b) a minimum width (for the core) of 40% of the water head, say H ; hence the half width of the central core is $0.2H$.

The expression for λ is

$$\lambda = \frac{0.2H}{10} \frac{k_{\text{drain}}}{k_{\text{core}}} = 0.02H \frac{k_{\text{drain}}}{k_{\text{core}}} . \quad 5.3$$

Table 5.3 gives the values for λ for various values of the head of water impounded (which for practical purposes is the height of the dam). It can be seen that for a given height of the dam built to conservative standards, the successful behavior of the dam (and the drain) depends primarily on

the ratio of the permeabilities (i.e., for given core and drain materials). The greater is this ratio the better is the performance of the dam. Further, for a given value of the ratio of permeabilities, the value of λ is higher for high dams when compared to that for low dams. Thus for the same materials a higher dam functions more satisfactorily than a low dam. In other words, a more permeable filter drain is to be provided for a low dam when compared to a high dam for the same performance. The performance is measured in terms of the ease with which water squeezed from the core due to consolidation is drained through the filter.

Table 5.1 Values of pore pressure for a Rectangular
Section of Side Ratio 2.4

At Mid Point on the Centre Line		At Quarter Point from Top on the Centre Line	
Days	Numerical	Days	Analytical
5	100.0	5	99.7
10	100.0	10	97.1
15	99.9	15	92.6
20	99.5	20	87.7
25	98.6	25	83.1
30	97.3	30	78.9
35	95.7	35	75.2
40	93.7	40	71.9
45	91.4	45	68.9
50	89.1	50	66.1
55	86.6	55	63.6
60	84.1	60	61.2
65	81.6	65	59.0
70	79.1	70	56.9
75	76.6	75	54.9
80	74.2	80	53.0
85	71.7	85	51.1
90	69.4	90	49.4
95	67.1	95	47.7
100	64.9	100	46.0

Table 5.2 Values of pore pressure for a Rectangular
Section of Side Ratio 1.5

At Mid Point
on the Centre Line

Days	Numerical	Analytical
15	99.9	99.6
20	99.5	98.7
25	98.6	97.3
30	97.3	95.5
35	95.5	93.3
40	93.4	90.9
45	90.9	88.2
50	88.3	85.3
55	85.5	82.4
60	82.5	79.4
65	79.6	76.4
70	76.6	73.4
75	73.6	70.5
80	70.6	67.6
85	67.7	64.7
90	64.9	61.9
95	62.1	59.3
100	59.4	

At Quarter Point from Top
on the Centre Line

Days	Numerical	Analytical
5	99.7	99.8
10	97.1	96.9
15	92.6	92.0
20	87.7	87.1
25	83.1	82.5
30	78.9	78.4
35	75.1	74.7
40	71.7	71.3
45	68.5	68.2
50	65.5	65.3
55	62.7	62.5
60	60.1	59.9
65	57.5	57.4
70	55.1	54.9
75	52.7	52.6
80	50.4	50.3
85	48.3	48.2
90	46.2	46.1
95	44.1	44.0
100	42.2	42.1

Table 5.3 Values of λ for a
hypothetical dam

Head of Water feet	Impedance Factor λ
25	0.5 k_1/k_2
50	1.0 k_1/k_2
100	2.0 k_1/k_2
200	4.0 k_1/k_2

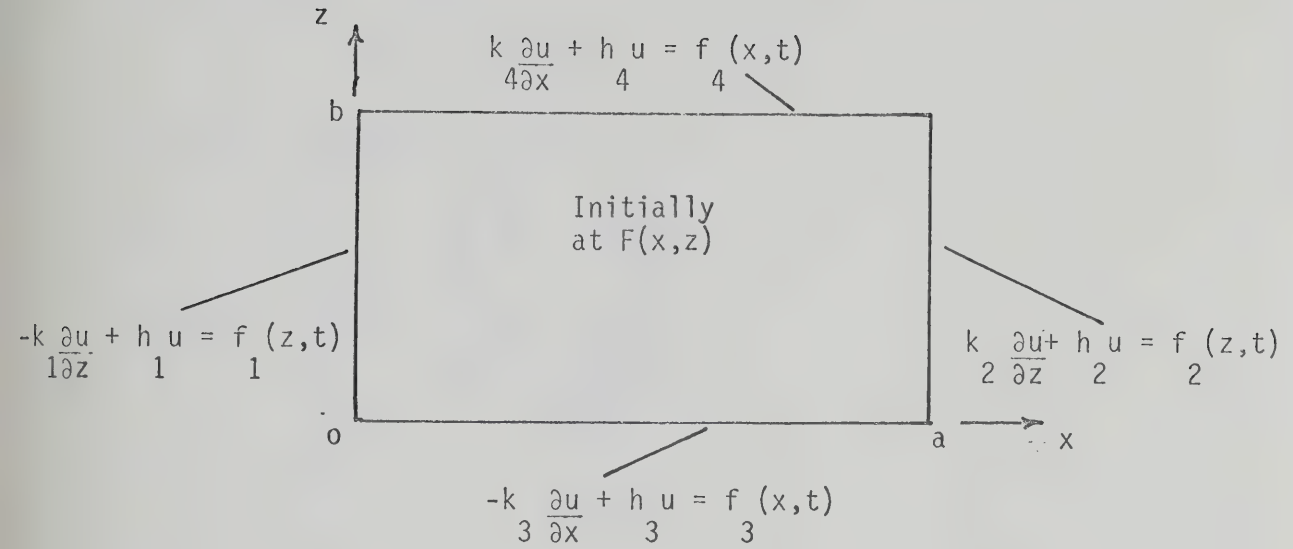


FIG. 5.1 A RECTANGLE WITH NONHOMOGENEOUS BOUNDARY CONDITIONS OF THE THIRD KIND.

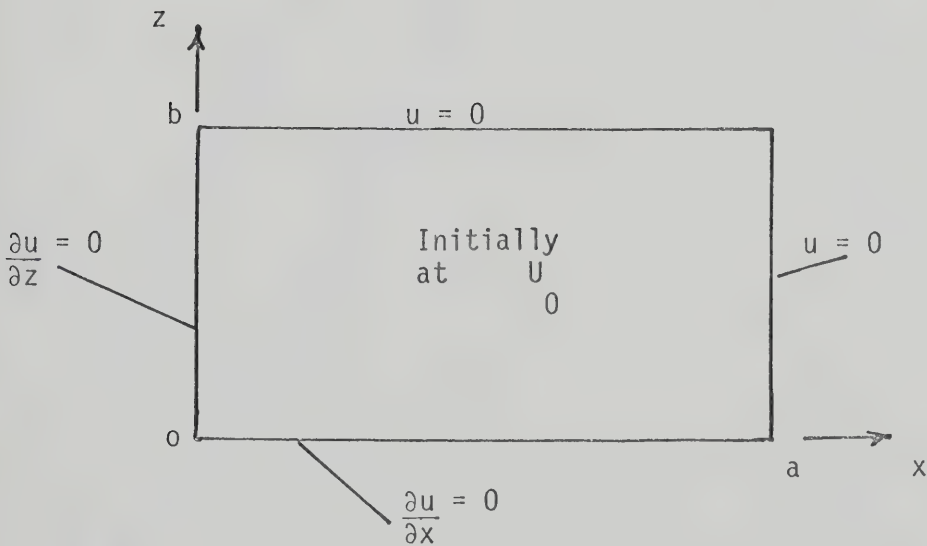


FIG. 5.2 A RECTANGLE WITH MIXED BOUNDARY CONDITIONS OF FIRST AND THIRD KIND.

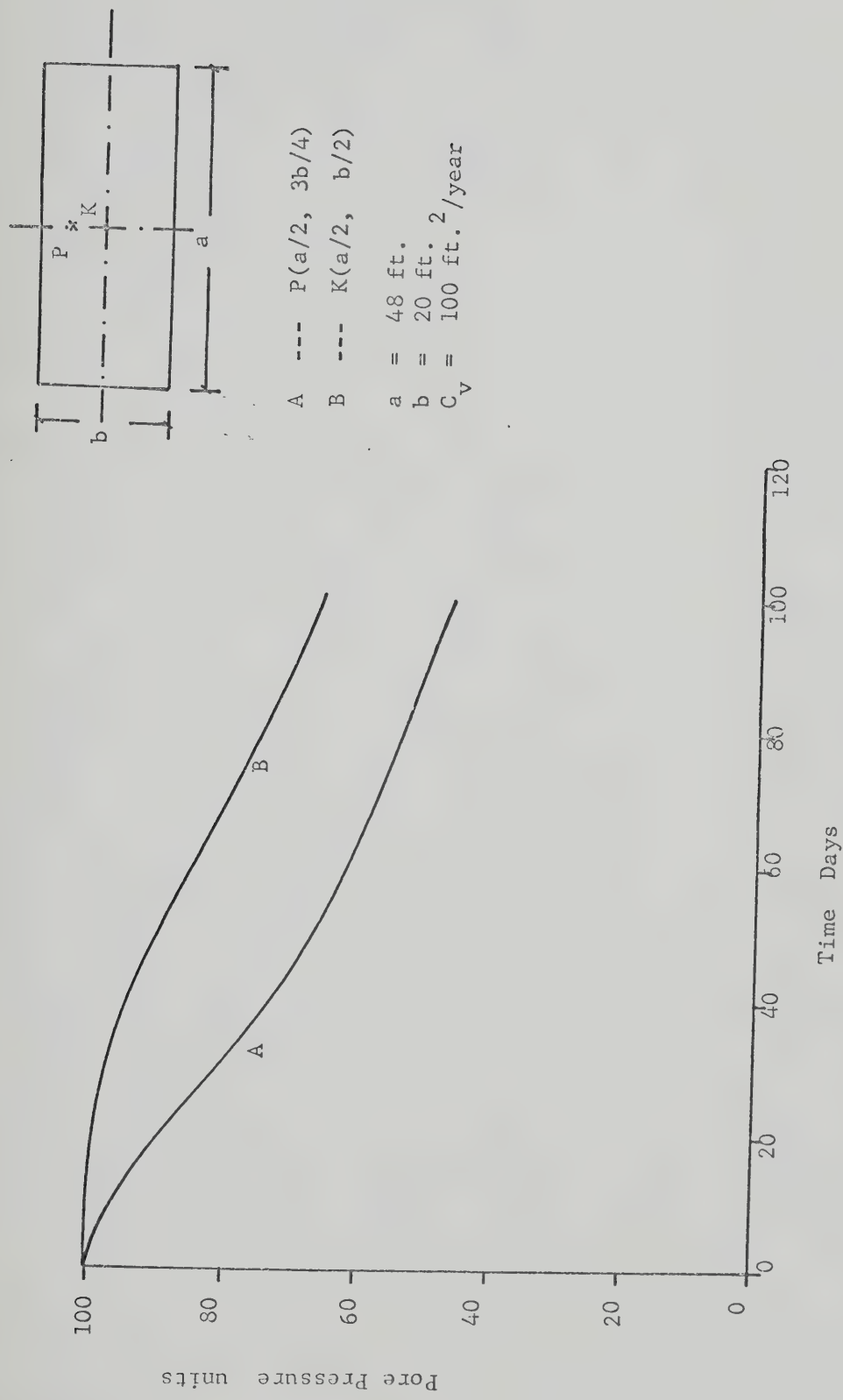


FIG. 5.3 a VARIATION OF PORE PRESSURE WITH TIME

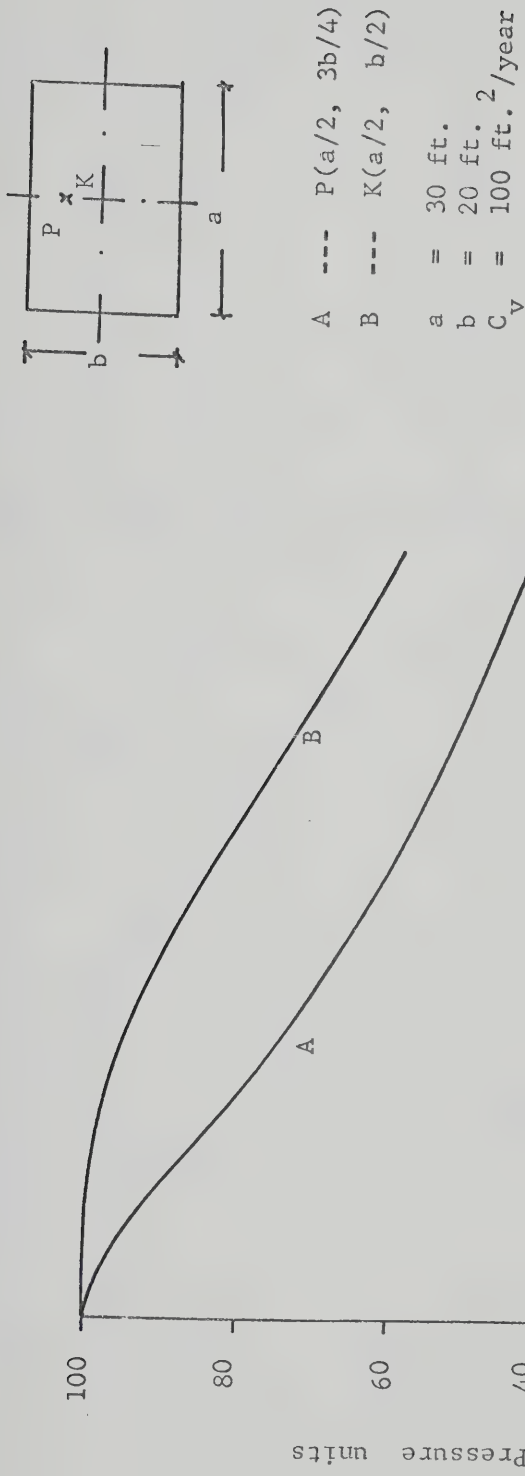


FIG. 5.3 b VARIATION OF PORE PRESSURE WITH TIME

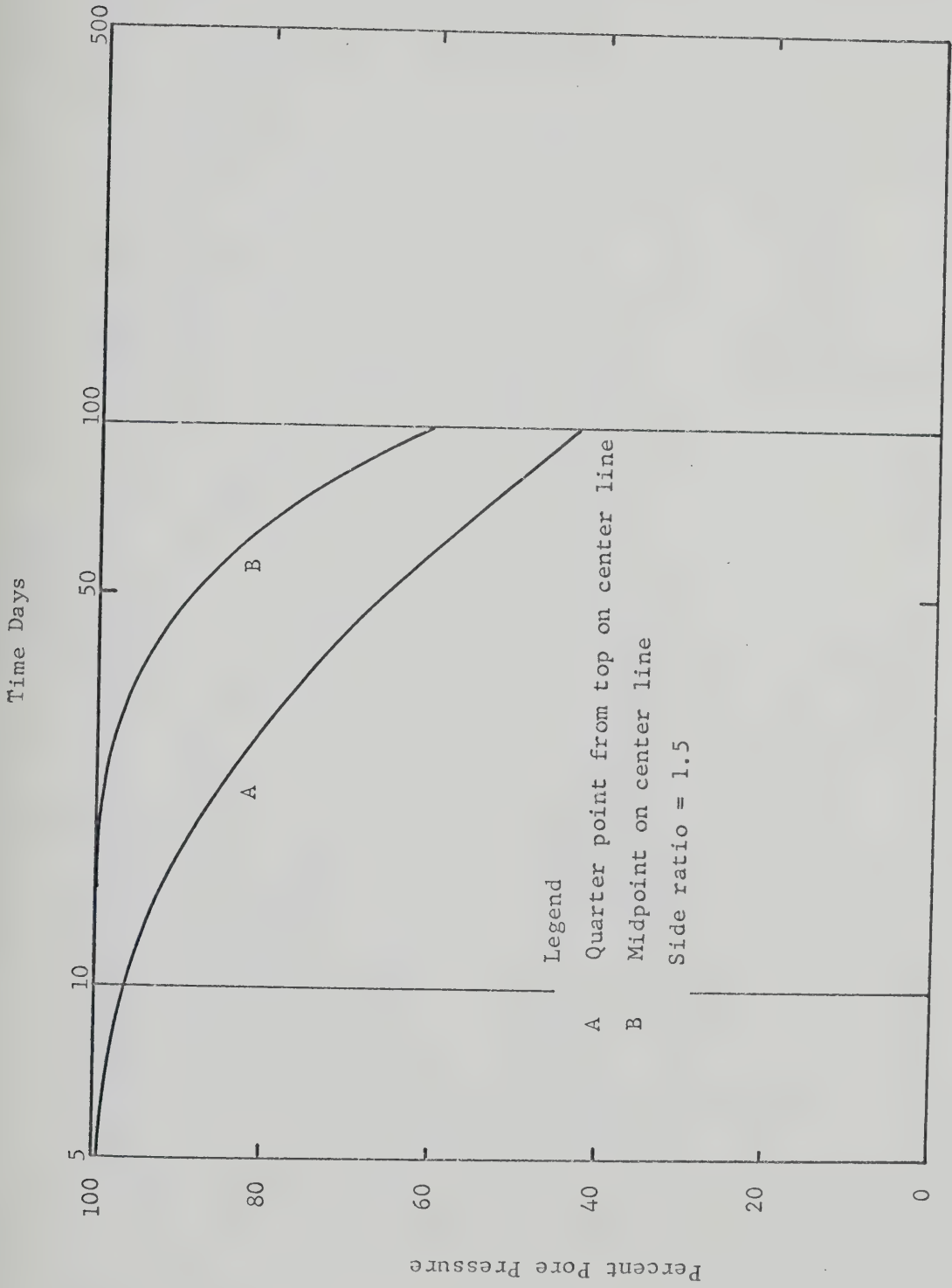


FIG. 5.3 c PERCENTAGE OF MAXIMUM PORE PRESSURE WITH TIME

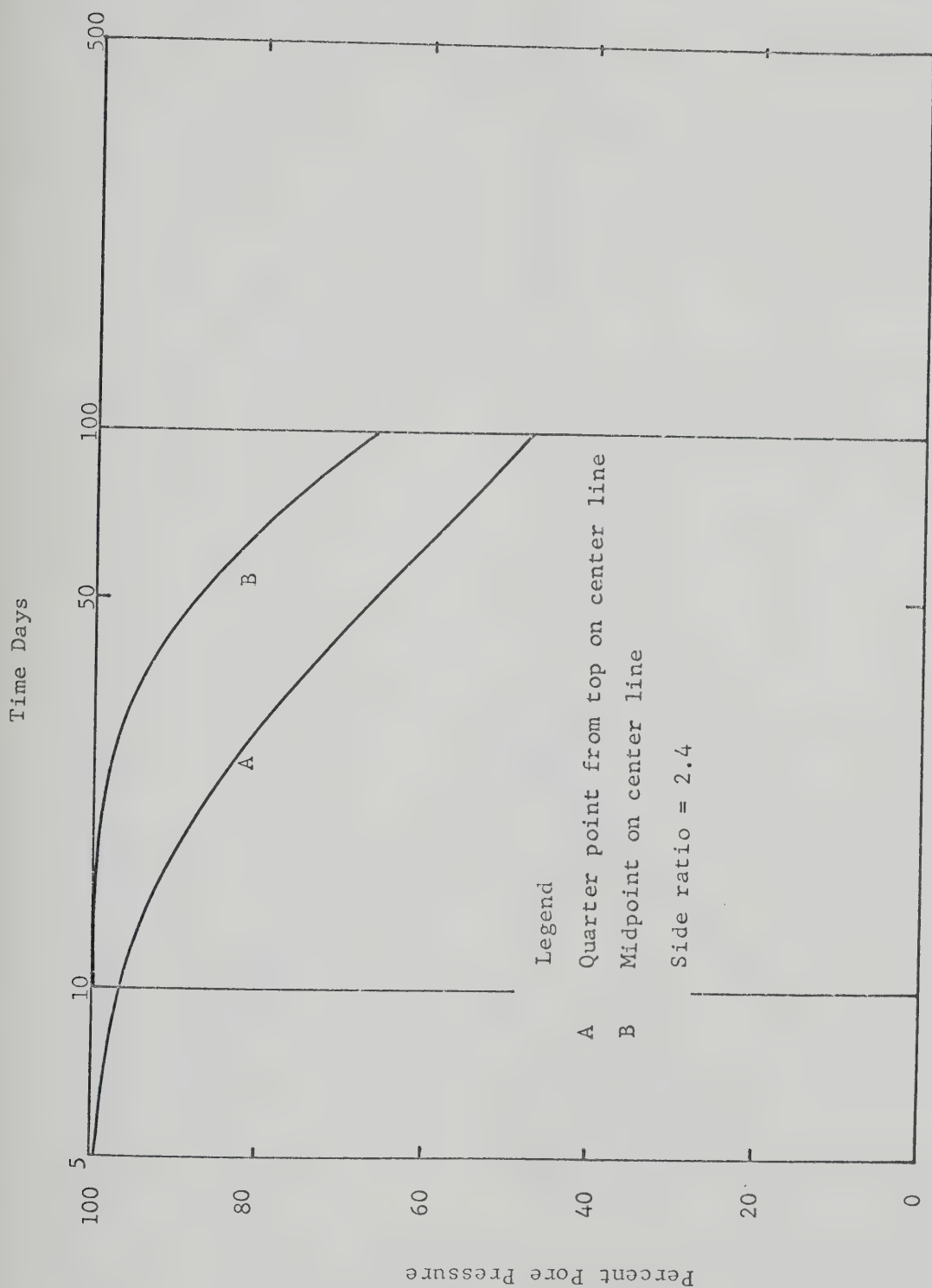


FIG. 5.3 d PERCENTAGE OF MAXIMUM PORE PRESSURE WITH TIME

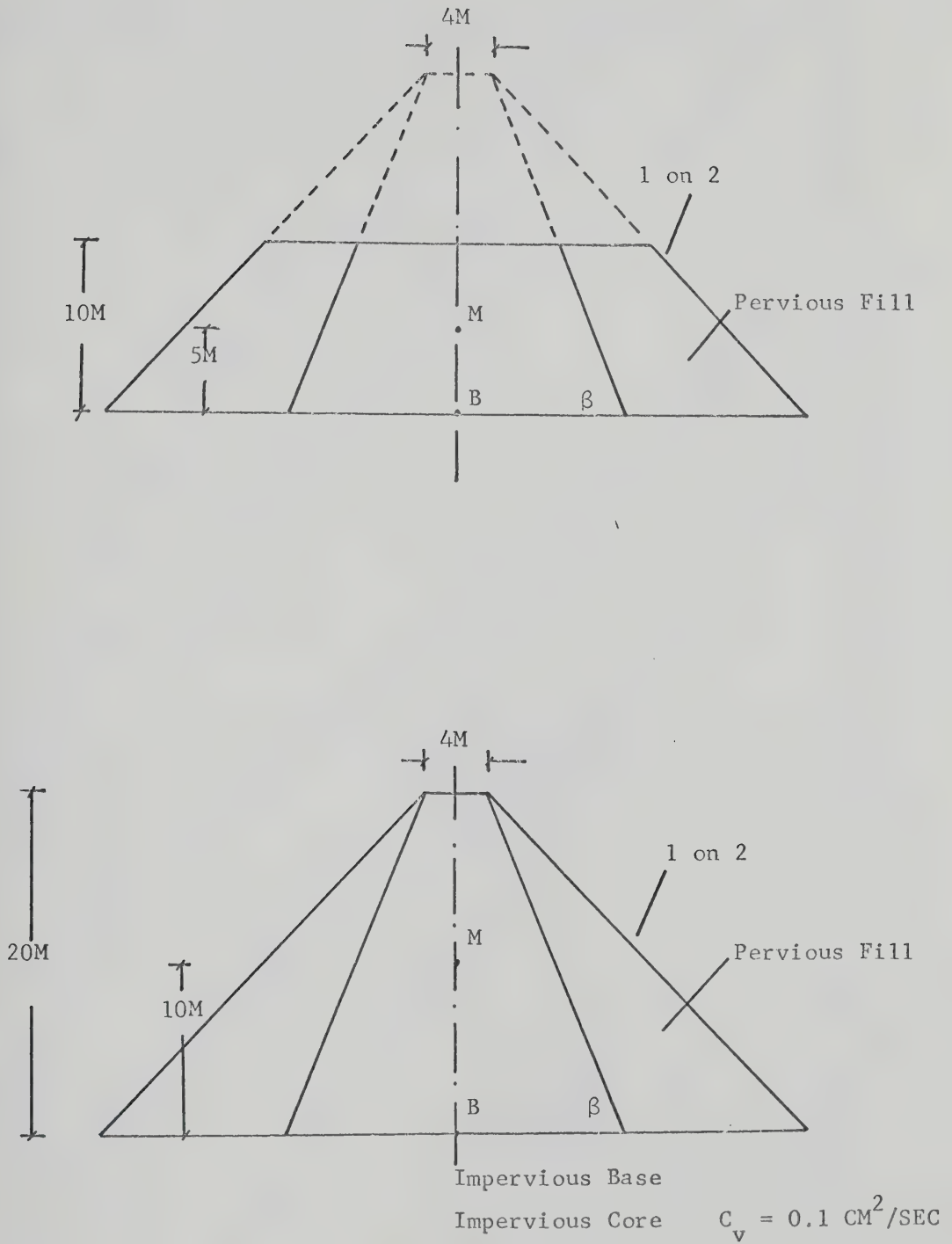


FIG. 5.4 IDEALIZED DAM CROSS-SECTION (Bernell, 1958)

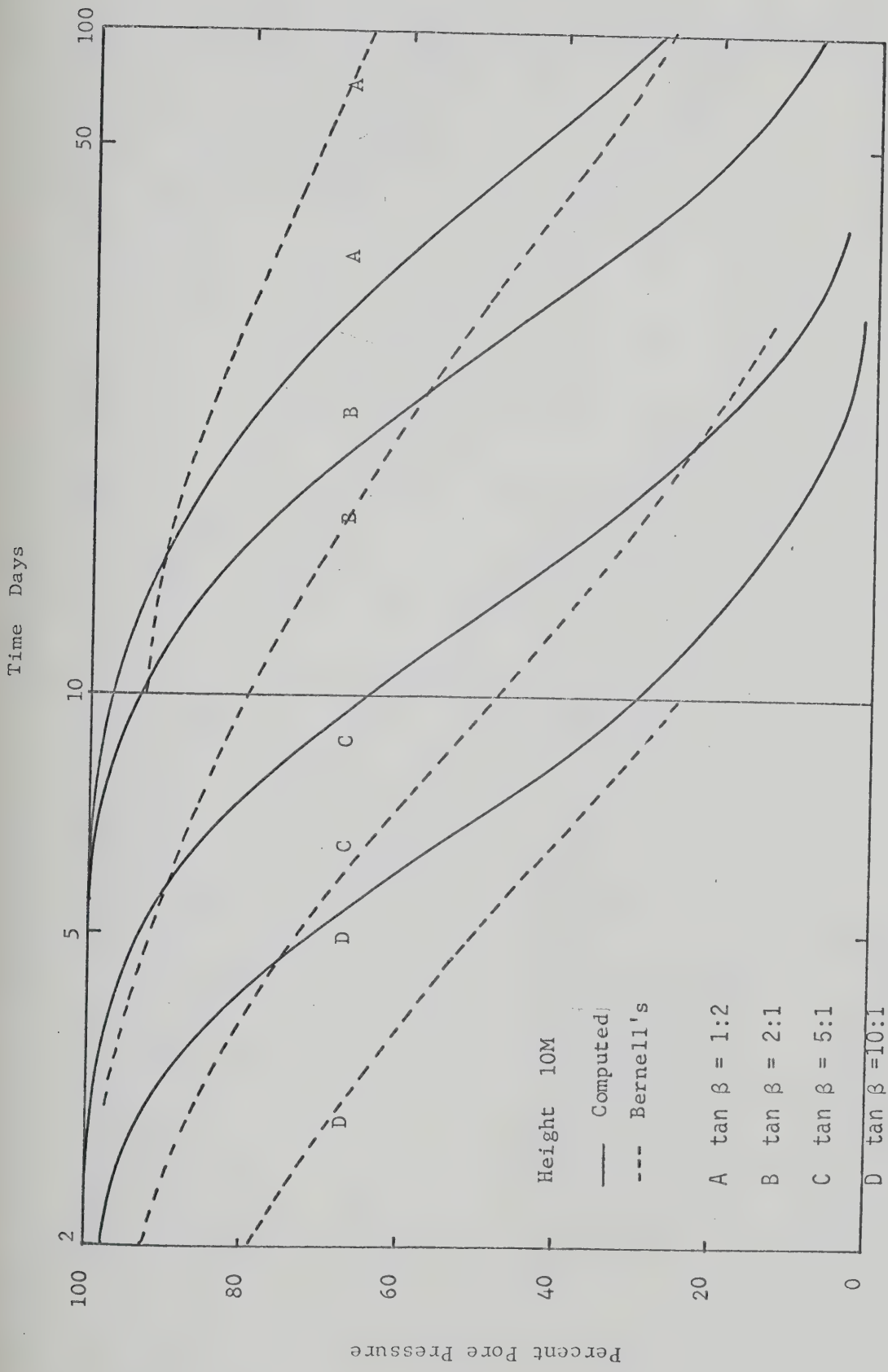


FIG. 5.5 a PERCENTAGE OF MAXIMUM PORE PRESSURE WITH TIME

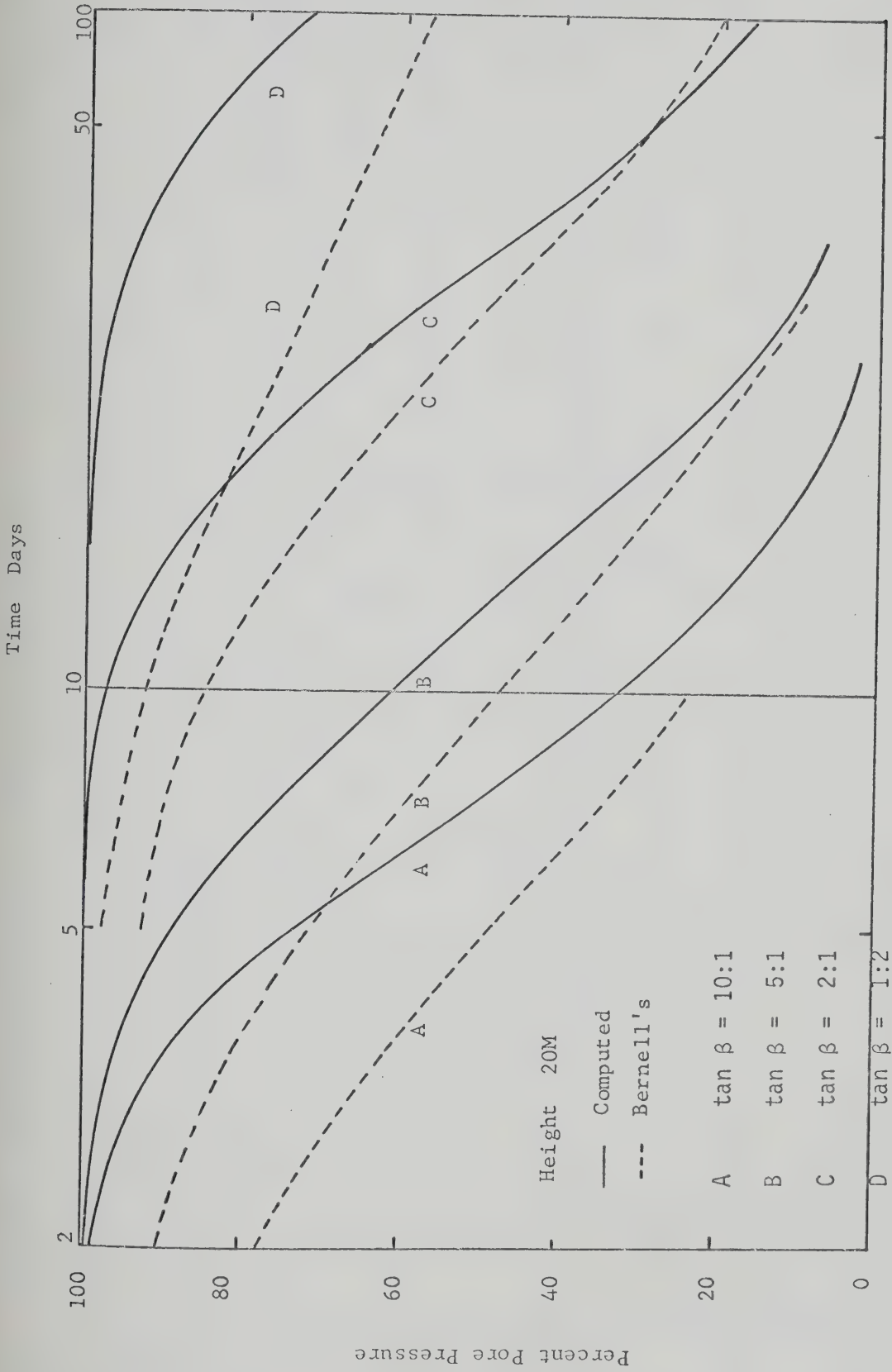


FIG. 5.5 b PERCENTAGE OF MAXIMUM PORE PRESSURE WITH TIME

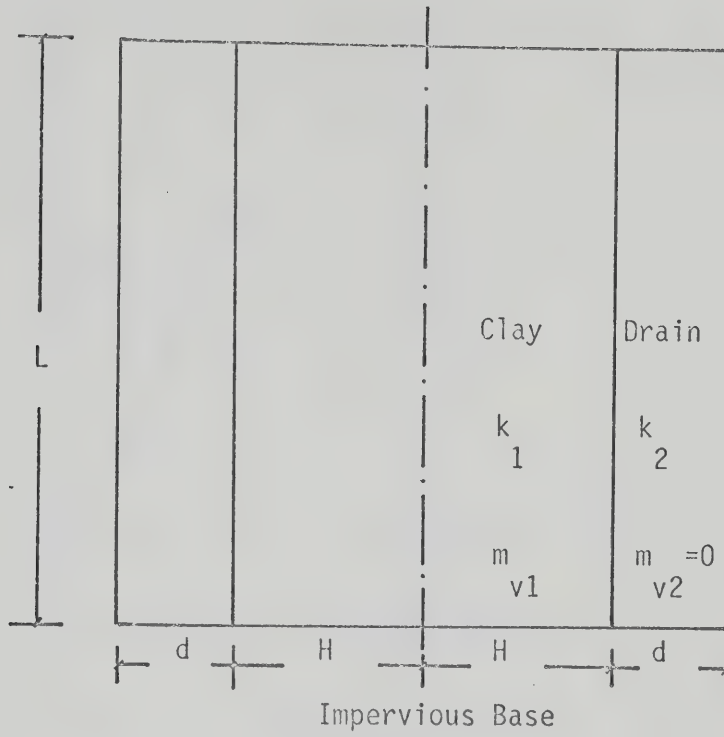


FIG. 5.6 a RECTANGULAR SECTION WITH SIDE DRAINS

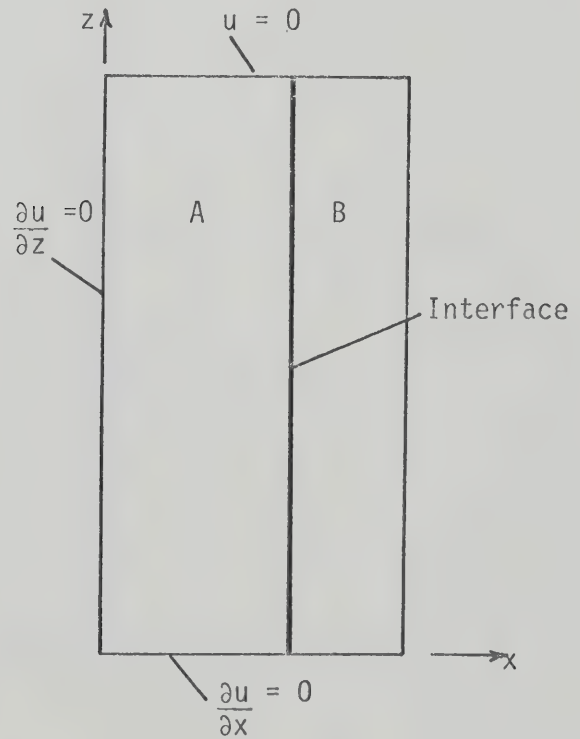


FIG. 5.6 b RECTANGULAR SECTION WITH SIDE DRAINS

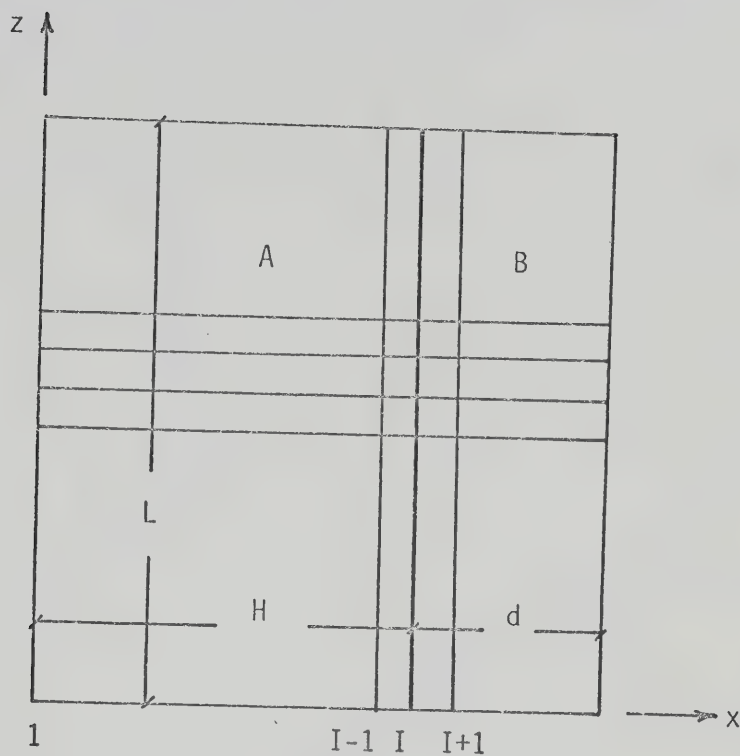


FIG. 5.7 a SPACE GRID FOR MATERIALS FOR A AND B

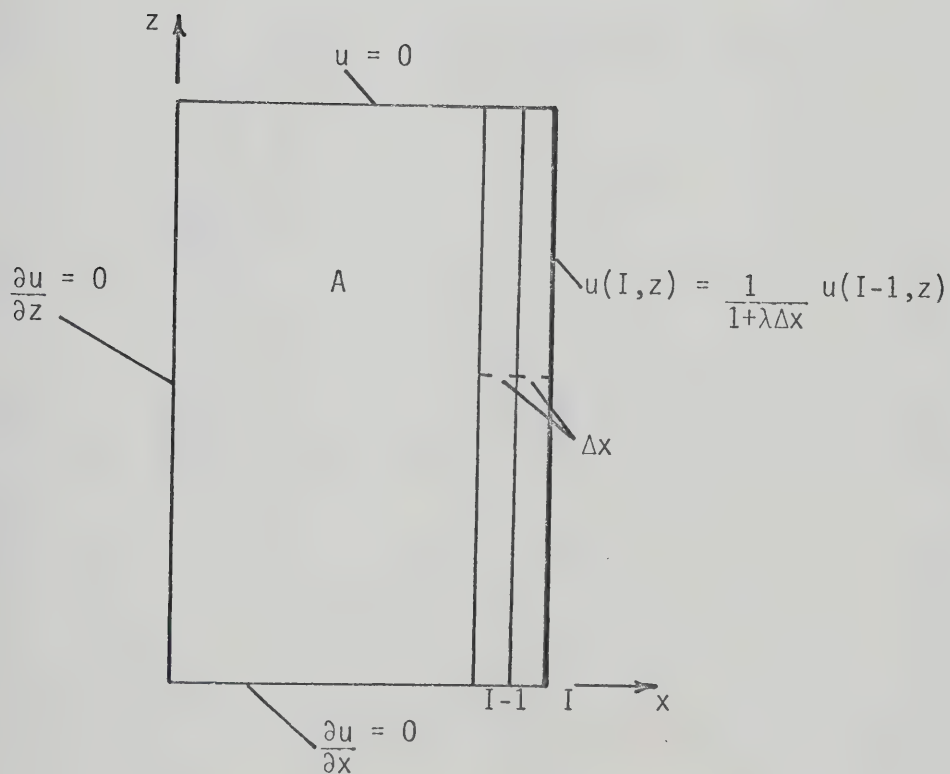


FIG. 5.7 b SPACE GRID FOR MATERIAL A ONLY

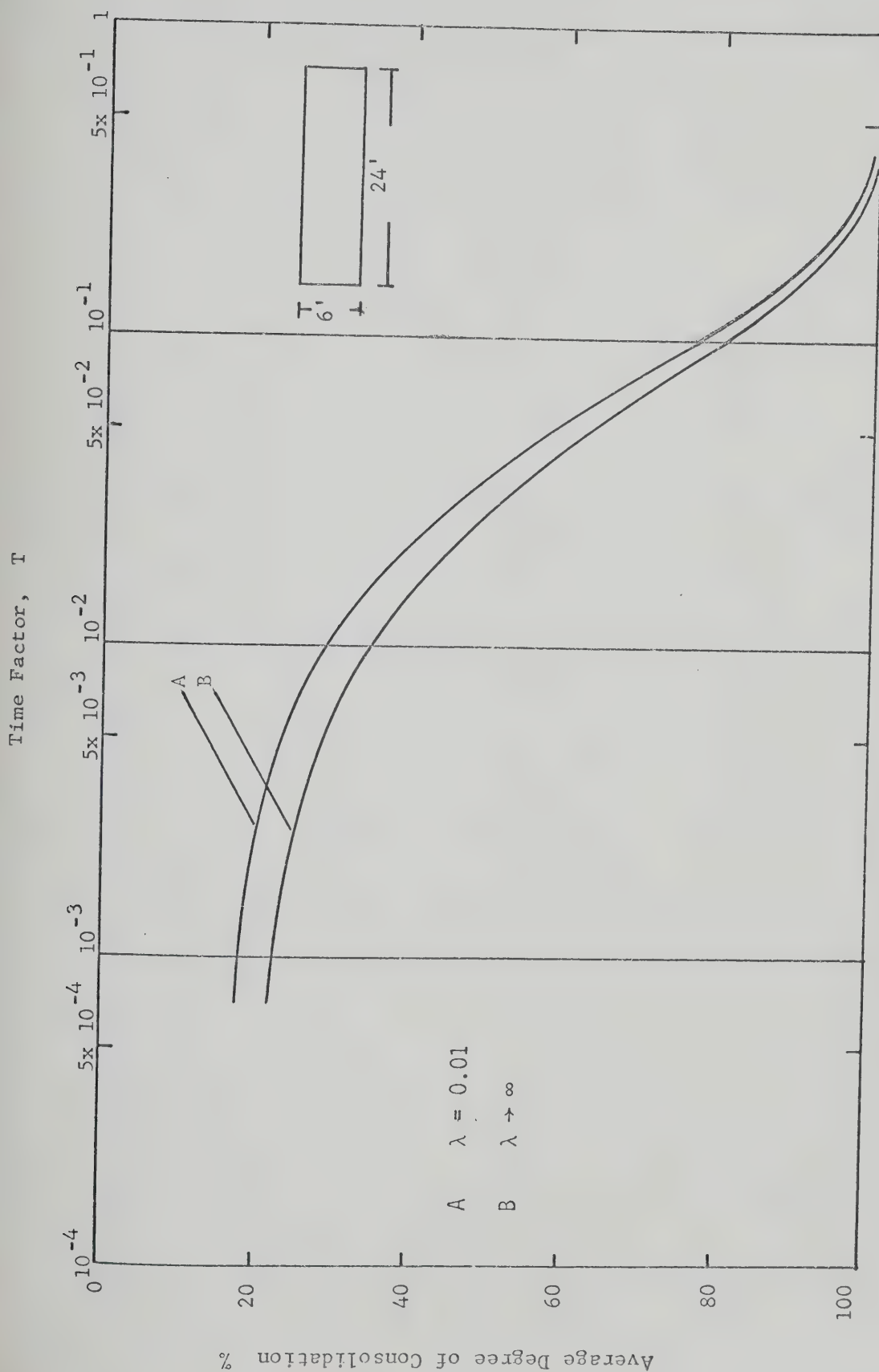


FIG. 5.8 RELATIONSHIP BETWEEN AVERAGE DEGREE OF CONSOLIDATION AND TIME FACTOR

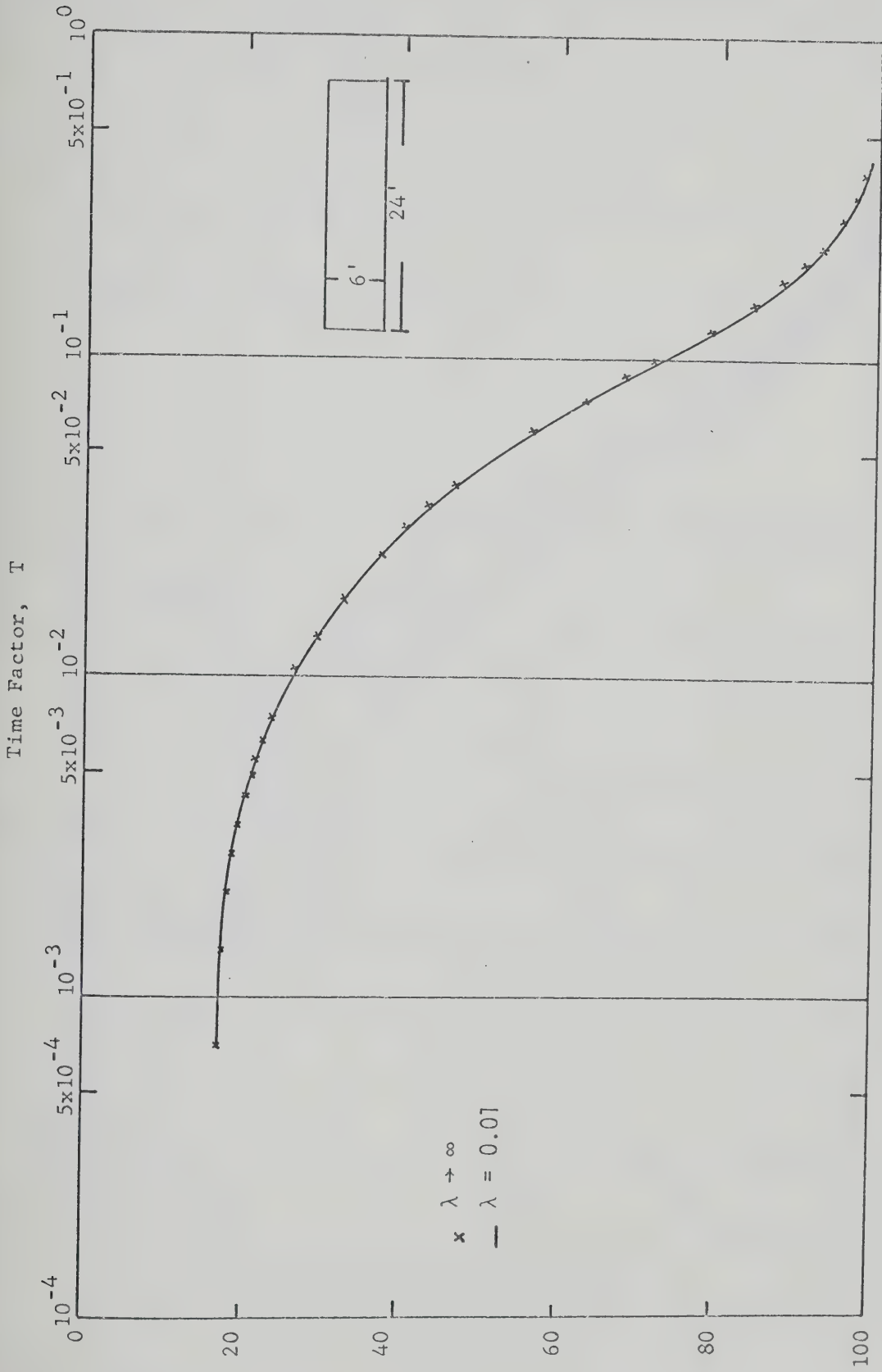


FIG. 5.9 RELATIONSHIP BETWEEN AVERAGE DEGREE OF CONSOLIDATION AND THE TIME FACTOR

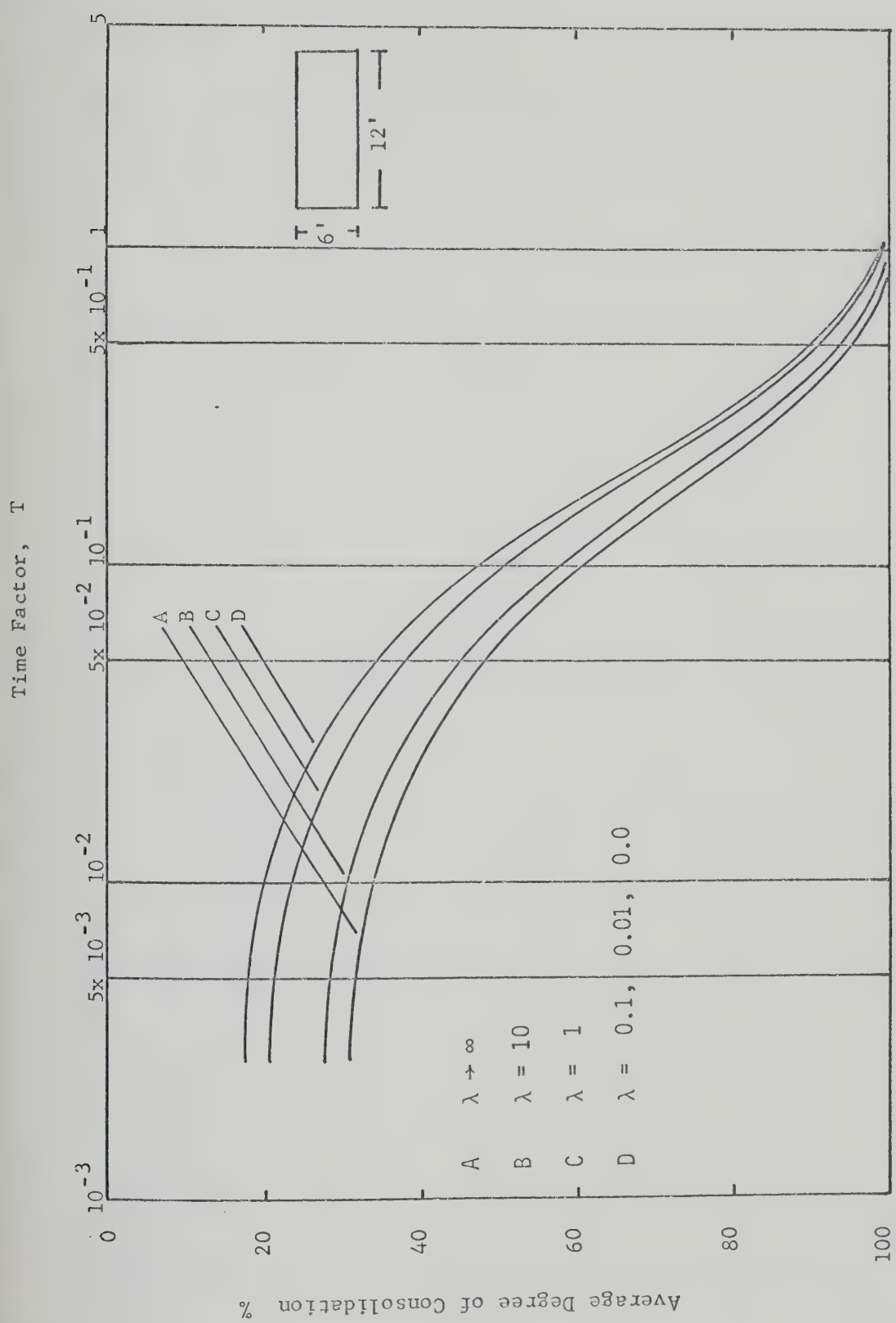


FIG. 5.10 RELATIONSHIP BETWEEN AVERAGE DEGREE OF CONSOLIDATION AND TIME FACTOR

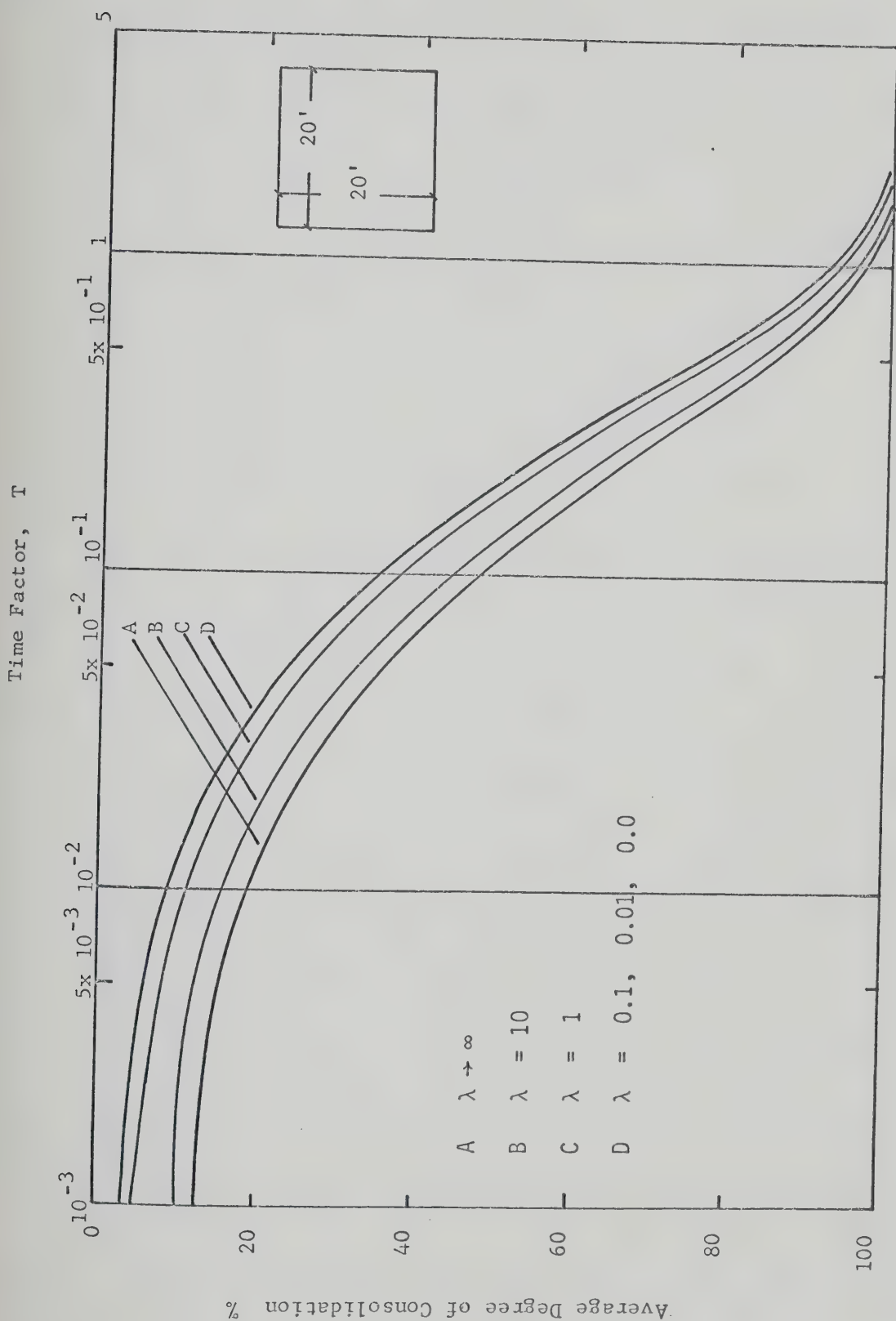


FIG. 5.11 RELATIONSHIP BETWEEN AVERAGE DEGREE OF CONSOLIDATION AND TIME FACTOR

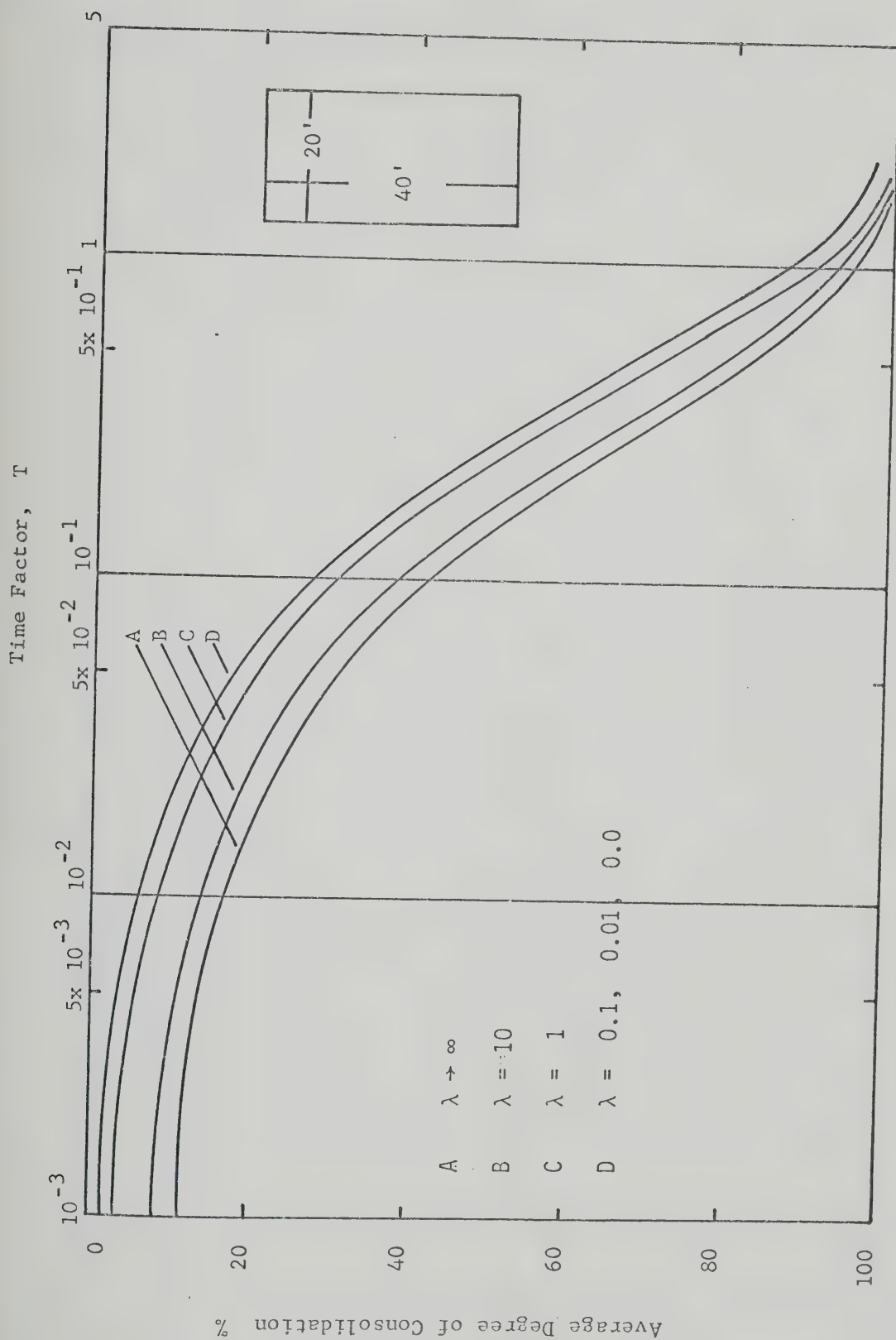


FIG. 5.12 RELATIONSHIP BETWEEN AVERAGE DEGREE OF CONSOLIDATION AND THE TIME FACTOR

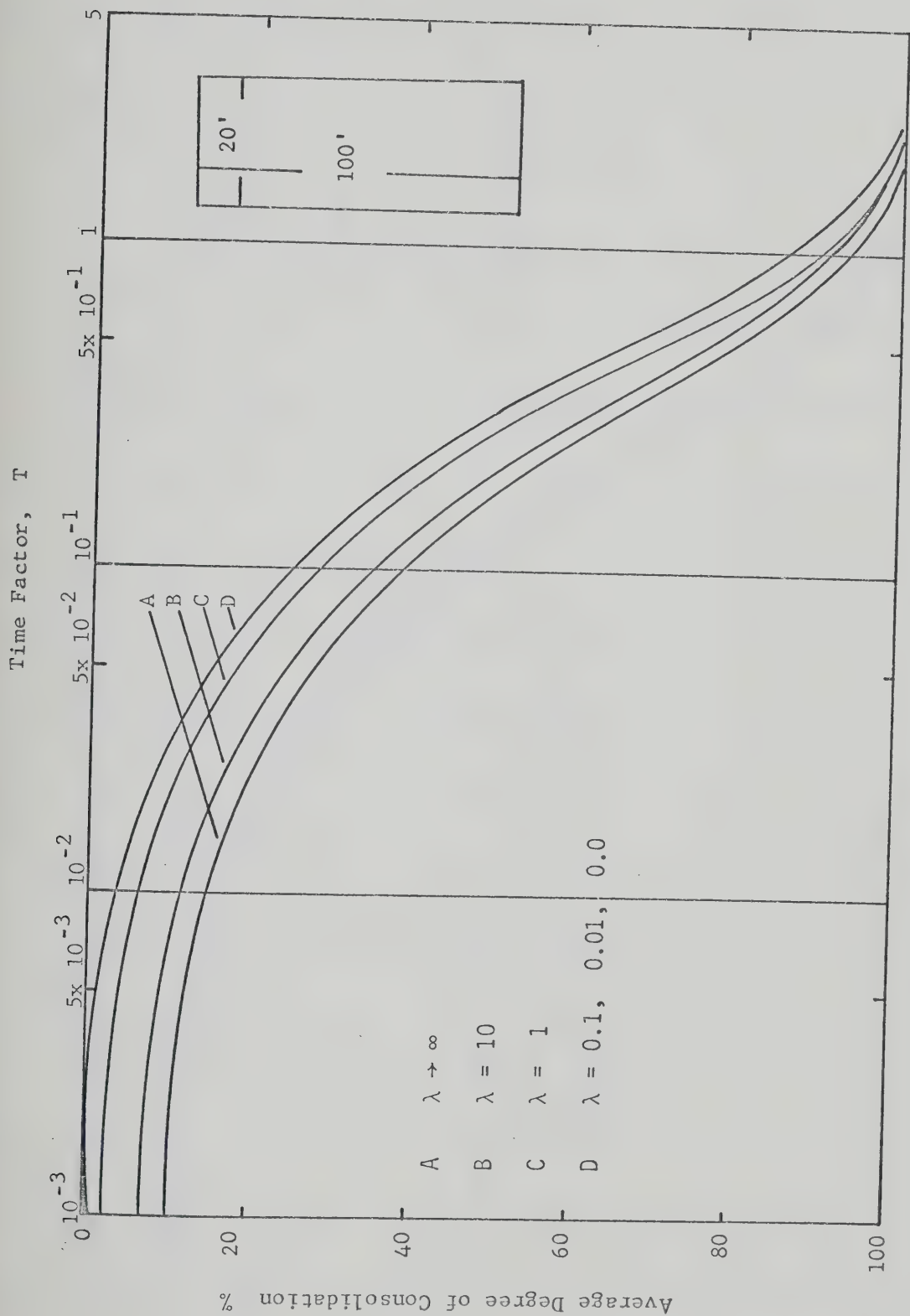


FIG. 5.13 RELATIONSHIP BETWEEN AVERAGE DEGREE OF CONSOLIDATION AND TIME FACTOR

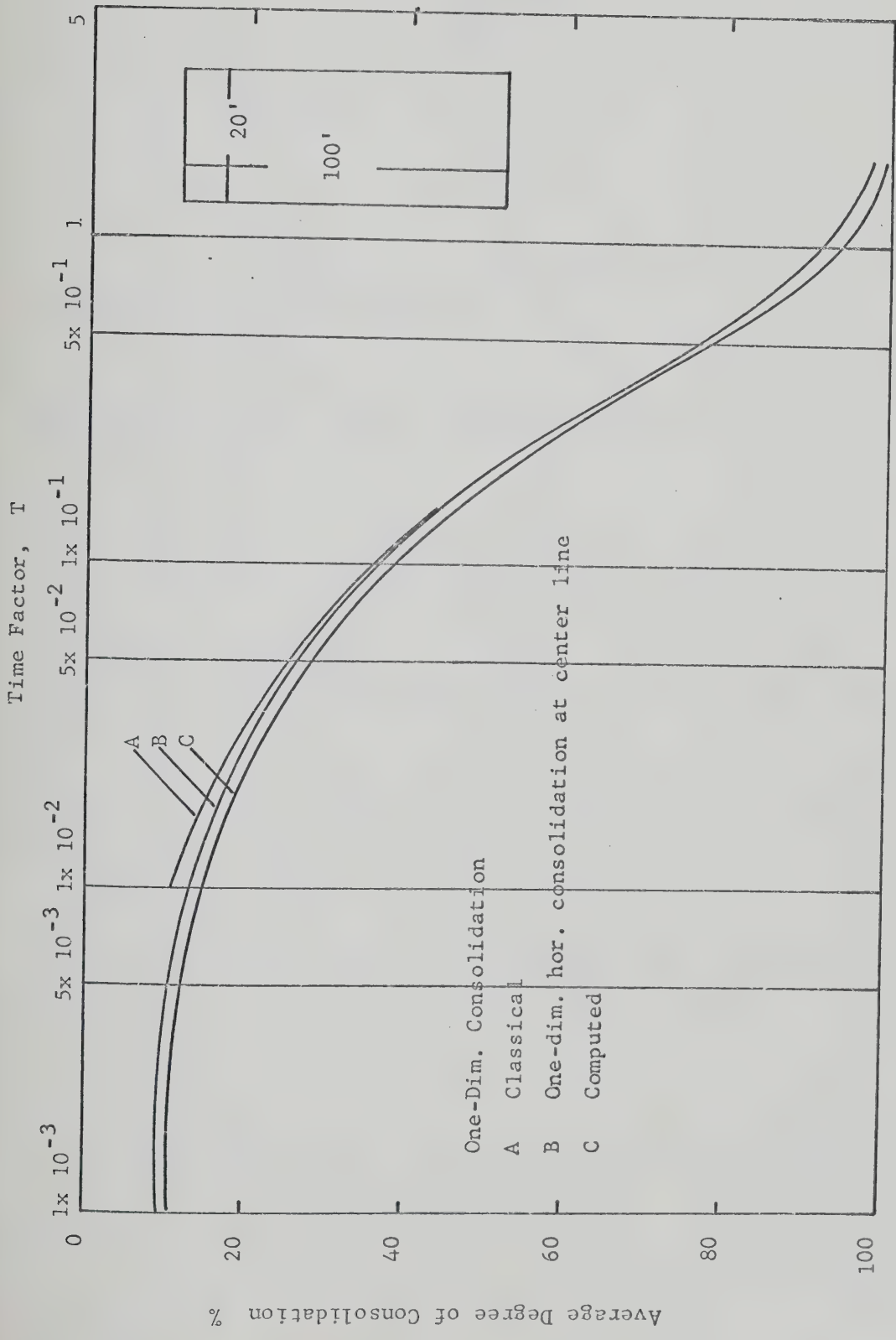


FIG. 5.14 RELATIONSHIP BETWEEN AVERAGE DEGREE OF CONSOLIDATION AND TIME FACTOR

CHAPTER VI

INFLUENCE OF DISSIPATION ON CONSTRUCTION PORE PRESSURES

6.1 GENERAL

A theoretical analysis is developed to determine the influence of dissipation on construction pore pressures developed in earth embankments. Using a multiple lift construction procedure and assuming conditions of plane strain, embankments with linear, isotropic, and homogeneous material properties are studied. The equation 6.4 governing the dissipation of excess pore pressure developed in partially saturated soils is solved using the ADI technique which was developed and tested in Chapter V. Six field cases are studied and the comparison between the calculated and measured pore pressures is good within practical limits of accuracy. The results indicate that the construction pore pressures are very sensitive to the assumed construction sequence and that in the analysis the construction stoppages and the resulting pore pressure dissipation must be considered to make reasonable pore pressure predictions.

6.2 SUMMARY OF THEORETICAL METHODS FOR PREDICTING CONSTRUCTION PORE PRESSURES

During construction of a rolled embankment temporarily

high pore water pressures develop. This development of high construction pore pressure presents a major design problem from the viewpoints of safety and economy. Numerous methods are available to predict the development and consequent dissipation of pore pressures during the construction of earth dams. Few of them have general application. For this reason, many practicing engineers and designers use a rule-of-thumb, generally based on past experience, for estimating construction pore pressures. Theoretical methods for predicting construction pore pressures are based on a minimum of assumptions and these methods provide an insight into the variation of pore pressures with different soil types and conditions. In the following the available theoretical methods are summarized.

The first analytical method for dealing with construction pore pressures in an embankment was published by the U.S. Bureau of Reclamation (1939). The basic development rests on the assumption that the time rate of change of the sum of the volume of moisture and free air in an earth mass is caused by:

- (i) flow into the unit volume due to percolation; and
- (ii) change in the free-air volume due to changes in pressure and temperature.

This time rate of change is equated to the time rate of consolidation, and the integration of this equation provides the solution for the problem of transient pore pressures.

Hilf (1948) proposed a solution to the unsteady flow

of water with the assumption that no drainage occurs and surface tension can be neglected. Pore pressures in a partly saturated cohesive soil mass are caused by the compression of the two phase pore fluid comprising a mixture of air and water as a result of an increase in superimposed load. An expression has been derived by Hilf (op. cit.) for such pressures by combining Boyle's law for compression of gases and Henry's law for solubility of gases and assuming the soil to be completely non-draining.

$$u = \frac{p_a \Delta_1}{v_a + H v_w - \Delta_1} + U_c$$

where u = total air pressure after consolidation, i.e.,
pore pressure

p_a = air pressure after initial compaction very close
to atmospheric pressure

Δ_1 = consolidation or volume change in percentage of
initial volume of soil mass

v_a = volume of free air in voids after initial com-
paction in percentage of initial volume of soil
mass

H = Henry's constant of solubility of air in water
by volume = 0.0196

$H v_w$ = volume of dissolved air in percentage of initial
volume of soil mass

U_c = capillary tension, usually of small order.

Upon saturation of the soil mass by pressure, $\Delta_1 = v_a$, and the expression is reduced to

$$u = (p_a v_a) / (H v_w)$$

if surface tension is neglected and no drainage occurs.

Although the assumptions used in the development of Hilf's method limit its applicability, the method eliminated complex mathematical difficulties. Hilf criticized his own assumption of no surface tension. The assumption of no drainage is overconservative particularly where internal drainage is provided. Despite the drawbacks inherent in Hilf's method, it often enables a reasonable estimate of the construction pore pressure to be made with the available data from consolidation and compaction tests.

An approximate method of allowing for the various factors leading to the dissipation of pore pressures in the field has been developed by Bishop (1957). The method comprises step computations of pore pressures by Hilf's equation at certain arbitrary intervals during which some pressure release is permitted so as to simulate the combined action of various factors leading to dissipation in the field. The various steps in the analysis are shown in Figure 6.1. The effective stress-volume change curve is first plotted from the laboratory consolidation test. For an arbitrary assumed

increment σ'_1 in effective stress, the volume change Δ_1 is obtained. The pore pressure u_1 corresponding to Δ_1 assuming no drainage is computed from Hilf's equation and point A_1 obtained. Next, the assumed percentage of dissipation is applied, bringing down the pore pressure and increasing the effective stress. Let this be represented by B_1 on the curve. The pore pressure corresponding to this stage is represented by C_1 . For the next stress increment of σ'_2 , the corresponding volume change is Δ_2 . For this stage of loading the conditions at points B_1 and C_1 are assumed as initial conditions. The pore pressure dissipation is again allowed to take place in the same ratio and the process repeated. The points C_1 , C_2 , ... etc. thus obtained indicate the pore pressure after allowing for the assumed dissipation rate. The ratio in which the pressure relief is permitted, known as the dissipation factor, depends on soil characteristics, rate of construction, and cross-section of the embankment. Even a low value of this dissipation factor (as low as 1/7) leads to considerable lowering of pore pressures:

- (a) directly as a result of dissipation itself,
- (b) due to increase in effective stress which leads to the application of flatter portion of the consolidation curve for the same range of loading; thus corresponding to a greatly reduced compressibility.

The step computations are based on the assumptions that:

- (i) Hilf's equation continues to be valid throughout the step computation;
- (ii) during dissipation, the mixture of air and water drained away has the same proportion by weight as that remaining in it, or in other words, the degree of saturation remains unchanged before and after drainage.

The method has been used for a number of dams having different design problems and has provided reasonable estimates of the construction pore pressures (Sherman and Clough, 1968). For example in the case of Usk dam (Bishop, 1957) this method proved very useful.

Skempton (1954) proposed a solution for determining the pore water pressure set up in a fully saturated soil, expressed in terms of the major and minor principal stresses, assuming that the undrained soil behaved in accordance with elastic theory. To compensate for the discrepancy between the elastic behavior and actual behavior of the soil, Skempton replaced the elastic constants in the expression by a factor found in a laboratory triaxial test, the well known A factor. Hence,

$$\Delta u = \Delta \sigma_3 + A(\Delta \sigma_1 - \Delta \sigma_3)$$

where Δu - the change in pore pressure

$\Delta \sigma_3$ - the change in all round pressure

$\Delta \sigma_1$ - the change in axial stress.

Through development by Skempton and others, a practical pore pressure theory for use in predicting embankment pore pressure during construction was established.

Skempton extended his expression for pore water pressure in saturated soils to unsaturated soils in which

$$\Delta u = B[\Delta\sigma_3 + A(\Delta\sigma_1 - \Delta\sigma_3)]$$

and B is another experimentally determined factor. The value of B was found to range from zero for completely dry soils to unity for completely saturated soils. For any given soil, the coefficient A was found to vary with stresses and strains.

Bishop (1954) rearranged Skempton's expression as

$$\Delta u / \Delta\sigma_1 = \bar{B} = B[1 - (1 - A)(1 - \frac{\Delta\sigma_3}{\Delta\sigma_1})]$$

The above equation involves the assumption of no dissipation of pore pressures, since excess pore pressure is a function of applied stress only. Also the factor \bar{B} was found to be not constant. The factor \bar{B} depends on the pore pressure coefficients A and B which vary with the amount of strain that takes place. Further Skempton and Bishop (1954) have shown that the value of B varies nonlinearly with the degree of saturation.

Bishop (1957) noted that the above method gave over-

conservative results if allowances were not made for drainage in dams. In the case of the Usk Dam, a dam compacted wet of optimum with numerous drainage blankets in the core, Bishop (op. cit.) found the assumption to be overconservative and contended that pore pressure dissipation during construction shutdown resulted in a two-fold effect on the value of excess pore pressure at the end of construction. The first and most obvious effect is that of relief of pore pressure by dissipation. The second effect occurs because of compaction wet of optimum. After a period of dissipation, the increase in pore water pressure with increase in stress was found to be less than the increase before dissipation.

Bernell and Nilsson (1957) developed an electric analogue equipment for the study of transient, two-dimensional flow problems in earth dams. The equipment permitted the analysis of construction pore pressures at any time during the construction of the dam. The pore pressure u at a time t can be determined by the following equation for two-dimensional consolidation:

$$C_v \left(\frac{\partial^2 u}{\partial x^2} + \frac{\partial^2 u}{\partial y^2} \right) = \frac{\partial u}{\partial t}$$

where C_v is the coefficient of consolidation whose value may be obtained from a triaxial consolidation test. From the illustrations presented, it appeared that difficult boundary conditions can be adequately reproduced in the equipment.

Bernell (1958) reported that the model analogy approach to the problem transient pore pressure dissipation is less difficult than the complex mathematical approach. However, it has been demonstrated in section 5.A.5 that the results presented by Bernell (op. cit.) are misleading and not trustworthy. Also with the progress of numerical analysis and advances in computer technology more accurate results can be obtained.

Li (1959) on analysis of pore pressure data from the construction of the Quebradona Dam, Colombia, South America, concluded that allowance should be made for dissipation of pore pressure during construction in predicting pore pressures. In a subsequent publication Li (1967) made a comparative study of the influence of various factors on the development of construction pore pressures in three earth dams, namely Quebrandona Dam, Troneras Dam and Miraflores Dam (all in Colombia, South America). Li (op. cit.) concluded that the pore pressure development is due to the combined effect of many factors and it would be an oversimplification and subject to serious inaccuracy to estimate construction pore pressure without an overall evaluation of all possible factors involved. Factors which affect the build-up of construction pore pressures are numerous (Sherman and Clough, 1968) and are discussed in section 6.5.

6.3 ANALYSIS AND TECHNIQUE OF SOLUTION

Equation 2.11 represents the consolidation of a soil mass when three-dimensional drainage is taking place and is reproduced below as

$$c \nabla^2 u = \frac{\partial u}{\partial t} - \frac{1}{3} \frac{\partial \theta_1}{\partial t} \quad 6.1$$

where θ_1 is the sum of the externally applied stresses. And $\theta_1 = \sigma_1 + \sigma_2 + \sigma_3$. Herein σ_1 and σ_3 are respectively major and minor principal stresses and σ_2 is the intermediate principal stress. Equation 6.1 may be written as

$$c \left(\frac{\partial^2 u}{\partial x^2} + \frac{\partial^2 u}{\partial z^2} \right) = \frac{\partial u}{\partial t} - \frac{\partial (\Delta \sigma)}{\partial t} \quad 6.2$$

for the case of plane strain and where the strain in the y-direction is considered zero. The quantity $\Delta \sigma$ is the change in the principal stresses at any point. Further, if it be assumed that change in principal stress at every point along the depth of the soil is equal to the change in the externally applied load, then it will be inferred that the rate of change in the external applied load is only time-dependent. Thus the term $\frac{\partial (\Delta \sigma)}{\partial t}$ in equation 6.2 assumes the form $\frac{d(\Delta \sigma)}{dt}$. Hence the equation 6.2 reduces to

$$c \left(\frac{\partial^2 u}{\partial x^2} + \frac{\partial^2 u}{\partial z^2} \right) = \frac{\partial u}{\partial t} - \frac{d(\Delta \sigma)}{dt} \quad 6.3$$

The added weight at the top, which is time-dependent, may be due to the variation in the external loading in form of surficial loads. Also load at the top may vary because of the addition of supplementary layers and thereby cause an increase in the maximum principal stress. In this case the top boundary is moving with time (moving boundary problem) while in the former case the top boundary does not move.

The presentation has been restricted to fully saturated clays, but the analysis may be extended to partially saturated soils by introducing the pore water pressure parameter \bar{B} (Skempton, 1954). This is necessary to estimate the pore pressures set up in an earth embankment during and after construction. Equation 6.3 is made use of to estimate the construction pore water pressures (and those during post-construction conditions) and is expressed as

$$c' \left(\frac{\partial^2 u}{\partial x^2} + \frac{\partial^2 u}{\partial z^2} \right) = \frac{\partial u}{\partial t} - \gamma \bar{B} \frac{dh}{dt} \quad 6.4$$

where the parameter \bar{B} is the fraction of the water pressure set up at any point under conditions of no drainage in the partially saturated soil to the water pressure that would be set up under the same conditions in a fully saturated soil; and c' is the coefficient of consolidation in two-dimensional

dissipation. The term γ is the bulk density of the soil and the term dh/dt is the time variation in the thickness of the soil layer that is added at the top. Thus it is seen that equation 6.4 has been derived with the usual assumptions made in the classical one-dimensional Terzaghi theory except for the following modifications:

- (a) the drainage of the pore water takes place in two directions, i.e., along x- and z-dimensions;
- (b) the soil is partly saturated as opposed to fully saturation; and
- (c) there is addition of soil layers at the top, i.e., the load application is time-dependent and the top boundary is moving.

It will be seen on comparing equations 6.3 and 6.4 that any solution obtained for a partly saturated soil is equally valid for a fully saturated soil if the term $\gamma\bar{B}$ is replaced by γ .

Equation 6.4 is useful in predicting pore pressures at any instant during and after construction of an earth-fill dam. This equation yields the excess pore water pressure provided certain physical constants such as the properties of the material going into the embankment; the rate of construction, and the cross-section of the dam together with the boundary conditions are known.

The solution to equation 6.4 may be obtained with the use of numerical technique ADI. For this to be feasible, the cross-section must be discretized in the x-z plane at

any instant of time. In order to achieve this symmetrical cross-sections are most helpful but in practice symmetrical sections are very rarely found. Dams and embankments with non-symmetrical central cores are more common. In the event of a non-symmetrical core, the cross-section has to be idealized as follows:

(a) Real boundary conditions expressed in finite differences are easy to satisfy if a rectangular mesh is used. An idealization (mentioned below) is made use of where a rectangular mesh is developed at the expense of real boundary conditions.

The idealization affected is for the upstream and downstream slopes. This stems from the fact that usually the values of upstream and downstream slopes bear a whole number relationship. This relationship is used in making up the mesh pattern. When the mesh is made up, usually the slopes (upstream and/or downstream) are approximated as steps (Figure 6.4(b)). This results in widening of the cross-section of the dam at certain sections. The space step in the vertical direction is so chosen that the height of the embankment never exceeds the actual height. Thus the lengths of the seepage paths in the horizontal direction is affected to a certain extent but care was taken not to lengthen unduly the lines of seepage. To assess the effect of this lengthening of the seepage path, two different idealized cross-sections for the Seitenoikea Dam (Arhippainen, 1964) were drawn and the values of pore pressure were determined. It was

found that the pore pressure values agree remarkably well (within an order of 0.1%). The line of seepage along the vertical direction is not affected and also the weight of the soil above the points of comparison (piezometer locations) were maintained the same as in the field.

(b) The actual rate of construction is usually adhered to. However in many cases, the rate of construction over few weeks or even few days is not uniform (e.g., Figure 6.3). If these rates are taken into calculation, the program becomes unduly unwieldy and may run into computational difficulties. In order to facilitate computation, the rate of construction over a region of time is chosen so that the assumed rate of construction is approximately an average of the actual rates in that interval of time. Thus instead of having a large number of varying construction stages, the entire construction season is divided into a small number of easily manageable rates of construction. The duration of construction stoppages is rigidly adhered to.

(c) One of the most important parameters that must be known in calculating the dissipation of excess of pore pressures is the coefficient of consolidation c_v of the material that goes into the embankment. Alternatively, the coefficient of permeability and the compressibility characteristics of the core material should be made known. Only, occasionally are such data available in the literature. If available, such information leads directly to the determination of the parameter c_v .

Frequently, however, only the recorded pore pressure readings during and after construction are available, and a representative value of c_v must be determined. The following procedure has been adopted.

A particular pore pressure cell is selected with respect to the boundary conditions. The recorded pore pressure readings are considered starting immediately after construction is completed. The pore pressure value just at the end of construction (i.e., beginning of post-construction period) is considered as the datum. Based on this datum, the degree of consolidation at various time intervals is calculated; and then the degree of consolidation values for the time intervals are compared with the theoretical one-dimensional consolidation curves for the appropriate boundary conditions. Thus the values of time factor for consolidation are determined at any time interval starting from the post-construction period as the initial time. Making use of the respective time factors, T , the time interval t and the length of the drainage path H , the value of c_v ($= \frac{TH^2}{t}$) is calculated. The value of c_v thus obtained is on the assumption of one-dimensional dissipation. This value gives an idea of the order of magnitude of the coefficient of consolidation for two-dimensional dissipation. However, the magnitude of c_v obtained is not the correct value nor can it be used for the duration of the construction period.

—By the above procedure a rough approximation of the order of magnitude of c_v is obtained and it is suitably modi-

fied to arrive at an appropriate value. Some of the published literature, however, yields the laboratory (or field) compression characteristics together with the permeability tests. This information directly leads to the determination of the parameter c_v .

(d) \bar{B} , the ratio of pore pressure developed to the principal stress, may be varied. The variation depends mainly on the moisture content of the soil going into the dam as referred to the optimum moisture content determined in the laboratory compaction tests. In a saturated soil the compressibility of the soil skeleton is almost infinitely greater than that of the pore water, and thus essentially all of a stress increment applied to a saturated soil is carried by the pore fluid and hence $\bar{B} = 1$. In a dry soil the compressibility of the pore air is almost infinitely greater than the compressibility of the soil skeleton, and thus essentially all of the increment in total stress applied to the dry soil element is carried by the soil skeleton, i.e., $\bar{B} = 0$. In partly saturated soils the very high compressibility of air relative to those of water and the soil skeleton results in values for the parameter \bar{B} somewhere between 0 and 1 until the percent saturation approaches 100%.

If the field moisture is above the optimum moisture content determined in the laboratory, then the soil is very nearly saturated and a value for \bar{B} may vary between 0.8 and 1.0. On the contrary, if the material has gone into the fill dry of optimum, the value of \bar{B} may be taken as varying between

0.6 and 0.7. The response to a variation in \bar{B} is reflected in the different results obtained and may be compared with actual performance in the field.

6.4 CASE HISTORIES

Six case histories have been studied and analyzed with respect to pore pressure development. The pore pressure data used in this study consisted of measurements in the embankments during and/or after construction, as indicated by piezometers installed prior to the completion of the embankments. The dams analyzed together with observational data are listed in Table 6.1. Materials and construction procedures varied widely for the dams, as is natural, reflecting the various countries and their organizations. In the following sections, a detailed analysis and the comparison between calculated and observed results are given for each of the cases considered.

6.4.A OTTER BROOK DAM

The cross-section of the Otter Brook Dam (New Hampshire, U.S.A.) with the piezometer locations is shown in Figure 6.2. Otter Brook dam is of rolled fill construction. The height is about 133 feet. It is of homogeneous impervious cross-section, except for the pervious fill drainage blanket and chimney, and rockfill and gravel slope protection. Both the

upstream and downstream slopes are 1 on 2 1/2.

On the right abutment the foundation is rock consisting of mica schist with some granite and gneiss. The left abutment consists of a deep deposit of glacial till. Impervious fill was placed directly on bedrock on the right abutment.

The glacial till embankment material was obtained from a borrow area opened in the left abutment above the elevation of the top of the dam. It consisted of well-graded gravelly clayey sand having 10-20% gravel and boulder-size material. The material was placed slightly dry of optimum moisture content and the average dry unit weight exceeded that at laboratory optimum. Explorations during design of the dam had indicated that the borrow material would be 2 to 3% wet of optimum. However, these explorations were made in winter and spring when the borrow area would have been at its wettest. Actually, the summer of 1957 proved to be one of the driest on record, and substantial drying of the material occurred both in the borrow pit and on the embankment. As a result, the material as actually placed averaged slightly dry of optimum moisture content and the average dry unit weight exceeded that at laboratory optimum.

Six closed-type piezometers were installed in the impervious fill during construction. After the upstream slope movements (bulging by about 3 feet), an additional five open-type piezometers were installed. At completion of the embankment, pore pressures ranged from 30 to 65% and 38 to 55%, of the pressure of the overlying fill as indicated by the closed-

type and open-type piezometers respectively. Since completion of the dam, all piezometers have shown decreasing pore pressures

The actual rate of construction is as shown in Figure 6.3. This figure has been redrawn from the original given by Linell and Shea (1960). The assumed rate of construction is also shown in the same figure by dotted lines. The assumed rates of construction are very close to the actual rates. The minor variations in actual rate of construction are smooth in this idealization. This is done so as to avoid programming and computational difficulties.

The assumed cross-section of the dam considered for analysis is as shown in Figure 6.4. That portion of the dam beyond the chimney drain was not considered. For this assumed cross-section, the upstream and downstream slopes bear an integer ($=4$) relationship; and the idealized cross-section of the dam is shown in Figure 6.4(b). Thus it may be seen, the idealized cross-section does not differ to any appreciable degree from the original cross-section. The height of the dam remains the same; while the length of the drainage path in the horizontal direction at the upper reaches is affected; it has been found, however, the length increase is very small. The section shown in Figure 6.4(b) is used for the calculation of pore pressures in conjunction with the assumed rate of construction.

The construction pore pressures in Otter Brook dam as observed are shown in Figure 6.5. A value for c_v was estimated using the method outlined in section 6.3 (Table 6.2). From

these calculations the value of c_v obtained was 1200 feet square per year. This value is for the after-construction period and is overconservative. As such a value of 1500 feet square per year for the coefficient of consolidation c_v was chosen for the duration of the construction and is made use of in the analysis of the estimation of construction pore pressures.

The value of \bar{B} was varied from 0.5 to 0.7 since the core material went in dry of optimum.

Using these values, the analysis was carried out with the assumed cross-section. The pore pressures computed are expressed as a percentage of the existing overburden and plotted against time (Figure 6.5). The computed values have been plotted only for the piezometer location 3A. Also the ratio of the computed pore pressure to the observed pore pressure is plotted against time. If the computed and the observed pore pressures are the same over the entire period of observation, the resulting curve should be parallel to the time axis and have a value of 1. The obtained results for various values of \bar{B} equal to 0.5, 0.6, and 0.7 are shown in Figure 6.6 for the piezometer location 3A. As may be inferred, the \bar{B} value, which not only depends on the moisture content of the material but also on the stress increment ratio, operating during construction was between 0.5 and 0.6.

6.4.B TOOMA DAM

Tooma Dam (Pinkerton and McConnell, 1964) is an earth and rockfill structure 68 meters high, situated at an elevation of 1220 meters on the Tooma river in the Snowy mountains of south eastern Australia. The dam forms a reservoir which essentially operates to provide flood retention and diversion of the waters of Tooma river.

The dam site is located in a V-shaped section of the valley with steep abutments rising about 80 meters above the river bed. The foundations for the dam consist of biotite granite, except for the upper part of the left abutment, the spillway and the downstream toe where the bedrock is granitic gneiss. In the river bed and lower parts of the abutments the dam is founded on sound rock.

The zoning of the embankment as constructed is shown in Figure 6.7. A description of the materials in each zone is as follows:

(1) IMPERMEABLE ZONE

The material used in the impermeable zone was a residual soil resulting from complete weathering of the biotite granite. The density of the material in place was required to be not less than 98% of the laboratory maximum dry density. The moisture limits specified were 1% on either side of the optimum moisture content, although for the upper reaches of the embankment these limits extended to 2% below optimum and

1.3% above optimum. During handling and compaction of this material, considerable breakdown occurred and substantially different properties were obtained for the material in the fill as compared with those obtained from samples tested for design purposes.

(2) FILTER AND DRAINAGE ZONES

The material placed in the filter and drainage zones consisted of selected quarry fines blended as necessary with crushed sand to give the required gradation for satisfactory filter and drainage properties.

(3) ROCKFILL ZONES

The rockfill was dense, fine grained quartzite which was hard and resistant to weathering. It consisted of a free-draining, well-graded mixture of rock fragments with maximum size about 15 centimeters.

The embankment was constructed in two distinct seasons embracing the 1959-1960 and 1960-1961 summer and autumn periods. Moisture conditions in the borrow area for impermeable material were markedly influenced by air temperature and humidity and it was only during these periods that the moisture content was low enough for placement.

The complete instrumentation is given by Pinkerton and McConnell (op. cit.) and installations for

measuring pore pressures are shown in Figure 6.7. Typical pore pressures recorded within the impermeable zone by vibrating wire type gauges during construction are given by Pinkerton and McConnell op. cit.). These show a characteristic build-up during periods when construction is in progress and dissipation during the off-season and after completion of construction.

The cross-section of Tooma dam is as shown in Figure 6.7. The assumed cross-section of the core for purposes of this analysis is given in Figure 6.8(a). The upstream and downstream slopes for the assumed section respectively are 1 vertical to 0.225 horizontal and 1 vertical to 0.9 horizontal. The downstream slope is a multiple '4' of the upstream slope. The upstream slope is approximated by steps as shown in Figure 6.8(b). The number of layers in the vertical direction can always be so chosen that the number is always a whole number multiple of '4'. Under such conditions the upstream slope can be approximated by steps. The idealized section (Figure 6.8(b)) is made use of in the analysis.

To obtain a representative value for c_v post-construction pore pressure values are very useful (section 6.3). In the case of Tooma dam such data is not available. However, the authors have cited the in-place coefficient of permeability as 0.5×10^6 centimeter per second. They have also presented the compression characteristics from which a value for the coefficient of volume compressibility is obtained as varying between 0.002 and 0.0025 centimeters square per kilo-

gram. From these values c_v has been calculated and it ranges from 0.25 to 0.35 centimeters square per second. In other words, the value of c_v ranges from about 8000 to 12,000 feet square per year. These values are conservative since they were obtained from one-dimensional dissipation.

To carry out the analysis a choice has to be made for the value of c_v . The measured pore pressures indicate that the pore pressures developed during the first stage of construction are quite low, and they almost remain at those values during the construction stoppage. This behavior indicates that the core material was able to dissipate the pore pressures quickly during the construction phase and during stoppage and dissipation was slower. Hence it is concluded that the c_v had a certain value during construction and it was reduced during the subsequent period of construction stoppage. With this in view and the values for c_v calculated from field data (a value of 12000 feet square per year during construction and 8000 feet square per year during shutdown) are chosen for the analysis.

The rate of construction made use of in the analysis is as shown in Figure 6.9. This is redrawn from the rate of construction supplied in the original contribution.

The in-place moisture content of the fill was 17.9%. The optimum moisture content determined in the laboratory from soil samples for design was on the average 18.4%. Thus it is inferred that the fill went in dry of optimum. Hence, the value of \bar{B} is varied through 0.6, 0.7, to 0.8.

The analysis was performed for the idealized section and for the material properties and the rate of construction noted above. The computed results were compared with the observed values of pore water pressure. There was a wide variation in the computed values and in the recorded pore pressures. The authors attributed the difference in theoretical curves (one-dimensional consolidation) and the recorded values due to erratic behavior of the piezometers. Flushing of piezometers at and soon after installation may have contributed to the relatively high initial pore pressures recorded at some points.

The computed results are expressed in terms of pore pressure ratio, r_u . The computed and observed pore pressure ratios are then compared (Figures 6.10 and 6.11) for the two piezometer locations P_5 and P_{10} . Figures 6.10 and 6.11 illustrate the variation of the pore pressure ratio with time. The computed values are in agreement with the observed values within practical limits. Both the figures indicate that during initial stages of construction a value of \bar{B} between 0.6 and 0.7 may be operating. During the next construction season, an average value of 0.50 for \bar{B} seems to be most appropriate.

6.4.C SEITENOIKEA DAM

The Seitenoikea Dam was built in 1960 across the Ema River, Finland (Arhippainen, 1964). The main section of the

dam crossing the river is 900 meters long, has a maximum height of 35 meters. It has a composite earth and rock-fill section with a central rolled earth-fill core surrounded by transition zones of graded filter material and supported by upstream and downstream rockfill zones (Figure 6.12). The foundation material at the site was mostly unconsolidated coarse silt and fine sand. Underlying this sediment was glacial moraine and bedrock. The silt was excavated under the highest part of the dam and the core was founded either on moraine or on bedrock.

The embankment core material which was glacial moraine has the following characteristic properties.

- (i) Average dry density in place was 2.01 tonnes/meter³. The fill dry density was expected to reach at least 95% of the Standard Proctor dry density.
- (ii) Average moisture content in place was 10.2%, while the average optimum moisture content obtained in the laboratory was 8.8%. That means that the fill went in wet of optimum.
- (iii) The degree of saturation of the placed material was in the range of 64% to 82% with an average value of 74%.

The location of the three pore pressure cells is given in Figure 6.12. The pore pressures recorded during the construction period and after the construction are given by Arhippainen, op. cit.

The rate of construction, as reported, has three different stages:

July 15 - Aug 10 1960	0.22 m/day
Aug 11 - Aug 28 1960	0.10 m/day
Aug 29 - Sept 20 1960	0.41 m/day.

This data is plotted in Figure 6.13.

The assumed cross-section of the Seitenoikea dam for analysis is shown in Figure 6.14(a). The approximation is made so as to result in side slopes bearing a definite integer relation to each other. The downstream and upstream slopes chosen are 0.8 on 1 and 1.2 on 1 respectively. The idealized cross-section of the dam (Figure 6.14(b)) is then worked out on the basis of the assumed cross-section. As can be seen, the height of the idealized dam section remains the same as that of the assumed section while the lengths of seepage in the horizontal direction are somewhat longer than the actual lengths (of seepage). To investigate if these lengthened seepage lines have any effect on the pore pressure dissipation, another idealized section for the assumed cross-section was chosen (Figure 6.14(c)). Pore pressures were calculated for both the sections (Table 6.3) and it has been found that the differences in values at the points of comparison (pore pressure cell locations) are very small. Thus the former idealization (Figure 6.14(a)) though it lengthens the seepage path to a certain extent, in no way affects the ultimate results.

The recorded pore pressures are quite difficult to reproduce. Arhippainen (op. cit.) has quoted the pore pressure ratios at the end of construction. The pore pressure ratio r_u at a point (Bishop and Morgenstem, 1960) is defined as the ratio of the pore pressure to the overburden weight above that point. The values are

$$\text{cell no. 4} \quad r_u = 0.37$$

$$\text{cell no. 5} \quad r_u = 0.20$$

$$\text{cell no. 6} \quad r_u = 0.29.$$

These values are made use of for the purposes of comparison. Also the values for pore pressure ratio during the construction stages are retrieved from the published results and are presented in Table 6.4.

To obtain a representative value of the coefficient of consolidation c_v for the core material, the procedure outlined in section 6.3 was used. The values of c_v obtained (Table 6.5) for various piezometer locations were examined. The values thus obtained are for the after construction period and are conservative since only one-dimensional consolidation was supposed to have taken place. As such the value for c_v was varied from 5.0 to 6.0 meters squared per day.

The material for the core construction was placed wet of optimum and as such the value of \bar{B} will be in the range of 0.80 to 0.90.

Making use of the above values together with the construction sequence noted above, a detailed comparison with

field observation may be made. The pore pressure ratios, r_u are computed at several time intervals and compared with the observed values, Table 6.4 (see Figure 6.15). From Figure 6.15 it may be concluded that a value of 6 meter squared per day for c_v and a value between 0.85 and 0.90 for \bar{B} give values of pore pressure very close to the observed values. The values of pore pressure ratios calculated are within practical limits of accuracy.

6.4.D MIRAFLORES DAM

The Miraflores Dam (Colombia), Figure 6.16 is located in an area of a deep seated intrusive formation of igneous rock known as 'Antioqueno Batholith'. The bedrock is quartz-diorite and is generally found approximately 60 feet or more below the ground level.

The soil varies from a pinkish silt having an average in-situ density of 80 pounds per cubic foot to a gray silty sand (locally termed 'decomposed rock') of average in-situ density of about 105 pounds per cubic foot. The Miraflores dam was built with predominantly sandy silt because there was not enough 'decomposed rock' readily available.

For measuring pore pressures, the twin-tube piezometers of USBR type were installed (31 numbers). Almost all the piezometers recorded consistent and valid readings. It is interesting to note that the piezometers were found to be so sensitive that it was often possible to tell from their read-

ings the fill placement activities such as starting or stopping the fill placing operations and the thickness of the layer placed.

The construction pore pressures developed are given by Li (1967) who reported that very high pore pressures developed in Miraflores dam. In general, the ratio of pore pressure to vertical stresses (assuming that vertical stress equals the vertical load of the fill) is very high during the initial stages of construction and decreases gradually as the height of fill increases, as shown by the convex shape of the observed pore pressure curves.

The major part of the earth fill was placed in one dry season (3 1/2 months - mid-December to beginning of April) round the clock. The rate of construction of the dam is shown in Figure 6.17. The assumed rate of construction is as shown in Figure 6.17. The assumed rates are very close to the actual rates of construction. The local minor variations in the actual rate of construction are smoothened by the assumed idealization.

Miraflores dam (Figure 6.16) is non-symmetrical in section and is provided with a chimney filter. For purposes of this study the portion upstream from the chimney filter is considered and the assumed cross-section is shown in Figure 6.18(a). The upstream and downstream slopes bear an integer relationship. The idealized cross-section of the dam (Figure 6.18(b)) is very close to the assumed cross-section. The percentage increase in length of seepage lines is very small.

The average in-place moisture content was 21.5% and is greater than the Proctor optimum moisture content, Li (1967) which ranges from 19-20%. It is inferred, hence, that the fill went in wet of optimum. The value of \bar{B} may be varied from 0.8 to 0.9.

A value for the coefficient of consolidation c_v is obtained on the lines outlined in section 6.3. The post-construction recorded pore pressures are used and the values for c_v obtained are given in Table 6.6.

Also the core material characteristics and behavior are reported by Li (1967). The coefficient of permeability of the fill material in Miraflores dam is of the order of 1×10^{-5} centimeter per second as determined by laboratory tests. The compression characteristics of the fill material are given in Figure 4 (Li, 1967). From these curves an average value of 0.011 feet square per ton for the coefficient of compressibility is obtained. Using these values the coefficient of consolidation c_v is calculated and c_v is 950×10^{-4} centimeters square per second.

Li (op. cit.) calculated a value for c_v using the 50% time factor to compare the calculated (one-dimensional dissipation) and actual measured pore pressure values. The approximate value for c_v is 1000×10^{-4} centimeters square per second.

Comparing the values of c_v obtained by above methods, it is seen that they agree very well in their numerical values. For purposes of computation a representative value of 1000×10^{-4} centimeters square per second for c_v is chosen.

Using the above values for the pertinent parameters the construction pore pressures were determined. The computed results at the end of construction are used to draw pore pressure contours which are compared with the measured values (Figure 6.19). As can be inferred from Figure 6.19 the computed values are lower than the measured values but are within 10% to 15% of the measured values. Figure 6.20 depicts the ratio of pore pressure to vertical load of the fill. In general, these ratios are very high at the initial stages of construction and decrease gradually as the height of fill increases.

6.4.E JARI DAM

The Indus Basin Project (Pakistan) is the largest single water development in the world and its two storage dams, Mangla and Tarbela are both exceedingly large. The substitution of Jari Dam (Binnie, *et al.*, 1967) in place of Mirpur dyke increased the capacity of Mangla reservoir without any increase in the reservoir level.

The Jari dam (Figure 6.21) is so positioned that the axis of the dam is parallel to the strike of the bedrock. The core, which is composed of rolled silt, covers a sandstone bed α_1 , which is continuous across the site. The higher sandstone bed α_2 is either covered by the core or outcrops in the upstream side of the core trench. Thus the continuous clay bed between α_1 and α_2 forms a cutoff connected to the

core. It was at Jari that shear zones were first discovered, and it was during the redesign that different design parameters for clay along and across the bedding were first used.

The instrumentation on the Mangla dam project has been designed to assist the detailed study of the construction and performance of all the major structures. Selected cross-sections of the dams have been instrumented in detail; Jari dam was instrumented in cross-sections at chainages 161 + 50 and 171 + 50. Pore pressure values are given for selected few points in Figure 103 (Binnie et al., op. cit.).

The cross-section of Jari dam is as shown in Figure 6.21. Only the portion of the dam between the upstream filters and the downstream drained silt (type B) is considered. The assumed cross-section for analysis is as shown in Figure 6.22(a). The upstream and downstream slopes are 1 vertical to 0.2 horizontal and 1 vertical to 0.5 horizontal respectively. The upstream and downstream slopes bear a relation of 5:2 and hence an idealized cross-section is made up as shown in Figure 6.22(b). By this idealization a rectangular mesh is obtained which is suitable for numerical analysis. Also as can be seen the ideal cross-section is very nearly the same as the actual section except for negligible lengthening (or occasional shortening) of the seepage lines. Care, however, has been taken not to unduly lengthen the seepage lengths. The height of the dam remains the same as the actual section.

The rate of construction of the dam at chainage 161 + 50

is obtained from Binnie, et al., (op. cit) and is reproduced in Figure 6.23. The assumed rate of construction is as depicted in Figure 6.23. As can be seen the assumed rates adhere to the actual rates very closely.

To obtain a representative value for the coefficient of consolidation of the silt type A, the detailed pore pressure readings recorded were obtained from Little (1969). The calculated values (obtained on the lines mentioned in section 6.3) of the coefficient of consolidation c_v showed a wide irregularity and no consistent results could be obtained (Table 6.7). This is thought to be due to a number of construction shutdowns in between the construction seasons. The values of c_v obtained seem to be small for the silty type of material that makes the core of the Jari dam. On observing the measured pore water pressures at various locations, it was found that the development of construction pore pressures at the initial stages is small thereby indicating that dissipation is rapid. At later stages of construction it has been observed that the pore pressure values maintain almost at the same level as the values at the initial stages. This concludes that as construction proceeded either the value of \bar{B} is decreasing or the value of c_v has decreased considerably. In the absence of any other data, the value of c_v is decreased in this analysis starting from a value of c_v that yields comparable pore pressure results to the measured values. The average values of c_v used in a set of calculations are:

4000 feet squared per year	during first 3 months of construction
3000 feet squared per year	during next 3 months of shutdown
3000 feet squared per year	during next 7 months of construction
2500 feet squared per year	during next 1 1/2 months of shutdown
2500 feet squared per year	during next 7 1/2 months of construction
2000 feet squared per year	during next 1 1/2 months of shutdown
2000 feet squared per year	during next 3 months of construction
1000 feet squared per year	during remaining post-construction season.

There is no record available for a value of \bar{B} made in the laboratory. \bar{B} determinations for the Jari core fill material were not made on site. The original calculations for the estimated construction pore water pressures refer only to a pore pressure ratio of 0.4, and not to any specific \bar{B} value (Little, 1969).

The idealized cross-section of the dam was analyzed for the specified rates of construction and the material properties mentioned above. Comparisons were made of the computed results with the observed data. To fit the computed values to the recorded data, a variation in set of values for c_v is envisaged. Other sets of values used for c_v are 4000 - 3500 - 3000 - 2000 - 1000 and 3500 - 3000 - 2750 - 2500 - 2000 feet squared per year for the same time sequence.

The measured and calculated values of pore pressure are shown in Figure 6.24 for the piezometer locations 27 and 28. The figures indicate that the computed results are in close agreement with observed values within practical limits of accuracy. It may be inferred that a value of 0.6 for \bar{B} is operative for a set of values for c_v 4000 - 3500 - 3000 - 2000 - 1000 feet squared per year.

6.4.F USK DAM

The earth dam situated at the upper reaches of the Usk River (U.K.) is 1575 feet long at crest level, 109 feet high with a cut off trench of maximum depth 77 feet. The volume of water impounded is 2700 million gallons.

The dam is made of boulder-clay fill carefully compacted in 12 inch layers sloping slightly away from the center line so as to avoid ponding. In the center, there is a diaphragm of puddle clay 6 feet wide at the top and increasing to 16 feet at the deepest part where it joins the 'spear head' of the 6 feet concrete filling in the cut off trench.

Embankment construction began in April 1951 and proceeded rather slowly at first (Sheppard and Ayles, 1957). Weather was an important factor controlling the use of equipment and placing of fill was possible for only part of the available time. With the comparatively high rainfall of about 60 inches per annum - half of which can fall during the construc-

tion season - it was realized that the fill was being compacted in a very wet state and a watch was kept on the pore water pressures.

Pressure cells were placed in the embankment fill as the work proceeded. These cells showed that the pressures resulting from the placing of the first 30 feet of embanking during the summer dissipated very slowly during the following winter season and that either the rate of construction would have to be reduced or some method found of speeding the rate of dissipation of pore pressures. The investigation of this problem, and its eventual solution by incorporating horizontal drainage blankets in the body of the dam, was the most interesting and unusual feature of the scheme (Sheppard and Aylen, op. cit.). The subsequent pore pressure readings have supported the theoretical anticipations. A detailed comparison between calculated and observed pore pressures has shown that towards the end of construction there was not good agreement when the lateral flow of pore water became important (Gibson, 1958).

The drainage blankets, which stopped 20 feet from the puddle core, consisted of 12 inches of river gravel placed on the prepared surface of the previous season's fill; then 6 to 9 inches of broken stone sized from 1/2 to 3 inches, followed by 18 inches of river gravel. The new season's fill was directly placed on this.

The actual rate of construction and the adopted (for calculations) rate of construction are given in Figure

6.26. The difference in the two rates is because of the thickness of the drainage layers (two in number at elevations 948 and 980). In the numerical calculations, the drainage layers are assumed to be thin layers (of no thickness) and also are assumed not to contribute substantially to the overburden weight.

The actual cross-section of the dam at chainage 800 + 00 is shown in Figure 6.25. The cross-section assumed for analysis is given in Figure 6.27. Only the downstream half of the dam cross-section is considered. The boundary along the center line of the puddle core is considered impervious. The bottom of the assumed cross-section is on a drainage mattress and hence it is considered a pervious boundary.

A value for the coefficient of consolidation c_v for the fill material is quoted as equal to 11 feet square per month (Gibson, 1958). This was a value determined in the laboratory. This value of c_v is made use in the present analysis. Gibson (op. cit.) quotes average values of \bar{B} and γ respectively as equal to 0.85 and 142 pounds per cubic foot obtained from laboratory and field tests. Later field evidence showed that \bar{B} associated with further load increments (after first construction season) decreased with increasing consolidation (Skempton, 1957). This phenomenon has been discussed in detail by Bishop (1957). The value of \bar{B} used in this analysis varies from 0.8, 0.85, to 0.90. This is so because the field moisture content was 2 to 3% more than the optimum moisture content determined in the laboratory (the wet site

conditions resulted in the material being placed on the wet side of the Proctor optimum moisture content).

The pore water pressures at the end of the October 1953 construction season are computed and drawn (Figure 6.28(a)) for a value of \bar{B} equal to 0.85. The pore pressure contours are mainly parallel to each other in the body of the dam. They are nearly horizontal with a close spacing near the drainage blankets. Thus it can be easily inferred that the principal dissipation of pore pressures is in the vertical direction. Similar pore pressure contours are drawn at the end of the completion of the dam, September, 1954 (Figure 6.28(b)). These figures also show that the main dissipation is in the vertical direction. This compares very well with the actual pore water pressures measured. Hence the contention of Gibson (op. cit.) that 'there was not good agreement between the calculated and the observed pore water pressures towards the end of construction when the lateral flow of pore water became more important' does not seem to hold good. Gibson (op. cit.) predicted the pore pressure values based on one-dimensional dissipation in the vertical direction. Figure 6.28 show the calculated as well as the measured pore water pressures. The observed and computed values agree very well. There were very few pore pressure cells installed near the downstream side of the cross-section and as such probably the pore pressure contours were drawn the way they were presented. It may be concluded that a two-dimensional study of the effect of dissipation on construction pore pressures

yields an assessment of the pore pressures within acceptable accuracy.

6.5 DISCUSSION

The method of solution presented in this study to predict pore pressures during and after construction is found to be very useful as the results of the six case histories suggest. As remarked earlier, the method is applicable to two-dimensional problems. The results obtained yield representative values on which basis a rational design of dams and embankments can be made. Also the method suggests an approach to control the rates of construction and the provision of drainage features in a dam or an embankment.

The ADI method is very versatile and can handle any changes in input values of material properties as time progresses. It also can handle any type of cross-section (with any form of drainage features incorporated) provided the cross-section is idealized.

The one important property of the embankment material that should be made known is the coefficient of consolidation, c_v . The method (section 6.3) adopted in this study to determine a representative value of c_v has proved to be very good. For example, in the case of Miraflores Dam (section 6.4.D), a value of 950×10^{-4} centimeters square per second for c_v was calculated from the available laboratory and field data. The value for c_v obtained using the method mentioned

in section 6.3 is 1000×10^{-4} centimeters square per second. Thus the values for c_v compare very well. However, it may be noted here that the coefficient of consolidation c_v has a different definition (section 2.4) depending on whether the consolidation is one- or two-dimensional. As such the value obtained for c_v by this process is only approximate. All the same this approach yields representative values to give an idea of the order of magnitude for c_v .

There are a number of limitations to the analysis presented here. In the process of idealization (to discretize an embankment cross-section), the resulting embankment used for analysis will be slightly different from the actual cross-section. Also the paths of seepage, especially in the horizontal direction, are lengthened (or shortened, as the case may be) at certain sections. By this means, the pore pressure dissipation is delayed and the time taken is longer. With judicious arrangement of the mesh size this discrepancy can be minimized but cannot be overcome altogether.

As the embankment is being constructed, fresh layers of soil are being added at the top. At any vertical section of the embankment, it was assumed that the increase in the maximum principal stress (in the vertical direction) at any point is the same and is equal to the weight of the added soil layer. Thus the increase in principal stress at all points along the depth is assumed uniform. This is at variance with reality. Any increase in load at a particular height is not felt uniformly throughout the soil depth; the load increase

is maximum at the top and decreases along the depth. At a certain depth and below it, any variation in the load at the top does not have any effect. However, the actual distribution of the load along a vertical section is hard to get, especially in a moving boundary problem where the thickness is changing with time. For purposes of simplicity, it is assumed that all points (along the depth) in a vertical section are affected to the same extent (equal to the weight of the soil layer added), i.e., there is a uniform distribution of added stress throughout the depth.

Due to the addition of load (because of the growing layers) at the top, the total principal stress at all points in the central portion of the dam increases by the magnitude of the added load. Because of dissipation of pore pressure there will be changes in effective stress in both , vertical and horizontal directions. What proportion of the load contributes to the horizontal stress is not known.

While developing the computer program for the solution of non-symmetrical sections of dams, it was assumed that the weight added at the top is operative on all nodal points then existing irrespective of their location. Thus the algorithm yields conservative results and are on the safe side.

Thus the algorithm developed in this study solves dam cross-sections in a grid form. All the grid points are subjected to the same load irrespective of its position; at the same time, the lines of seepage are almost the same as in the original cross-section(s). In other words, the analysis is

concerned with rectangular cross-section embankments as far as the load is concerned, while the solution actually treats real drainage paths. This approximation could be eliminated in subsequent work.

The observations made from the examples presented in section 6.4 are intended to present a new approach for predicting pore pressures developed during and after the construction of embankments. The following observations may be made in this connection.

There are a large number of factors which influence the build up of construction pore water pressures. Because of their interdependence, it is difficult to isolate the influence of any one factor on the development of construction pore pressures. The influencing factors may be summarized as: rate of construction including construction stoppages, nature of the core material, the location of drainage features, the length of the drainage path, the overburden weight, and the placement-water content.

The rate of construction definitely influences the pore pressures developed during construction. Increasing the rate of construction results in an increasing rate of pore pressures with overburden weight. Bishop (1957) has shown that if dissipation of pore pressures occurs during construction stoppages the rate of increase in pore pressure with subsequent increases in overburden pressure is lessened. This has been found to be true in the case of Jari and Miraflores.

The higher the value of the coefficient of consolidation c_v of a core material the quicker the dissipation of pore pressure. Thus the soil type has a certain influence on the build up of construction pore pressures.

Where internal drainage is provided adjacent to or within the core, dissipation of pore pressure occurs (e.g., Usk and Miraflores). This helps in lowering subsequent increases in pore pressures with increasing fill height.

The fill height influences the length of the drainage path and the overburden weight. Thus the dissipation of excess pore pressures developed are influenced to a certain extent.

Sherard et al. (1963) stated that 'water content at which the embankment is constructed has the largest influence on the magnitude of the pore pressures which develop'. This study, in general, supports this conclusion. For placement water contents on the wet side of optimum water content, pore pressures rapidly increase with increasing water content.

At this stage some of the anomalies occurring in the field may be mentioned. All values of water content, density, etc. reported are usually the weighted mean values found by various sampling techniques. Some random variation of these quantities is expected. However, in several cases because of the erratic nature of the weather during placement, or the borrow material significant deviations may be observed.

Also the type of piezometer used has an influence on the measured value of the pore pressure. Piezometer designs

have been modified and made more efficient. Bishop et al. (1964) have pointed out the difficulties in measuring pore pressure in partly saturated compacted soil and conclude that much of the standard equipment currently used for pore pressure measurements in rolled fills is not in fact suitable for this purpose. The accurate measurement of pore water pressure in partly saturated soils requires properly designed piezometers if the difference between pore air and pore water pressure is significant. The importance of the error due to inadvertent measurement of air pressure will depend on the soil type, the placement water content and the height of fill above the piezometer.

Table 6.1 Observational data for impervious core zones, dams

Dam	Location	Height of Dam	Compaction Data			Field Deviation from Std. Proctor	Max Pore Pressure Ratio at end of Construction
			Std. Proctor γ_D	Proctor OMC	Av. in-place γ_D	OMC	
Otter Brook	U.S.A.	130 ft.	125.7 lb/ft ³	11.3%	120 lb/ft ³	14.3% +3%	0.65
Tooma	Australia	68 m	1.68 t/m ³	18.4%	1.73 t/m ³	17.9% -0.5%	0.20
Seitenoikea	Finland	35 m	2.10 t/m ³	8.8%	2.01 t/m ³	10.2% +1.4%	0.30
Miraflores	Colombia	55m	102.0 lb/ft ³	19.6%	103 lb/ft ³	21.6% +2.0%	0.70
Jari	Pakistan	230 ft.	97.0 lb/ft ³		102 lb/ft ³	dry of OMC	0.35
Usk	U.K.	109 ft.	142 lb/ft ³		142 lb/ft ³	wet of OMC	0.25

Table 6.2 Calculation for a representative value of co-efficient of consolidation, Otter Brook Dam

Piezometer Location	Time t in Months	Pore Pr % of Over Burden	Degree of Consolidation	H Ft.	a/H	Time Factor T	$c_v = \frac{TH^2}{t}$ Ft ² /Month
3A	3.5	52.0	-	120	0.2		
	8.0	42.0	0.19	120	0.2	0.030	96
	10.0	40.0	0.23	120	0.2	0.040	92
2A	3.5	42.0	-	120	0.2		
	8.0	39.0	0.07	120	0.2	0.020	64
	10.0	38.0	0.10	120	0.2	0.025	60
2B	3.5	64.0	-	120	0.2		
	8.0	52.0	0.20	120	0.2	0.032	102
	10.0	50.0	0.22	120	0.2	0.040	92

Table 6.3 Values of pore pressure at cell
no. 5, Seitenoikea Dam

$$\bar{B} = 0.90 \quad c_v = 6.0 \text{ meter}^2/\text{day}$$

Time (days)	Pore Pressure Values (t/m) ²	
	Cross-Section 1	Cross-Section 2
1	6.951	6.949
14	9.112	9.109
27	9.100	9.100
45	11.223	11.220
56.5	13.210	13.210
68.0	9.332	9.330

Table 6.4 Observed values of r_u ,
Seitenoikea Dam

Time (days)	r_u
1	0.55
27	0.40
56	0.30
68	0.20

Table 6.5 Representative value for c_v , Seitenoikea Dam

Pore Pressure Cell	Time t (days)	r_u	Degree of Consolidation	Height $H(m)$	a/H	Time Factor T	$c_v = \frac{TH^2}{t}$ m^2/day
5	-	0.20	-	22.5			
	10	0.19	0.05	22.5	0	0.10	5.06
6	-	0.30	-	22.5			
	10	0.28	0.07	22.5	0	0.11	5.56

Table 6.6 Representative value for c_v , Miraflores Dam

Piezometer Location	Time	Pore Pressure in Meters	Degree of Consolidation	H Meters	z/H	Time Factor T	$c_v = \frac{TH^2}{t}$ meter ² /day
17	April 10	2065.0	-				
	June 30	2055.5	0.005	36	0	0.05	0.80
18	April 10	2065.5	-				
	June 30	2055.0	0.005	36	0	0.05	0.80

Table 6.7 Representative value for c_v , Jari Dam

Piezometer Location	Time (days)	Pore Pressure lb/ft ²	Degree of Consolidation %	H Ft.	z Ft.	Time Factor T	$c_v = \frac{T-H^2}{t}$ ft ² /year
80	-	6440	-	230	75		
	35	6252	2.92			0.005	2758
	124	6159	4.36			0.007	1090
	155	6096	5.34			0.008	997
28	-	6926	-	230	35		
	35	6864	0.89			0.0	495
	90	6738	2.71			0.002	429
	124	6614	4.55			0.004	311
27	-	5585	-	230	35		
	35	5398	3.35			0.0025	1379
	90	5148	7.82			0.0060	1287
	124	4961	11.17			0.0080	1246

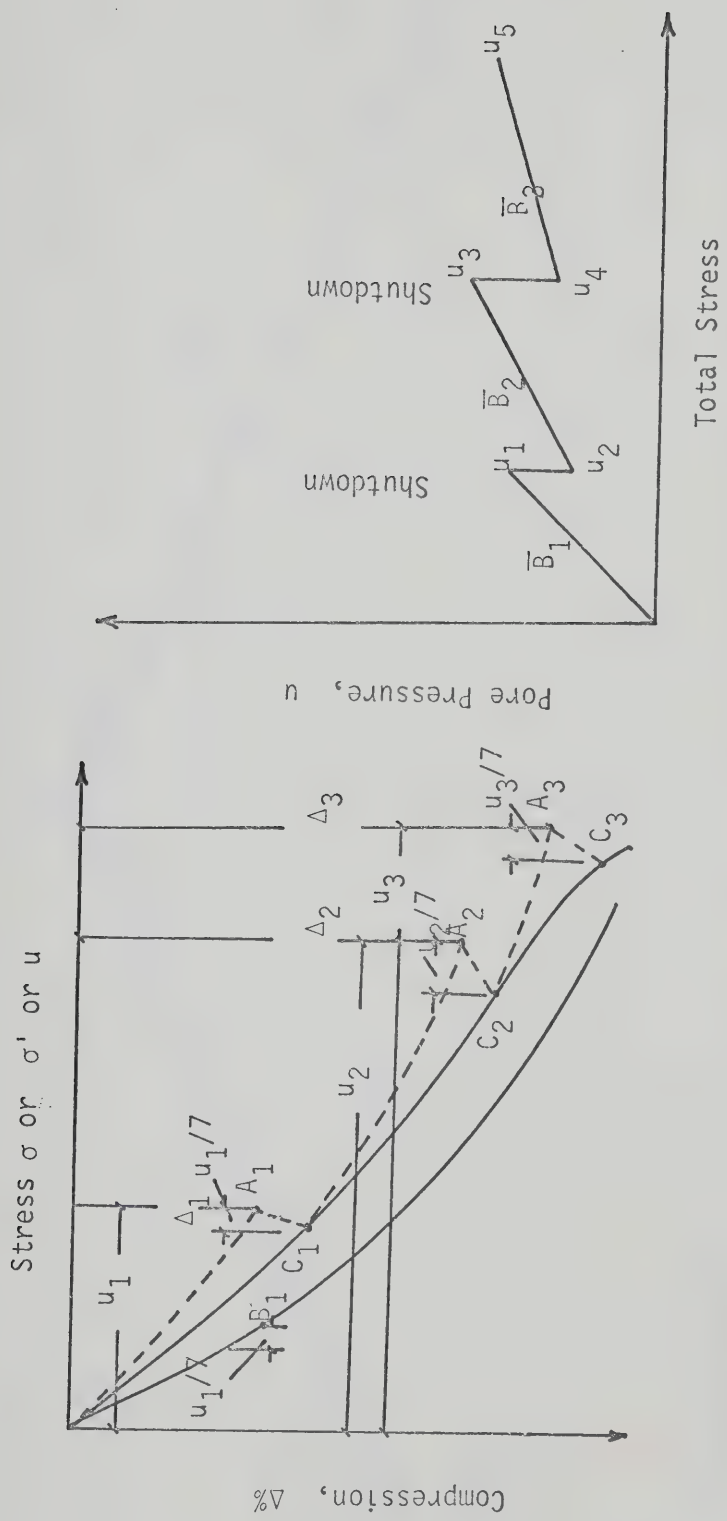


FIG. 6.1 COMPUTATION OF PORE PRESSURE ALLOWING DRAINAGE (Bishop, 1957)

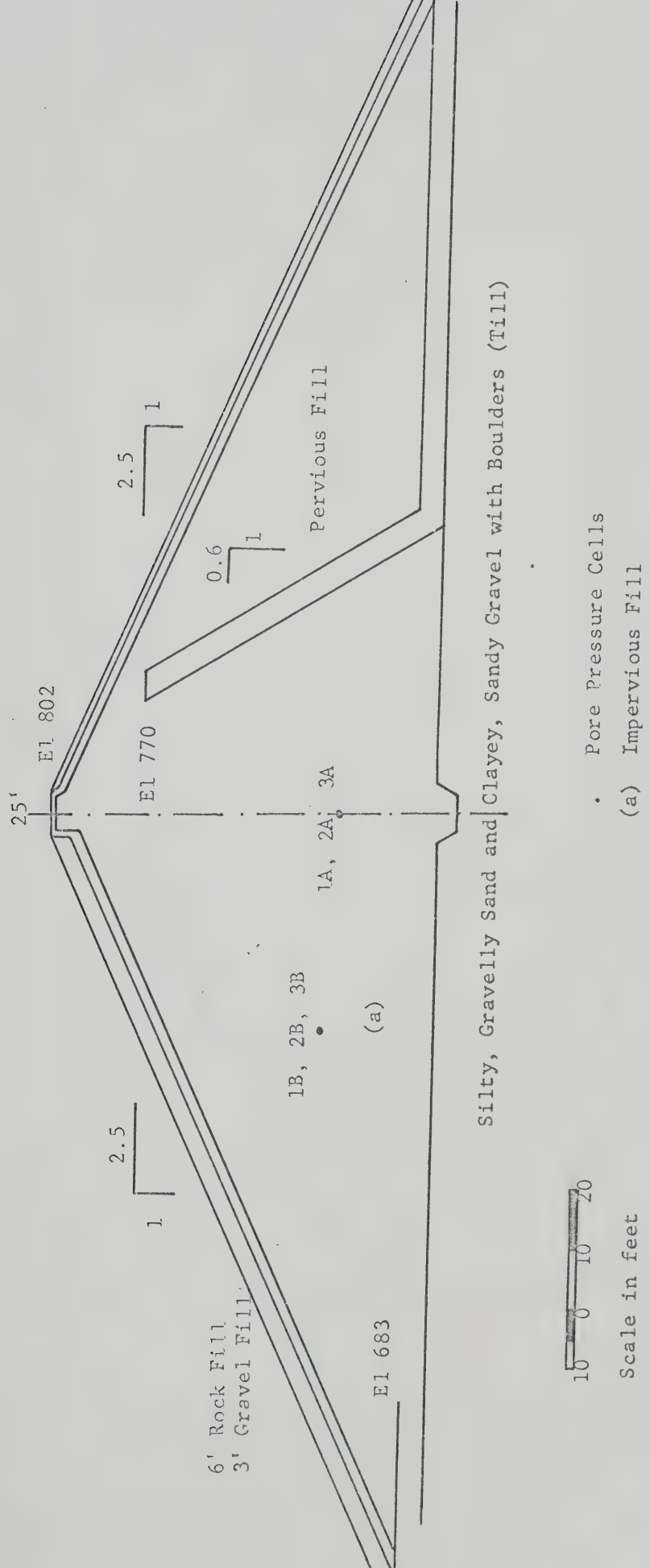


FIG. 6.2 CROSS-SECTION OF OTTER BROOK DAM

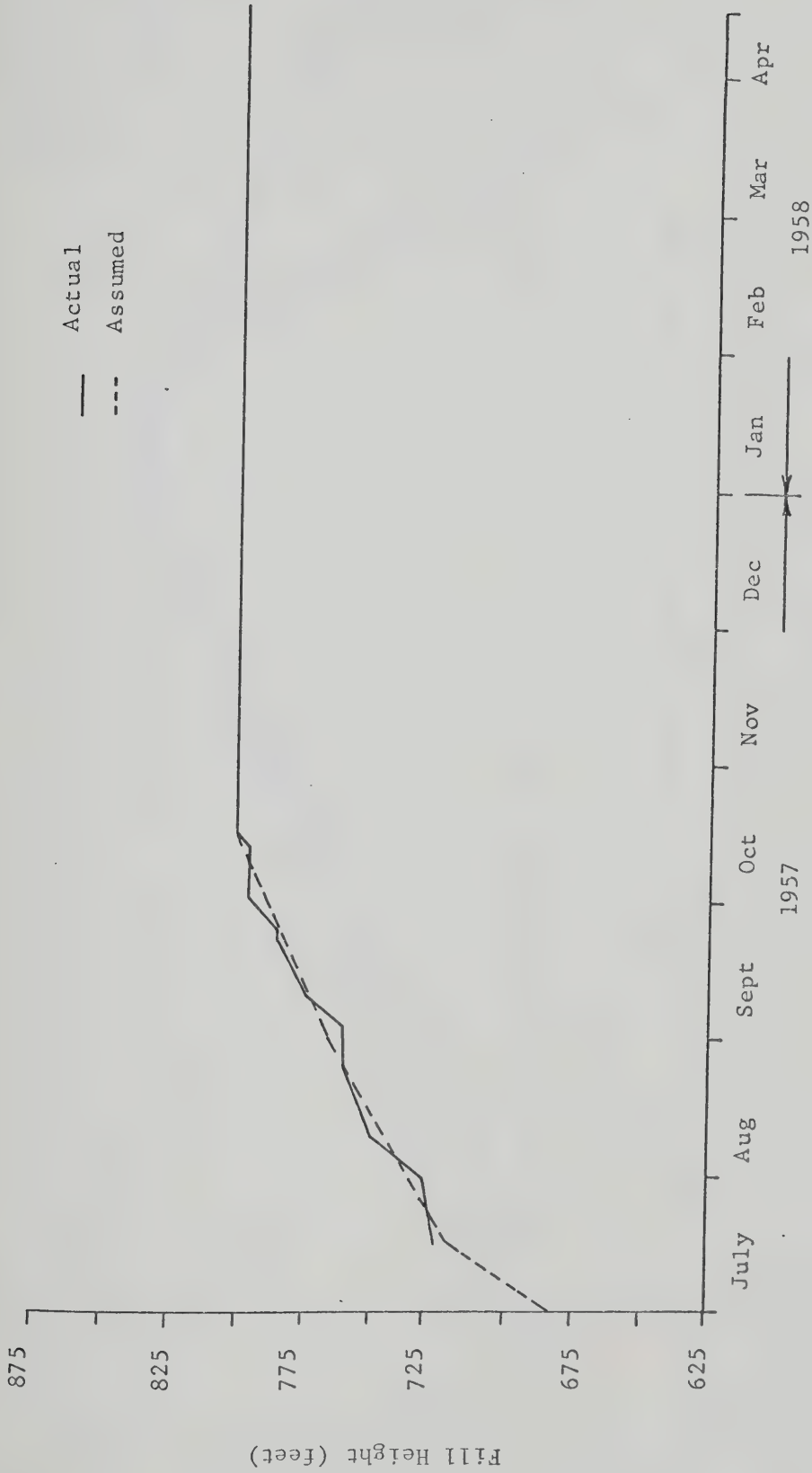


FIG. 6.3 RATE OF CONSTRUCTION OF OTTER BROOK DAM (Linell and Shea, 1960)

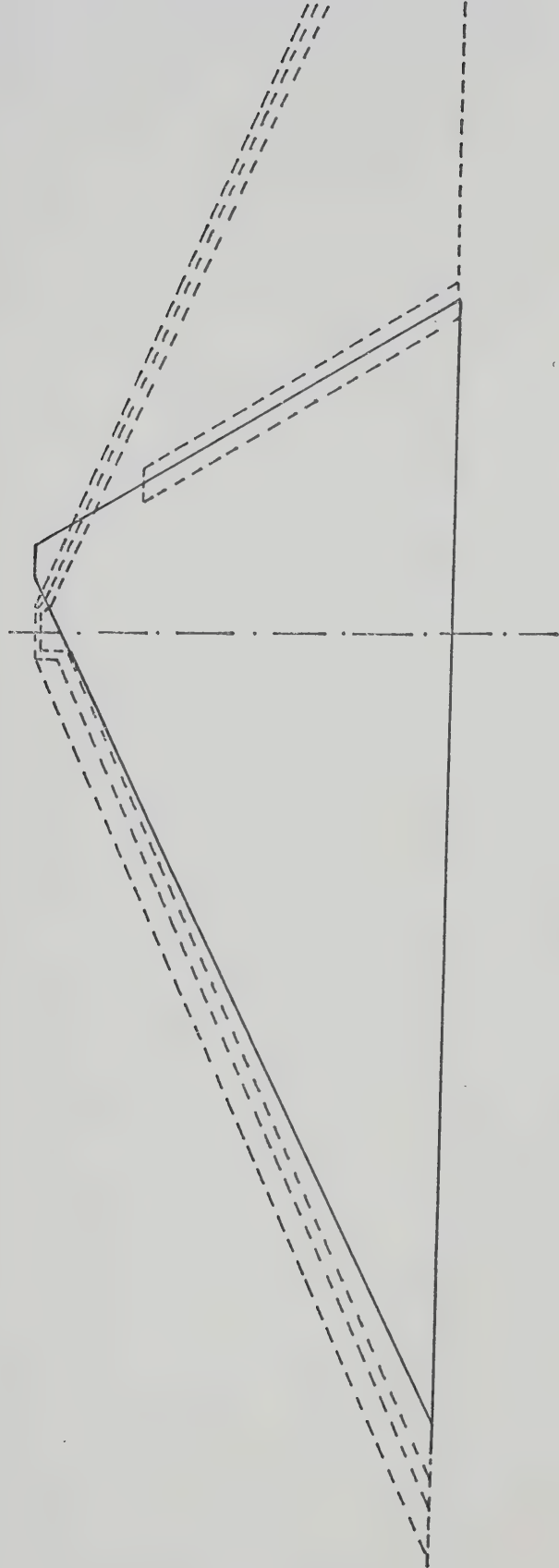


FIG. 6.4 a ASSUMED CROSS-SECTION OF OTTER BROOK DAM

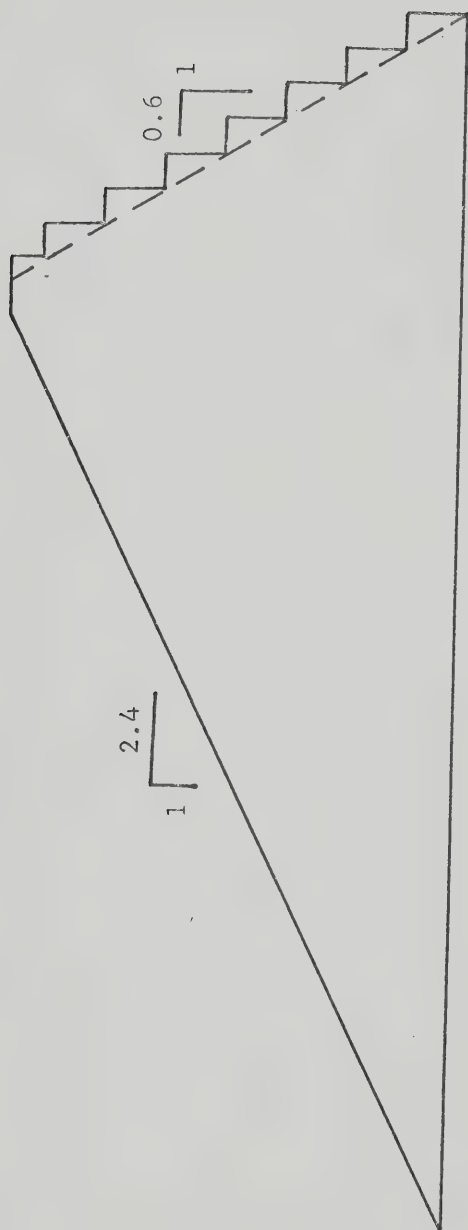


FIG. 6.4. b IDEALIZED CROSS-SECTION OF OTTER BROOK DAM

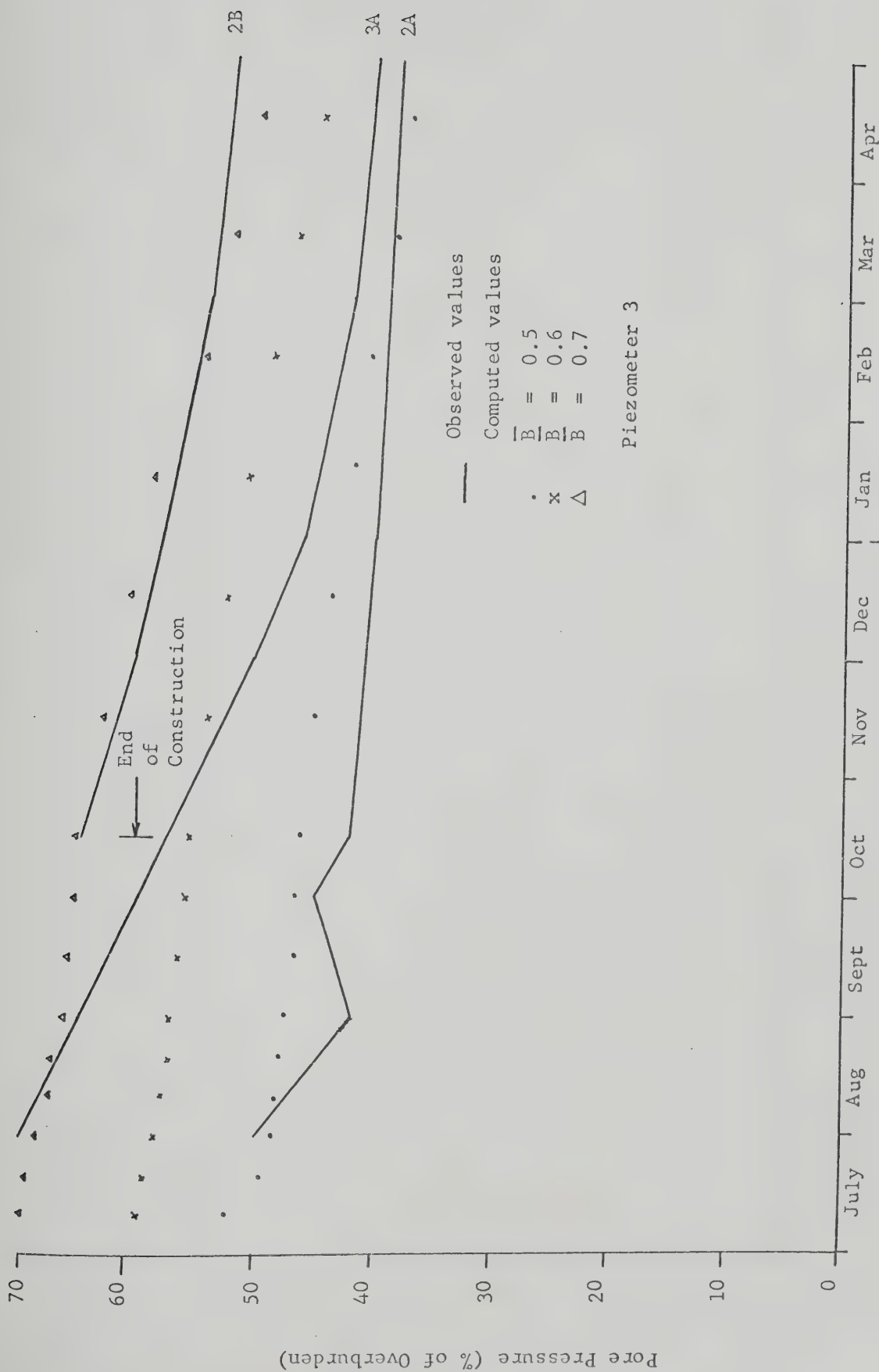


FIG. 6.5 DEVELOPMENT OF CONSTRUCTION PORE PRESSURES, OTTER BROOK DAM

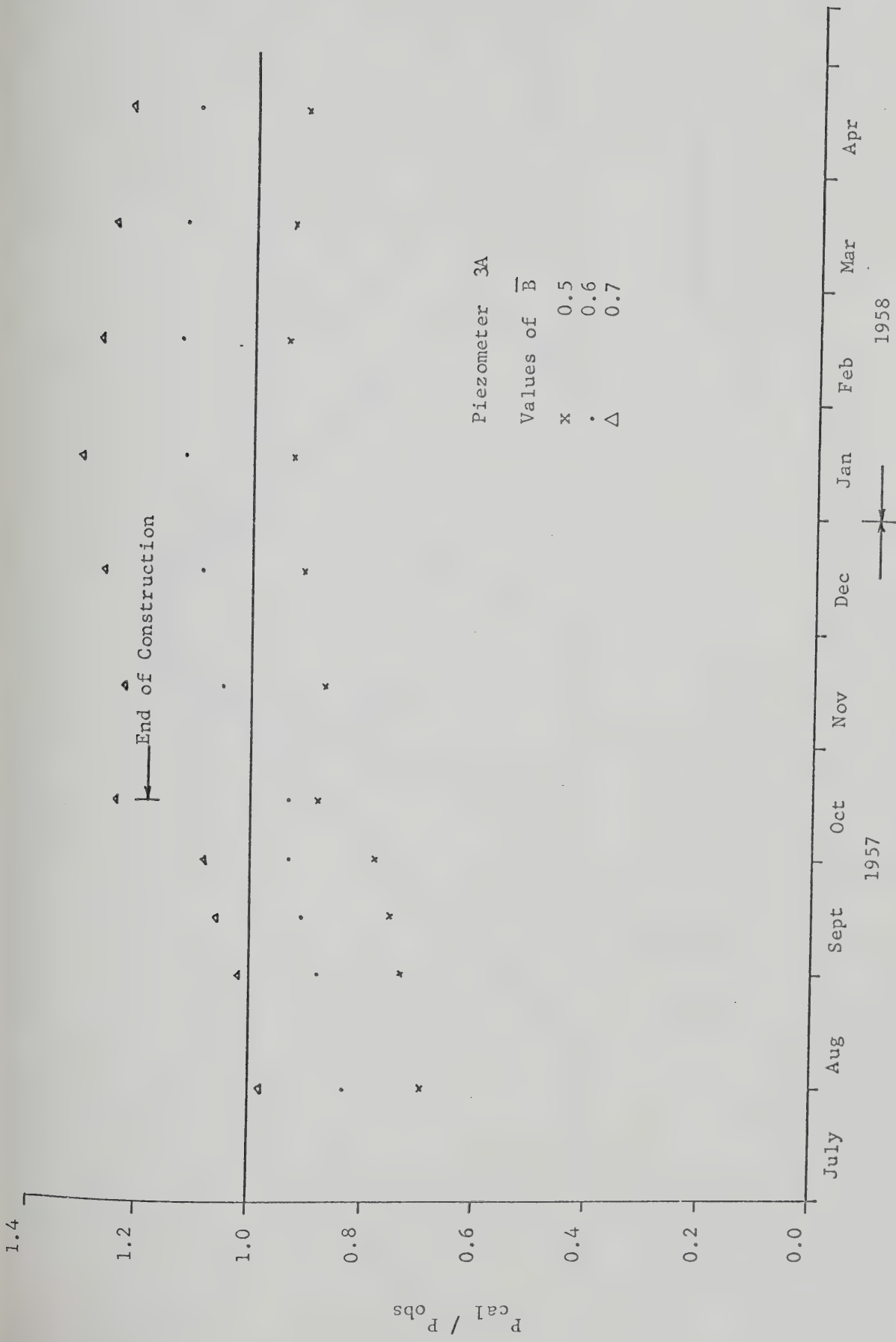


FIG. 6.6 PORE PRESSURE RATIO WITH TIME, OTTER BROOK DAM

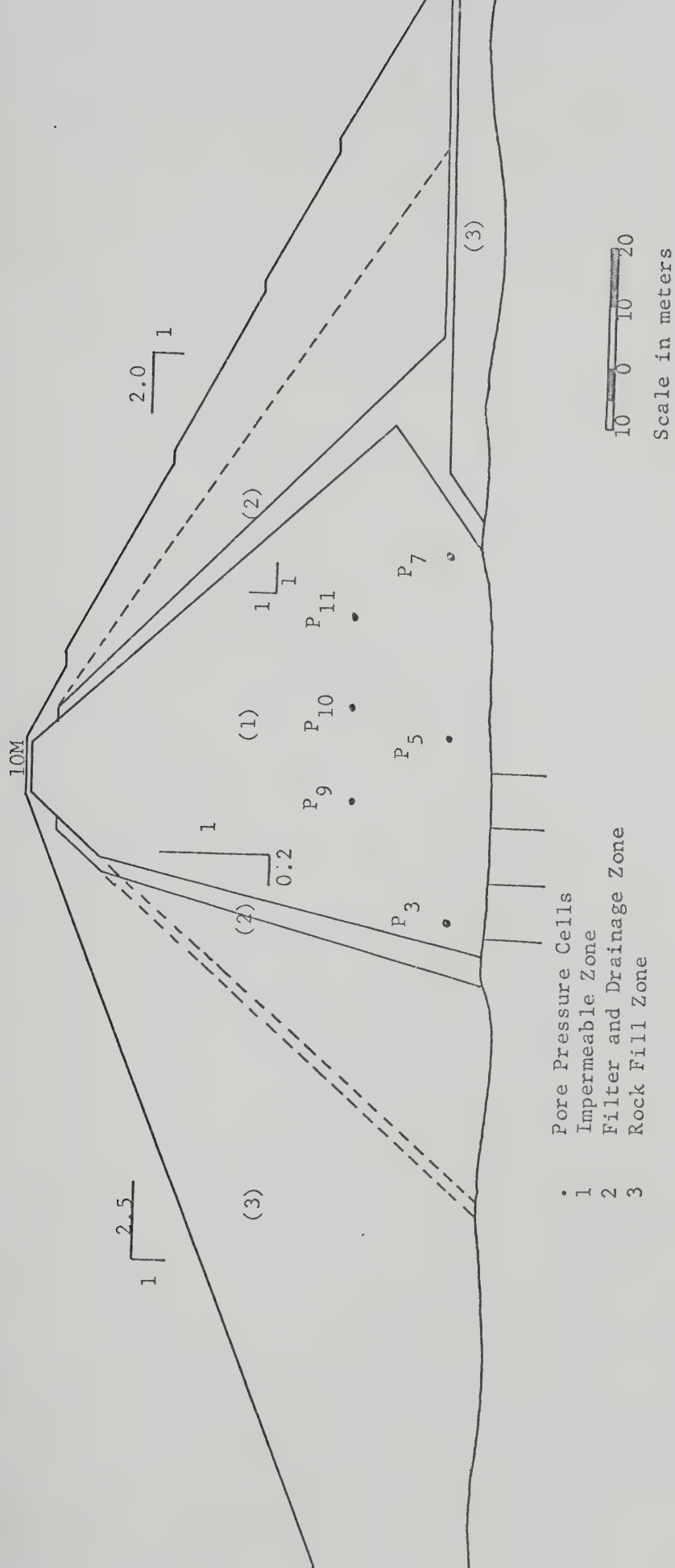


FIG. 6.7 CROSS-SECTION OF TOOMA DAM

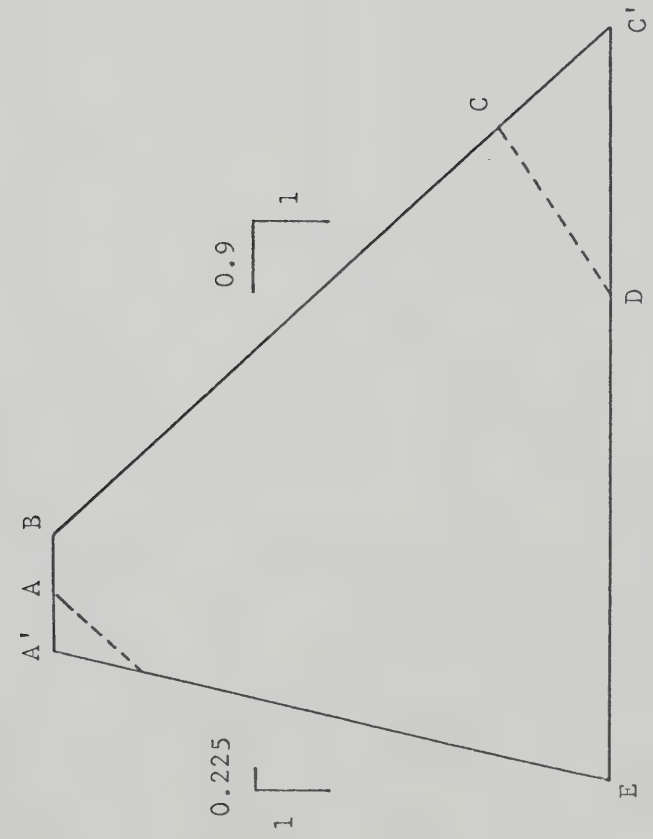


FIG. 6.8 a CROSS-SECTION OF CORE OF TOOMA DAM

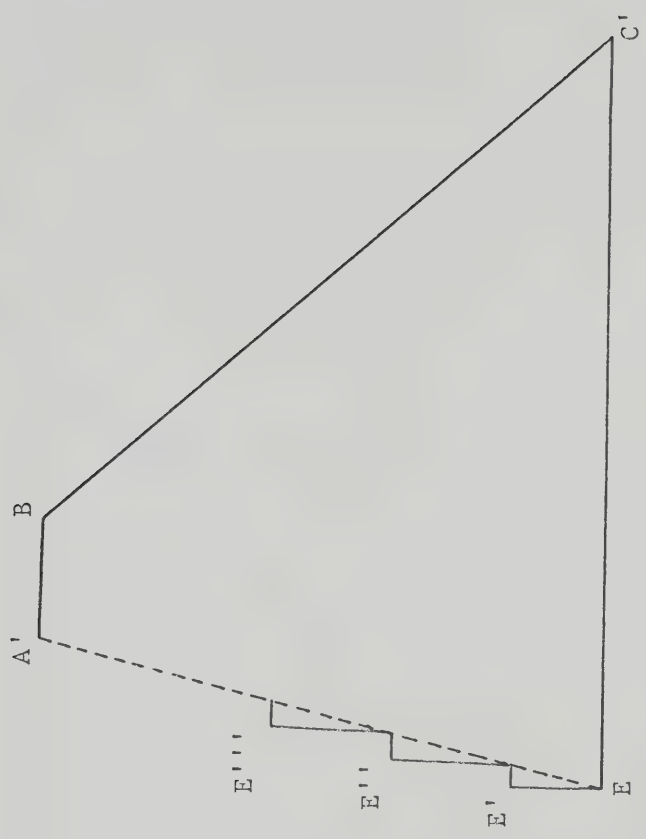


FIG. 6.8 b IDEALIZED CROSS-SECTION OF CORE OF TOOMA DAM

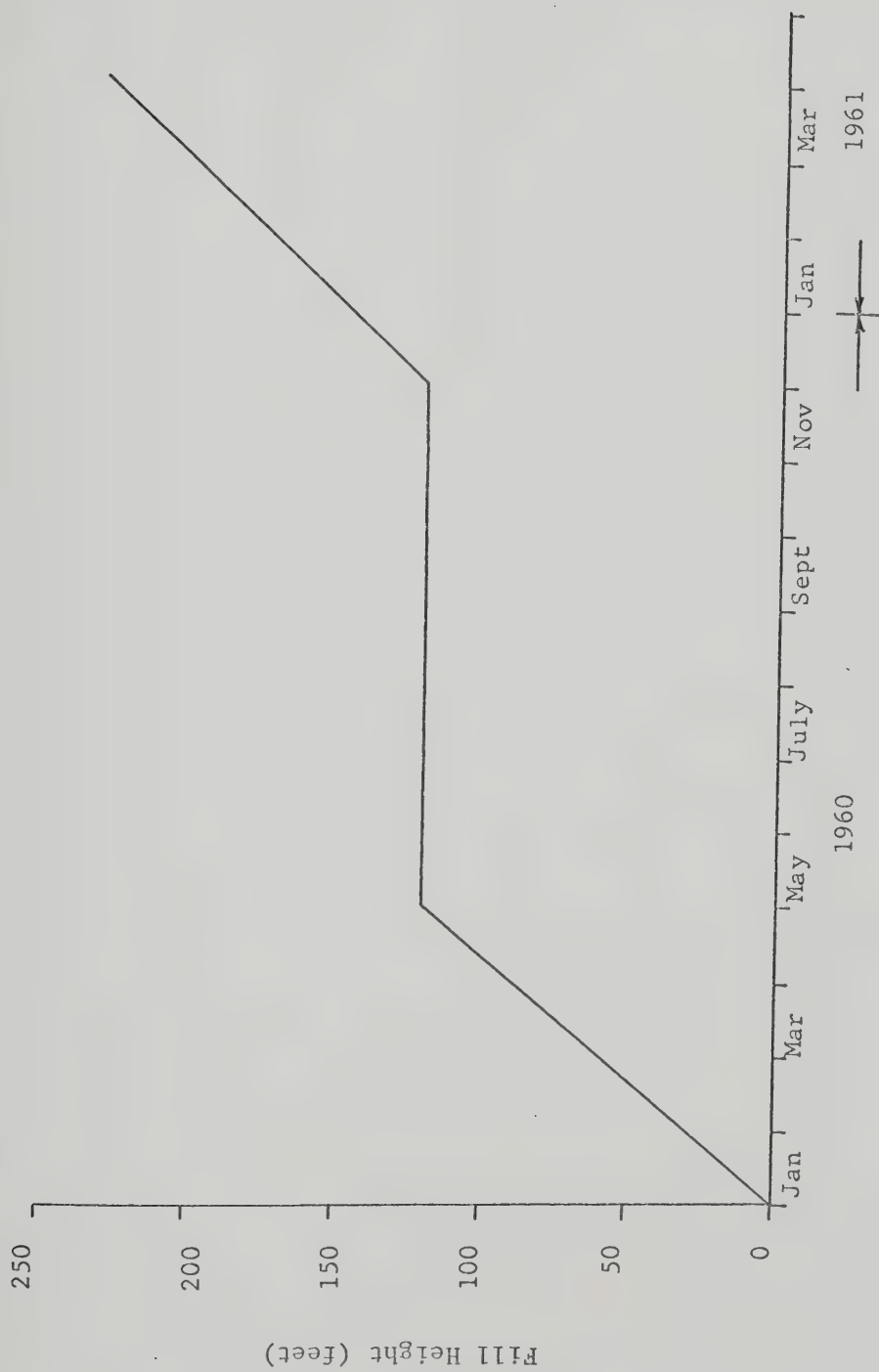


FIG. 6.9 RATE OF CONSTRUCTION OF TOOMA DAM (Pinkerton and McConnell, 1964)

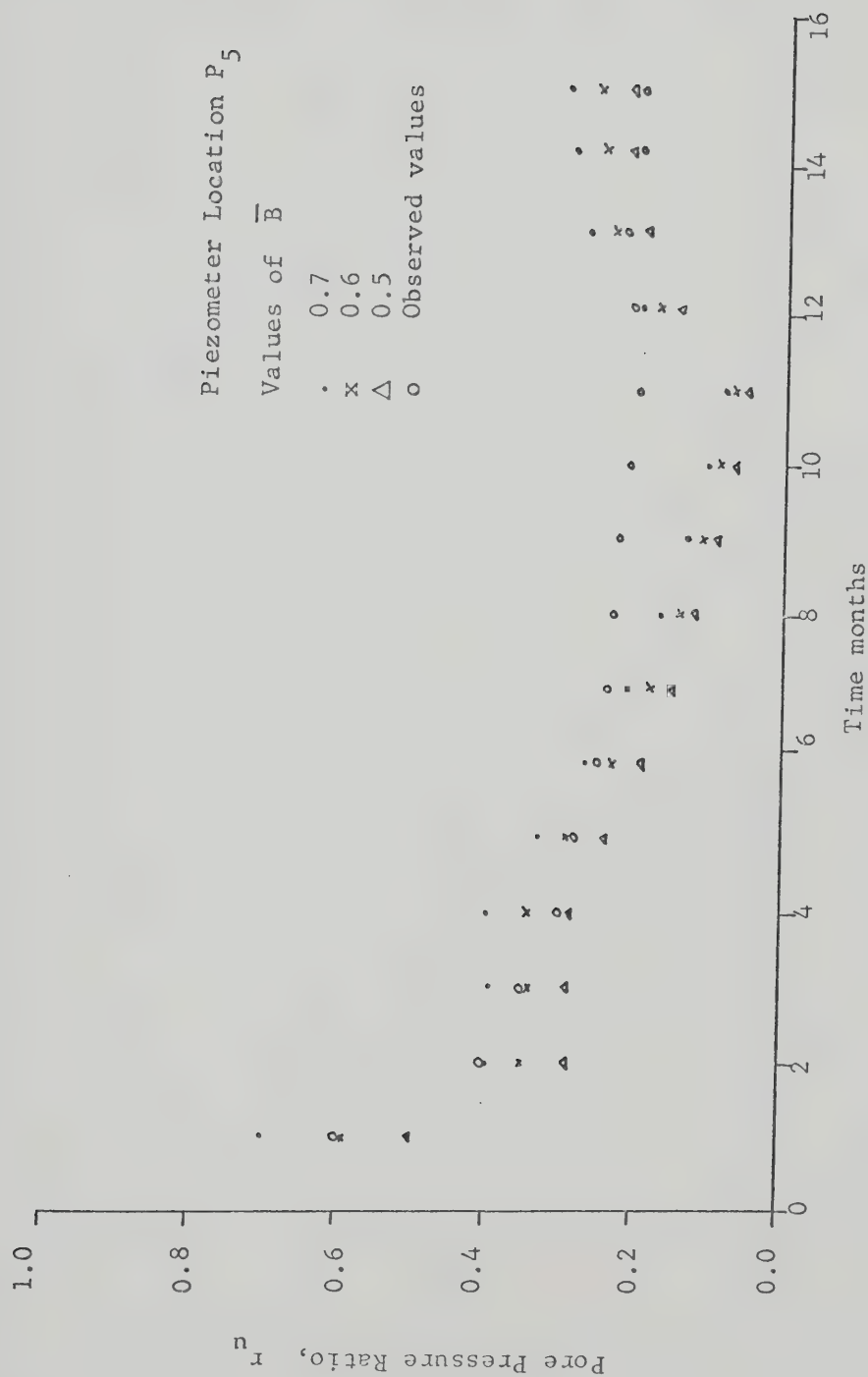


FIG. 6.10 VALUES OF PORE PRESSURE RATIO, TOOMA DAM

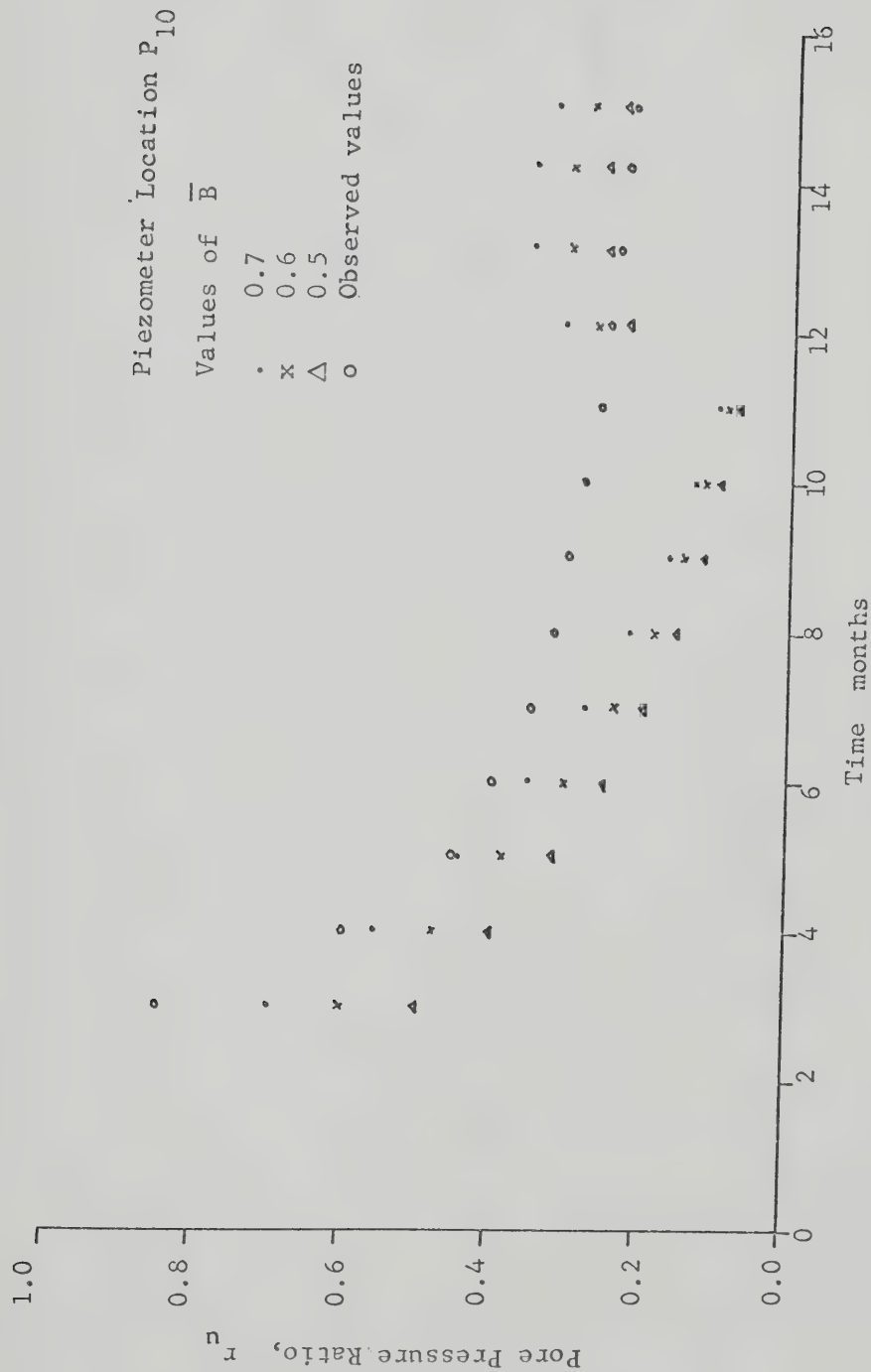


FIG. 6.11 VALUES OF PORE PRESSURE RATIO, TOOMA DAM

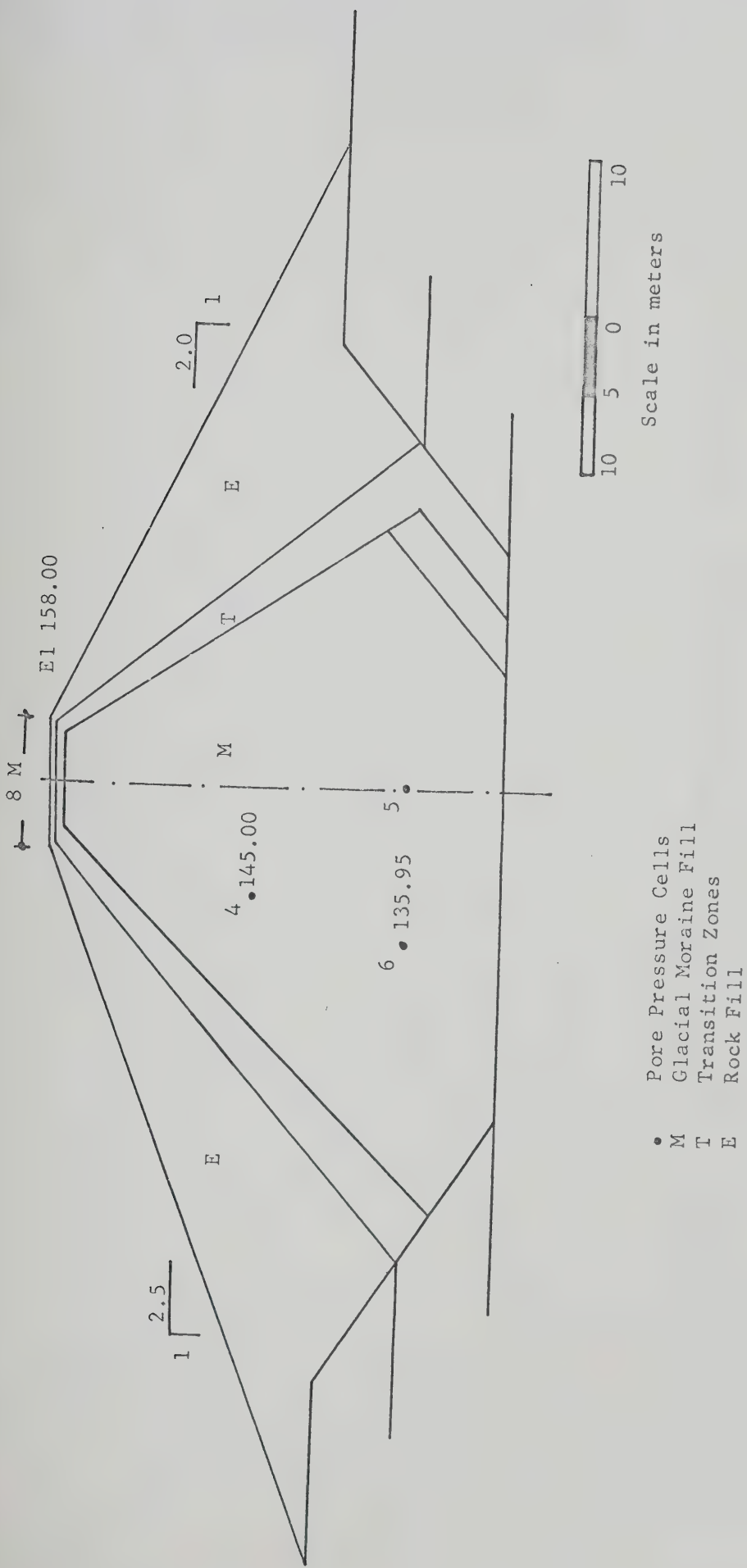


FIG. 6.12 CROSS-SECTION OF SEITENOIKEA DAM

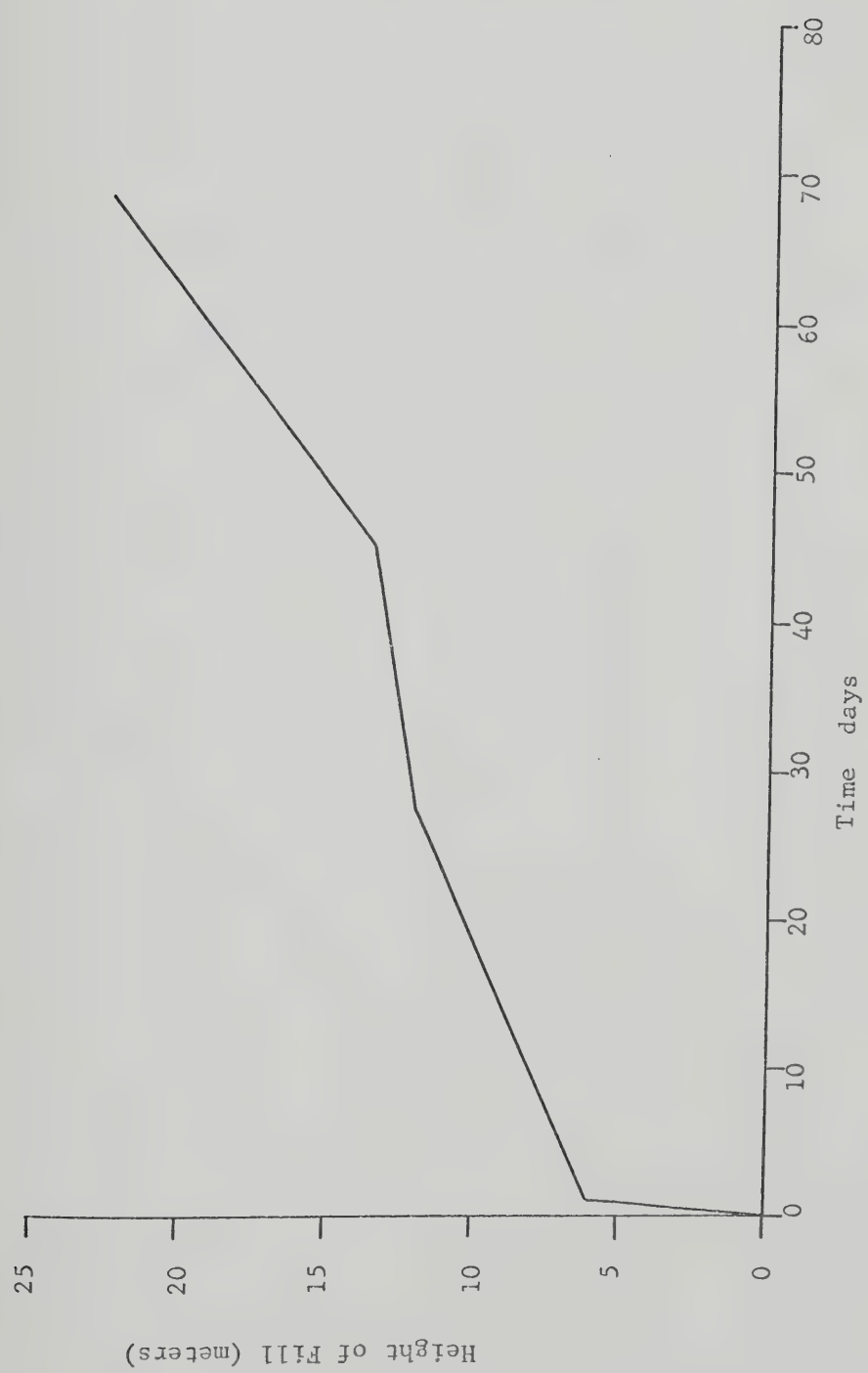


FIG. 6.13 RATE OF CONSTRUCTION OF SEITENOIKEA DAM (Arhippainen, 1964)

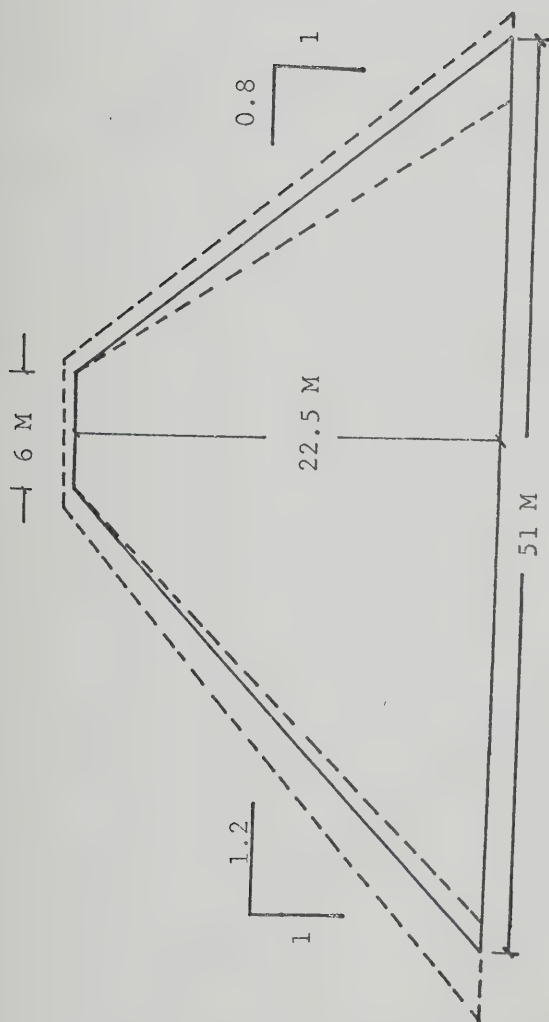


FIG. 6.14 a ASSUMED CROSS-SECTION OF SEITENOIKEA DAM

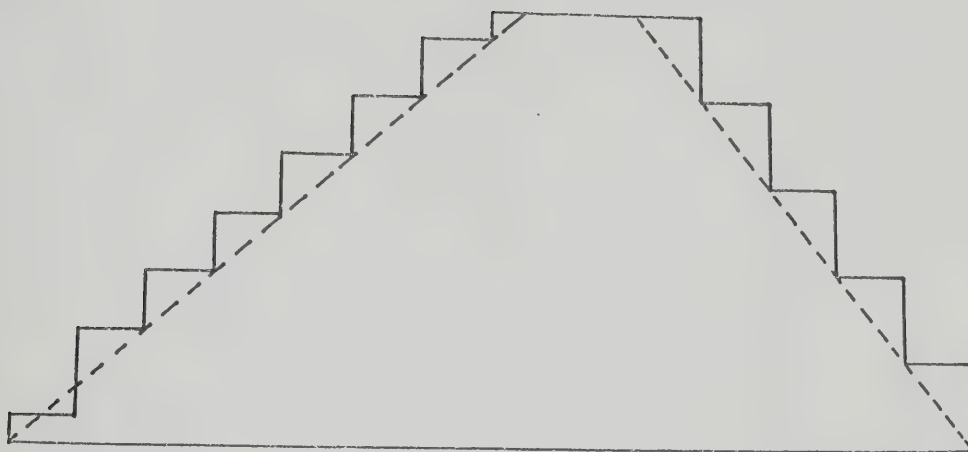


FIG. 6.14 b IDEALIZED CROSS-SECTION

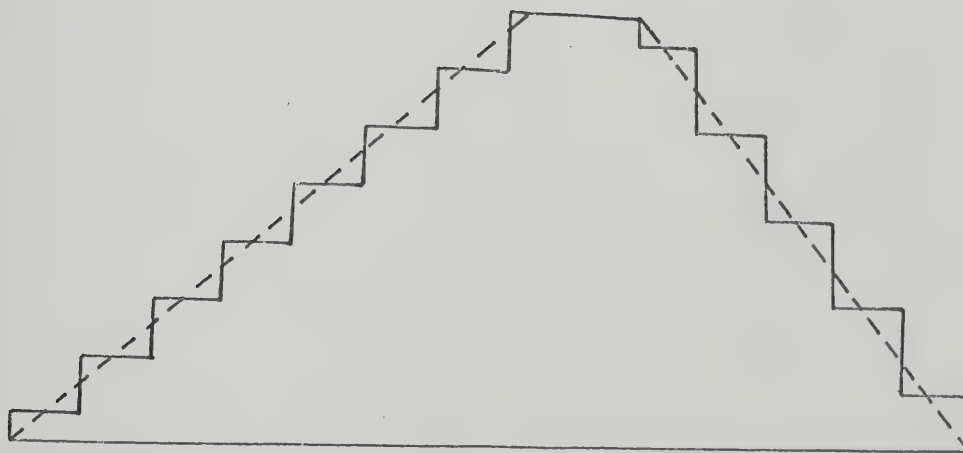


FIG. 6.14 c ALTERNATE IDEALIZED CROSS-SECTION

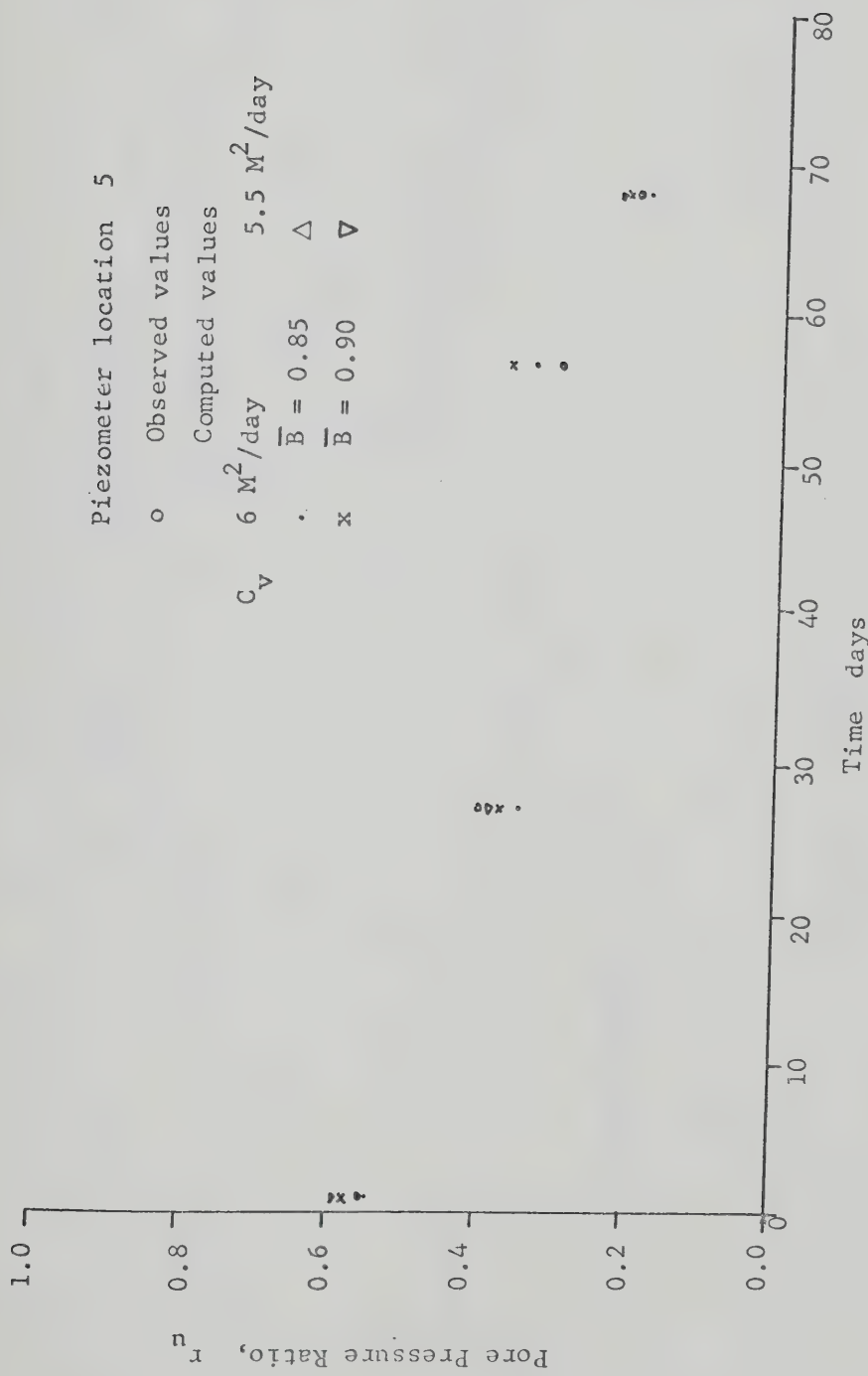


FIG. 6.15 VALUES OF PORE PRESSURE RATIO, SEITENOIKEA DAM

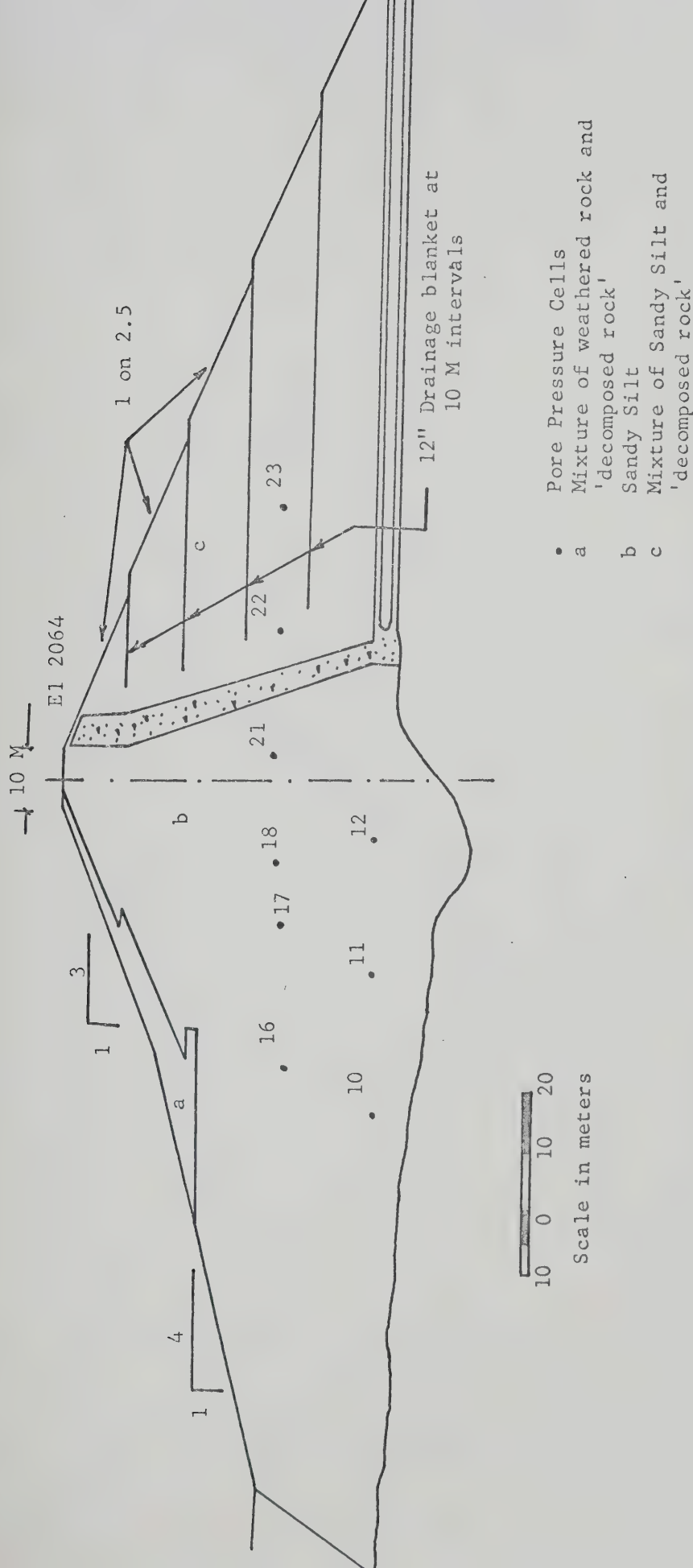


FIG. 6.16 CROSS-SECTION OF MIRAFLORES DAM

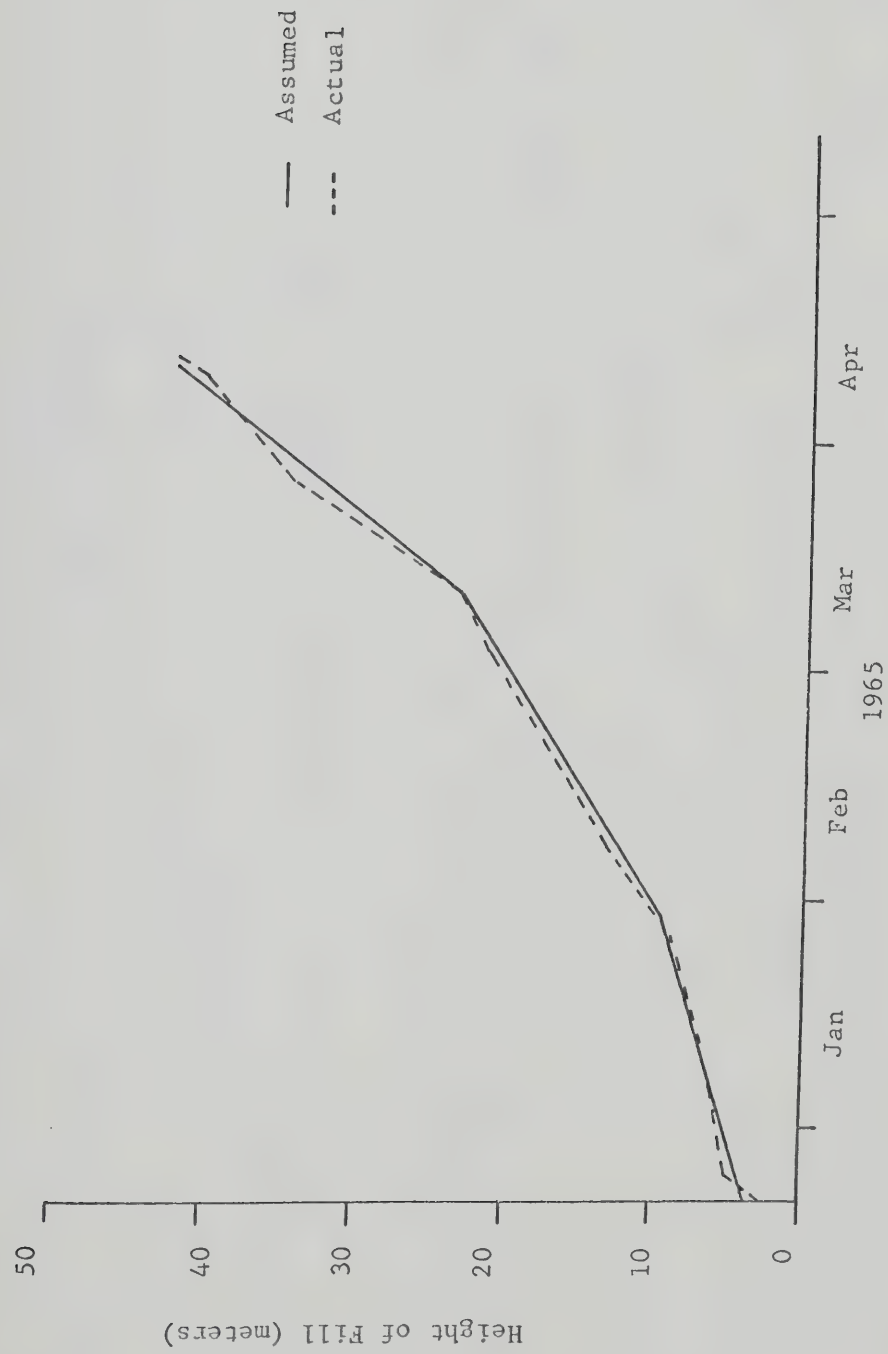


FIG. 6.17 RATE OF CONSTRUCTION OF MIRAFLORES DAM (Li, 1967)

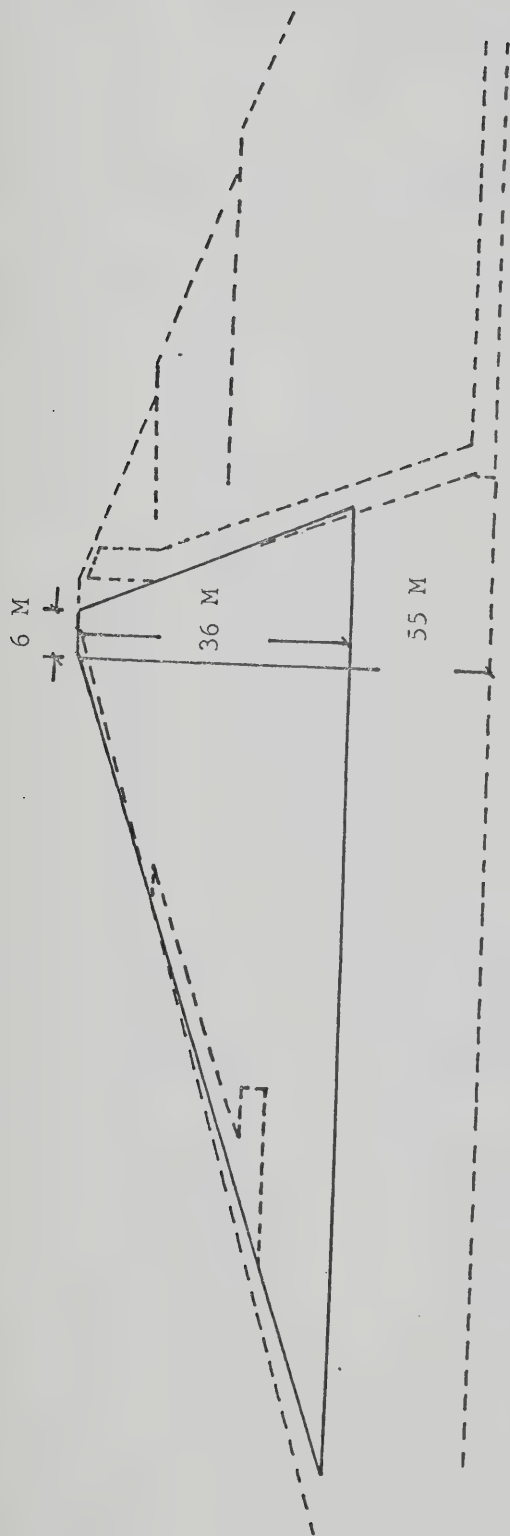


FIG. 6.18 a ASSUMED CROSS-SECTION OF MIRAFLORES DAM

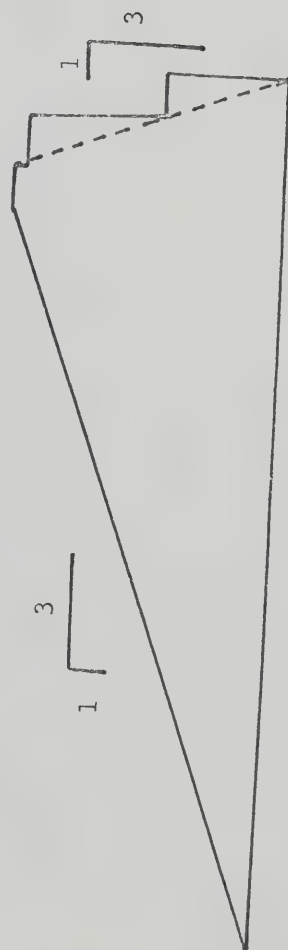


FIG. 6.18 b IDEALIZED SECTION OF MIRAFLORES

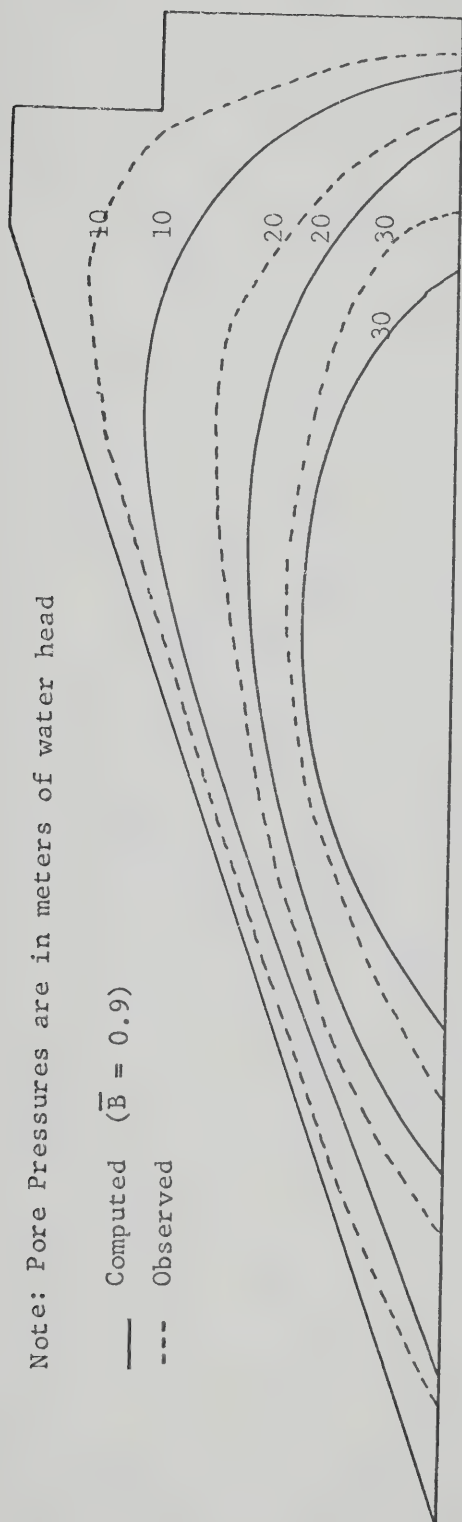


FIG. 6.19 PORE PRESSURES IMMEDIATELY AFTER CONSTRUCTION, MIRAFLORES DAM

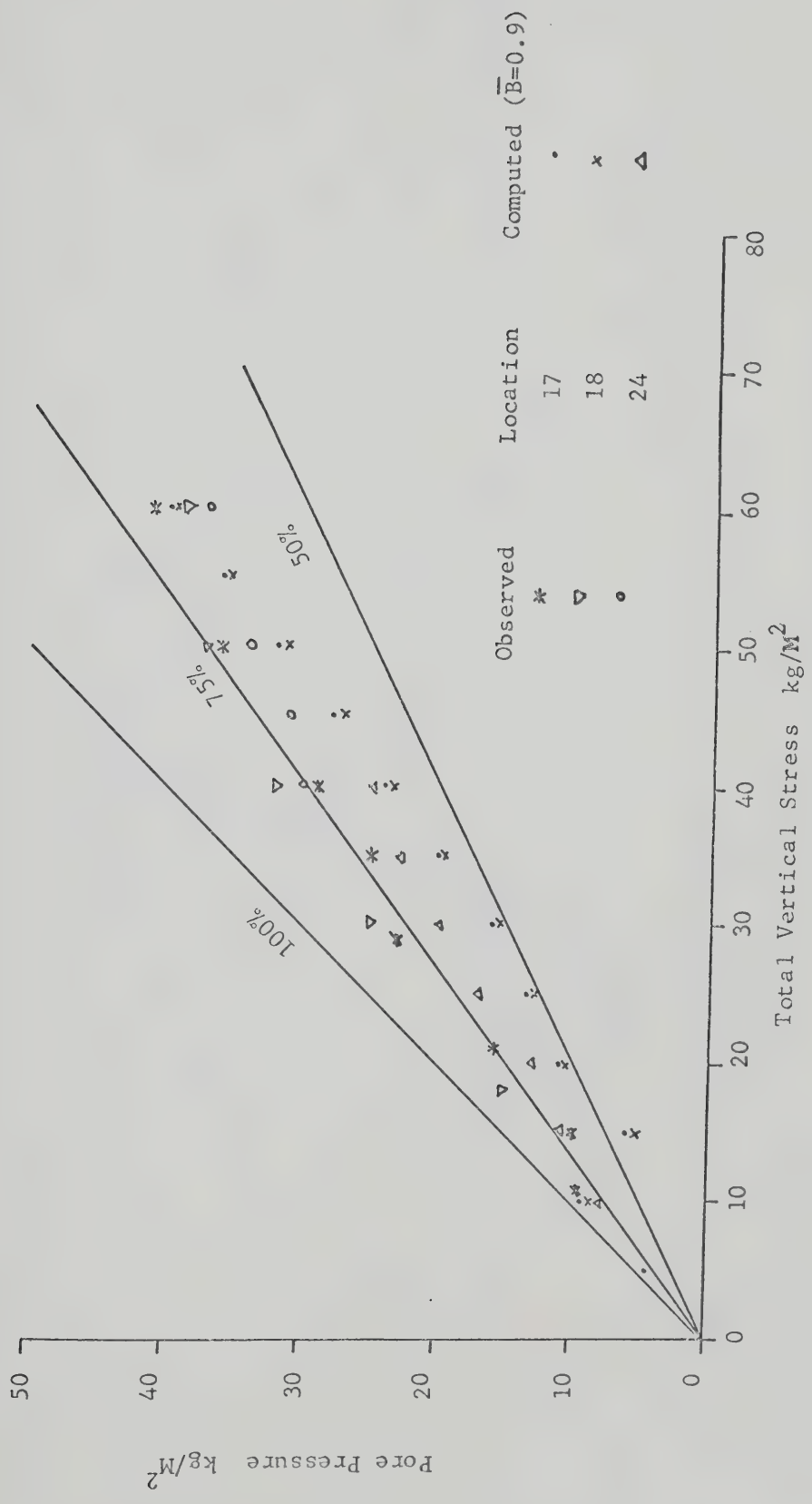


FIG. 6.20 SUMMARY OF PORE PRESSURES, MIRAFLORES DAM

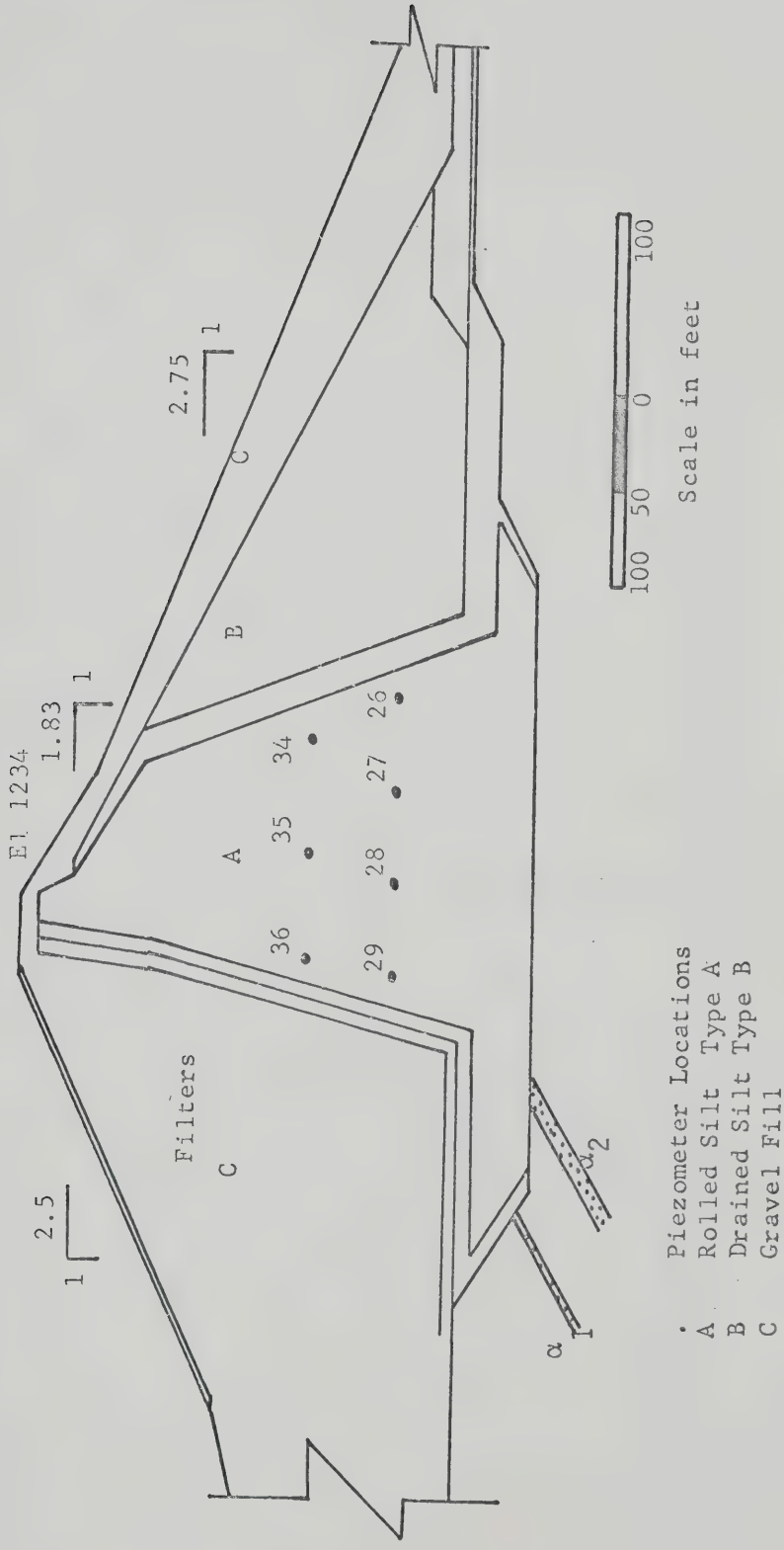


FIG. 6.21 CROSS-SECTION OF JARI DAM

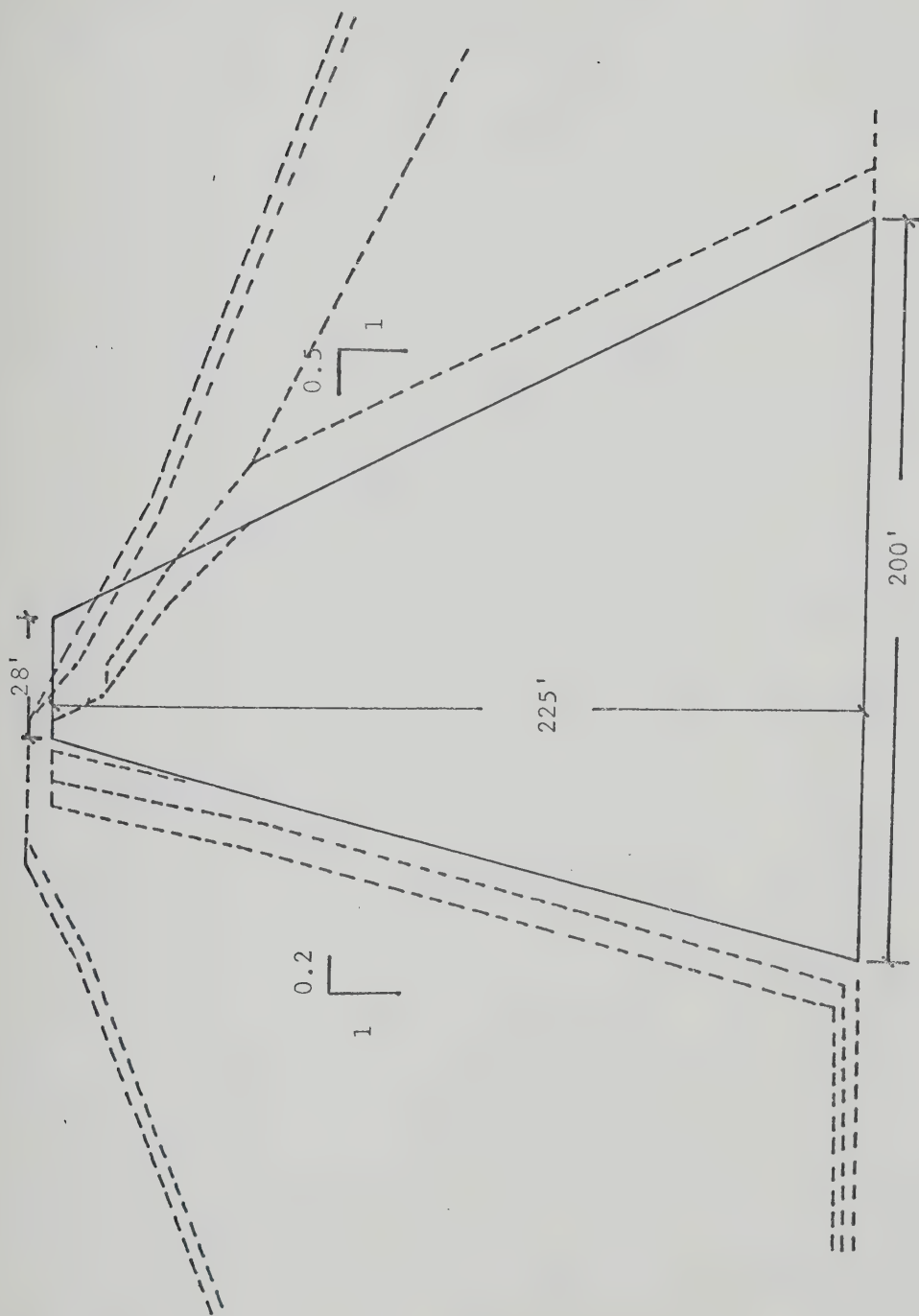


FIG. 6.22 a ASSUMED CROSS-SECTION OF JARI DAM

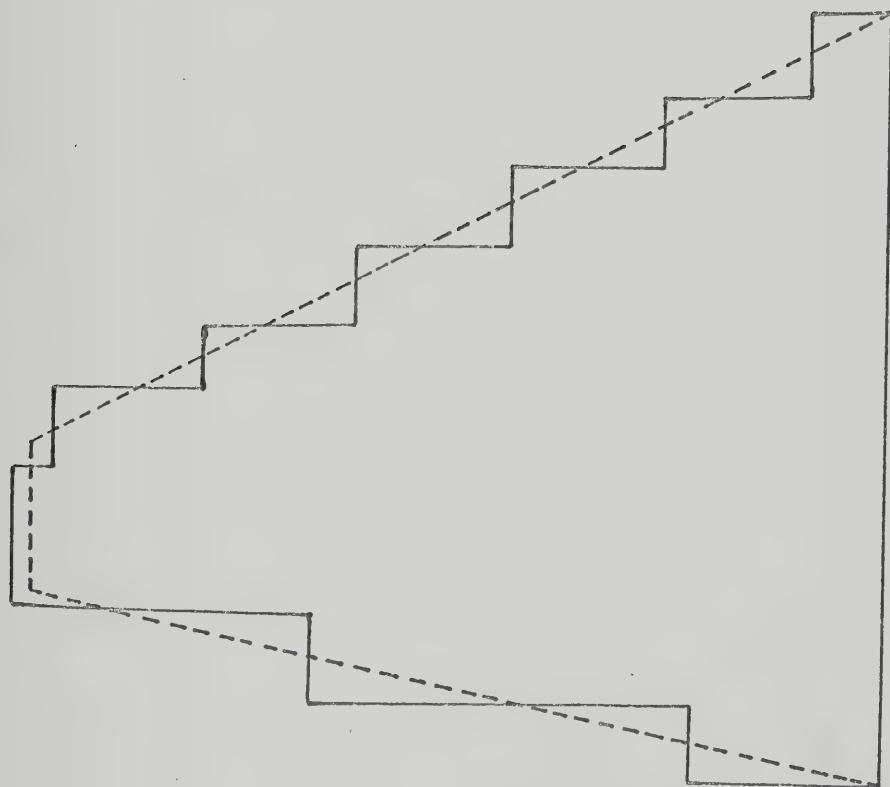


FIG. 6.22 b IDEALIZED SECTION OF JARI

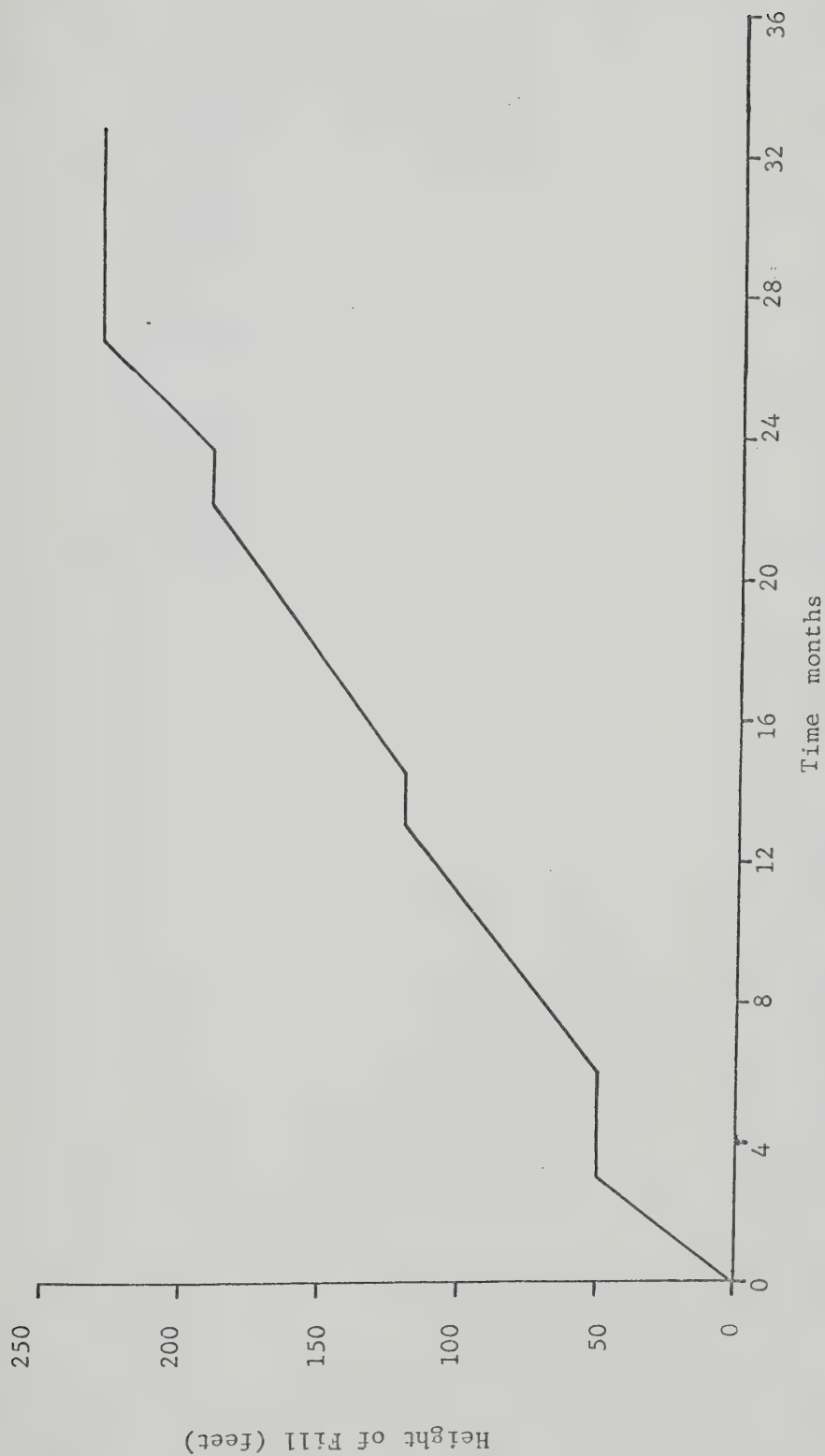


FIG. 6.23 RATE OF CONSTRUCTION OF JARI DAM (Binnie et al., 1967)

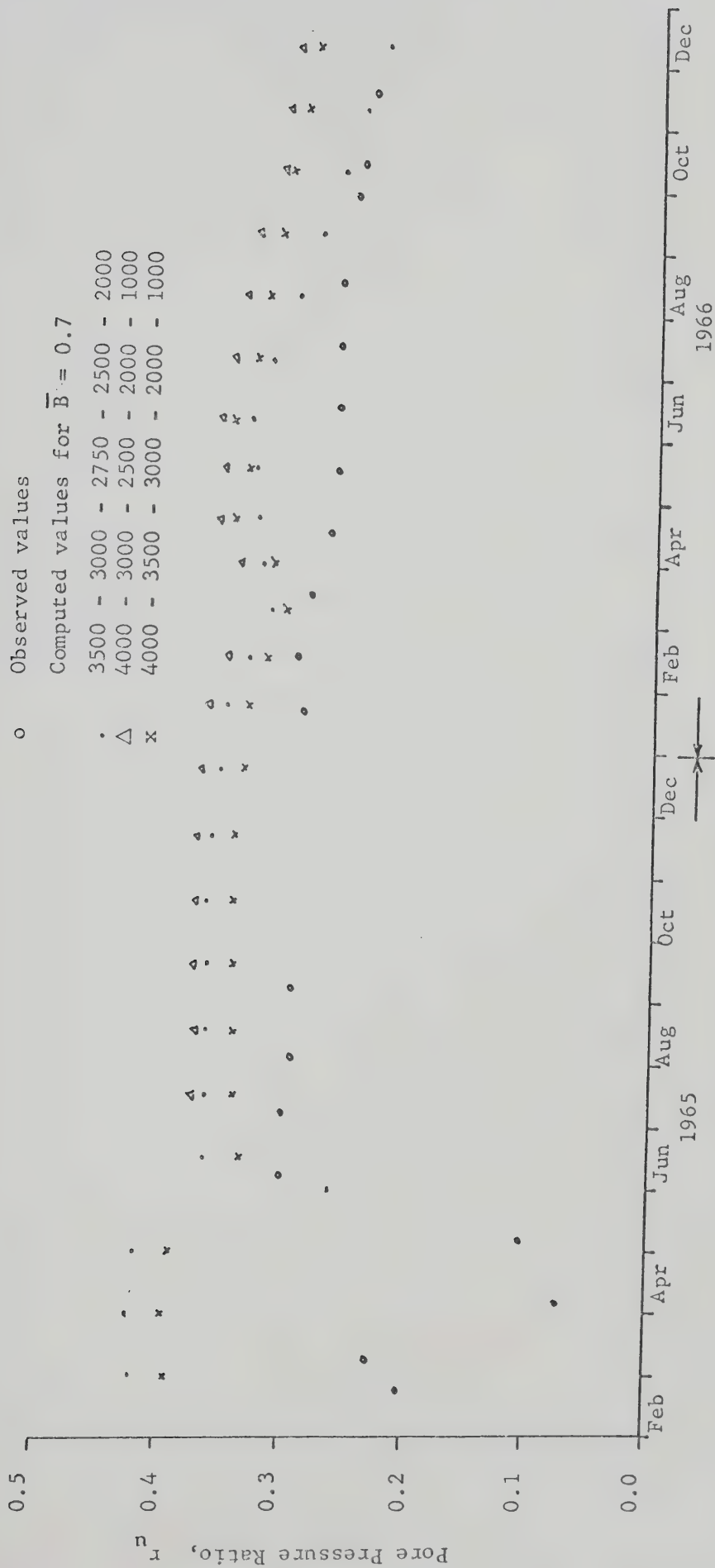


FIG. 6.24 a CONSTRUCTION PORE PRESSURES, JARI DAM

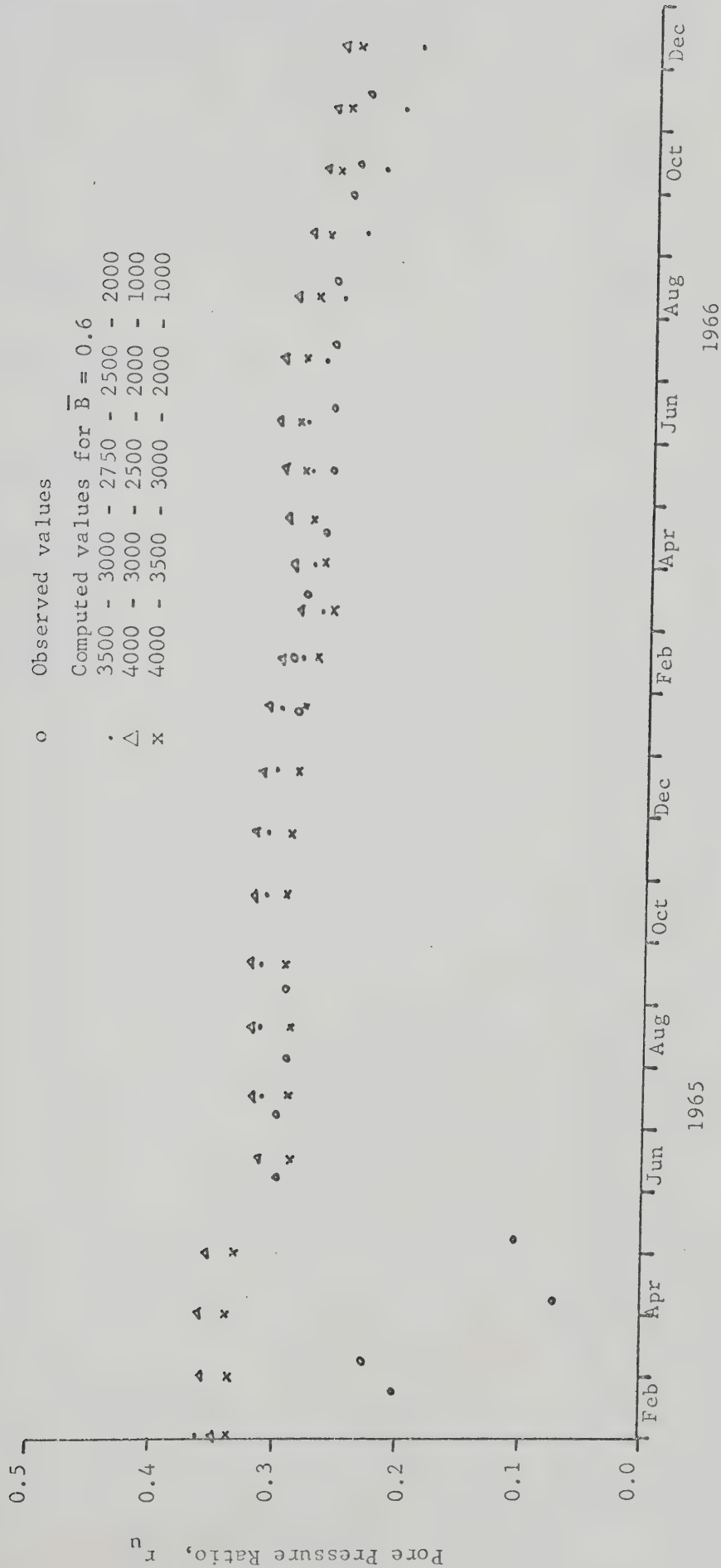


FIG. 6.24 b CONSTRUCTION PORE PRESSURES, JARI DAM

o Observed values
 Computed values for $\bar{B} = 0.6$
 . 3500 - 3000 - 2750 - 2500 - 2000
 Δ 4000 - 3000 - 2500 - 2000 - 1000
 x 4000 - 3500 - 3000 - 2000 - 1000

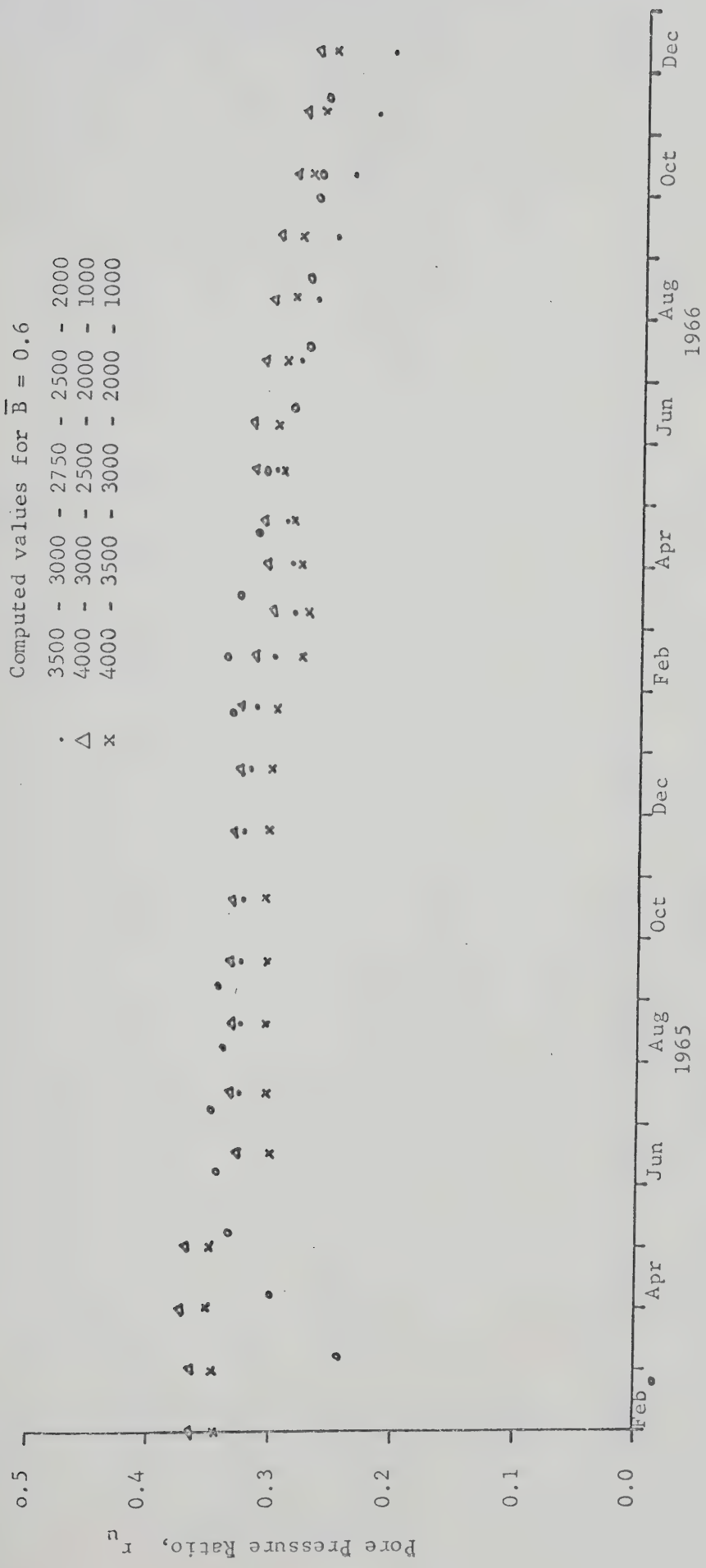


FIG. 6.24 c CONSTRUCTION PORE PRESSURES, JARI DAM

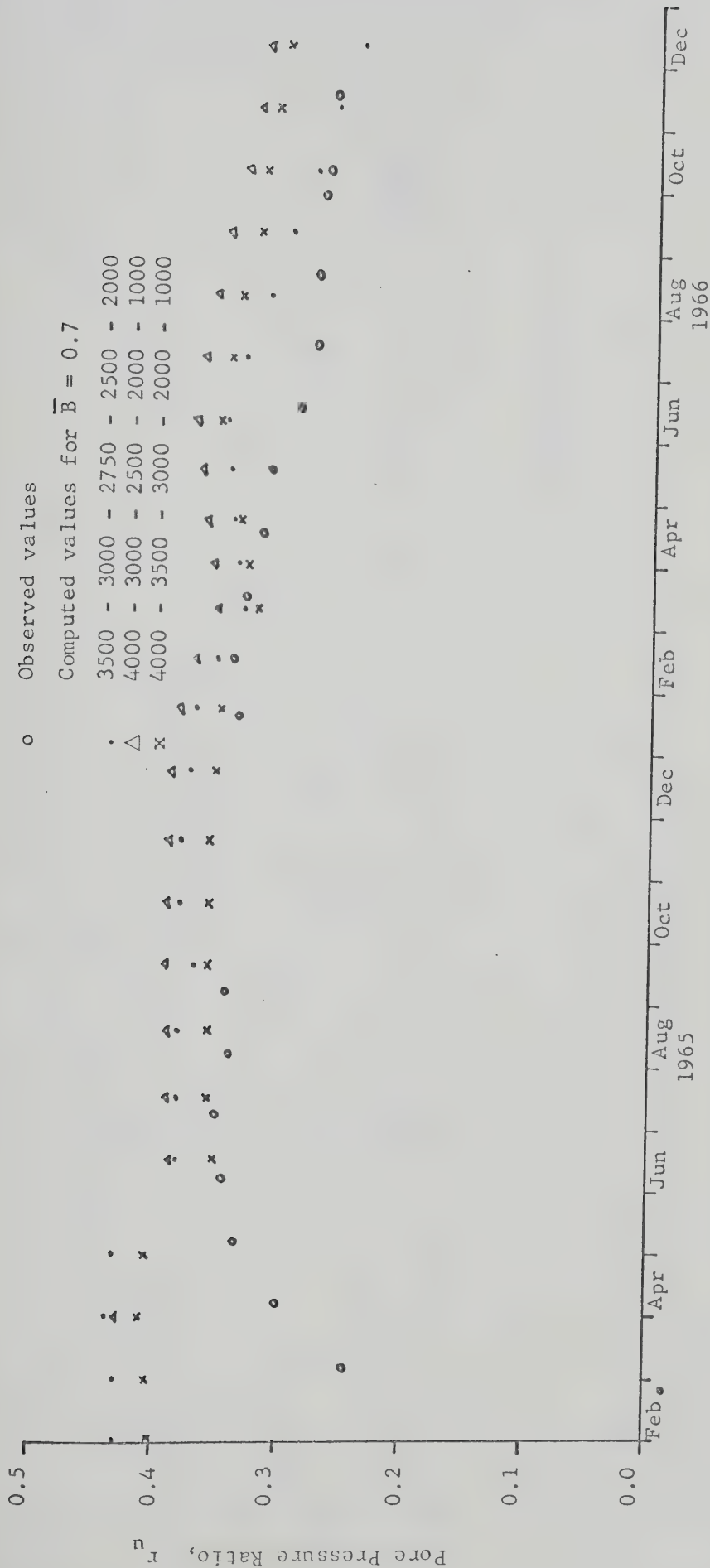


FIG. 6.24 d CONSTRUCTION PORE PRESSURES, JARI DAM

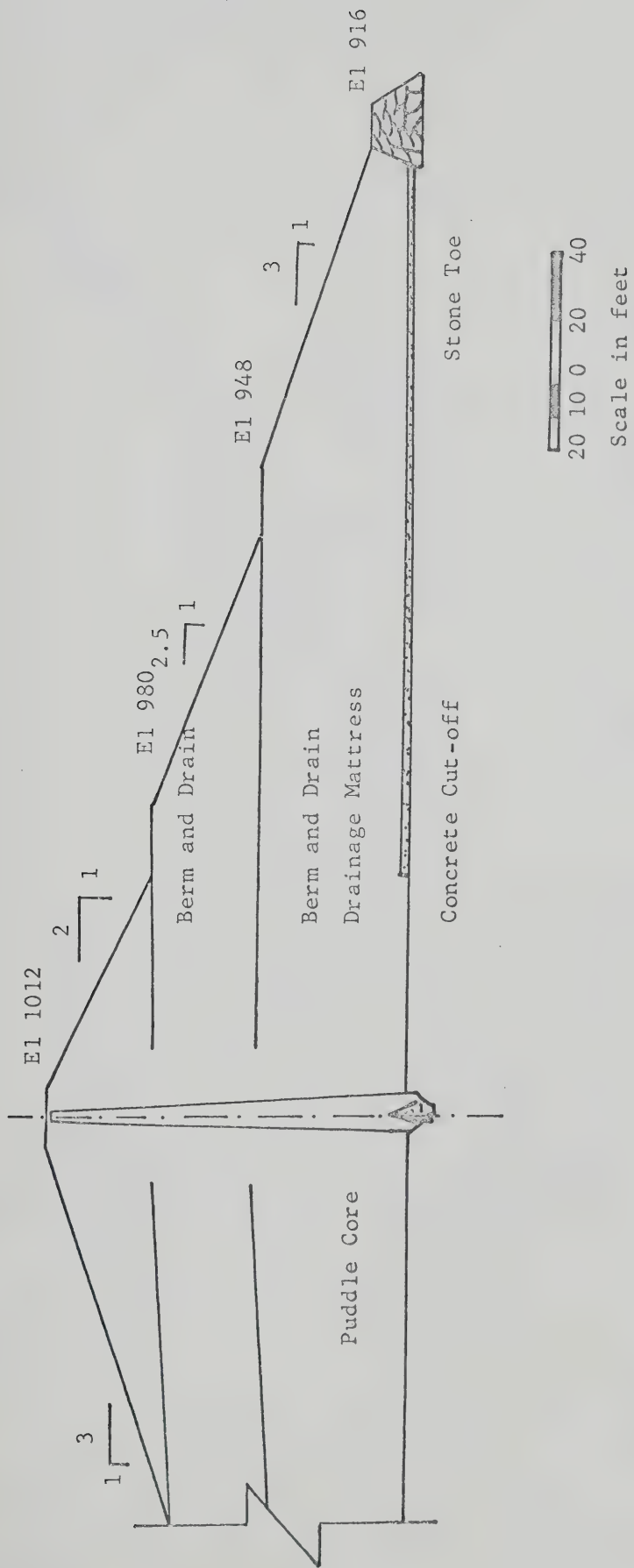


FIG. 6.25 CROSS-SECTION OF USK DAM

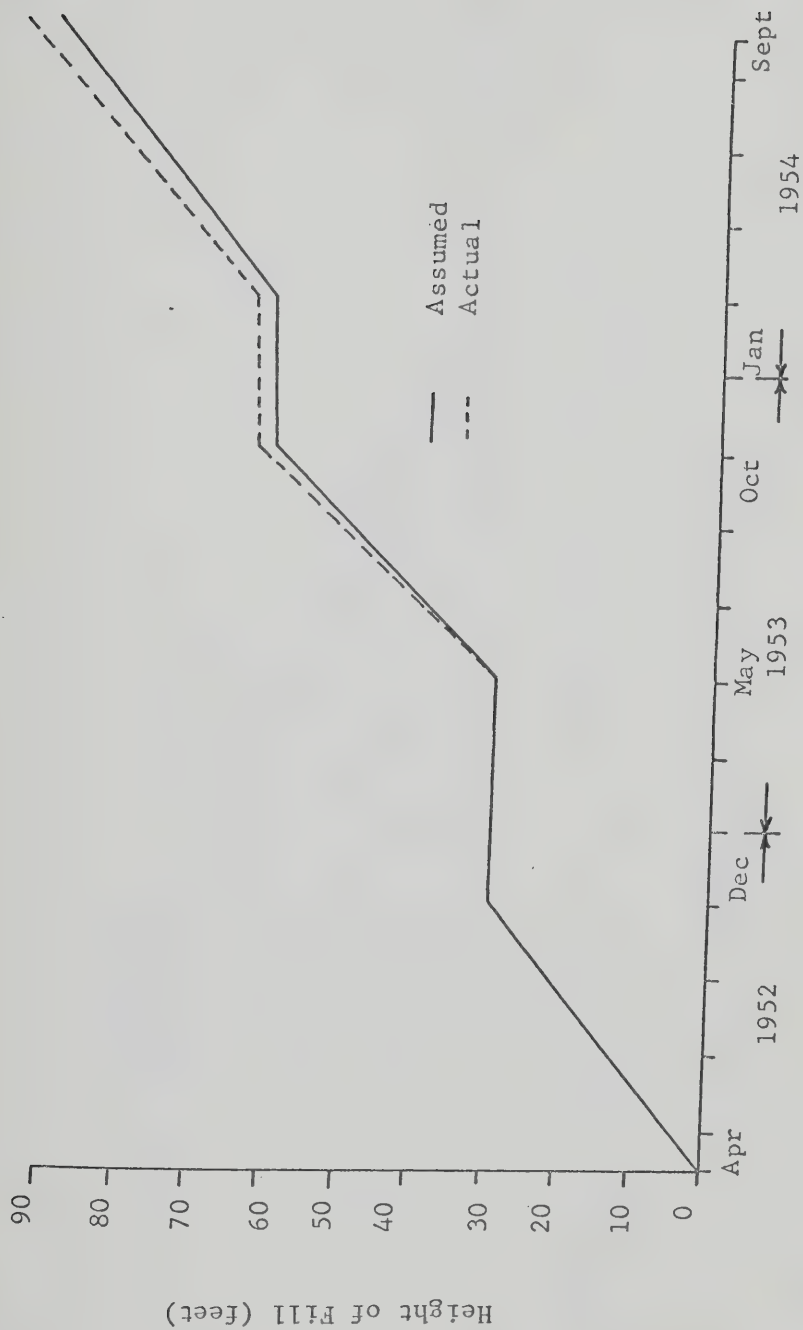


FIG. 6.26 RATE OF CONSTRUCTION OF USK DAM (Sheppard and Aylen, 1957)

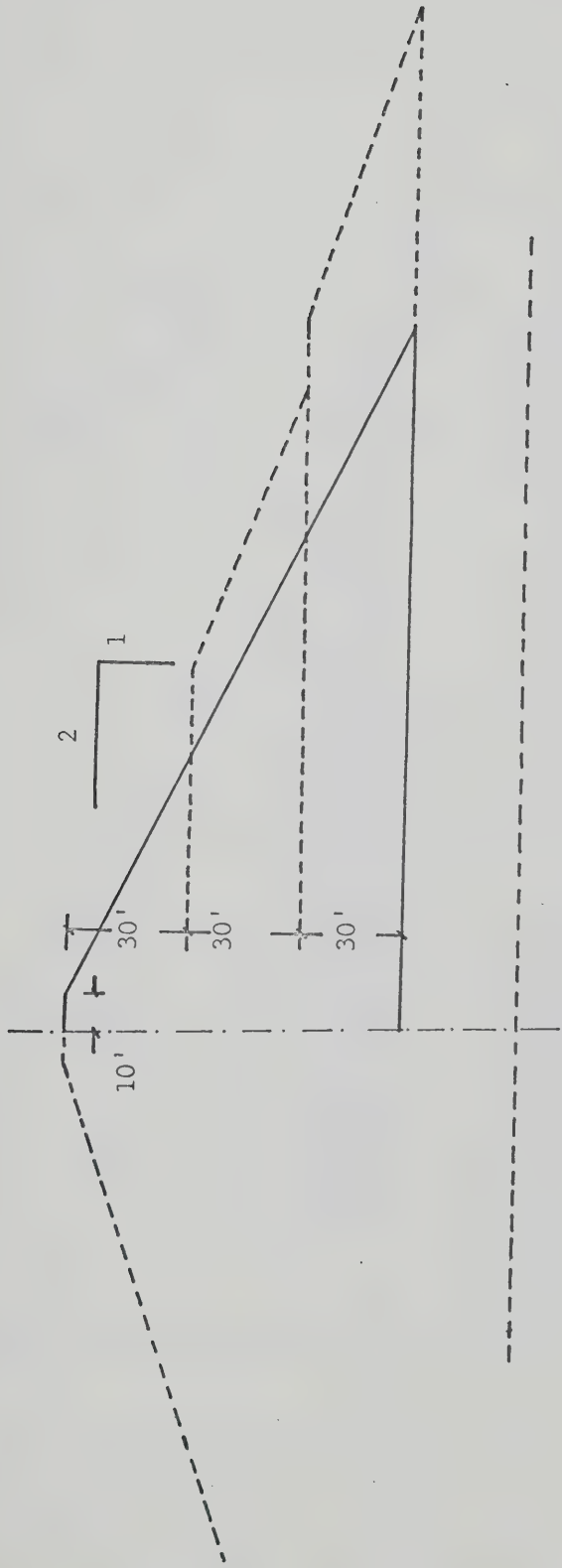


FIG. 6.27 ASSUMED CROSS-SECTION OF USK DAM

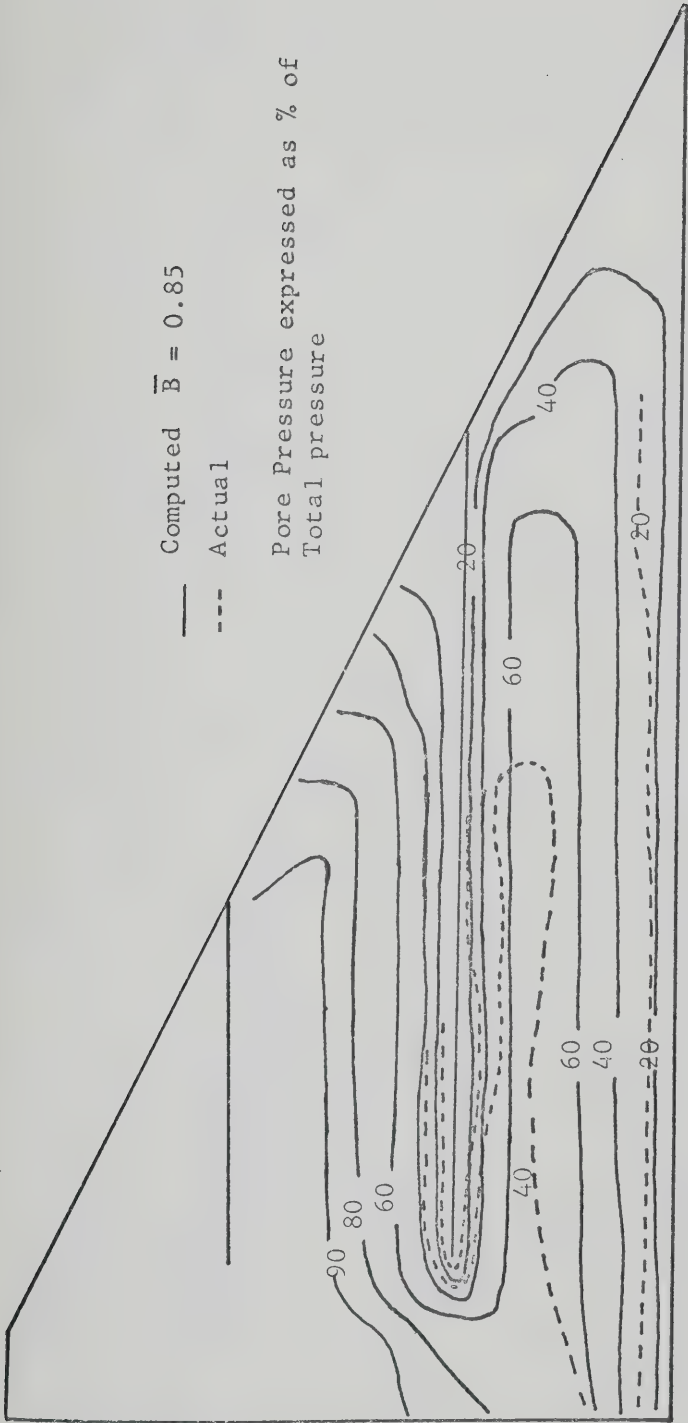


FIG. 6.28 a PORE WATER PRESSURES IN OCTOBER, 1953 USK DAM

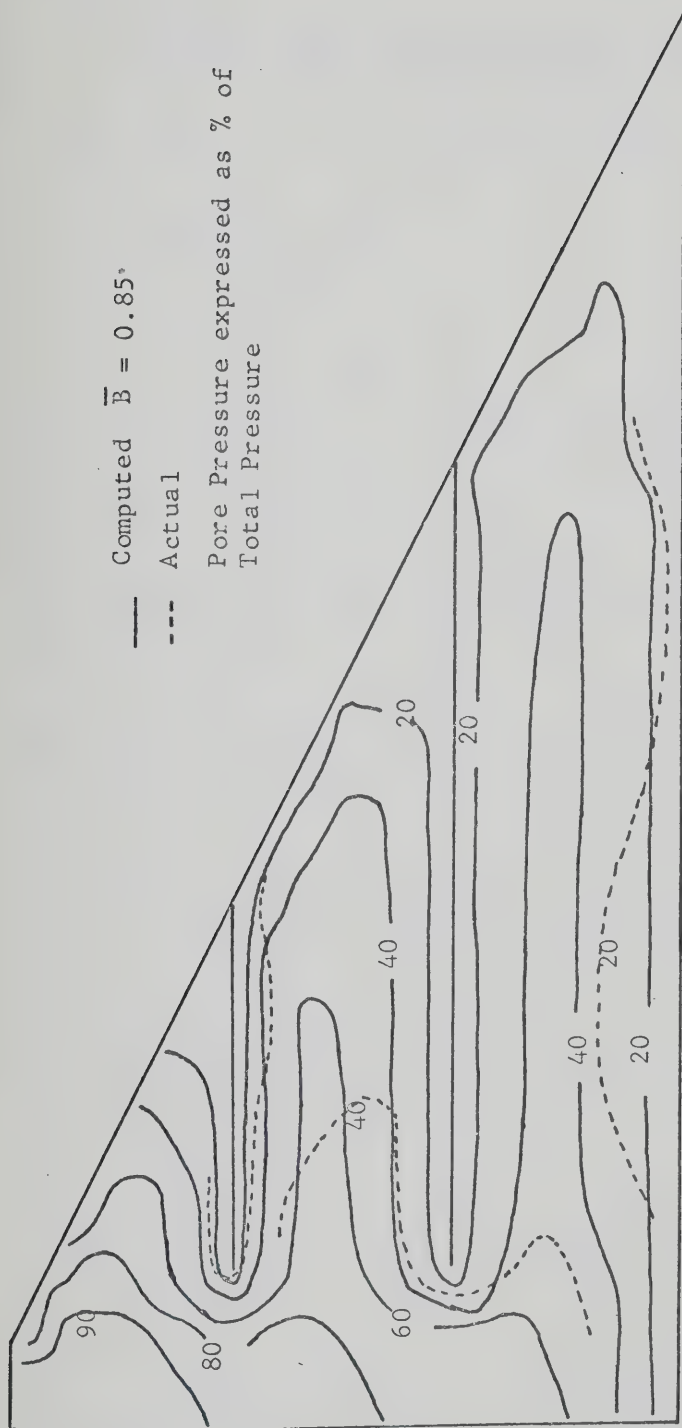


FIG. 6.28 b PORE WATER PRESSURES AT END OF CONSTRUCTION, USK DAM

CHAPTER VII

FINITE STRAIN ONE-DIMENSIONAL CONSOLIDATION SEDIMENTATION

7.1 GENERAL

This study attempts a comprehensive solution for the estimation of excess pore pressure in sedimented layers during one-dimensional consolidation. The original theory of consolidation due to Terzaghi (1923) assumes that several soil parameters such as compressibility, permeability, and coefficient of consolidation remain constant throughout the process of consolidation. In most of the theoretical results published so far, it has been assumed that the soil behaves linearly, both with respect to permeability, and with respect to its stress strain properties. That is to say, it has been assumed that the coefficient of permeability is constant throughout the layer and remains unchanged as consolidation proceeds, and that the compressibility or modulus of elasticity of the soil is also constant. In fact the permeability of real soil decreases with decreasing void ratio and hence with increasing effective compressive stress. Thus in a deep bed of clay the initial permeability will be appreciably less at the bottom than at the top due to overburden effects and the permeability will decrease during consolidation as the stresses transfer to the soil skeleton

and compress it. The compressibility of the soil skeleton will always vary with depth and time in a similar manner.

It is certain that observed soil behavior, in requiring a large number of linear elements to describe it, is in fact nonlinear. The treatment in terms of linear elements has been necessary because exact mathematical treatment is then possible. However, the mathematics become more difficult as the number of parameters increases. For solutions to be of more practical use, they must involve a minimum of parameters. It is perhaps timely to investigate the possibility of introducing nonlinear terms involving the minimum number of parameters necessary to describe the essential physics of the problem, and to produce sufficiently accurate numerical solutions on a computer.

The major sources of nonlinear behavior for clayey soils are (Barden, 1968):

- (a) finite strain;
- (b) varying permeability;
- (c) varying compressibility;
- (d) compressible pore fluid in partly saturated soil;
- and (e) secondary creep effects - nonlinear structural viscosity.

It is possible to include all these various nonlinearities into a single general treatment. However, it is usual to consider various common types of soil and to include only the dominant nonlinearities relevant to each case.

Theoretical analysis of the effects of nonlinear

behavior of a real soil could be carried out for general conditions but so far most results have been published for one-dimensional conditions. Davis and Raymond (1965) gave the results of a theory which assumes the coefficient of consolidation c_v to remain constant, while still permitting k and m_v to vary. Their results only encompassed the variation with time, not with depth, so their results are applicable to oedometer tests and thin layers in the field. Barden and Berry (1965) analyzed the case of a soil whose permeability at any instant is expressed as a polynomial approximation of the excess pore pressure at that instant. Gibson et al. (1967) have produced general equations assuming one-dimensional finite strain and any arbitrary variation of compressibility and permeability. An extension of the work of Davis and Raymond (op. cit.) to include the depth effect is presented by Davis and Lee (1969) and by Raymond (1969). Zaretsky et al. (1969) derive a basic system of differential equations for three-dimensional consolidation of a soil. Nonlinear relations between stresses and strains in the soil skeleton, the dependence of permeability on water saturation and the effect of the rheological properties of the soil skeleton are taken into account.

In the case of a compressible saturated clay, the assumptions of nonlinearity may involve the following empirical relationships:

- (a) void ratio - logarithm of permeability is a straight line (Raymond, 1966; Raymond and

Azzouz, 1969); and

- (b) void ratio - logarithm of effective stress is a straight line (Raymond, op. cit.; Raymond and Azzouz, op. cit.).

Lai (1968) noted these empirical relationships and generalized the assumptions so as to achieve any arbitrary variation in permeability and compressibility with effective stress. The coefficient of permeability k and the coefficient of compressibility m_v are related to effective stress $\sigma'(z,t)$ by power laws. These relations in turn mean that the coefficient of consolidation c_v is a function of the effective stress. In all these cases, the results show that the rate of pore pressure dissipation in an oedometer test is affected by the load increment ratio used, a property not predicted by the classical theory.

7.2 MATHEMATICAL FORMULATION

It was mentioned earlier in section 7.1 that changes in layer thickness with time occur due to the finite strains involved in the process of consolidation. This implies that the quantity $(1+e)$, where e is the current void ratio, representing the thickness of the sample at a given depth and time can no longer be considered a constant during consolidation.

It is customary, when deriving the equation governing a physical process which involves a region of space and time,

to fix attention on the physical phenonema which occur at any single point of space (Gibson, et al., 1967). More correctly the neighbourhood of this point is considered and this leads to the discussion of the events taking place in an element of volume. We can arbitrarily fix our attention on an element of space through which the medium moves and to consider the sequence of events in this element. This is Euler's approach. Alternatively, an element of mass which always encloses the same material particles may be chosen and we describe the events taking place in this moving and distorting element as time progresses. This is the method adopted by Lagrange.

Since in a finite strain consolidation problem the thickness of the soil sample is continuously changing, the top boundary is always moving. Thus at the top, the boundary is time dependent. Since this condition is both the answer we are seeking and the condition required to obtain the answer, this type of problem is normally solved by trial and error. This is an impossible task with a partial differential equation of second order with variable coefficients which governs the consolidation process (Gibson, et al., op. cit.). This difficulty may completely be overcome if the problem is presented in terms of Lagrangean coordinates. In this approach the boundary is always identified and the boundary conditions on it introduced into the analysis, although we are ignorant of its exact location.

In the Lagrangean system of coordinates, an element

is considered to enclose always the same soil grains, and hence the element does not always embrace the same pore water. (By the same token, an element enclosing always the same pore water may be chosen). In this system the element moves and its dimensions change as time progresses. On the other hand, in Euler's approach attention is fixed on an element which is assumed not to distort. It may be noted that when the displacements and strains are small the distinction between the two approaches becomes negligible. Thus in small strain theories it is of no consequence which system of coordinates is employed. However, in finite strain theory, an element has to be defined rigorously.

An element may be located at a distance 'a' from any prescribed datum plane at a given time (Figure 7.1). Let the element be at a distance 'x' from the same datum, at any subsequent time 't'. Then,

$$x = x(a,t) \quad 7.1$$

which indicates that x depends on time as well. Thus the element is fixed no more in space as in the case of Euler's approach and the dimension dx varies with time.

(a) The vertical equilibrium of the solids and fluid currently occupying the element dx yields

$$\frac{\partial \sigma}{\partial a} + \frac{e\gamma_w + \gamma_s}{1 + e} \frac{\partial x}{\partial a} = 0 \quad 7.2$$

where σ denotes the total stress

e denotes the void ratio

γ_w denotes the unit weight of water

and γ_s denotes the unit weight of solids

Since the chosen element always contains the same weight of solids this leads to the equation of continuity of solids as,

$$\gamma_s \left(\frac{1}{1+e_0} \right) = \gamma_s \left(\frac{1}{1+e(a,t)} \right) \frac{\partial x}{\partial a} \quad 7.3$$

where γ_s is considered to remain constant.

(b) Darcy's law is generally given as

$$v = ki$$

where v is the discharge velocity of the water and i is the hydraulic gradient. A more general form (Scheidegger, 1960) may be used relating the law as function of the velocity of the water relative to that of the soil skeleton. Thus,

$$n(v_w - v_s) = - \frac{k}{\gamma_w} \frac{\partial u}{\partial x} \quad 7.4a$$

where n denotes porosity of the soil skeleton ($= e/1+e$),

and u denotes the excess pore water pressure,

v_w denotes the velocity of pore water,

v_s denotes the velocity of solid particles.

In the case of steady seepage, $v_s = 0$ leading to the familiar form. If the entire continuum moved bodily, $v_w = v_s$ and the equation then correctly predicts that this movement is not associated with the development of a hydraulic gradient.

Equation 7.4a may be expressed as

$$\frac{e}{1+e} (v_w - v_s) = - \frac{k}{\gamma_w} \frac{\partial u}{\partial a} \frac{\partial a}{\partial x}$$

$$\text{i.e.,} \quad \frac{e}{1+e} (v_w - v_s) \frac{\partial x}{\partial a} = - \frac{k}{\gamma_w} \frac{\partial u}{\partial a} \quad 7.4b$$

(c) Continuity of flow of water demands that the rate of weight inflow of water must equal the rate of change of weight of water in the element.

Rate of weight inflow of the water is

$$\frac{\partial}{\partial a} \left(\frac{e}{1+e} \gamma_w (v_w - v_s) \right) da$$

Rate of change of weight of the water in the element is

$$\frac{\partial}{\partial t} \left(\frac{e}{1+e} \gamma_w \frac{\partial x}{\partial a} \right) da$$

Therefore

$$\frac{\partial}{\partial a} \left(\frac{e}{1+e} \gamma_w (v_w - v_s) \right) + \frac{\partial}{\partial t} \left(\frac{e}{1+e} \gamma_w \frac{\partial x}{\partial a} \right) = 0 \quad 7.5$$

It is convenient to introduce at this stage (Gibson et al., op. cit.) a new independent variable z to replace a , such that

$$z(a) = \int_0^a \frac{1}{1+e(a',0)} da' \quad 7.6$$

This implies that a point of the soil skeleton is identified now by the volume of solids z in a prism of unit cross-sectional area lying between the datum and the point (McNabb, 1960). Clearly, z is independent of time. All the relations so far derived may now be expressed in terms of the new variable z . Thus,

Equation 7.2 becomes

$$\frac{\partial \sigma}{\partial z} + \frac{e\gamma_w + \gamma_s}{1+e} \frac{\partial x}{\partial z} = 0 \quad 7.7$$

Equation 7.3 becomes

$$\frac{1}{1+e_0} = \frac{1}{1+e} \frac{\partial x}{\partial z} \frac{dz}{da}$$

dz/da from equation 7.6 is

$$dz/da = 1/1+e_0$$

Therefore equation 7.3 is expressed as

$$\frac{1}{1+e_0} = \frac{1}{1+e} \frac{\partial x}{\partial z} \quad \frac{1}{1+e_0}$$

$$\text{i.e.,} \quad \frac{\partial x}{\partial z} = 1+e \quad 7.8$$

Equation 7.4b, expressed in the new variable z , is

$$\frac{e}{1+e} (v_w - v_s) \frac{\partial x}{\partial z} = - \frac{k}{\gamma_w} \frac{\partial u}{\partial z}$$

$$\text{i.e.,} \quad e(v_w - v_s) = - \frac{k}{\gamma_w} \frac{\partial u}{\partial z} \quad 7.9$$

Equation 7.5 becomes

$$\frac{\partial}{\partial z} \left(\frac{e}{1+e} \gamma_w (v_w - v_s) \right) + \frac{\partial}{\partial t} \left(\frac{e}{1+e} \gamma_w \frac{\partial x}{\partial z} \right) = 0$$

$$\text{i.e.,} \quad \frac{\partial}{\partial z} \left(\frac{e}{1+e} (v_w - v_s) \right) + \frac{\partial e}{\partial t} = 0 \quad 7.10$$

assuming that the unit weight of water does not alter during the process of consolidation.

The governing equation can now be developed using the equations 7.7, 7.8, 7.9, and 7.10. Substituting equation 7.9 in the equation 7.10, yields

$$\frac{\partial}{\partial z} \left[- \frac{k}{\gamma_w(1+e)} \frac{\partial u}{\partial z} \right] + \frac{\partial e}{\partial t} = 0$$

$$\text{or} \quad \frac{\partial}{\partial z} \left[- \frac{k}{\gamma_w(1+e)} \frac{\partial u}{\partial z} \right] + \frac{de}{d\sigma'} \cdot \frac{\partial \sigma'}{\partial t} = 0 \quad 7.11a$$

where $\sigma' = \sigma'(e)$; and σ' , the effective stress at any point at a given time is expressed as

$$\sigma' = \sigma - u + \gamma_w x \quad 7.11b$$

where x is considered positive when measured against gravity. Therefore

$$\frac{\partial \sigma'}{\partial t} = \frac{\partial \sigma}{\partial t} - \frac{\partial u}{\partial t} + \gamma_w \frac{\partial x}{\partial t} \quad 7.11c$$

$$\text{Also} \quad \frac{\partial x}{\partial z} = 1+e$$

$$\text{i.e.,} \quad x = \int_0^z (1+e) dz$$

$$\text{Therefore} \quad \frac{\partial x}{\partial t} = \int_0^z \frac{\partial e}{\partial t} dz \quad 7.11d$$

$$\text{Again} \quad \sigma(z,t) = \sigma_i(z) + \Delta\sigma(t)$$

where $\Delta\sigma(t)$ is the load increment, which generates the excess

pore water pressure. Differentiating with respect to t , gives:

$$\frac{\partial \sigma}{\partial t} = \frac{d(\Delta \sigma)}{dt} \quad 7.11e$$

Substituting equations 7.11c, 7.11d, and 7.11e in 7.11a yields

$$\frac{\partial}{\partial z} \left[-\frac{k}{\gamma_w(1+e)} \frac{\partial u}{\partial z} \right] + \frac{de}{d\sigma'} \left[\frac{d}{dt} (\Delta \sigma) - \frac{\partial u}{\partial t} + \gamma_w \int \frac{\partial e}{\partial z} dz \right] = 0 \quad 7.12$$

Equation 7.12 is the governing general relationship of the excess pore water pressure as a function of time t and space z .

As a check, the familiar Terzaghi equation may easily be recovered. On the basis of small strains (i.e., void ratio e is constant), Terzaghi made the rational assumption that the permeability k , the compressibility $de/d\sigma'$, the quantity $1/(1+e)$ are constant during consolidation. Therefore, equation 7.12 reduces to

$$-\frac{k}{\gamma_w(1+e)} \frac{\partial^2 u}{\partial z^2} + \frac{de}{d\sigma'} \left[\frac{d}{dt} (\Delta \sigma) - \frac{\partial u}{\partial t} \right] = 0$$

$$\text{or} \quad \left(\frac{1}{1+e_0} \right)^2 c_v \frac{\partial^2 u}{\partial z^2} = \frac{\partial u}{\partial t} - \frac{d}{dt} (\Delta \sigma) \quad 7.13a$$

which is the equation derived by Gibson (1958) except for the

term $1/(1+e_0)^2$. The term $1/(1+e_0)^2$ arises because the z reference plane is with respect to the volume of the solids as explained following equation 7.6 which may be expressed as

$$dz/da = 1/1+e_0$$

where 'a' refers to the soil as a whole from any arbitrarily chosen datum. The equation derived by Gibson (op. cit.) is with respect to 'a'. Equation 7.13a expressed in terms of the variable 'a' yields

$$c_v \frac{\partial^2 u}{\partial a^2} = \frac{\partial u}{\partial t} - \frac{d}{dt} (\Delta \sigma) \quad 7.13b$$

which is exactly the form given by Gibson (op. cit.).

If it is assumed, further, that there is no change in superincumbent load with respect time, 7.13b yields

$$c_v \frac{\partial^2 u}{\partial a^2} = \frac{\partial u}{\partial t} \quad 7.14$$

which is the classical Terzaghi equation for one-dimensional dissipation of excess pore water pressure.

BOUNDARY CONDITIONS

The solution of equation 7.12 will be unique depending

on the boundary conditions. At the top, the layer of soil is always free to drain and is open to the atmosphere. As such excess pore pressures will dissipate almost instantaneously. Thus the top boundary of the soil will have zero excess pore pressure. That is, a free draining boundary is one for which the excess pore pressure is always zero. There is a possibility that the bottom boundary may also be free draining.

If the soil layer is in contact with an impermeable rock stratum it will be impossible for water to drain across the boundary. Also no movement of solid particles occurs across the boundary. Therefore

$$v_w = 0 \quad \text{and} \quad v_s = 0$$

Substituting the above equations in the equation 7.9 yields

$$\frac{\partial u}{\partial z} = 0 \tag{7.15}$$

Equation 7.15 implies that the flow velocity induced by the excess pore pressure is zero. That is, an impervious boundary is one for which the excess pore pressure gradient is zero.

The impervious boundary condition can also be expressed in terms of the void ratio e at any given instant of time. Equation 7.15 is made use of in conjunction with equations 7.7, 7.8, and 7.11b to arrive at the desired result.

Differentiating the equation 7.11b with respect to z ,

gives:

$$\frac{\partial u}{\partial z} = \frac{\partial \sigma}{\partial z} - \frac{\partial \sigma'}{\partial z} + \gamma_w \frac{\partial x}{\partial z}$$

Using equation 7.15, the above reduces to

$$\frac{\partial \sigma}{\partial z} - \frac{\partial \sigma'}{\partial z} + \gamma_w \frac{\partial x}{\partial z} = 0 \quad 7.15a$$

where

$$\frac{\partial \sigma}{\partial z} = - \frac{e\gamma_w + \gamma_s}{1+e} \frac{\partial x}{\partial z} \quad 7.7$$

and

$$\frac{\partial x}{\partial z} = 1+e \quad 7.8$$

Combining equations 7.7, 7.8, and 7.15a, we have

$$- \gamma_w(e + G_s) - \frac{\partial \sigma'}{\partial z} + \gamma_w(1+e) = 0$$

i.e.,
$$\frac{d\sigma'}{de} \cdot \frac{\partial e}{\partial z} = \gamma_w(1 - G_s)$$

or
$$\frac{\partial e}{\partial z} = \gamma_w \cdot \frac{de}{d\sigma'} (1 - G_s) \quad 7.15b$$

Equation 7.15b thus gives an expression for an imper-

vious boundary condition in terms of void ratio, i.e., it yields the variation of void ratio with depth at the boundary across which no movement of pore water or solids takes place. The expression for $\partial e / \partial z$ indicates that, at the impervious boundary, the variation in void ratio with depth depends on such soil characteristics as specific gravity and the current compressibility.

As in thin layers, if the self weight of the soil is not considered correctly and the buoyant weight is assumed to be unity, i.e., $G_s = 1$, equation 7.15b reduces to

$$\frac{\partial e}{\partial z} = 0 \quad 7.15c$$

at the impervious boundary.

The free draining and impervious boundary conditions form the two extremes of a real situation in which there is partial drainage across the boundary.

INITIAL CONIDITION

In the case of sedimentation, the soil layers are gradually built up. Since layers are growing with time, at the initial time (i.e., say when $t = 0$) the initial excess pore pressure is zero. Also at that initial time, there will be no clay layer to start sedimentation with, which means that the void ratio at the beginning is zero. A zero void

ratio always relates to an effective stress which is not accountable. To surmount this predicament, the sedimentation shall start (at $t = 0$) with a negligibly thin layer at an initial void ratio e_0 , and a corresponding effective stress σ'_0 . At the next time step ($t = 0 + \Delta t$) a layer of thickness Δz shall be added at a given void ratio e_0 . This will generate excess pore water pressure, which dissipates depending on the boundary conditions.

The initial conditions thus are:

- (1) a soil layer of no measureable thickness with a definite void ratio e_0 and a corresponding effective stress σ'_0 is provided; and
- (2) there is no excess pore pressure, i.e., the excess pore pressure in the thin layer of void ratio e_0 is zero.

Equation 7.12 can be solved for given initial condition and a set of prescribed boundary conditions. Unfortunately it is impossible to give an analytical solution to the equation under these conditions. However, an approximate numerical solution can be arrived at (to determine u as a function of z and t) using an implicit finite difference technique. Once the value of the excess pore pressure is known, the quantities such as effective stress, void ratio, the height of the sediment (which is not the sum total of the layers added because of finite strains) and the density of the sediment may easily be obtained.

7.3 PERMEABILITY, COMPRESSIBILITY, VOID RATIO AND EFFECTIVE STRESS RELATIONSHIPS

In this section, a discussion, in general, of the possible relationships existing between compressibility, permeability, and effective stress is given.

Janbu (1963) concluded, after an extensive study of rocks and clays, that an effective stress-strain law may be expressed as

$$\frac{de}{d\sigma'} = \left(\frac{de}{d\sigma'}\right)_0 \left(\frac{\sigma'}{\sigma_0}\right)^p \quad 7.16$$

where the subscript '0' refers to an arbitrary reference state and the exponential p is a non-dimensional constant. The value of p ranges from -1 to 0. Equation 7.16 in its present form is the one adopted by Lai (1968); but is identical in all respects to that given by Janbu. When $p = 0$, $de/d\sigma'$ is a constant and hence the effective stress-strain curve is a straight line representing a linearly elastic material behavior. When $p = -1$, $de/d\sigma'$ varies inversely as the effective stress and a plot of e versus $\log \sigma'$ yields a straight line; thus representing a normally consolidated material. When $p = -0.5$, a plot of e versus σ' yields a parabolic curve; which may not in particular represent any one material. But this value of $p = -0.5$ represents a state which is somewhat in between the states represented by $p = 0$ (a linearly elastic material) and $p = -1$ (a normally consolidated soil). The

value of $p = 0$ roughly represents the case of an overconsolidated soil in a limited stress range. Thus $p = -0.5$ possibly represents the middle of a spectrum of soils, one end of which is represented by normally consolidated soils and the other end being represented by overconsolidated soils.

However, for purposes of this study equation 7.16 is made use of with a value of $p = -1$ because special attention is devoted here to normally consolidated soils.

A value of $p = -1$ yields a plot of e versus $\log \sigma'$ as a straight line; the equation of which may be written as

$$e = C - D \log \sigma' \quad 7.17$$

where C and D (both positive) depend on the soil characteristics such as liquid limit, plasticity index etc. Such an explicit relation as given by equation 7.17 is necessary for solving the nonlinear consolidation equation 7.12 as will be shown later.

An attempt was made to find a relationship between the permeability k and the effective stress σ' based on experimental evidence. Strangely enough there is little published evidence available for such a relationship to be evaluated. According to Taylor (1948), 'a plot of the void ratio to a natural scale against the coefficient of permeability to a logarithmic scale approximates a straight line for any soil'. Schmid (1957), based on a study of several published results, reached the same conclusion.

Figure 7.2 gives the variation in permeability caused by consolidation. The quantity $\log (k/1+e)$ bears a straight line relationship with $\log \sigma'$ for the soils studied. At low consolidation pressures, the curves are not strictly straight lines; though they are perfect straight lines at higher effective stresses. For purposes of this study the plot of $k/1+e$ versus σ' is considered a straight line on a log - log scale. (The curves are plotted from the data of Normand, 1964.)

Thus it may be assumed that an experimental curve relating the effective stress σ' and the ratio $k/1+e$ can be represented by

$$\frac{k}{1+e} = \left(\frac{k}{1+e}\right)_0 \left(\frac{\sigma'}{\sigma_0}\right)^q \quad 7.18$$

where q is a non-dimensional constant to be determined by curve fitting. As in the equation 7.16 the subscript '0' refers to the same arbitrary strained state.

From Figure 7.2 it may be concluded that a given change in void ratio e causes a much larger change in k when e is large than when e is small. change in the ratio $k/1+e$ for a given change in e must approach zero as e becomes smaller. Also the rate at which the ratio $k/1+e$ changes decreases continuously. Equation 7.18 possesses these properties. The first derivative with respect to σ' yields

$$\frac{d}{d\sigma'} \left(\frac{k}{1+e} \right) = \frac{k}{1+e} \cdot \frac{q}{\sigma'}$$

which approaches zero as σ' approaches infinity. Its second derivative

$$\frac{d^2}{d\sigma'^2} \left(\frac{k}{1+e} \right) = \frac{k}{1+e} \cdot \frac{q(q-1)}{(\sigma')^2}$$

also approaches zero with σ' at a much faster rate.

7.4 ONE-DIMENSIONAL CONSOLIDATION EQUATION

Equations 7.16 and 7.18 may be substituted in equation 7.12 to yield

$$\begin{aligned} \frac{1}{\gamma_w} \frac{\partial}{\partial z} \left[- \frac{k_0}{1+e_0} \left(\frac{\sigma'}{\sigma'_0} \right)^q \frac{\partial u}{\partial z} \right] + \left(\frac{de}{d\sigma'} \right)_0 \left(\frac{\sigma'}{\sigma'_0} \right)^p \left[\frac{d}{dt} (\Delta\sigma) \right. \\ \left. - \frac{\partial u}{\partial t} + \gamma_w \int_0^z \frac{\partial e}{\partial t} dz \right] = 0 \end{aligned}$$

where $\left(\frac{de}{d\sigma'} \right)_0$ is negative. Therefore

$$\frac{k_0(1+e_0)}{\gamma_w(\frac{de}{d\sigma'})_0} \cdot \frac{1}{(1+e_0)^2} \cdot \frac{1}{(\sigma'_0)^q} \frac{\partial}{\partial z} [(\sigma')^q \frac{\partial u}{\partial z}] =$$

$$(\frac{\sigma'}{\sigma'_0})^p [\frac{\partial u}{\partial t} - \frac{d}{dt} (\Delta\sigma) - \gamma_w \int_0^z \frac{\partial e}{\partial t} dz]$$

7.19

where $(\frac{de}{d\sigma'})_0$ is positive. Let T be defined as

$$T = \frac{k_0(1+e_0)}{\gamma_w(\frac{de}{d\sigma'})_0} t, \text{ the time factor.}$$

Therefore

$$(\frac{\sigma'_0}{\sigma'})^{p-q} \frac{1}{(1+e_0)^2} \frac{\partial^2 u}{\partial z^2} + (\frac{\sigma'_0}{\sigma'})^{p-q} \frac{q}{(1+e_0)^2 \sigma'} [\gamma_w(1-G_s) - \frac{\partial u}{\partial z}] \frac{\partial u}{\partial z} =$$

$$\frac{\partial u}{\partial T} - \frac{d}{dT} (\Delta\sigma) - \gamma_w \int_0^z \frac{\partial e}{\partial T} dz$$

i.e.,

$$(\frac{\sigma'_0}{\sigma'})^{q-p} \frac{1}{(1+e_0)^2} \frac{\partial^2 u}{\partial z^2} = \frac{\partial u}{\partial T} - \frac{d}{dT} (\Delta\sigma) - \gamma_w \int_0^z \frac{\partial e}{\partial T} dz$$

$$+ (\frac{\sigma'_0}{\sigma'})^{q-p} \frac{q}{(1+e_0)^2 \sigma'} [(\frac{\partial u}{\partial z})^2 + \frac{\partial u}{\partial z} \gamma_w (G_s - 1)]$$

7.20

Equation 7.20 is the most general equation describing the one-dimensional consolidation process. In this study the quantities p , q , $k_0/(1+e_0)$, σ'_0 , and $(\frac{de}{d\sigma'})_0$ are considered to be constants. The time factor T is defined in the same manner as Terzaghi's except that this time factor T is not divided by the square of the length of the drainage path. The time factor T has a dimension of $(\text{length})^2$.

As mentioned earlier in connection with equation 7.17, the governing equation 7.19 involves the effective stress σ' and as such an explicit relation between void ratio e and effective stress σ' such as 7.17 is essential.

It can be shown that from the equation 7.19, the form of the governing equation as presented by Davis and Raymond (1965) for a normally consolidated soil may be derived. As assumed by Davis and Raymond in their formulation, the weight of a thin soil layer (for an oedometer case) may be taken such that $G_s = 1$. Also $\Delta\sigma(t) = 0$, since no additional layers are being added. Since it is a small strain theory $\frac{\partial e}{\partial T} = 0$. Again, for a normally consolidated soil $p = -1$. They further assumed that the decrease in permeability k is proportional to the decrease in compressibility $\frac{de}{d\sigma'}$; hence $q = -1$. All these parameters are substituted in the equation 7.20 to yield

$$\frac{1}{(1+e_0)^2} \frac{\partial^2 u}{\partial z^2} = \frac{\partial u}{\partial T} - \frac{1}{\sigma'_0} \left(\frac{\partial u}{\partial z} \right)^2 \frac{1}{(1+e_0)^2} \quad 7.21a$$

which is of the same form as given by Davis and Raymond (op. cit.). The presence of the term $(1/1+e)^2$ may be explained on the same basis as was done for the equation 7.13a. Equation 7.21a may be expressed to the independent variable 'a' to yield

$$\frac{\partial^2 u}{\partial a^2} = \frac{\partial u}{\partial T} - \frac{1}{\sigma'} \left(\frac{\partial u}{\partial a} \right)^2 \quad 7.21b$$

which is Davis and Raymond's equation for a normally consolidated soil with the value of the coefficient of consolidation c_v maintained constant.

Also the form of the equation governing one-dimensional consolidation with finite strains as derived by Lai (1968) can be extracted from the governing equation presented here. It would be much simpler and convenient to proceed from the equation 7.11a instead of the equation 7.12 or equation 7.20. Combining the equation 7.11a with equation 7.16 and 7.18 (as carried out by Lai), yields

$$\frac{k_0}{\gamma_w(1+e_0)} \cdot \frac{1}{\left(\frac{de}{d\sigma'}\right)_0} \frac{\partial}{\partial z} \left[\left(\frac{\sigma'}{\sigma_0}\right)^q \frac{\partial u}{\partial z} \right] = \left(\frac{\sigma'}{\sigma_0}\right)^p \frac{\partial \sigma'}{\partial t}$$

i.e.,

$$- c_{v0} \left[\frac{\partial^2 u}{\partial z^2} + \frac{q}{\sigma'} \frac{\partial \sigma'}{\partial z} \frac{\partial u}{\partial z} \right] = \left(\frac{\sigma'}{\sigma_0}\right)^{p-q} \frac{\partial \sigma'}{\partial t}$$

where

$$c_{v0} = - \frac{k_0}{\gamma_w(1+e_0)} \frac{1}{\left(\frac{de}{d\sigma'}\right)_0}$$

which is Lai's equation for one-dimensional finite strain consolidation.

7.5 THICKNESS OF THE SEDIMENT

During sedimentation, fresh layers are deposited on the existing layers. As the layers (say) of certain thickness are being deposited, the pore water dissipates whereby the thickness of the layer changes. The change in thickness depends, among other things, on the overlying sediment and the everchanging physical properties such as compressibility, permeability etc. These changing properties can be related by a single variable, namely the void ratio e . The value of the void ratio depends on the position of the point under consideration and also on time. A change in void ratio under the changing overburden reflects the changes in compressibility, the permeability and associated properties. Thus the change in thickness of a sediment, or the thickness of a soil layer may be designated in terms of the void ratio.

Because of the dissipation of the excess pore water pressures, the effective stresses change. In the case of finite strains, the thickness of a layer changes depending on its location. Let the thickness of the soil deposited be dz at a height z from the reference datum. Further, let the void ratio of this layer at any instant of time be $e(z,t)$. From the continuity of solids (equation 7.8), we have

$$\frac{\partial x}{\partial z} = 1 + e(z,t)$$

where dx is the current thickness of the soil layer. Therefore,

$$x = \int_0^z [1 + e(z,t)] dz \quad 7.22$$

The value of the void ratio $e(z,t)$ can be evaluated using the governing equation for a specified initial condition and assumed boundary conditions. Equation 7.22 may be utilized in computing the current height of a soil layer of given initial thickness.

7.6 DENSITY OF THE SEDIMENT

Since the void ratio e varies from position to position within the sediment and also from time to time, the unit weight at any given point in the sediment will change with time. Once the value of the void ratio $e(z,t)$ is known, the density of the sediment at any depth z and time t may be obtained as

$$\frac{e(z,t)\gamma_w + \gamma_s}{1 + e(z,t)} \quad 7.23$$

However, if the average density over the entire thickness of

the sediment is required, the individual values of density at various chosen intervals may be integrated by Simpson's rule and averaged. This leads to calculating the total weight of the sediment deposited.

7.7 FINITE DIFFERENCE REPRESENTATION

Exact solutions of equation 7.20 for specified boundary and initial conditions are difficult to obtain. The most general method for solving this equation is by finite differences. Equation 7.20 is reproduced below as

$$\begin{aligned}
 \left(\frac{\sigma'_0}{\sigma'_0}\right)^{-p+q} \frac{1}{(1+e_0)^2} \frac{\partial^2 u}{\partial z^2} &= \frac{\partial u}{\partial T} - \frac{d}{dT} (\Delta \sigma) - \gamma_w \int_0^z \frac{\partial e}{\partial T} dz \\
 &+ \left(\frac{\sigma'_0}{\sigma'_0}\right)^{q-p} \frac{q}{(1+e_0)^2} \frac{1}{\sigma'_0} \left[\left(\frac{\partial u}{\partial z}\right)^2\right. \\
 &\left.+ \frac{\partial u}{\partial z} \gamma_w (G_s - 1)\right]
 \end{aligned}$$

To write the above equation in a simpler form the following equivalences are made. Let

$$\begin{aligned}
 e_0 &= E0 & e &= E(L, N) \\
 \sigma'_0 &= \text{Sigmo} & u &= U(L, N)
 \end{aligned}$$

$$\gamma_w = UWW$$

$$\sigma' = \text{Sigma}(L)$$

$$\frac{DT}{(DZ)^2} = R$$

$$\gamma_w \frac{\partial e}{\partial T} dz = \text{DET}(L)$$

$$d(\Delta\sigma) = DH$$

$$\left(\frac{\sigma'}{\sigma_0}\right)^{q-p} \frac{1}{(1+e_0)^2} \cdot R = U1(L)$$

The governing equation in central differences may now be expressed as

$$U1(L) * (U(L-1, N+1) - 2U(L, N+1) + U(L+1, N+1)) \\ = U(L, N+1) - U(L, N) - DH - \text{DET}(L) (DT + (q * U1(L) / \text{Sigma}(L))) *$$

$$\left(\left(\frac{\partial u}{\partial z}\right)^2 + \frac{\partial u}{\partial z} \gamma_w (G_s - 1)\right) * (DZ)^2$$

$$\text{or} \quad -U1(L) * U(L-1, N+1) + (1. + 2. * U1(L)) * U(L, N+1) - U1(L) * U(L+1, N+1) \\ = D(L)$$

$$\text{where} \quad D(L) = U(L, N) + DH + \text{DET}(L) * DT - (q * U1(L) / \text{Sigma}(L)) *$$

$$((U(L-1, N) - U(L+1, N)) ** 2 / 4. + DZ * UWW * (G_s - 1) * (U(L-1, N) \\ U(L+1, N)) / 2.)$$

which is the difference equation for the governing differential equation.

When $L = 1$

$$-U_1(1)*U(0,N+1)+(1+2*U_1(1))*U(1,N+1)-U_1(1)*U(2,N+1) = D(1)$$

Since at $L = 1$ an impervious boundary exists, there is no hydraulic gradient; and as such

$$U(0,N+1) = U(2,N+1)$$

$$\text{Therefore } (1+2*U_1(1))*U(1,N+1)-U_1(1)*2*U(2,N+1) = D(1)$$

Thus the difference equations may be written for all values of L except when $L = N$; that is, at the top of the current sediment.

When $L = N$, i.e., at the top of the sediment at the instant $t = N$, the gradient $\frac{\partial u}{\partial z}$ equals $(U(N+1,N)-U(N-1,N))/2*DZ$ where the $(N+1,N)$ point (Figure 7.3) does not exist at the time t . To obviate this difficulty, it is safe to assume that the hydraulic gradient excess is linear between the mesh points $(N-1,N)$ and (N,N) , i.e., instead of taking central differences, backward differences are taken. Therefore:

$$\begin{aligned} -U_1(N)*U(N-1,N+1)+(1+2*U_1(N))*U(N,N+1)-U_1(N)*U(N+1,N+1) \\ = D(N) \end{aligned}$$

where $U(N+1,N+1) = 0$, always by assumption

$$\begin{aligned} \text{and } D(N) = U(N,N)+DH+DET(N)*DT-(q*U_1(N)/\text{Sigma}(N))*((U(N-1,N)- \\ U(N,N))*2+DZ*UWW*(G_s-1)*(U(N-1,N)-U(N,N))) \end{aligned}$$

where $DET(N) = DET(N-1)$

Thus the governing partial differential equation is

converted into a set of simultaneous algebraic equations using finite differences. These simultaneous equations may then be solved in the usual manner.

Once the values of $U(L,N)$ are known, the values of $U(L,N+1)$ can be computed. This procedure of 'marching out' the solution yields results at subsequent time intervals.

7.8 SUMMARY

A study has been made in order to ascertain the excess pore pressures developed in an environment, when sedimentation takes place. The treatment has been on the basis of general nonlinear behavior of the soil where the soil properties were assumed to vary with depth and time. To account for large changes in the void ratio (i.e., finite strains were allowed to develop) the continuity equation for one-dimensional fluid flow was derived in a general manner. Since large changes in void ratio usually entail large changes in soil properties of which the compressibility and the permeability are the main factors, these were taken into account by assuming that both the coefficients of compressibility and permeability are related to effective stress by power laws. These assumptions mean in turn that the coefficient of consolidation is also related to the effective stress by a power law. By combining these with other assumptions made in classical Terzaghi theory together with the vertical equilibrium of soil water system including the self weight

of the soil, the equation governing the process of consolidation was derived.

The consolidation equation obtained in this study, in general, is nonlinear. From this general nonlinear equation other published equations governing linear as well as nonlinear consolidation behavior of soils can be derived (as demonstrated on previous pages) provided the appropriate assumptions that have been made are incorporated.

7.9 A CASE HISTORY

Subject to some assumptions, the observations of Fisk and McClelland (1959) on the deltaic deposits of the Continental Shelf off Louisiana can be reproduced using the theory described in the previous sections. A brief description of the area is presented below.

The search for offshore oil was being conducted in shallow waters of the continental shelf along the entire Louisiana Coast (Fisk, 1956). Data from a number of test borings, from the gulf floor samples, indicate that the shelf surface throughout the region is underlain by relatively unconsolidated deposits of the Quaternary age. Laboratory investigations of the shelf sediments penetrated by those borings have been directed primarily toward the measurement of strength characteristics rather than consolidation properties. Consolidation tests have been performed for only a small percentage of the locations investigated (McClelland,

1967), Morgenstern (1967) calculated the degree of consolidation for a range of rates of sedimentation and coefficients of consolidation when the layer gradually grows upon an impermeable base. The results revealed that underconsolidation (average degree of consolidation was of the order of 0.10 to 0.50) is significant for silty clays and clays deposited at deltaic rates of sedimentation.

The general nonlinear one-dimensional consolidation theory developed in an earlier section may be applied to calculate the void ratio and effective stresses of any depth in the sediment. Some basic information pertaining to rates of sedimentation, type of sediment etc is obtained from McClelland (op. cit.).

The topstratum deposits of the continental shelf off Louisiana vary in thickness to a maximum of approximately 600 feet in the central area south of New Orleans. These recent deposits, together with the relatively firm soil layer upon which they rest locally, control foundation conditions at drilling platform sites. The nature and distribution of the uppermost layers of the sediments on the continental slope and in the deeper parts of the gulf have been discussed by Greenman and LeBlanc (1956) and appear to be largely clay deposits.

The principal control on the character of the topstratum deposits has been the Mississippi River, and their thickness depends mainly on the distance from sites of river-mouth sedimentation in the deltaic plain. The stream discharges more than one million tons per day of sediment through

the mouths of its birdfoot delta distributaries. The load of sediments carried to the gulf is more than 75 per cent silts and clays and less than 25 per cent very fine sands. The sands are deposited close to the mouths of the distributaries in river-mouth bars, whereas the silts and clays are carried by gulf currents for considerable distances from the delta.

The nature and distribution of Recent and late Pleistocene deposits and the physiographic features of the shelf provide evidence of events which have occurred in the region in the immediate geological past. The presence of buried valley systems across the shelf, the submarine canyon at the shelf margin, and the soil zone which mantles a buried erosional surface indicate that the shelf was exposed and was deeply eroded by stream systems in late Pleistocene time. The burial of the erosional surface by the sequence of recent deltaic deposits is proof that the sea level subsequently rose and flooded the shelf. The gradational sequence of recent deposits from a coarse substratum of sands and gravels through a fine-grained topstratum of silts and clays provides evidence of the gradual lowering the gradients of streams entering the gulf and the reduction of their carrying capacity while sea level was rising. A cycle of sea level change is represented by the erosion of the late Pleistocene valley system on the shelf area and by the subsequent flooding of the shelf by gulf waters. This cycle can logically be explained by appeal to the climatic cycle responsible for

the growth and retreat of glaciers during the closing stage of the Pleistocene. Radiocarbon dates (Fisk et al., 1954) suggest that the modern birdfoot delta began to develop 450 years ago. The deposition of the leaf-like mass of the bird-foot delta has proceeded uniformly and has resulted in the seaward elongation of the distributaries and has given rise to a pattern of diverging finger-like bar deposits of sands and sandy silts separated by wedges of silty clay. These sedimentary units, together with an underlying thin layer of prodelta marine clay, form the framework of the delta platform.

Fisk and McClelland (1959) have provided data for three locations of similar composition, but of different degrees of consolidation (Table 7.1).

To apply the nonlinear theory to the above cases the following information must be known.

- (a) The material input values, such as the initial void ratio, e_0 and the corresponding initial effective stress σ_0' .
- (b) The mass rate at which deposition over the years took place so as to yield the present thickness.
- (c) The compressibility and permeability characteristics; their initial values at e_0 and the manner in which they vary.

To determine the mass rate of deposition, the total weight and the original thickness of the sediment are calculated. From the data of McClelland (1967) the void ratio

and unit weight variation with depth are obtained. The total weight of the sediment is calculated. The average void ratio of the sediment is determined. It may be noted that the thickness of the sediment is proportional to the quantity $(1+e)$. Therefore

$$\text{Original thickness} = \text{Present thickness} \frac{(1+e_0)}{(1+e)} .$$

The value thus obtained gives a rough approximation of the actual rate at which sedimentation took place. The mass rate of deposition is then obtained by dividing the total weight with the original thickness.

The input initial void ratio e_0 may be termed as that void ratio of the sediment a few centimeters below the mud-line. Also the value of e_0 may be varied with the water content, $w\%$ ($e_0 = w G_s$, where G_s is the specific gravity of the solids).

To arrive at the input value for the effective stress, σ'_0 , a relation between e and σ' must be known. The sediment at Eugene Island Block 188 is fully consolidated and behaves as a normally consolidated soil (Figure 7.4). Thus the soil behaviour is expressed as

$$e = 1.84 - 0.75 \log_{10} \sigma'$$

This relation is made use of for the sediment at the other two locations

To determine the variation of permeability, a relation

between $m_v/1+e$ (m_v the coefficient of volume compressibility) and σ' is drawn (Figure 7.5). If the assumption is made that the value of the coefficient of consolidation, c_v is a constant, the following relation is obtained.

$$k/1+e \propto (\sigma')^{-0.814}$$

An estimate of the value of k_0 corresponding to σ_0' can then be made. The value of k_0 was varied together with the value for q (in the equation 7.18) for the underconsolidated sediment at Grand Isle Block 23 to fit the observed data of void ratio with depth (Figure 7.8). This is carried out since the rate of deposition for Eugene Island Block 188 sediment is so slow that a variation of c_v and/or q does not have any influence on the degree of consolidation. Figure 7.6 yields the variation of c_{v0} (i.e., the variation of k_0) with q . A decrease in the value of q is compensated by an increase in c_{v0} in the relation

$$c_v/c_{v0} = \left(\frac{1+e}{1+e_0}\right)^2 \left(\frac{\sigma'}{\sigma_0'}\right)^{1+q}$$

so as to yield the same void ratio-depth relationship as the observed (Figure 7.8). It has been observed from Figure 7.2 that the values of q for the various soils tested by Normand (1964) are:

Weald Clay	$q = - 0.67$
Avonmouth Clay	$q = - 0.60$
Kaolinite	$q = - 0.63.$

Also from Figure 7.5 for the fully consolidated sediment at Eugene Island Block 188 the value of q obtained is -0.814 (when c_v is assumed constant). Keeping these values in view, for purposes of this study, the following set of values are chosen:

$$q = - 0.70 \quad c_{v0} = 40 \text{ FT}^2/\text{YR.}$$

$$q = - 1.05 \quad c_{v0} = 50 \text{ FT}^2/\text{YR.}$$

A value of 1×10^{-6} cm/sec to 1.5×10^{-6} cm/sec for k_0 is obtained, which is quite reasonable for the type of sediment dealt with. The properties of the sediments used in the analysis are:

$$e_0 = 2.3$$

$$e = 1.84 - 0.75 \log_{10} \sigma'$$

Figures 7.7, 7.8, and 7.9 illustrate the relationship between the void ratio and depth for the three locations. The observed data is represented by points while the calculated results are shown by full lines. The calculated values agree very well with the observed data. Figure 7.7 yields the relationship between void ratio and depth for two input void ratios (i.e., e_0) of 2.7 and 2.3. As can be seen the differ-

ence in the curves lies only in upper few feet of the sediment. A similar trend was observed at the other two locations (this is not shown in Figures 7.8 and 7.9).

Figures 7.10, 7.11, and 7.12 show the manner in which permeability decreases with depth at the end of deposition. The variation is typical and it decreases from a value of 1.0 for k/k_0 to a value of the order of 0.04. However, it is noted that the variation of permeability with depth for the South Pass Block 20 sediment (Figure 7.12) is very small in the upper few feet and then gradually the decrease grows rapidly. This is because the sediment is very underconsolidated and the upper few feet are almost at the input void ratio e_0 (and effective stress σ_0'). As the sediment is being built up the effective stress increases and hence a decrease in the permeability occurs.

Figures 7.13, 7.14, and 7.15 illustrate the variation of the coefficient of consolidation with depth for the input values of

$$q = -0.70 \quad c_{v0} = 40 \text{ FT}^2/\text{YR.}$$

$$q = -1.05 \quad c_{v0} = 50 \text{ FT}^2/\text{YR.}$$

The variation (increase or decrease) of c_v/c_{v0} with depth is mainly dependent on the value of q . The smaller the value of q (smaller than -1.0) the value of c_v decreases with depth. However, a value of q greater than -1.0 makes the value of c_v increase with depth although the increase is very small.

This demonstrates the manner in which the magnitude of q affects both k and c_v with depth.

7.10 DISCUSSION

In this study the state of consolidation at several locations on the continental shelf off Louisiana is studied. The one-dimensional consolidation theory adopted for analysis is the most general accounting for a mass input at a prescribed initial void ratio. The results calculated are in good agreement with the observed field values. The rate of deposition and the soil characteristics such as the compression index, initial void ratio, and coefficient of permeability control the pore pressure dissipation (and hence the effective stress).

A close study of the equation 7.20 reveals that a value for the exponential q has a significant influence on the ultimate results. A value of zero for q reduces the equation 7.20 to

$$\left(\frac{\sigma_0'}{\sigma_1'}\right)^p \frac{1}{(1+e_0)^2} \frac{\partial^2 u}{\partial z^2} = \frac{\partial u}{\partial T} - \frac{d}{dT} (\Delta\sigma) - \gamma_w \int_0^z \frac{\partial e}{\partial T} dz \quad 7.24$$

The above equation does not embody any more the term containing G_s . In other words, if by any chance the ratio $k/(1+e)$ remains constant (i.e., $q = 0$) which is most unlikely, during consolidation the specific gravity G_s (or the self weight) of

the consolidating material does not contribute anything to the progress of consolidation.

Also from equation 7.20 the expression $\frac{\partial u}{\partial z} \gamma_w (G_s - 1)$ contains both the hydraulic gradient $\frac{\partial u}{\partial z}$ and G_s is the specific gravity of solids. If either one of these terms is zero then the expression $\frac{\partial u}{\partial z} \gamma_w (G_s - 1)$ vanishes. The hydraulic gradient ($\frac{\partial u}{\partial z}$) is zero at an impervious boundary where there is no exchange of water across it. At such a boundary, it seems, the influence of G_s is not felt although at all other sections G_s has its influence. By the same token the influence of G_s is the maximum where the hydraulic gradient is the highest. The hydraulic gradient is the highest at the top of the sediment and hence the influence of G_s is maximum in the upper layers of the sediment.

To assess the influence of G_s analytical solutions were obtained for values of $G_s = 2.7$ and $G_s = 1.0$ (buoyant weight). It has been observed that the computed results of void ratio (with depth) and the degree of consolidation do not differ substantially. It may be concluded that G_s (i.e., self weight of the sediment) is not too important in quantitative results.

In summary the following may be expressed.

The deltaic sediment samples (very under consolidated to fully consolidated) reported by McClelland (1967) were examined in the light of the theory presented in section 7.4. The rate of deposition is believed to be the main factor most closely associated with the consolidation characteristics

observed. The rates of sedimentation and related properties are available in sedimentology literature. In regions of high rate of sedimentation, there will be a lag between the accumulation of the material and the consolidation associated with it. This gives rise to an excess pore pressure and the under consolidated material is prone to slumping. The prediction of excess pore pressure can be made to a high degree of accuracy by the analysis presented in section 7.4. The state of consolidation of the clay mass is very important in connection with foundation studies for offshore structures, for the strength of these deposits is a function of pre-consolidation pressure.

Other parameters that affect the build up pore pressures during sedimentation are the material properties such as

- (a) the consolidation characteristics of the sediment;
- (b) the variation of compressibility and permeability;
- and (c) the environment in which deposition takes place.

It has been demonstrated by Skempton (1970) that the behavior of (fully consolidated) deltaic sediments is mostly normally consolidated. And hence the value of p in equation 7.16 may be taken as equal to -1.0 for all practical considerations.

The sedimented void ratio e_0 (and hence the corresponding effective stress) depends on the type of environment in which the sedimentation takes place. Depending on the sedimented material properties such as e_0 and the rate of sedimentation the behaviour of the sediment at any stage of

accumulation can be predicted provided the value of sedimented permeability k_0 (i.e., the input coefficient of consolidation c_{v0}) and its behaviour during sedimentation are known. The magnitude of the values of k_0 and q of the sediments off Louisiana are precisely not known. It has been shown that q has a significant influence on the variation of the coefficient of consolidation and the consolidation characteristics of the sediment.

Table 7.1 Deltaic deposits off Louisiana

Location	State	Liquid Limit %	Plasticity Index %	Depth Feet	Age Years
Eugene Island Block 188	Fully Consolidated	80-90	53	96	not less than 10000
Grand Isle Block 23	Under Consolidated	80-90	53	170	not more than 1500
South Pass Block 20	Very Under Consolidated	60-100	53	320	450

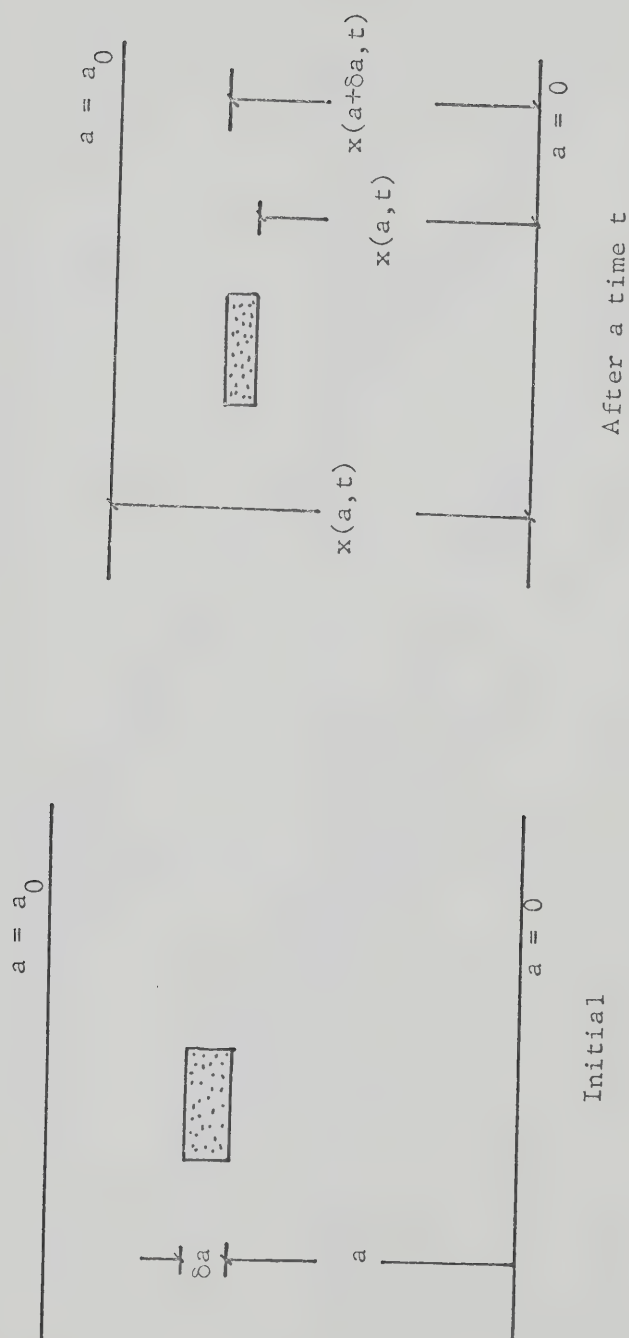


FIG. 7.1 CONFIGURATION OF SOIL ELEMENT

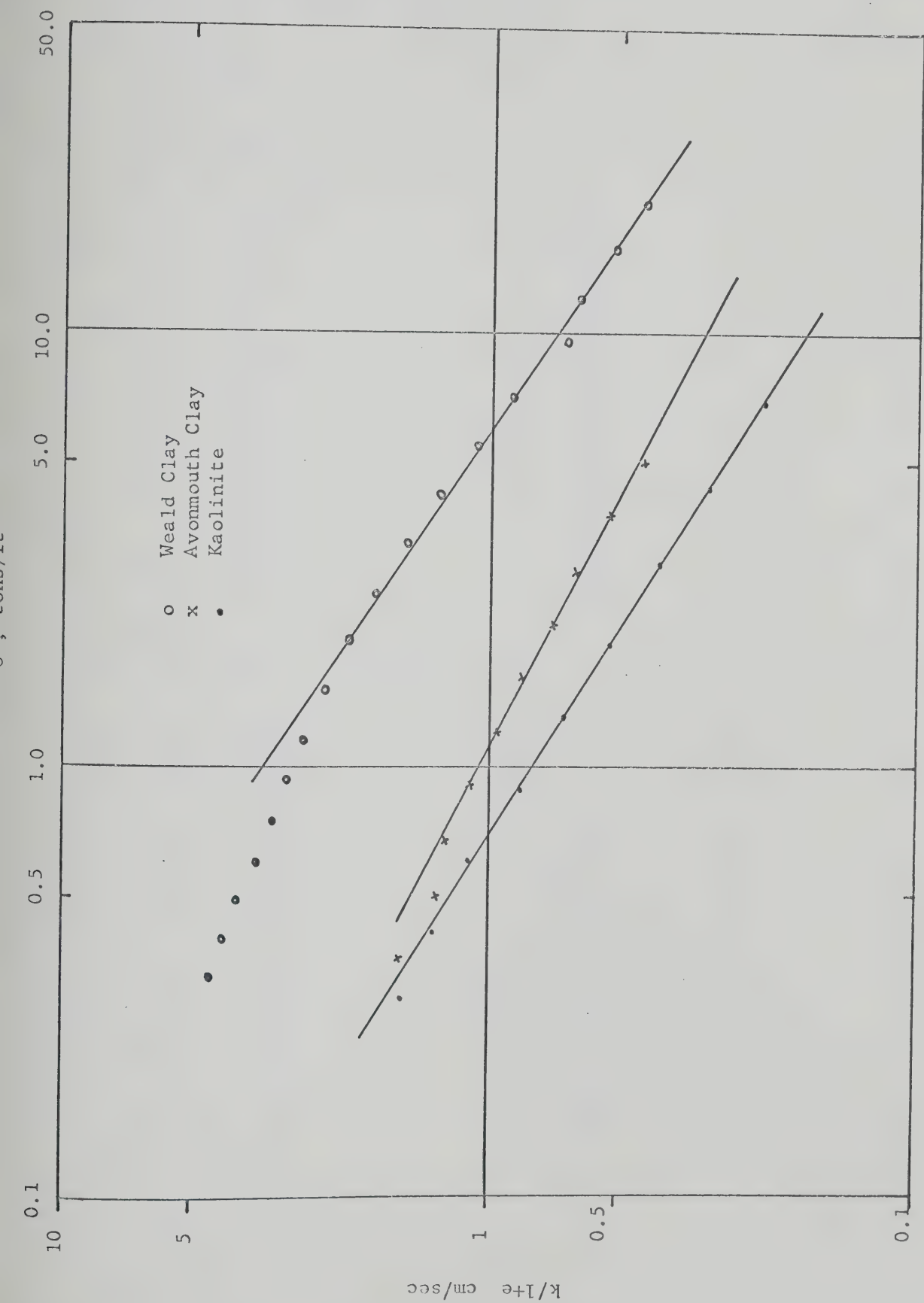


FIG. 7.2 PERMEABILITY - EFFECTIVE STRESS RELATIONSHIP FOR N. C. CLAYS

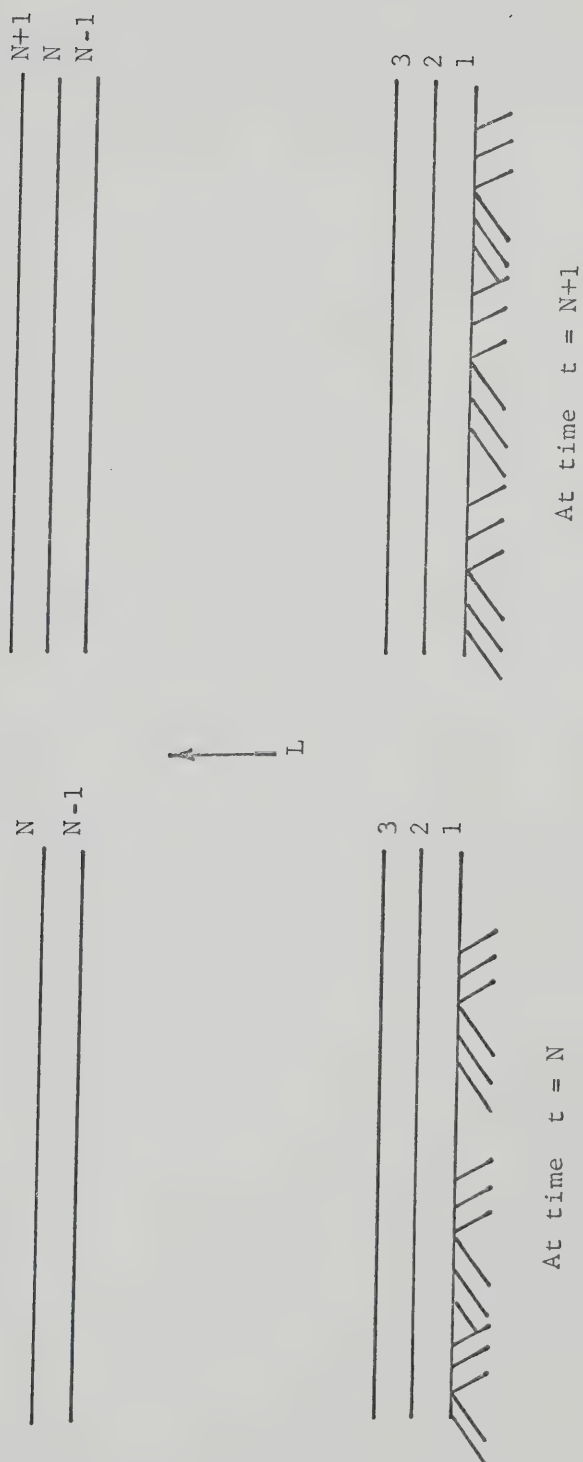


FIG. 7.3 SEDIMENT LAYER GROWTH

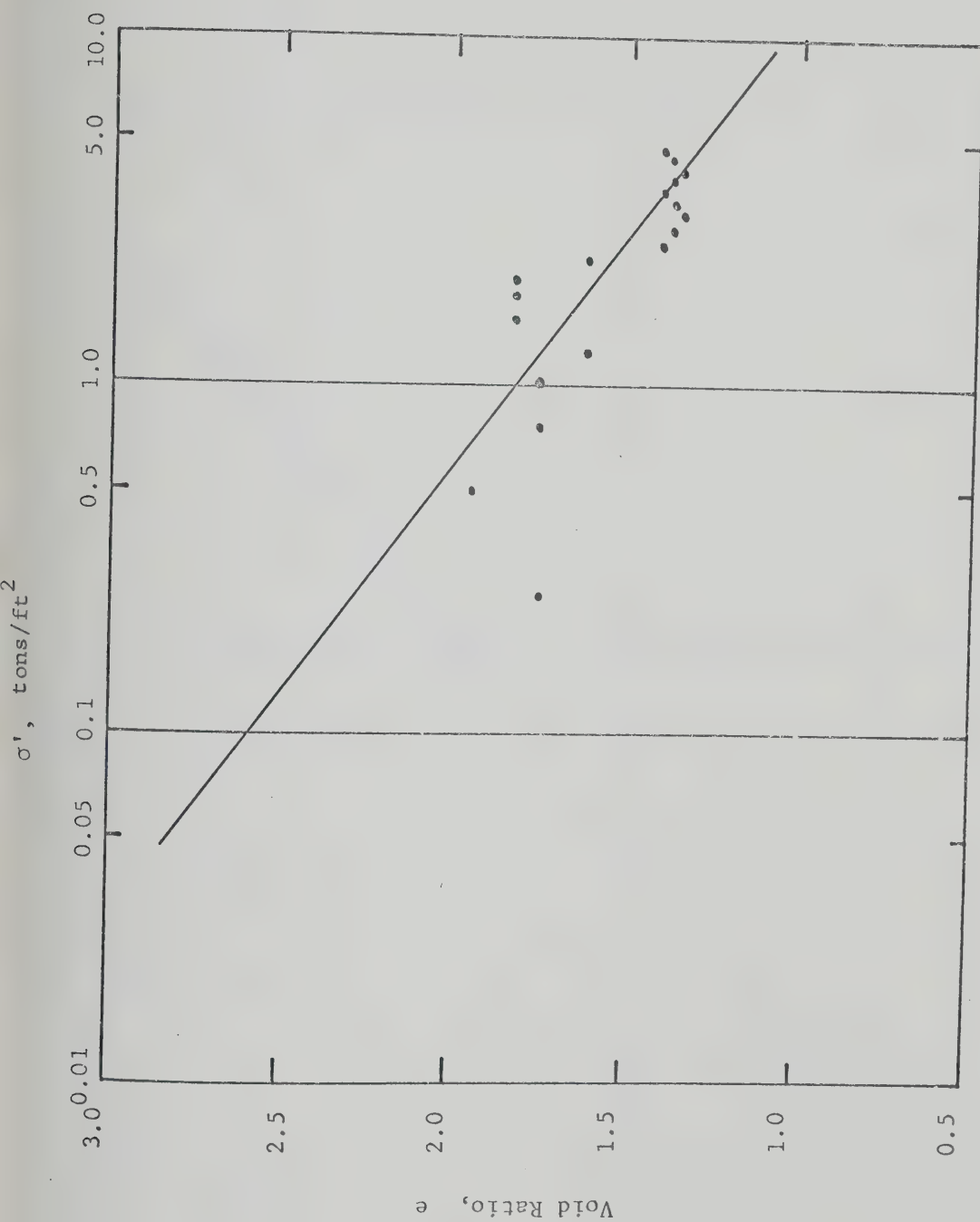


FIG. 7.4 RELATIONSHIP BETWEEN VOID RATIO AND EFFECTIVE STRESS,
EUGENE ISLAND BLOCK, 188.

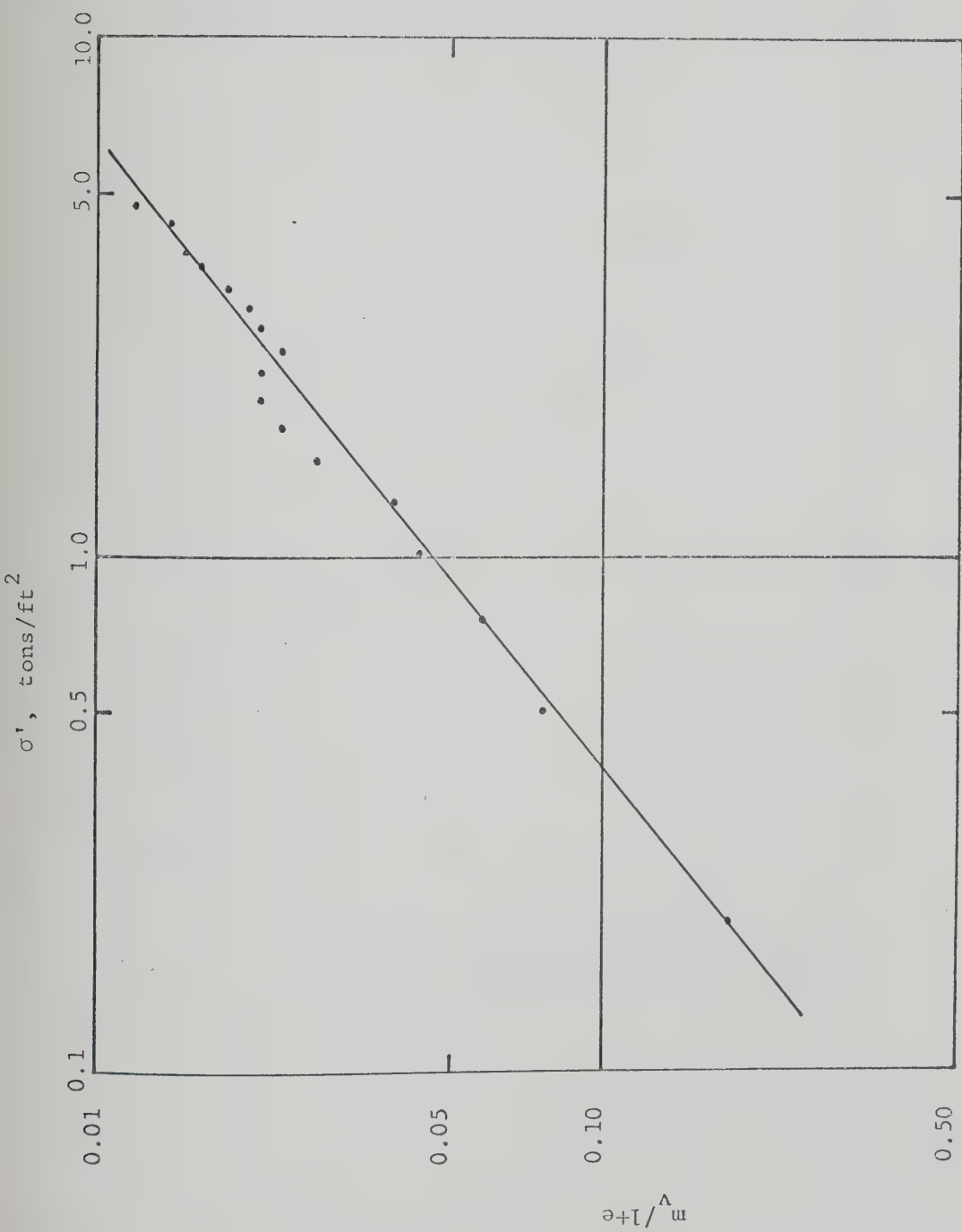


FIG. 7.5 RELATIONSHIP BETWEEN COMPRESSIBILITY AND EFFECTIVE STRESS,
EUGENE ISLAND BLOCK, 188.

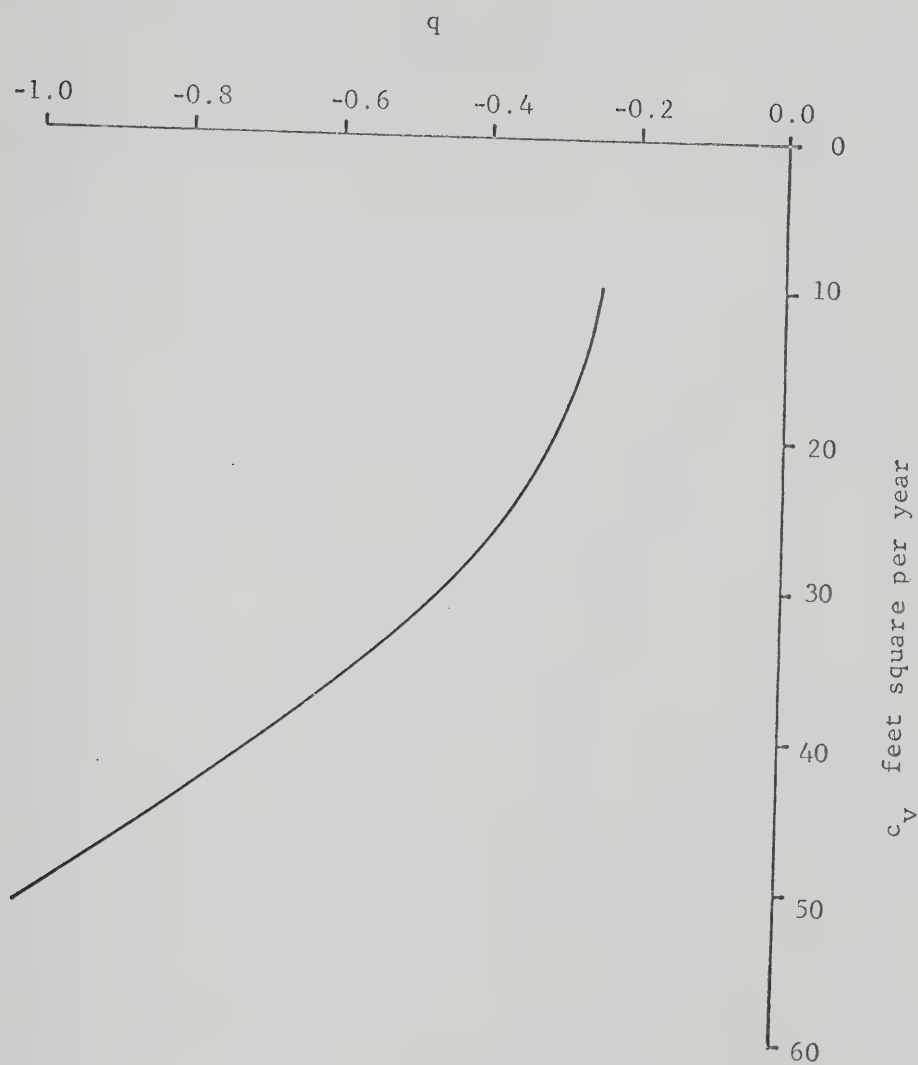


FIG. 7.6 RELATIONSHIP BETWEEN c_v and q ,
EUGENE ISLAND BLOCK, Y88.

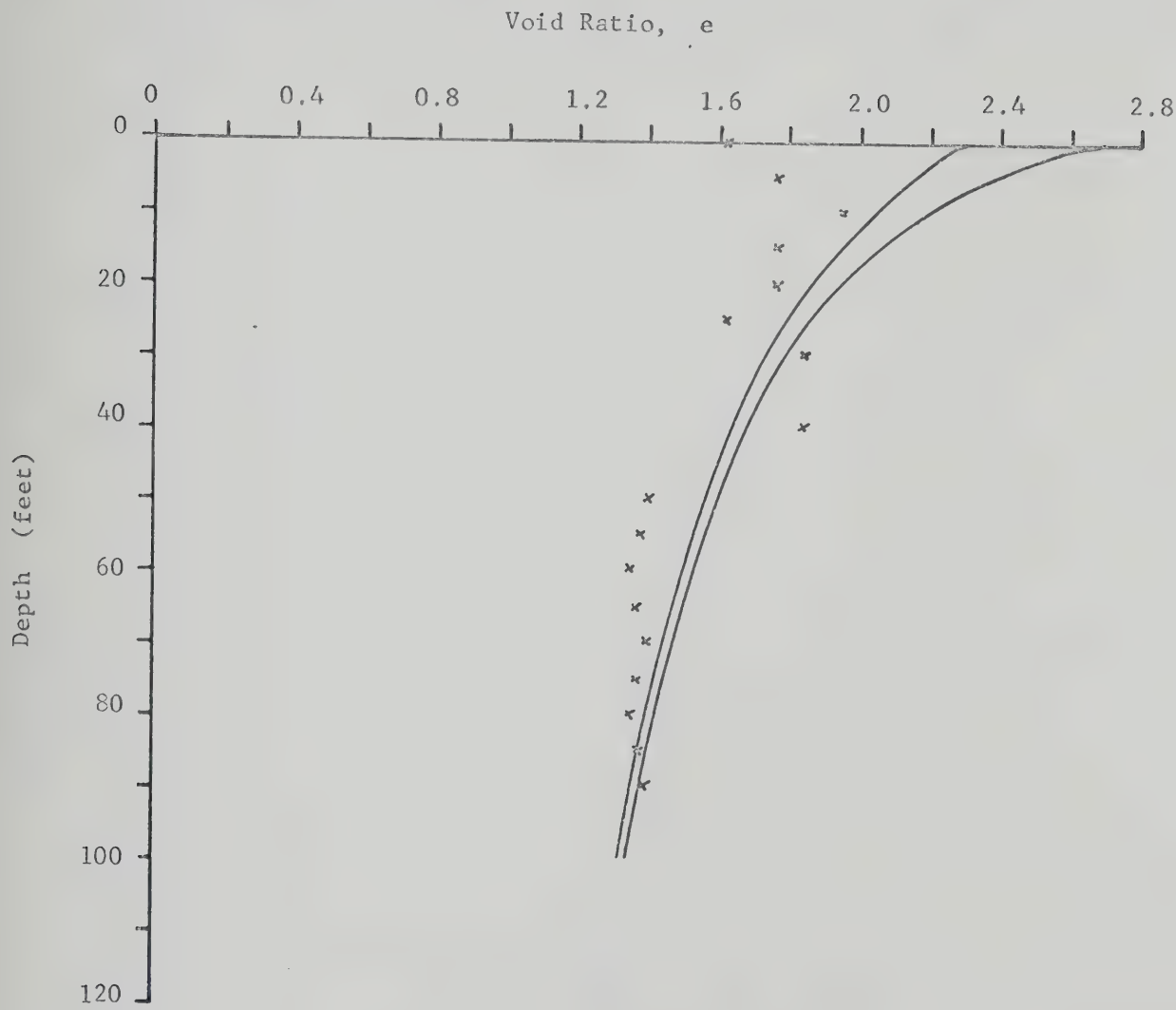


FIG. 7.7 RELATIONSHIP BETWEEN VOID RATIO AND DEPTH, EUGENE ISLAND BLOCK, 188.

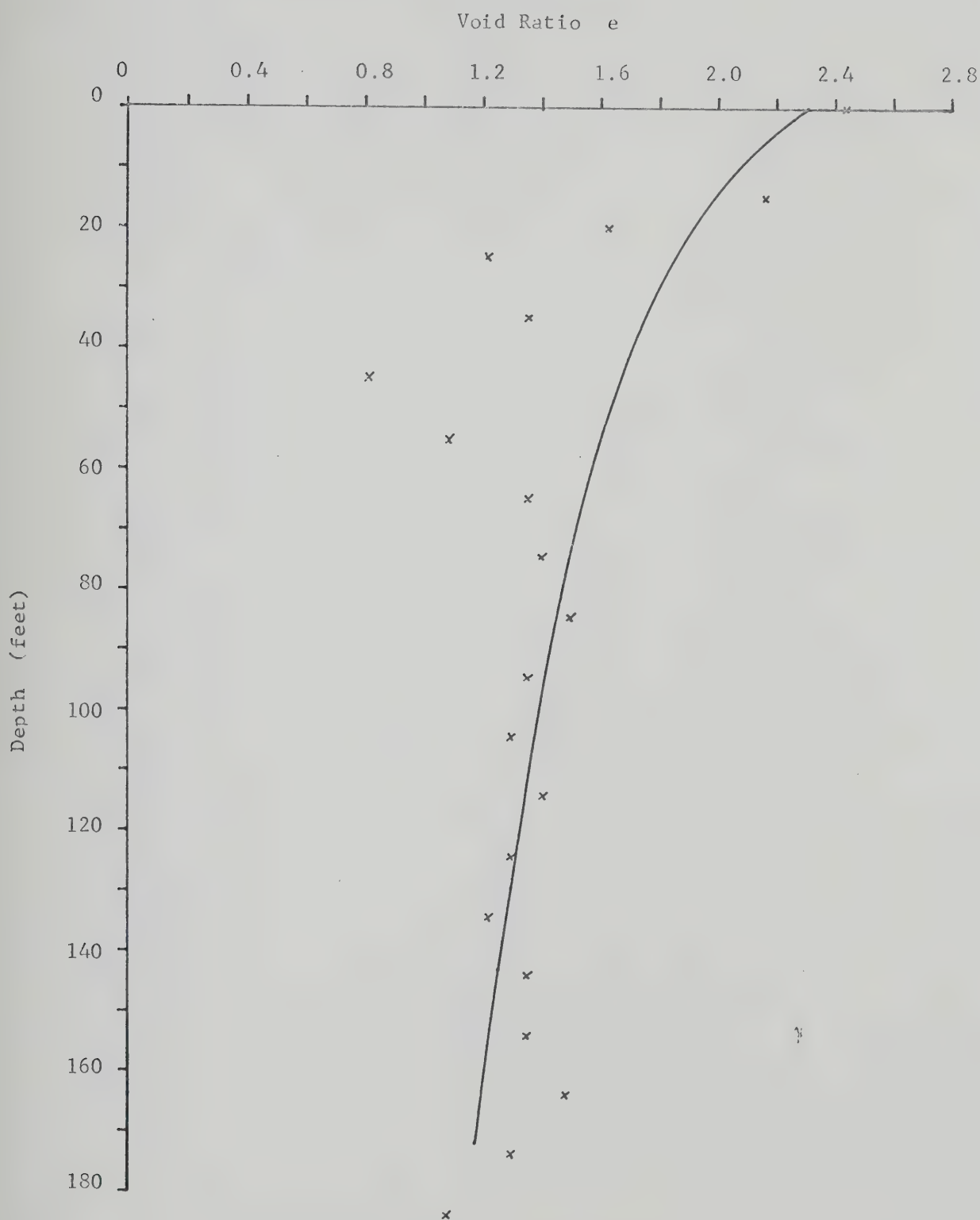


FIG. 7.8 RELATIONSHIP BETWEEN VOID RATIO AND DEPTH, GRAND ISLE BLOCK, 23.

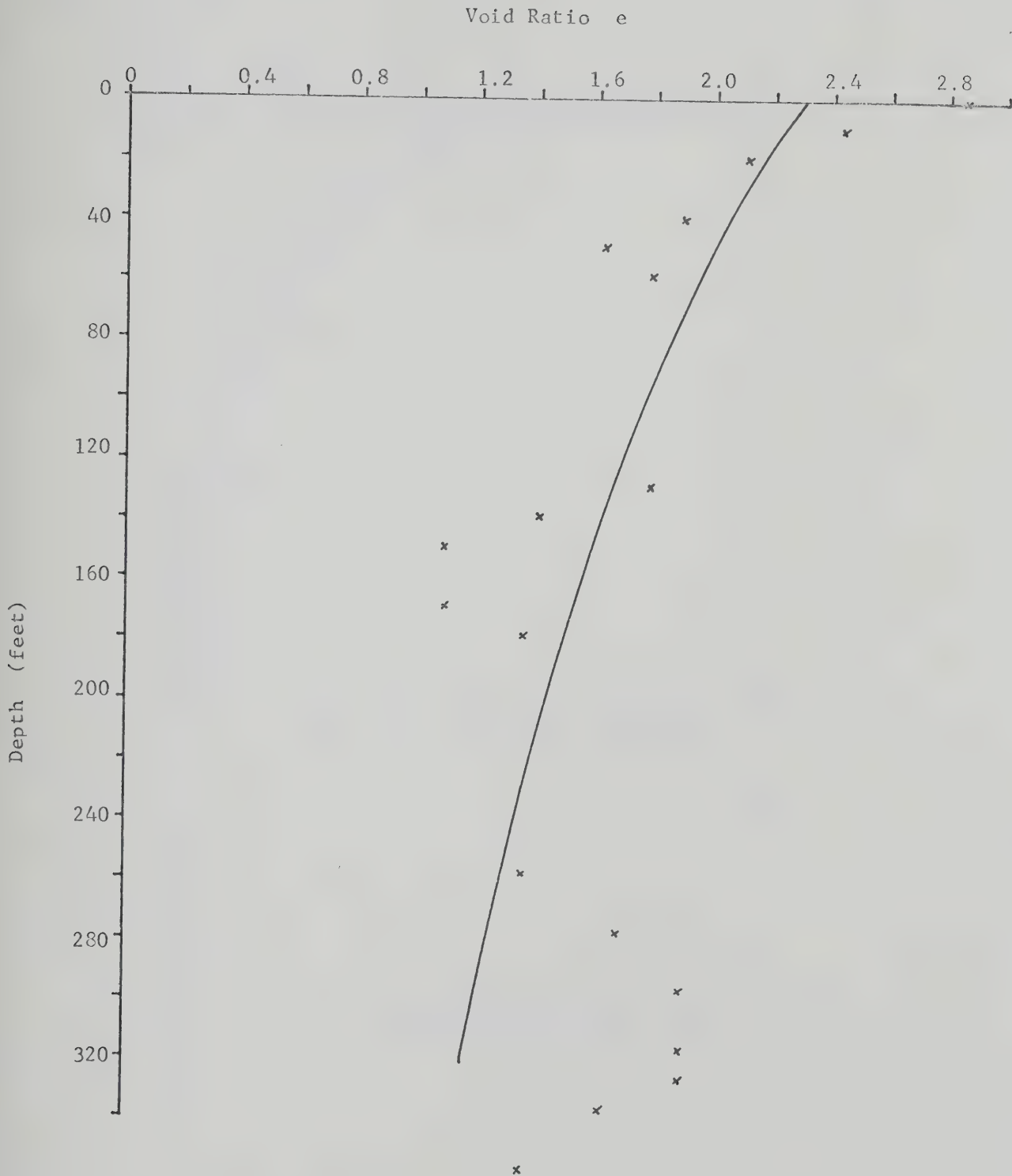


FIG. 7.9 RELATIONSHIP BETWEEN VOID RATIO AND DEPTH,
SOUTH PASS BLOCK, 20.

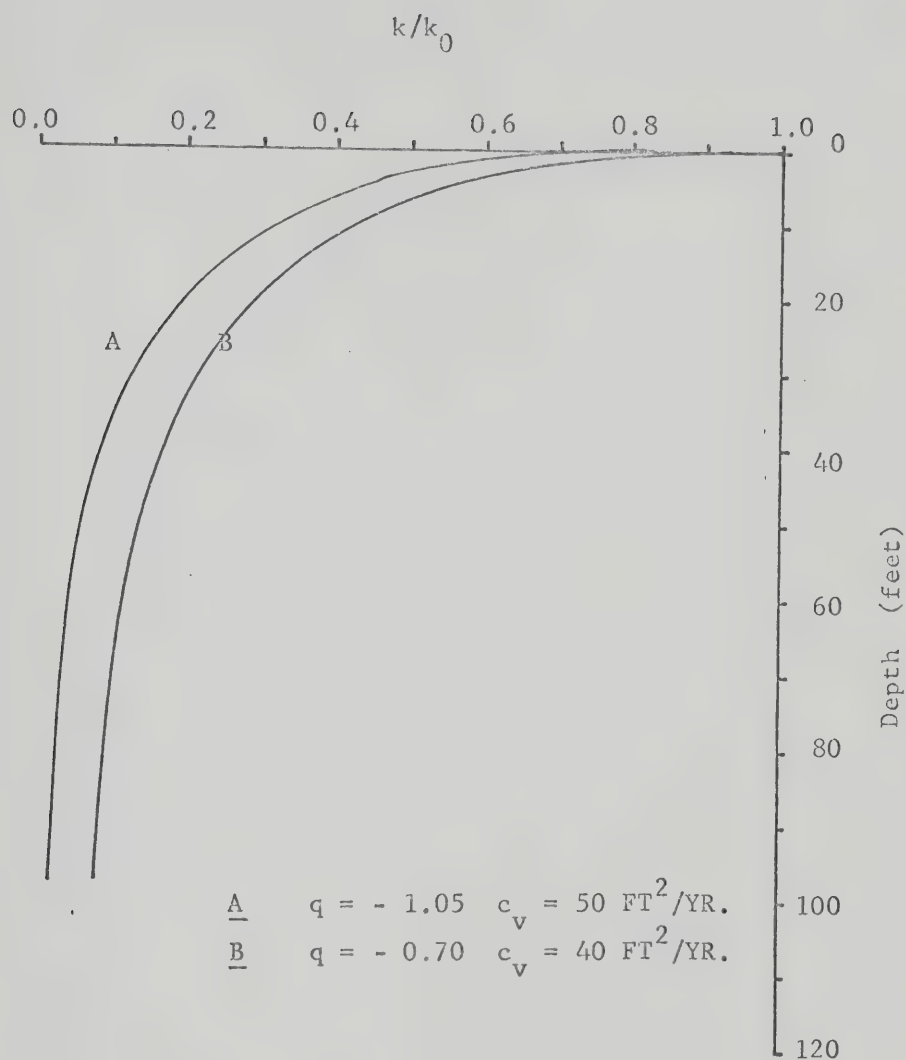


FIG. 7.10 VARIATION OF PERMEABILITY WITH DEPTH,
EUGENE ISLAND BLOCK, 188.

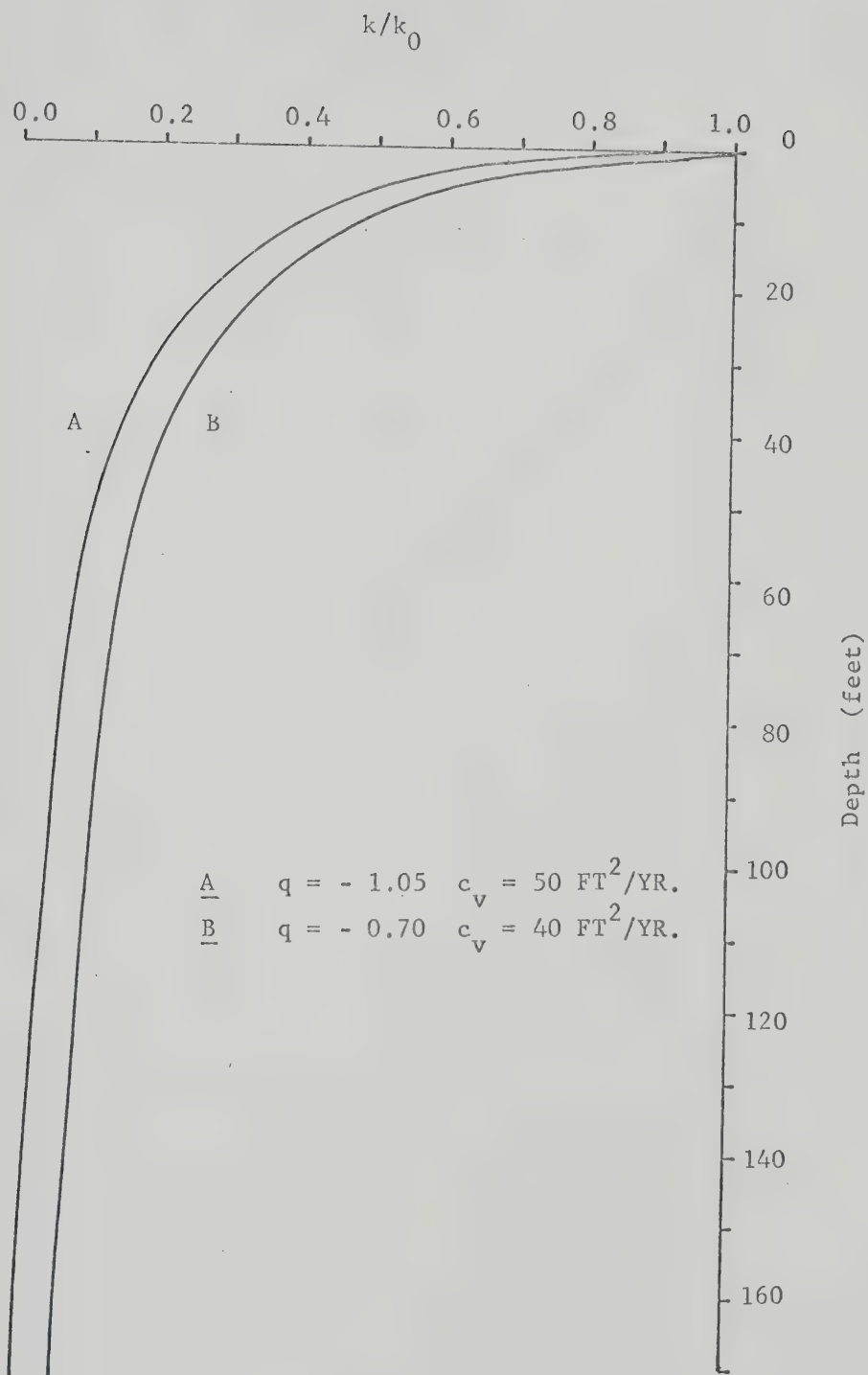


FIG. 7.11 VARIATION OF PERMEABILITY WITH DEPTH,
GRAND ISLE BLOCK, 23.

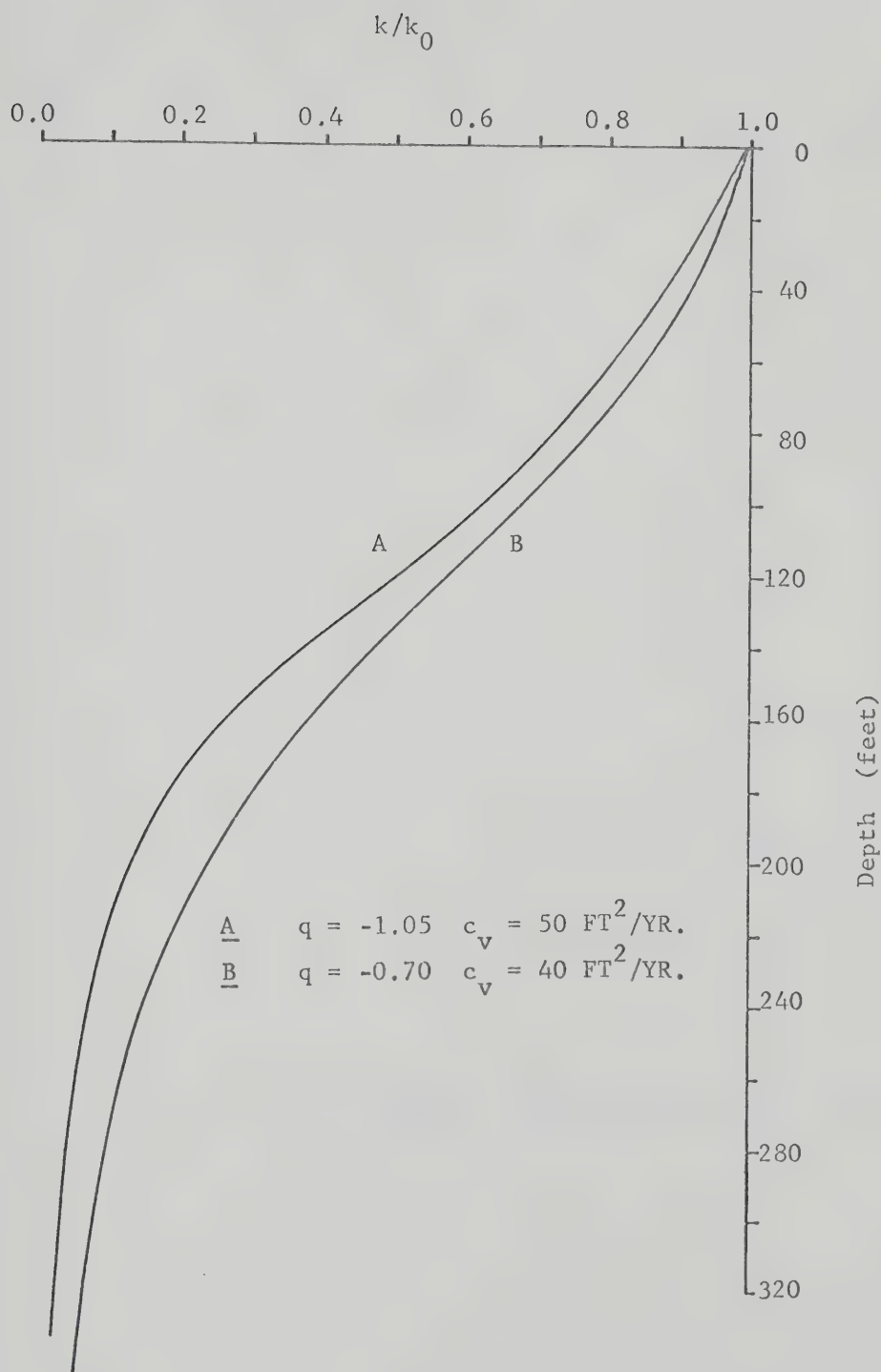


FIG. 7.12 VARIATION OF PERMEABILITY WITH DEPTH,
SOUTH PASS BLOCK, 20.

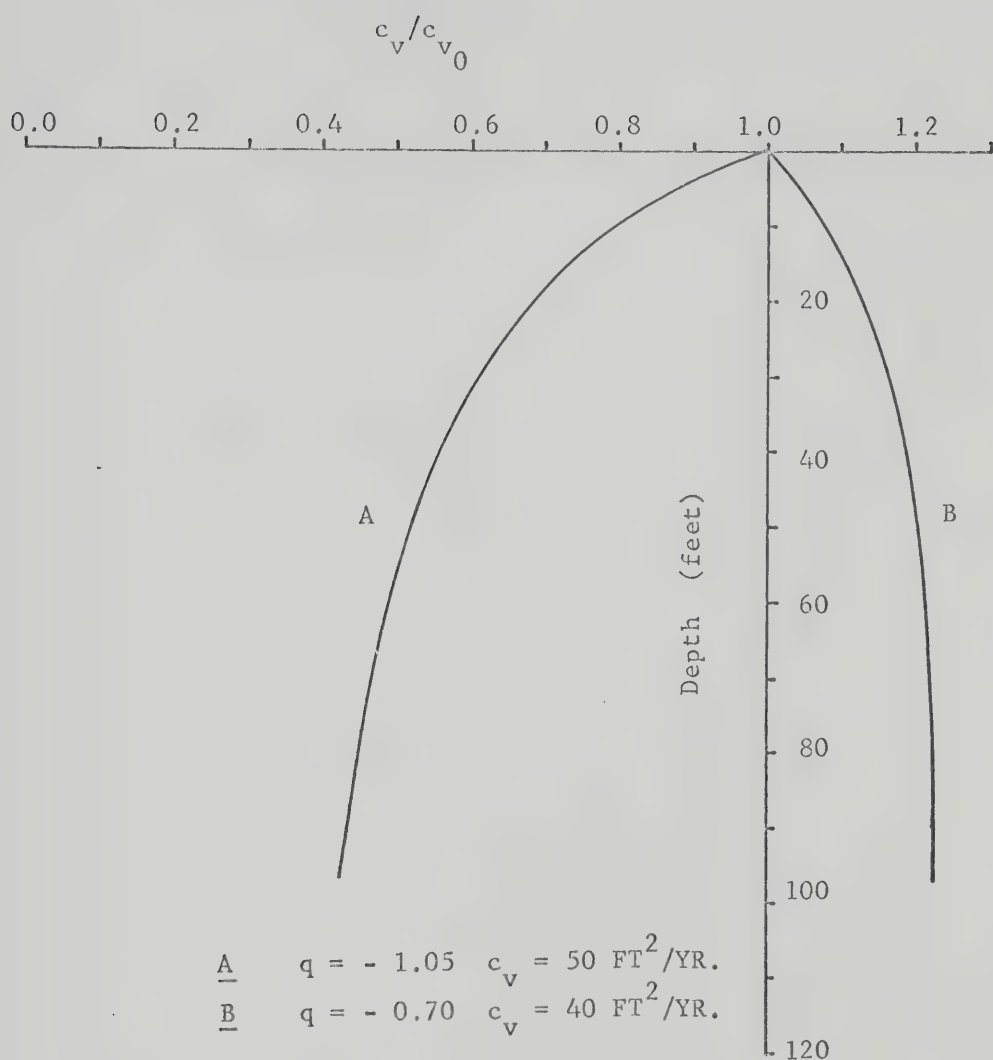


FIG. 7.13 VARIATION OF COEFFICIENT OF CONSOLIDATION WITH DEPTH, EUGENE ISLAND BLOCK, 188.

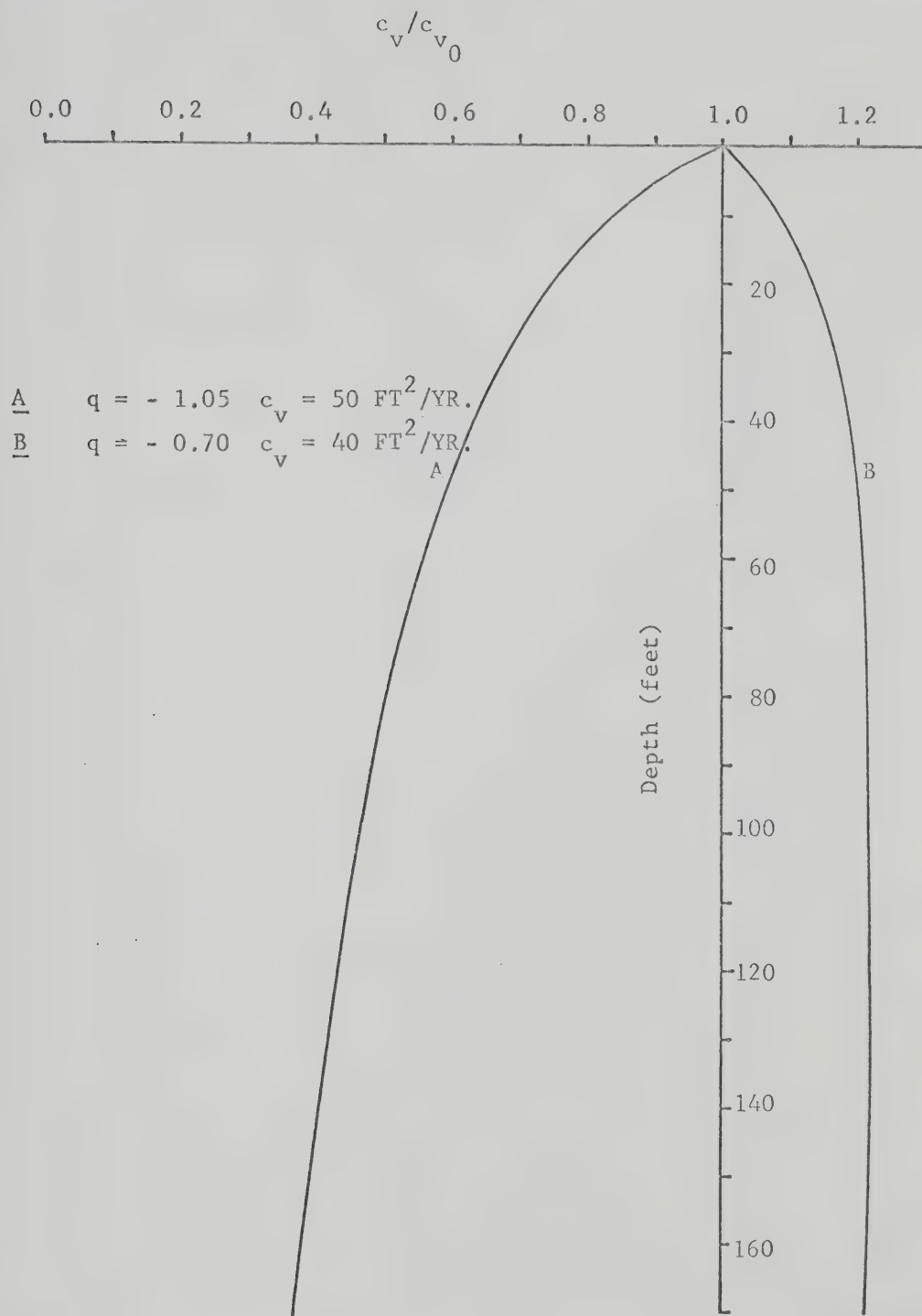


FIG. 7.14 VARIATION OF COEFFICIENT OF CONSOLIDATION WITH DEPTH, GRAND ISLE BLOCK, 23.

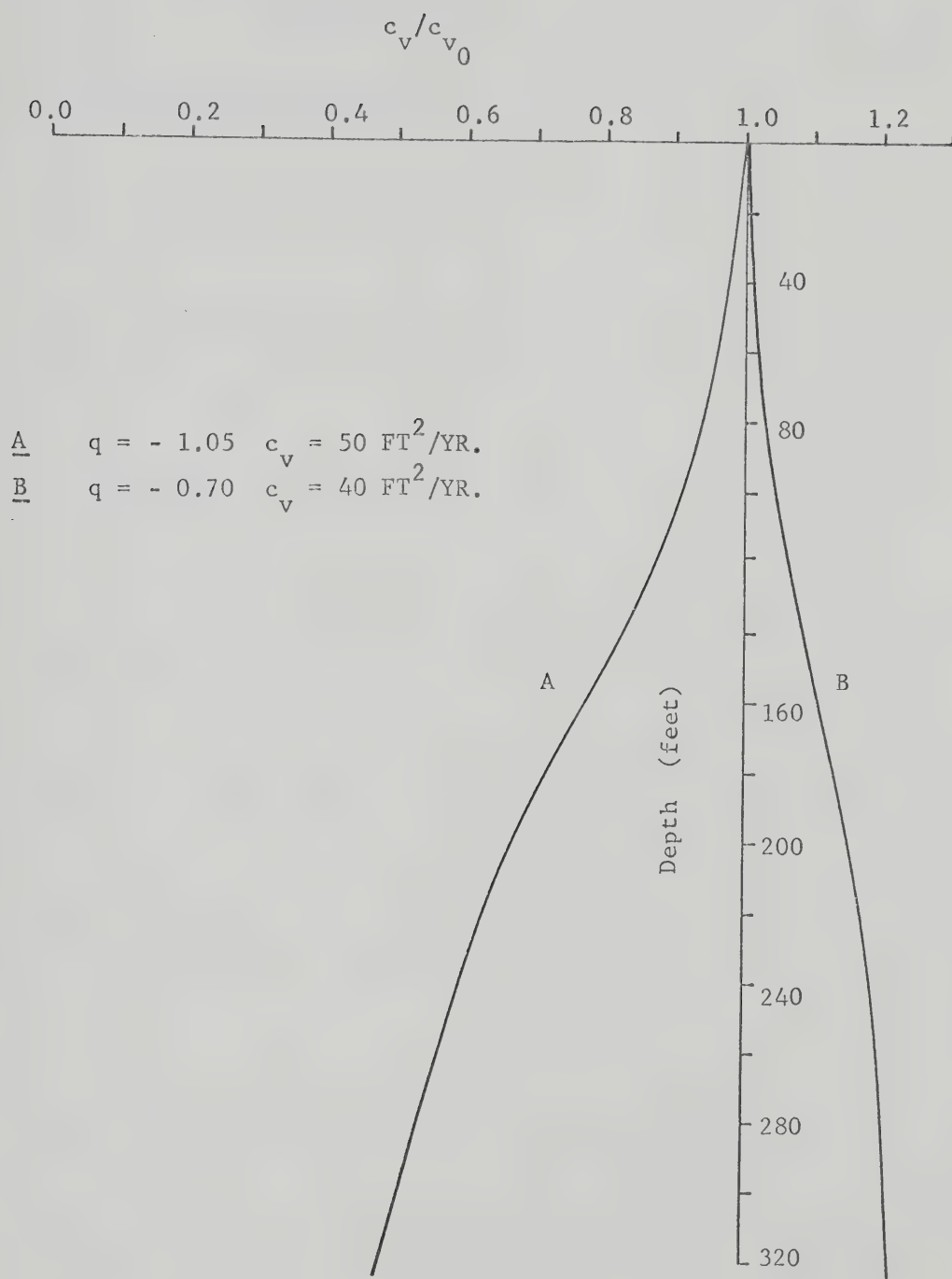


FIG. 7.15 VARIATION OF COEFFICIENT OF CONSOLIDATION WITH DEPTH, SOUTH PASS BLOCK, 20.

CHAPTER VIII

EROSION AND SWELLING IN VALLEY FORMATION

8.1 GENERAL

This chapter deals with the pore water pressure-time relationship for a fully saturated clay layer subjected to a uniformly-distributed eroding load. The governing equation is developed on the basis of the Terzaghi's classical one-dimensional consolidation theory and it is weakly nonlinear in character. With this nonlinearity and the boundary conditions encountered, it is difficult to obtain a closed form solution. A numerical solution based on finite difference approach is presented. The study is of practical value in the assessment of pore pressure equalization of an eroded soil mass. Further, the study aims at correlating geological and physical parameters involved with the theoretical solution.

8.2 FORMULATION

The problem considered is that of a semi-infinite mass of soil eroded at a prescribed arbitrary rate at the top. The properties of a real soil are time and space dependent. For purposes of this study, however, the material properties are assumed constant (on the lines of Terzaghi's classical theory), i.e., the physical properties of the soil such as the coefficient of swelling (consolidation), the coefficient of perme-

ability etc. are constant.

The problem may be considered to represent any of the following categories:

- (a) the eroded material removed instantaneously; and
- (b) the usual case of finite rate of removal of eroded material.

Thus the problem is one of a moving boundary condition.

Generally, two types of moving boundary problems are encountered:

- (i) motion of the boundary is due to the rigid body motions of the entire body (Carslaw and Jaeger, 1959);
- (ii) motion of the boundary is due to local conditions near the boundary.

Further, in type (ii) two cases can be distinguished:

- (a) problems in which the motion of the boundary is prescribed; and
- (b) problem in which the boundary must be determined as a part of the solution of the erosion problem.

The problem of erosion is developed along the lines given by Gibson (1958) for sedimentation. In the case of sedimentation fresh layers of soil are added at the top whereby the thickness of the sediment increases with time. In the erosion study, the layers are removed gradually at the top and hence the thickness of sediment decreases with time. Thus erosion may be looked upon as similar to sedimentation except that instead of soil layers being added at the

top, the soil layers are removed gradually at a constant rate. Thus the quantity $\Delta\sigma$ in Gibson's (1958) equation for sedimentation (equation 7.13b) may be changed to $-\Delta\sigma$; then equation 8.1 will describe a process of erosion.

$$c_v \frac{\partial^2 u}{\partial z^2} = \frac{\partial u}{\partial t} + \frac{d}{dt} (\Delta\sigma) \quad 8.1$$

where c_v denotes the coefficient of swelling of the material

u denotes the deficient pore pressure

$\Delta\sigma$ denotes the weight of the soil removed by erosion.

Equation 8.1 governs the dissipation of deficient pore water pressures in one dimension when erosion takes place at a prescribed rate of $d(\Delta\sigma)/dt$. The expression $\Delta\sigma$ is equal to $\gamma dh/dt$ where γ is the bulk unit weight of the soil and dh/dt is the rate of removal of the soil with time.

BOUNDARY CONDITIONS

A unique solution to equation 8.1 depends primarily on the boundary conditions. The top of the sediment is always open to the atmosphere and is free to drain; the pore pressures will dissipate almost instantaneously. Thus at the top the excess (deficient) pore pressure will always be zero. But then the top boundary is 'moving' with time. The top boundary is to be located at any instant of time.

At the instant of time $t = 0$ (i.e., initially) the top of the sediment is designated by $z = 0$. The rate of erosion dh/dt , is equal to m ; the amount of sediment eroded out is $z = mt$ after a time t . Thus the top boundary at time $t = t$ exists at a distance $z = mt$ from the original reference plane. It is at this boundary the deficient pore pressure is zero. Therefore the top boundary condition may now be defined as

$$u(z,t) = 0 \quad \text{at } z = mt, \quad t > 0 \quad 8.2a$$

The bottom boundary condition must also be specified. It is tacitly assumed that the problem involves a semi-infinite homogeneous soil medium. It may be said with no loss of generality that at a great depth (i.e., $z \rightarrow \infty$), there will be no change in the deficient pore pressure (equal to the weight of soil removed) at any given time. Or, in other words, at infinite depth the soil will in effect act as an impermeable layer since across that layer no hydraulic gradient will be set up. Thus the bottom boundary may be defined as

$$\frac{d}{dt} u(z,t) = 0 \quad z \rightarrow \infty, \quad t > 0 \quad 8.2b$$

The soil mass as a whole may be assumed to be in equilibrium with its surroundings before the process of

erosion sets in. As such it may be said that no deficient pore pressure exists throughout the soil mass at the instant when erosion is about to set in. The initial condition, thus, is

$$u(z,t) = 0 \quad 0 \leq z \leq \infty, \quad t = 0 \quad 8.2c$$

Making use of the boundary and initial conditions given by equations 8.2 a unique solution to equation 8.1 may be obtained. A closed form solution of the equation 8.1 for the nonlinear boundary conditions specified is difficult to obtain. Hence a numerical method is sought.

The procedure for the numerical solution of equation 8.1 involves replacing the equation by a finite difference form. That is accomplished by central differences using Crank-Nicolson's implicit method. The resulting set of simultaneous linear equations is solved by the Gaussian elimination procedure.

However, the nature of the bottom boundary condition specified may influence the accuracy of the results. Hence, the artificial boundary specified by $z \rightarrow \infty$ (equation 8.2b) was carefully studied, both with respect to its location and with respect to its assigned boundary condition, to determine its effect on the computed results. The conclusions were:

- (a) that a distance L of approximately 2000 feet is adequate in order to neglect the influence of the boundary; and

- (b) that consideration of this boundary as impermeable ($\frac{\partial u}{\partial z} = 0$), or that at this boundary the pore pressure $u(z,t)$ is always equal to the weight of the soil eroded at that instant had no significant effect; hence the solution was obtained for $L = 2000$ feet. The solution was found to be stable.

According to this method of solution, the behavior of the soil mass is determined at a finite number of discrete nodal points; if values of the parameter u are desired at points intermediate to the nodal points, linear interpolation may be employed.

8.3 DISCUSSION OF NUMERICAL RESULTS

Typical results are presented for the erosion of a low-swelling clay sediment under constant rate of erosion. The clay deposit may be considered as recently glaciated (quaternary age) and as being eroded by fluvial action. The sediment is assumed to be fully saturated and on the top of the eroded layer, it is assumed, water is always available. By this means, the deficient pore pressures developed are satisfied at the boundary. Further it is assumed that uniform pressure distribution takes place throughout the depth when a soil layer is removed by erosion.

Figures 8.1 to 8.4 show the deficient pore pressure isochrones at the end of erosion and also at the end of the duration of standstill. The depth of erosion is arbitrarily

chosen at 250 feet. The plots have been obtained for various values of the coefficient of consolidation (i.e., the coefficient of swelling). The values for the coefficient of swelling C_s used are 0.1, 1.0, 10.0, and 100.0 feet square per year. Also varying periods of erosion and subsequent standstill are tried. The combinations are:

- (a) 5000 years of erosion and 15000 years of subsequent swelling;
- (b) 10000 years of erosion and 10000 years of subsequent swelling; and
- (c) 15000 years of erosion and 9000 years of subsequent swelling.

In each case the value of the coefficient of swelling is varied through the specified ranges.

Since it was assumed that the sediment is fully saturated and also that the groundwater level is flush with the top of the (eroded) sediment, prior to erosion there exists a hydrostatic pressure of water which would be recovered after equilization. Combining the deficient pore pressure with the hydrostatic pressure at each level the resulting pore water pressure isochrones, that are existing, are obtained. Figures 8.1 to 8.4 illustrate that at the end of the period of erosion, substantial deficient pore pressures remain at the top within few feet although the sediment is fully saturated; thus there exist very high negative hydraulic gradients at the top. These high deficient pore pressures still exist after a large number of years of standstill, when neither

deposition nor erosion takes place.

These figures show that the dissipation of deficient pore pressure depends, largely upon the coefficient of swelling, C_s . The higher the value of C_s the quicker the dissipation and the greater is the depth to which pore pressures are equated. Thus the behaviour of a soil sediment depends mainly on the permeability and compressibility characteristics (on which C_s depends). The lower the permeability, the longer the time needed for the dissipation of deficient pore pressures.

For a given value of C_s , the duration of erosion and subsequent period of standstill have a profound influence on the magnitude of the developed deficient pore pressure. The smaller the duration of erosion (for a given erodable depth), the greater the effect on the deficient pore pressures and the hydraulic gradient at upper layers is very large. The longer the duration of erosion (for the same eroded depth), comparatively the hydraulic gradients are smaller. To illustrate the above statements, the total water pressure at any point (as it exists at the end of the duration of standstill) is expressed as a percentage of the hydrostatic pressure at that point that would have existed had there been no swelling. The calculated per cent of hydrostatic pressure is plotted against depth for a given value of C_s . Figures 8.5 to 8.8 illustrate the effect of rates of erosion and subsequent standstill on the pore water pressure for a specified soil mass (whose coefficient of swelling is known). The

values expressed, e.g., as 5000 + 10000 years on Figures 8.5 to 8.8 denote 5000 years (first term) of erosion to form a 250 feet valley and 10000 years (second term) of subsequent standstill with no erosion or deposition.

Figures 8.5 and 8.6 suggest that whatever be the rates of erosion and subsequent swelling for soil masses with a value of C_s of the order of 0.1 or 1.0 foot square per year, the per cent hydrostatic pressure does not alter with depth. This means to say that in low swelling soils the dissipation of pore pressure is very slow. Figure 8.8 suggests that for soils with a high value of C_s (e.g., 100 feet square per year), the rate of erosion and swelling have almost the same effect. In other words, the high swelling soils adjust themselves to the surroundings very quickly. A value of 10.0 feet square per year for C_s (Figure 8.7) shows a marked influence of the various rates of erosion and subsequent swelling. All the curves (Figures 8.5 to 8.8) become parallel to the depth axis at large values of depth.

Essentially the same remarks (as for the rate of erosion) may be made for the duration of subsequent standstill. The length of the duration of swelling has a significant influence on the deficient pore pressures. The longer is this duration the more is the degree of dissipation.

It is of interest to investigate if cases exist in nature that confirm to the type of behavior described earlier in this section. Large areas of Western Canada and the North Central States (USA) are underlain by Bearpaw Shale.

This material geologically is classed as bedrock.

In the undisturbed state Bearpaw Shale is dense, homogeneous and impervious (Peterson, 1954). Some of the pertinent material properties are:

Average Degree of Saturation	96.4%
Coefficient of Permeability cm/sec	10^{-5} to 10^{-9}
Average Water Content	25%

Tests conducted at this University yield an average value of 0.10 feet square per year for the coefficient of swelling, c_s . Same order of magnitude for c_s is quoted in the published literature.

The analysis presented in the previous section is relevant to the valley formation in Bearpaw Shale. South Saskatchewan River drains most of the Prairie provinces and has cut deep valleys in the Bearpaw Shale formation. In the immediate vicinity of Gardiner Dam the valley is approximately 200 feet deep. Thus the river flows through a deep bed of homogeneous, low swelling, (almost) saturated sediment and has cut a valley 200 feet deep. Figures 8.1 and 8.5 are ideal for comparison for this case and the figures indicate that a substantial deficit pore pressures may exist.

Although it has been assumed that large depths of homogeneous material are involved, the analysis can be applied to homogeneous materials of limited thickness underlain by relatively impermeable material such as most rocks. However, any inhomogeneity in form of stratification in the material will yield substantially different results.

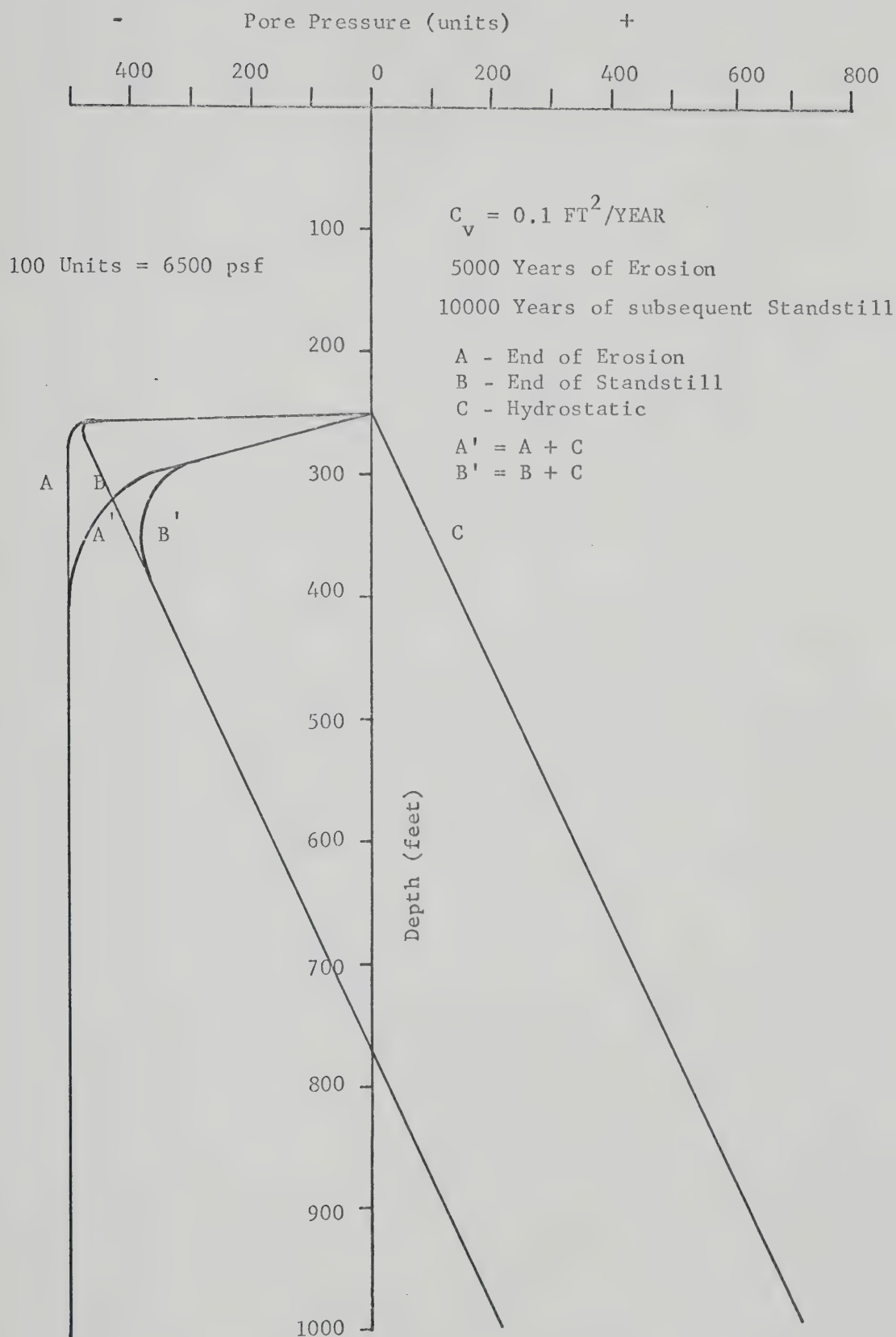


FIG. 8.1 PORE PRESSURE ISOCHRONES

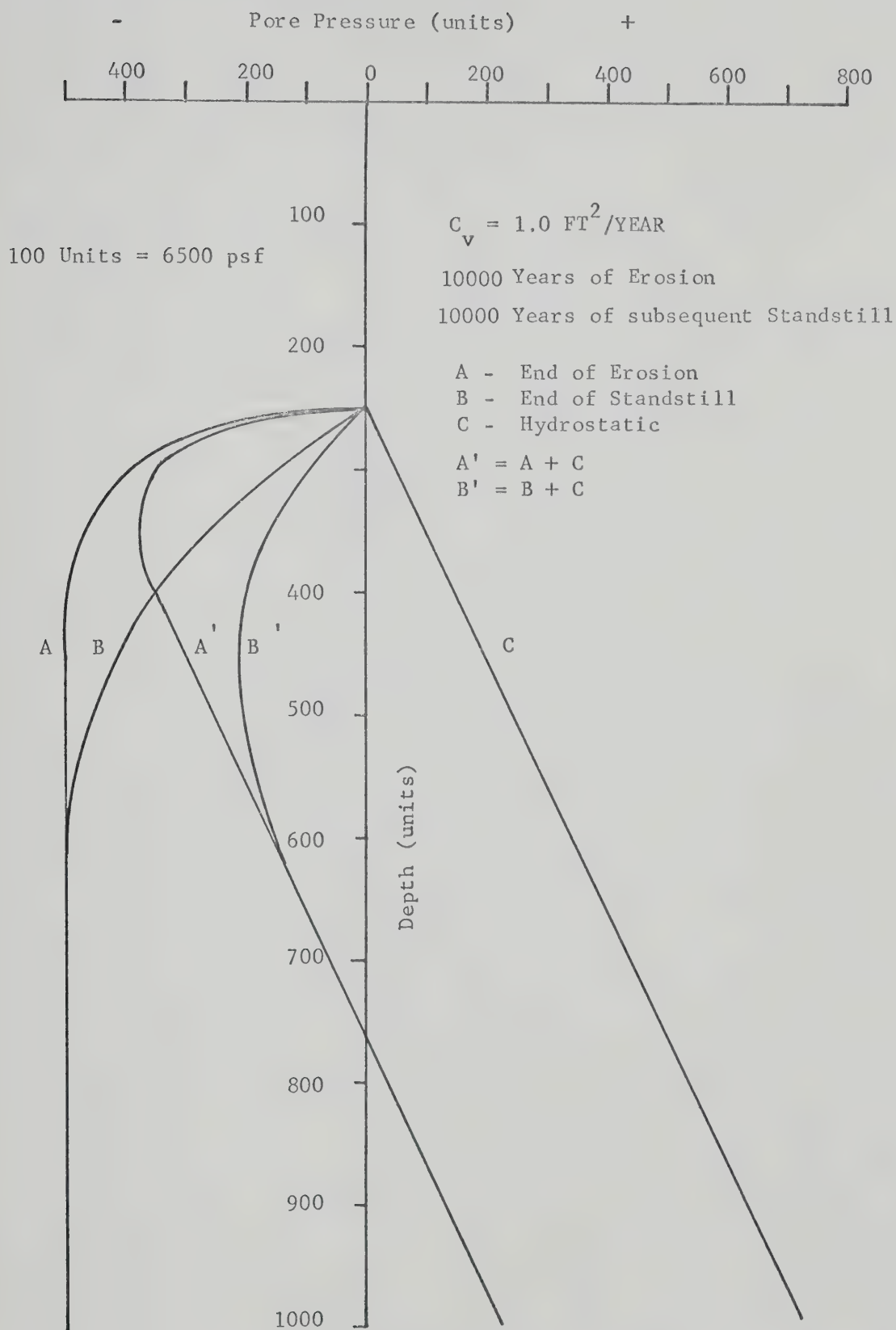


FIG. 8.2 PORE PRESSURE ISOCHRONES

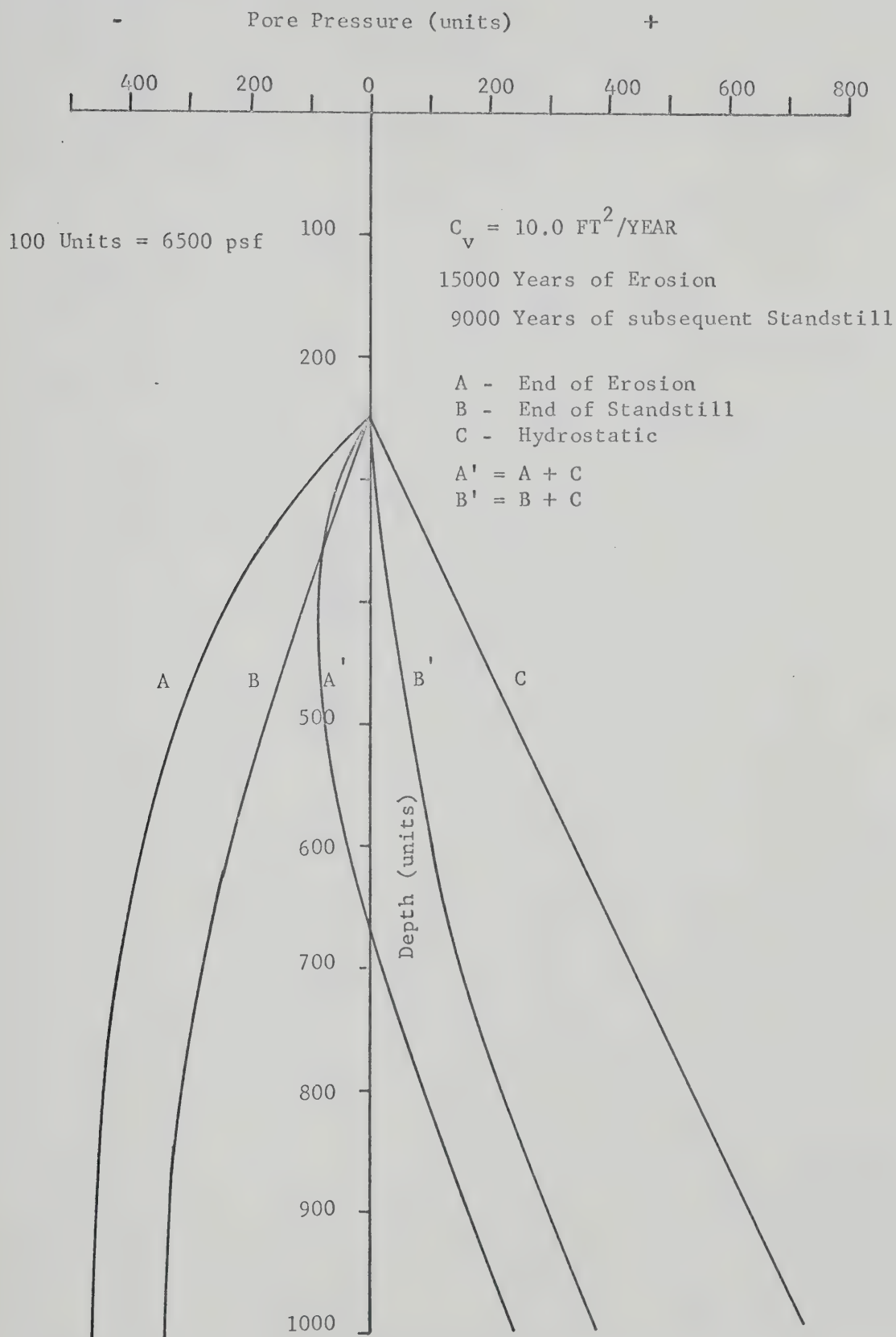


FIG. 8.3 PORE PRESSURE ISOCHRONES

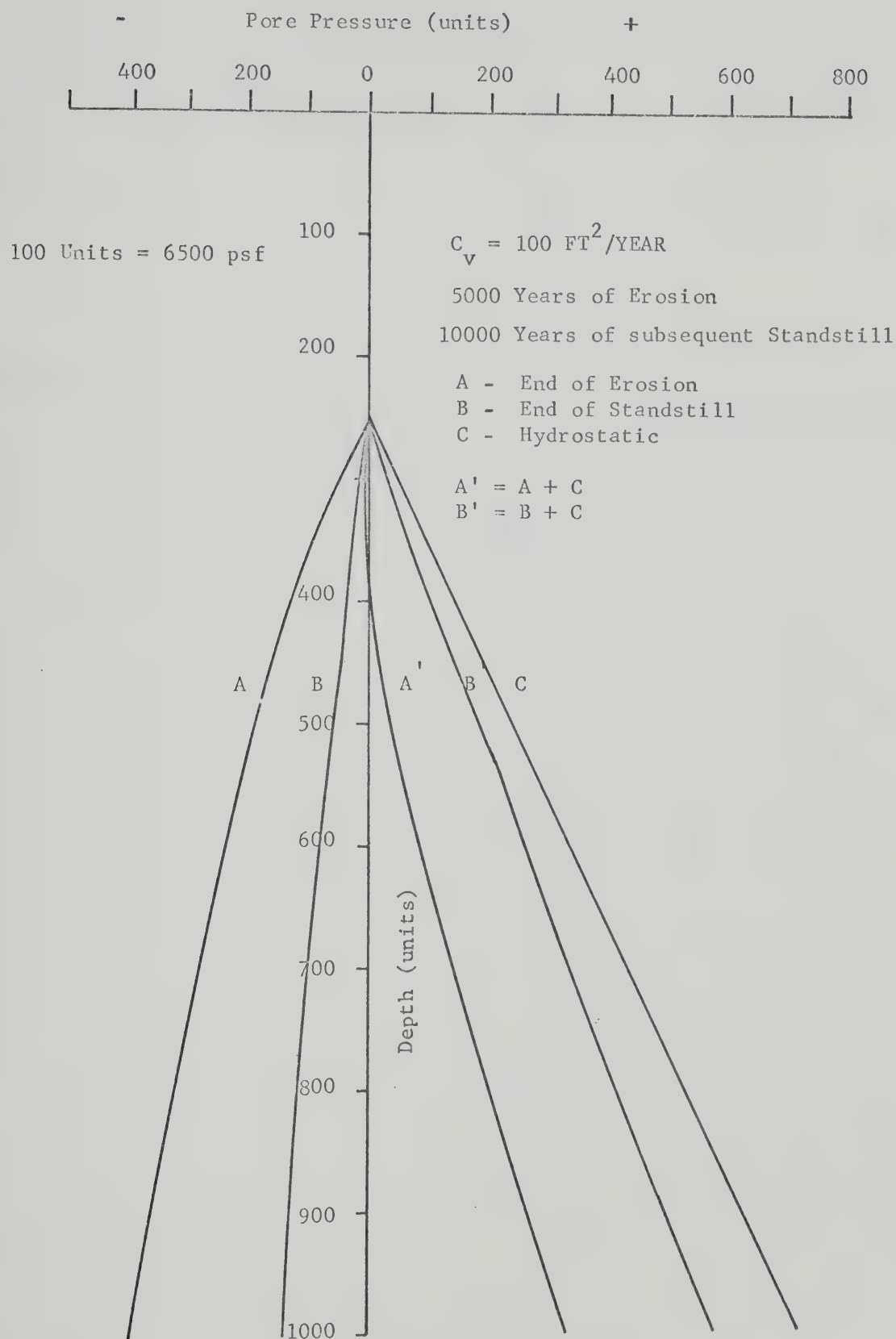


FIG. 8.4 PORE PRESSURE ISOCHRONES

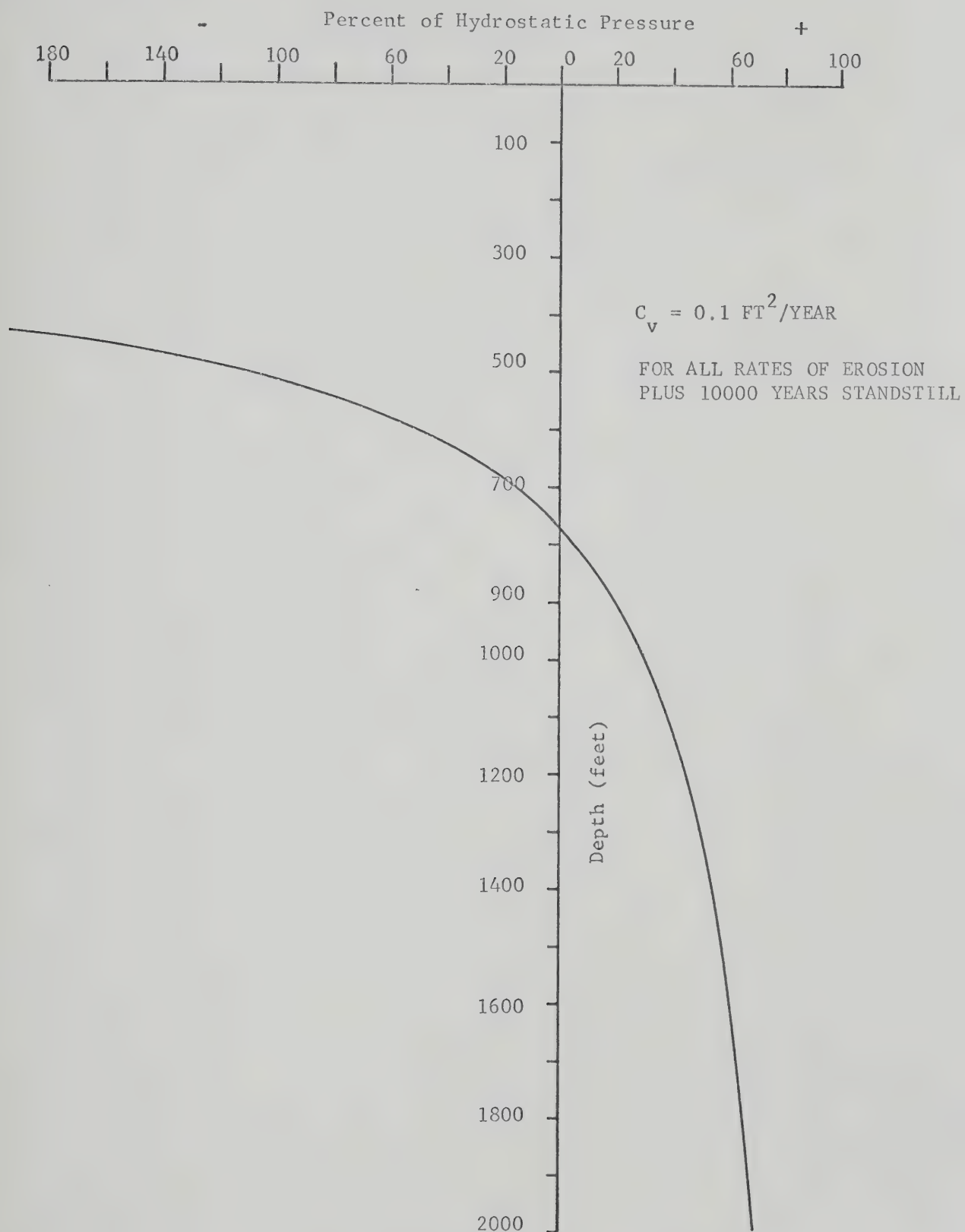


FIG. 8.5 PERCENT OF HYDROSTATIC PRESSURE vs DEPTH

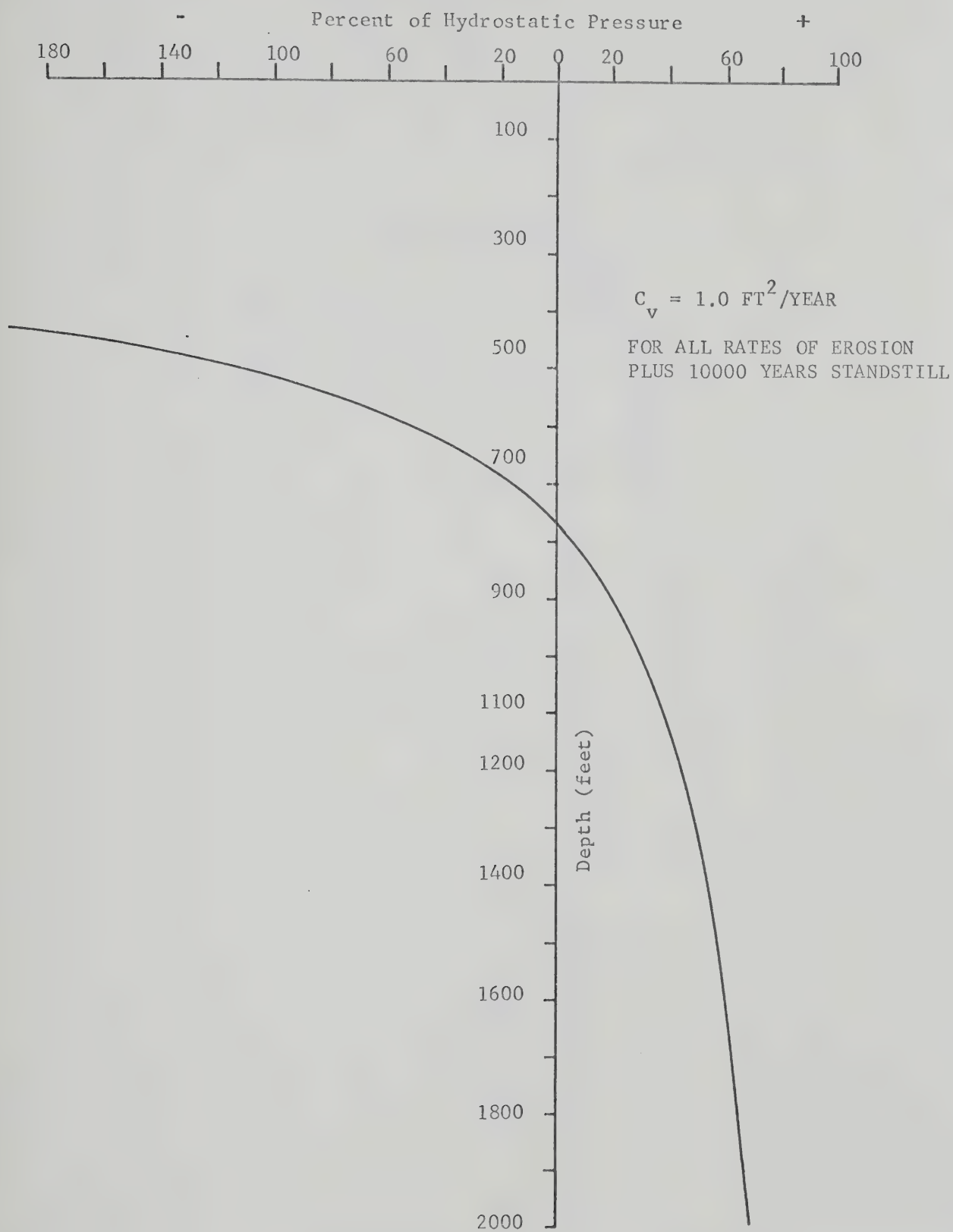


FIG. 8.6 PERCENT OF HYDROSTATIC PRESSURE vs DEPTH

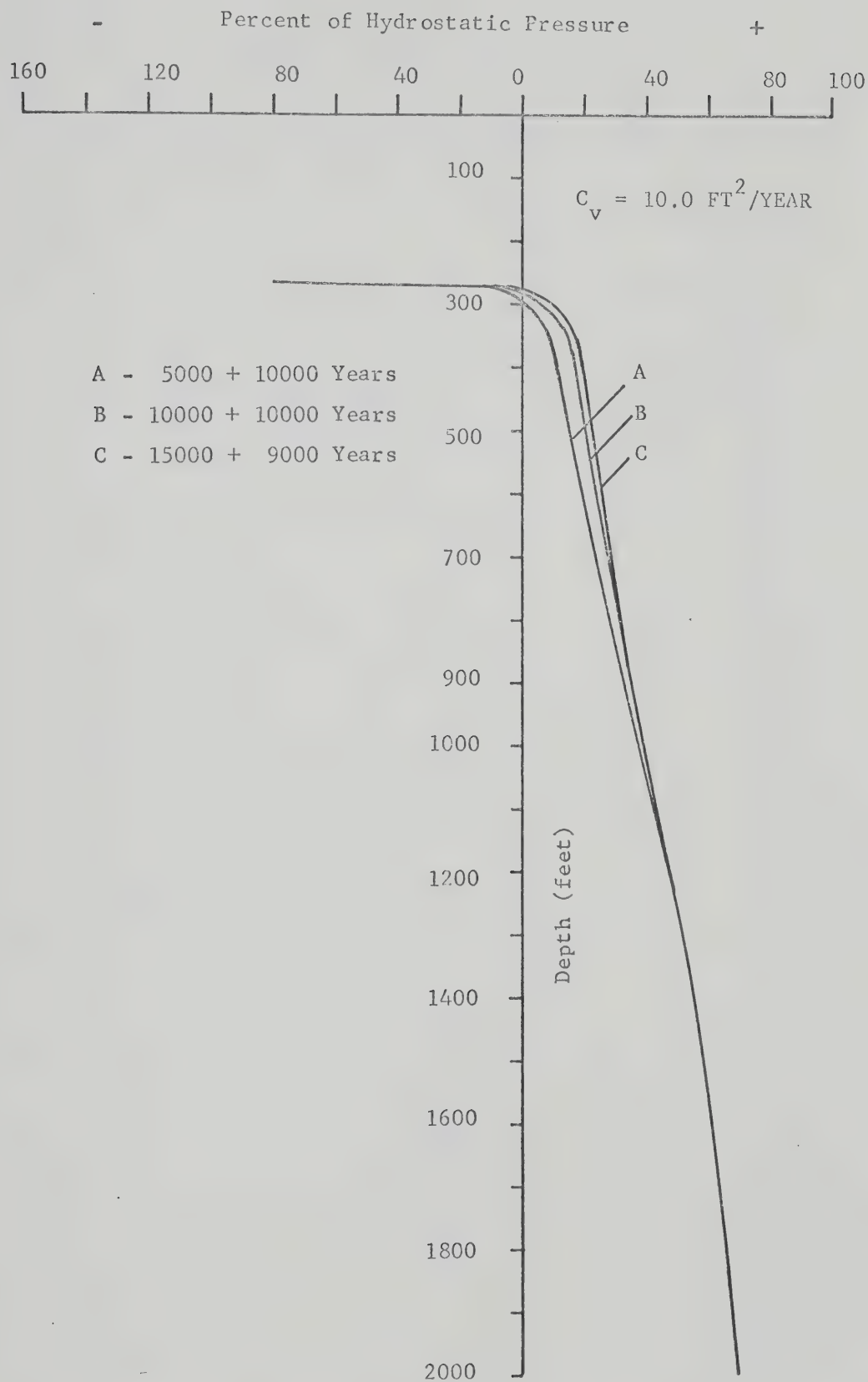


FIG. 8.7 PERCENT OF HYDROSTATIC PRESSURE vs DEPTH

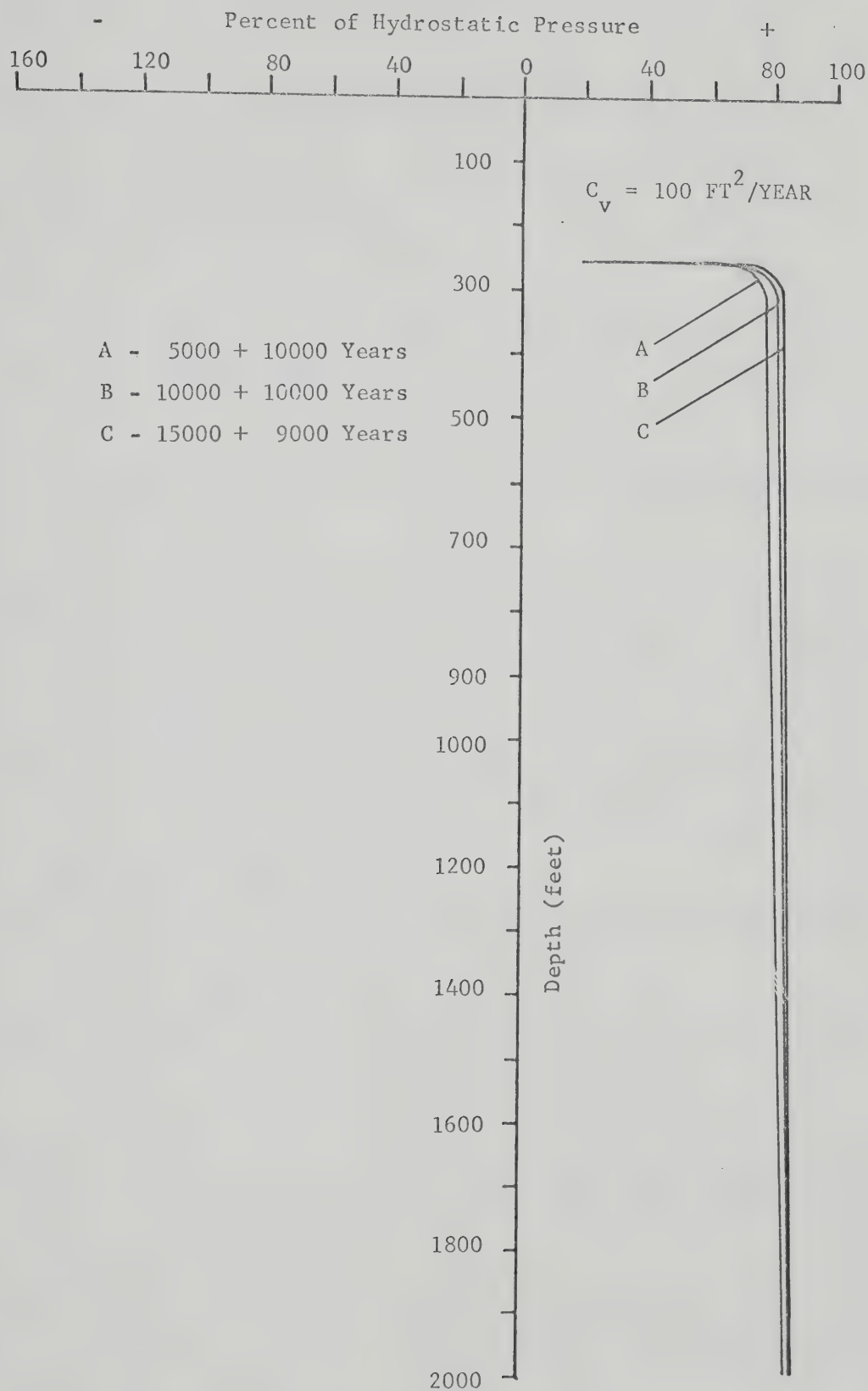


FIG. 8.8 PERCENT OF HYDROSTATIC PRESSURE vs DEPTH

LIST OF REFERENCES

- Abbott, M.B., 1960. "One-dimensional consolidation of multilayered soils". Geotechnique, 10, 151-165.
- Abbott, M.B. and Shrivastava, S.P., 1967a. "A note on one-dimensional consolidation of spatially non-homogeneous soils". LGM Mededelingen, 11, 96-101.
- Abbott, M.B. and Shrivastava, S.P., 1967b. "A note on one-dimensional consolidation of a clay layer that increases in thickness with time". LGM Mededelingen, 11, 102-105.
- Arhippainen, E., 1964. "Pore pressure measurements in two Finnish earthfill dams". Trans. 8th Int. Congress on Large Dams, 2, 503-515.
- Barakat, H.Z. and Clark, J.A., 1966. "On the solution of diffusion equation by numerical methods". J. of Heat Transfer, ASME, 88, 421-427.
- Barden, L., 1965a. "Consolidation of compacted unsaturated clays". Geotechnique, 15, 267-286.
- Barden, L., 1965b. "Consolidation of clay with nonlinear viscosity". Geotechnique, 15, 345-362.
- Barden, L., 1968. "Recent developments in consolidated theory and techniques", Civil Engg. and Public Works Review, 63, 52-54.
- Barden, L. and Berry, P.L., 1965. "Consolidation of normally consolidated clay". J. Soil Mechs. and Found. Div., Proc. ASCE, 91, SM5, 15-35.

- Barron, R.A., 1948. "Consolidation of fine-grained soils by drain wells". Trans. ASCE, 113, 718-754.
- Bernell, L., 1958. "Determination of pore pressures in earth dams during construction". Proc. 6th Int. Congress on Large Dams, 2, 1171-1177.
- Bernell, L. and Nilsson, R., 1957. "Electrical analog equipment for solving nonstationary two-dimensional flow problems". Proc. 4th Int. Conf. Soil Mechs. Found. Engg., 2, 291-293.
- Binnie, G.M. et al., 1967. "Engineering of Mangla". Proc. I.C.E., 38, 337-576.
- Biot, M.A., 1941. "General theory of three-dimensional consolidation". J. App. Physics, 12, 155-164.
- Bishop, A.W., 1954. "The use of pore pressure coefficients in practice". Geotechnique, 4, 148,152.
- Bishop, A.W., 1957. "Some factors controlling the pore pressures set up during the construction of earth dams". Proc. 4th Int. Conf. Soil Mechs. Found. Engg., 2, 294-300.
- Bishop, A.W., Kennard, M.F. and Vaughan, P.R., 1964. "Developments in the measurement and interpretation of pore pressure in earth dams". Trans. 8th Int. Congress on Large Dams, 2, 47-72.
- Carillo, N., 1942. "Simple two- and three-dimensional cases in the theory of consolidation of soils". J. Math. Physics, 21, 1-4.

- Carslaw, H.S. and Jaeger, J.C., 1959. "Conduction of Heat in Solids". Clarendon Press, Oxford.
- Cryer, C.W., 1963. "A comparison of three-dimensional consolidation theories of Biot and Terzaghi". Quart. J. Mech. App. Math., 16, 401-412.
- Davis, E.H. and Lee, I.K., 1969. "One-dimensional consolidation of layered soils". Proc. 7th Int. Conf. Soil Mechs. and Found. Engg., 2, 65-72.
- Davis, E.H. and Raymond, G.P., 1965. "A nonlinear theory of consolidation". Geotechnique, 15, 161-173.
- De Jong, Josselin, 1957. "Applications of stress functions to consolidation problems". Proc. 4th Int. Conf. Soil Mechs. Found. Engg., 1, 320-323.
- Douglas, J. Jr., 1955. "On the numerical integration of $\frac{\partial^2 u}{\partial x^2} + \frac{\partial^2 u}{\partial y^2} = \frac{\partial u}{\partial t}$ by Implicit methods". J. SIAM, 3, 42-65.
- Fisk, H.N., 1956. "Nearsurface sediments of the continental shelf off Louisiana". Proc. 8th Texas Conf. Soil Mechs. and Found. Engg., 1-35.
- Fisk, H.N., McFarlan, E., Kolb, C.R. and Wilbert, L.J., 1954. "Sedimentary framework of the modern Mississippi delta". J. Sed. Petrology, 24, 76-99.
- Fox, L., 1962. "Numerical solution of Ordinary and Partial Differential Equations". Addison-Wesley, Reading, Mass.

- Gibson, R.E., 1958. "The progress of consolidation in a clay layer increasing in thickness with time". Geotechnique, 8, 171-182.
- Gibson, R.E. and Lumb, P., 1953. "Numerical solution of some problems in the consolidation of clay". Proc. I.C.E., 1, 182-198.
- Gibson, R.E. and McNamee, J., 1957. "The consolidation settlement of a load uniformly distributed over a rectangular area". Proc. 4th Int. Conf. Soil Mechs. Found. Engg., 2, 297-299.
- Gibson, R.E., England, G.L. and Hussey, M.J.L., 1967. "The theory of one-dimensional consolidation of saturated clays". Geotechnique, 17, 261-273.
- Gould, J.P., 1959. "Construction pore pressures observed in rolled earth dams". Tech. Memo. 650, USBR.
- Greenman, N.M. and LeBlanc, R.J., 1956. "Recent marine sediments and environments of Northern Gulf of Mexico". Bull. Am. Assoc. of Petro. Geologists, 90, 813-847.
- Gröber, Erk and Grigull, 1963. "Die Grundgesetze der Wärmeübertragung". Springer Verlag, Berlin.
- Gupta, S.N. and Sharma, H.D., 1964. "Pore pressure and settlement observations at Nanak Sagar Dam". Proc. 8th Int. Congress on Large Dams, 2, 865-882.
- Hilf, J.W., 1948. "Estimating construction pore pressures in rolled earth dams". Proc. 2nd Int. Conf. Soil Mechs. Found. Engg., 3, 234-240.

- Horne, M.R., 1964. "The consolidation of a stratified soil with vertical and horizontal drainage". Int. J. Mech. Sciences, 6, 187-197.
- Janbu, N., 1963. "Soil compressibility as determined by oedometer and triaxial tests". Proc. European Conf. Soil Mechs. and Found Engg., Wiesbaden, 1, 19-25.
- Lai, J.Y., 1968. "Effects of Compressibility, Permeability and Void Ratio Variations on the Classical Theory of Consolidation". Ph.D. Thesis, Univ. of Illinois.
- Li, C.Y., 1959. "Construction pore pressures in an earth dam". J. Soil Mechs. and Found. Div., Proc. ASCE, 85, SM5, 43-60.
- Li, C.Y., 1967. "Construction pore pressures in three dams". J. Soil Mechs. and Found. Div., Proc. ASCE, 93, SM2, 1-26.
- Linell, K.A. and Shea, H.F., 1960. "Strength and deformation characteristics of various glacial tills in New England". Proc. ASCE Research Conf. on Shear Strength of Cohesive Soils, Boulder, 275-314.
- Little, A.L., 1969. "Personal communication".
- McClelland, B., 1967. "Progress of consolidation in delta front and prodelta clays of the Mississippi River". Marine Geotechnique, Univ. of Illinois Press, 22-40.
- McNabb, A., 1960. "A mathematical treatment of one-dimensional soil consolidation". Quart. App. Math., 17, 337-347.
- Mikasa, M., 1965. "The consolidation of soft clay - A new consolidation theory and its application". Civil Engg. in Japan, Japan Society of Civil Engineers, 21-26.

- Morgenstern, N., 1967. "Submarine slumping and initiation of turbidity currents". Marine Geotechnique, University of Illinois Press, 189-220.
- Normand, J., 1964. "One-dimensional Consolidation of Saturated Clays with Large Strains". M.Sc. Thesis, Univ. of London.
- Ozisik, M.N., 1968. "Boundary Value Problems of Heat Conduction". Int. Text Book Co., U.S.A.
- Peaceman, D.W. and Rachford, H.H. Jr., 1955. "The numerical solution of parabolic and elliptic differential equations". J. SIAM, 3, 28-41.
- Peterson, R., 1954. "Studies of Bearpaw Shale at a damsite in Saskatchewan". J. Soil Mechs. and Found. Div., Proc. ASCE, 80, Separate No. 476, 1-28.
- Pinkerton, I.L. and McConnell, A.D., 1964. "Behaviour of Tooma Dam". Trans. 8th Int. Congress on Large Dams, 2, 351-375.
- Raymond, G.P., 1965. "Rate of Settlement and Dissipation of Pore Water Pressure during Consolidation of Clays". Ph.D. Thesis, Univ. of London.
- Raymond, G.P., 1966. "Consolidation of slightly over-consolidated soils". J. Soil Mechs. and Found. Div., Proc. ASCE, 92, SM5, 1-20.
- Raymond, G.P., 1969. "Consolidation of deep deposits of homogeneous clay". Geotechnique, 19, 478-494.

- Raymond, G.P. and Azzouz, M.M., 1969. "Permeability determination for predicting rates of consolidation". Conf. In-situ Investigations in Soils and Rocks, London, 195-203.
- Rendulic, L., 1936. "Porenziffer and Porenwasserdruck in Tonen". Der Bauingenieur, 17, 559-564.
- Richtmyer, R.D., 1957. "Difference Methods for Initial-Value Problems". Interscience Publishers, Inc., New York.
- Scheideger, A.E., 1960. "Flow through porous media". App. Mech. Review, 13, 313-318.
- Sherard, J.L., Woodward, R.J., Gizziensky, S.F. and Clevenger, W.A., 1963. "Earth and Earth Rock Dams". John Wiley and Sons, New York.
- Schiffman, R.L., 1958. "Consolidation of soil under time-dependent loading and varying permeability". Proc. H.R.B., 37, 564-617.
- Schiffman, R.L., 1967. Discussion in "Bearing capacity and settlement of foundations". Edited by A.S. Vesic, Duke Univ., 107-110.
- Schiffman, R.L., 1969. "Role of theory and numerical methods". Discussion: Advances in consolidation theories for clays, Specialty Session 12, 7th Int. Cong. Soil Mechs. Found. Engg., 128-133.
- Schiffman, R.L., Chen, A.T.F. and Jordan, J.C., 1969. "An analysis of consolidation theories". J. Soil Mechs. and Found. Div., Proc. ASCE, 95, SM1, 285-312.

- Schiffman, R.L. and Gibson, R.E., 1964. "Consolidation of nonhomogeneous clay layers". J. Soil Mechs. and Found. Div., Proc. ASCE, 90, SM5, 1-30.
- Schmid, W.E., 1957. "The permeability of soils and the concept of a stationary boundary layer". Proc. ASTM, 57, 1195-1218.
- Sheppard, G.A.R. and Aylem, L.B., 1957. "The Usk scheme for water supply of Swansea". Proc. I.C.E., 7, 246-264.
- Sherman, W.C. and Clough, G.W., 1968. "Embankment pore pressures during construction". J. Soil Mechs. and Found. Div., Proc. ASCE, 94, SM2, 527-553.
- Skempton, A.W., 1954. "The pore pressure coefficients A and B". Geotechnique, 4, 143-147.
- Skempton, A.W., 1970. "The consolidation of clays by gravitational compaction". Quart. J. Geol. Soc. London, 125, 373-411.
- Taylor, D.W., 1948. "Fundamentals of Soil Mechanics". John Wiley and Sons, New York.
- Terzaghi, K., 1923. "Die berechnung der durchlassigkeitsziffer der tones aus dem verlauf die hydrodynamischen spannungserscheinungen". Akademie die Wissenschaften in Wein, 132, 125-138.
- Terzaghi, K. and Peck, R.B., 1967. "Soil Mechanics in Engineering Practice". John Wiley and Sons, New York.
- U.S. Bureau of Reclamation, 1939. "Notes on analytical soil mechanics". Tech. Memo No. 592.

Zaretsky, Y.K., Gorelik, L.V. and Nuller, B.M., 1969.

"Certain problems in the nonlinear consolidation theory". Proc. 7th Int. Conf. Soil Mechs. and Found. Engg., 2, 261-269.

APPENDIX A

COMPUTER PROGRAM AND USAGE
FOR TWO-DIMENSIONAL IMPEDED DRAINAGE

APPENDIX A

ORGANIZATION OF COMPUTER PROGRAM

The computer program described in this Appendix is based on the theory presented in Chapter V of this study. The program is in Fortran IV language and may be used directly on computers of the type IBM 360/67.

The program furnishes the excess pore pressure, and the average degree of consolidation of a rectangular wedge at any time. The program is applicable for a rectangular section of height L and width $2H$ provided with side drains of thickness d on either side. The program is based on the ADI method of analysis presented in Chapter V. The program is presented for uniform distribution of initial excess pore pressure which may exist at the start of the program and which will dissipate with time. However, the algorithm can easily be modified to incorporate a continuous variation across the entire height or width. The variation may be different from one direction to the perpendicular direction. The variation may be defined by a polynomial interpolation of input data.

The equation governing dissipation of excess pore pressure in two dimensions is given by 5.2. The extent of retardation to drainage is measured by a parameter called the Impedance Factor, λ . The treatment of the problem is in a dimensionless form.

The program reads all the input data regarding the

rectangular wedge and sets up the initial and boundary conditions. Also it establishes the impedance factor governing the retarded consolidation. Depending on the governing material and operating parameters, the program calculates the excess pore pressure at each nodal point at prescribed time intervals. The average degree of consolidation both by two-dimensional and one-dimensional (along a specified section) are calculated using the pore pressure values obtained earlier. The Simpson's rule is made use of in obtaining the degree of consolidation. The calculated results are printed out as per the output formats.

COMPUTER PROGRAM USAGE

INPUT DATA

The first step in the analysis of retarded consolidation for a rectangular wedge with inefficient side drains is to determine

- (a) the height to half width ratio 'Beta' of the wedge;
- (b) the existing boundary and initial conditions;
- (c) the extent of impedance to drainage as measured by a numerical value of the impedance factor λ ; and
- (d) the space and time intervals to suit the computer memory requirements.

The input data cards reads the space steps in both the directions, the time (factor) steps and the ratio Beta.

The READ variables are:

I, J, K, BETA

The FORMAT is,

3I5, F10.2

OUTPUT INFORMATION

The following information is computed and printed by the program at specified time intervals:

- (a) the pore pressure excess at each nodal point; and
- (b) the square root of time factor, the time factor, the degree of consolidation (by two-dimensional integration) for the entire wedge, and the degree of consolidation (by one-dimensional integration) along a chosen section.

 THIS PROGRAM CALCULATES THE PORE PRESSURES AND
 ALSO THE AVERAGE DEGREE OF CONSOLIDATION BY BOTH TWO-DIMENSIONAL
 AND ONE-DIMENSIONAL INTEGRATION

ANALYSIS IS FOR A SYMMETRICAL RECTANGULAR SECTION
 L FT. HIGH 2*H WIDE
 H FT. HALF WIDTH
 LET THE RATIO L/H BE DENOTED BY BETA

IMPERVIOUS BOTTOM CONSTANT LOAD

TREATMENT IS IN A DIMENSIONLESS FORM

THIS IS ACHIEVED WITH RESPECT TO H
 SO THAT VARIATION IN THE QUANTITY IN THE DIRECTION OF H
 IS FROM 0.0 TO 1.0

THE VARIATION IN THE PERPENDICULAR DIRECTION
 IS FROM 0.0 TO BETA

THE TIME FACTOR IS NOW TRULY DIMENSIONLESS
 AND EQUAL TO $CV * \text{TIME} / H^2$
 THE VARIATION IN TIME FACTOR IS FROM 0.0 IN STEPS OF 0.001

DRAINAGE IS IMPEDED AT SIDES DUE TO INEFFICIENT SIDE DRAINS
 IMPEDANCE TO DRAINAGE IS GOVERNED BY THE IMPEDANCE FACTOR AMDA

AMDA IF INFINITY THE DRAIN IS EFFECTIVE

AMDA IF OF THE ORDER OF 0.1 OR 0.01 THE DRAIN IS IMPEDING

AMDA IF EQUALS ZERO THE DRAIN EFFECTIVELY IMPEDES

I, J, K ARE THE INPUT PARAMETERS

I - SPACE STEPS IN ONE DIRECTION
 J - SPACE STEPS IN THE PERPENDICULAR DIRECTION
 K - TIME FACTOR STEPS

DIMENSION X(51), Y(6), T(301), U(52,7,302), A(52), B(52), AV(302),
 CS(302), V(302), D(302), T1(302), T2(302), W(52,7,1), AD(302)


```

C
C      READ (5,10) I,J,K,BETA
10  FORMAT (3I5,F10.2)
C      WRITE (6,15) I,J,K,BETA
15  FORMAT (30X, 'INPUT DATA', 3I20, F10.2///)

C
C      *****
C      BOUNDARY AND INITIAL CONDITIONS
C      *****
C
C      IMPERVIOUS BOTTOM
C      THAT IS AT L=1 THE LAYER IS IMPERMEABLE
C
C      DO 50 N=1,K
C      DO 40 L=1,I
C      DO 30 M=1,J
C      IF (N.EQ.1) GO TO 20
C      IF (L.EQ.1) U(L,M,N) = 0.
C      GO TO 30
20  U(L,M,N) = 100.
30  CONTINUE
40  CONTINUE
50  CONTINUE

C
C      PHYSICAL CONSTANTS *****
C
C      DX = SPACE STEP IN ONE-DIRECTION
C      DY = SPACE STEP IN THE PERPENDICULAR DIRECTION
C      DT = TIME FACTOR STEP
C
C      DX = 0.2
C      DY = 0.2
C      DT = 0.001
C      R = DT/DX**2
C      WRITE (6,60) (H, DX, DY, DT, R)
60  FORMAT (20X, 'H =', 2X, F6.2, 10X, 'DX =', 2X, F6.2, 10X, 'DY =',
C      2X, F6.2, 10X, 'DT =', 2X, F6.2, 10X, 'R =', 2X, F6.2////)

C
C      *****
C      AMDA = IMPEDANCE FACTOR *
C      *****
C      AMDA = INFINITY
C      WRITE (6,70)
70  FORMAT (30X, 'IMPEDENCE FACTOR = INFINITY')

C
C      *****
C      THIS PART OF THE PROGRAM CALCULATES THE EXCESS PORE
C      PRESSURES BY THE ALTERNATING - DIRECTION IMPLICIT METHOD
C      *****
C
C      DO 600 N=1,K

```


C

```

KB=N/2.
RB=N/2.
IF (KB.EQ.RB) GO TO 260
IA = I-1
JA = J-1
DO 190 M=1,JA
IF (M.EQ.1) GO TO 155
A(1) = (2.*R)/(1.+2.*R)
B(1) = ((1.-2.*R)*U(1,M,N)+R*(U(1,M-1,N)+U(1,M+1,N)))/(1.+2.*R)
DO 150 LE = 2,IA
A(LE)=R/(1.+2.*R-R*A(LE-1))
B(LE) = (R*(U(LE,M-1,N)+U(LE,M+1,N))+(1.-2.*R)*U(LE,M,N)+
CR*B(LE-1))/(1.+2.*R-R*A(LE-1))
150 CONTINUE
GO TO 180
155 A(1) = (2.*R)/(1.+2.*R)
B(1) = (2.*R*U(1,M+1,N)+(1.-2.*R)*U(1,M,N))/(1.+2.*R)
DO 160 LE = 2,IA
A(LE)=R/(1.+2.*R-R*A(LE-1))
B(LE) = (2.*R*U(LE,M+1,N)+(1.-2.*R)*U(LE,M,N)+R*B(LE-1))/
C(1.+2.*R-R*A(LE-1))
160 CONTINUE
180 U(IA,M,N+1) = B(IA)
LLG = IA-1
DO 185 LGL = 1,LLG
KG = IA-LGL
U(KG,M,N+1) = B(KG)+A(KG)*U(KG+1,M,N+1)
185 CONTINUE
190 CONTINUE

```

C

C

```

C      IF  AMDA IS INFINITY  U(LE,J,N+1) = 0.
C      IF  AMDA IS A FINITE QUANTITY,  SAY = AMDA
C          U(LE,J,N+1) = U(LE,JA,N+1)/(1.+AMDA*DX)
C      IF  AMDA IS ZERO THE IMPEDANCE IS EFFECTIVE AND
C          U(LE,J,N+1) = U(LE,JA,N+1)
C      *****

```

52

2

```

DO 195 LE = 1,IA
U(LE,J,N+1) = 0.
195 CONTINUE
GO TO 600

```

C

C

```

260  IA = I-1
      DO 420 L = 1, IA
        JA = J-1
        U(L, J, N+1) = U(L, J, N)
        IF (L.EQ.1) GO TO 270
        A(1) = (2.*R)/(1.+2.*R)
        B(1) = ((1.-2.*R)*U(L, 1, N)+R*(U(L-1, 1, N)+U(L+1, 1, N)))/(1.+2.*R)
        DO 265 LA = 2, JA
          A(LA)=R/(1.+2.*R-R*A(LA-1))
          B(LA) = ((1.-2.*R)*U(L, LA, N)+R*(U(L-1, LA, N)+U(L+1, LA, N)))+

```



```

CR*B(LA-1))/(1.+2.*R-R*A(LA-1))
265  CONTINUE
GO TO 310
270  A(1) = (2.*R)/(1.+2.*R)
B(1) = ((1.-2.*R)*U(L,1,N)+2.*R*U(L+1,1,N))/(1.+2.*R)
DO 275 LA = 2,JA
A(LA)=R/(1.+2.*R-R*A(LA-1))
B(LA) = ((1.-2.*R)*U(L,LA,N)+2.*R*U(L+1,LA,N)+R*B(LA-1))/
C(1.+2.*R-R*A(LA-1))
275  CONTINUE
310  U(L,JA,N+1) = B(JA)
LLD = JA-1
DO 320 LLA = 1,LLD
KB = JA-LLA
U(L,KB,N+1) = B(KB)+A(KB)*U(L,KB+1,N+1)
320  CONTINUE
420  CONTINUE
600  CONTINUE

C
C
C
C *****
C THIS PART OF THE PROGRAM PRINTS OUT THE OUTPUT
C OF PORE PRESSURE VALUES AT VARIOUS NODAL POINTS
C
DO 900 N=1,K,10
NK = N
T(NK) = DT*(NK-1)
WRITE (6,650) (T(NK))
650  FORMAT ('1', 45X, 'T=', 3X, F8.2, 6X, 'UNITS'////)
DO 700 M = 1,J
700  Y(M) = DY*(M-1)
WRITE (6,750) (Y(M), M=1,J)
750  FORMAT (18X, 'X/Y', 6X, 6F10.3////)
DO 850 L = 1,I
X(L) = DX*(L-1)
WRITE (6,800) (X(L), (U(L,M,N), M=1,J))
800  FORMAT (15X, F6.2, 10X, 6E10.3/)
850  CONTINUE
900  CONTINUE

C
C
C *****
C THIS PART OF THE PROGRAM CALCULATES THE AVERAGE DEGREE
C OF CONSOLIDATION BY TWO-DIMENSIONAL INTEGRATION
C USING SIMPSON'S RULE
C *****
C
C THE NUMBER OF ORDINATES ON Y- AXIS IS EVEN
C AS SUCH A MODIFICATION IN SIMPSON'S RULE IS INCORPORATED
C
DO 945 N = 1,K
DO 930 M = 1,J
S1 = U(1,M,N)+U(I,M,N)
S2 = 0.

```



```

DO 920 L = 2,1,2
S2 = S2 + U(L,M,N)
920 CONTINUE
IA = I-1
S3 = 0.
DO 925 L = 3,IA,2
S3 = S3 + U(L,M,N)
925 CONTINUE
S(M) = (DX/3.)*(S1+4.*S2+2.*S3)
930 CONTINUE
JA = J-1
V1 = S(1)+S(JA)
V2 = 0.
DO 935 M = 2,JA,2
V2 = V2 + S(M)
935 CONTINUE
JB = JA-1
V3 = 0.
DO 940 M = 3,JB,2
V3 = V3 + S(M)
940 CONTINUE
V(N) = (DY/3.)*(V1+4.*V2+2.*V3)+(DY/2.)*(S(J)+S(J-1))
C TOTAL VOL. OF DIFF. NET INITIALLY = (6-1)*(51-1)*100.*DX*DY
C = 1000
D(N) = 1.-(V(N)/1000.)
945 CONTINUE
C
C
C *****
C THIS PART OF THE PROGRAM CALCULATES THE AVERAGE DEGREE
C OF CONSOLIDATION ALONG THE CENTRE LINE
C BY ONE-DIMENSIONAL INTEGRATION USING SIMPSON'S RULE
C *****
C
C THE CENTRE LINE IS ALONG L = 26
C
C L = 26
DO 952 N=1,K
AV(N) = (DY/3.)*(U(L,1,N)+U(L,5,N)+4.*(U(L,2,N)+U(L,4,N))+
C 2.*U(L,3,N))+(DY/2.)*(U(L,5,N)+U(L,6,N))
C AD(N) = 1.-(AV(N)/AV(1))
C AV(1) = 100. = DX*100.*(6-1)
C AD(N) = 1. - (AV(N)/100.)
952 CONTINUE
C
C *****
C THIS PART OF THE PROGRAM PRINTS THE OUTPUT FOR
C THE AVERAGE DEGREE OF CONSOLIDATION WITH CORRESPONDING
C TIME FACTORS
C
C WRITE (6,953)
953 FORMAT ('1', 20X, 'SQRT TF', 20X, 'TIME FACTOR', 20X,
C 'DEG OF CONS', 20X, '1-D HOR CONS'///)
DO 980 N=1,K

```



```
NK = N
T1(N) = DT*(NK-1)
T2(N) = SORT(T1(N))
WRITE (6,975) (T2(N), T1(N), D(N), AD(N))
975  FORMAT (15X, E12.5, 24X, E12.5, 19X, E12.5, 19X, E12.5//)
980  CONTINUE
STOP
END
```


APPENDIX B

COMPUTER PROGRAM AND USAGE FOR
PREDICTION OF CONSTRUCTION PORE PRESSURES

APPENDIX B

ORGANIZATION OF COMPUTER PROGRAM

The computer program presented in this Appendix describes the construction sequence of JARI Dam (section 6.4.5) and calculates the pore water pressures at several nodal points. The program is in Fortran IV language and may be used directly on computers of the type IBM 360/67.

The algorithm developed typically predicts the influences of dissipation on construction pore pressures. Of the six case histories studied, the program developed and written for Jari Dam is presented as an illustrative example.

The equation governing the dissipation of construction pore pressures is given by 6.4. The method of analysis is by the ADI technique described in Chapter V. The pore pressure generation term is $DH (= \gamma \bar{B} * DX$ where DX is the thickness of the added soil layer) and this is equated to zero when there is a construction stoppage.

The program furnishes the excess pore pressure at the nodal points of the idealized cross-section of the core of the Jari Dam. The first step in the analysis is to determine the construction sequence and the rates of construction and work stoppage. The material properties of the core such as unit weight and the coefficient of consolidation c_v (alternatively the permeability and compressibility characteristics) should be known. Incidentally, it may be mentioned

that the algorithm can handle any variation in the values of c_v or \bar{B} at any stage of construction or work stoppage. The program is furnished for a uniform distribution of the load added at the top (due to increase in layer thickness) on all the nodal points irrespective of their position and depth. This is justified to an extent because proper distribution of load along the depth and along the lateral direction for a moving boundary problem is difficult to assess.

The entire program consists of a main and fourteen subroutines. The main program reads in the input data and sets up the initial and boundary conditions. It establishes the physical constants such as core dimensions and the material properties. The main program also regulates the branching to the subroutines by setting up appropriate conditional statements.

Subroutine KOP generates the boundary conditions for the first construction stoppage of three months. Subroutines KOPPUL and KOPPU set up the boundary conditions for the second and third construction stoppages of one and half months each. Subroutine NMI computes the boundary conditions for the period after construction for the entire core section.

The subsequent subroutines calculate the excess pore pressures generated (or dissipated) at the current nodal points by the ADI technique. The computed quantities in all the subroutines are returned to the main program. The main program prints the desired information according to the out-

put formats.

COMPUTER PROGRAM USAGE

INPUT DATA

The first step in the analysis of the influence of dissipation on construction pore pressures is to decide on the cross-section of the core in the case of a dam to be built or to note the dimensions of an existing dam under examination. The core section is idealized on the basis described in Chapter VI to get a rectangular mesh amenable to finite difference approach. The boundary conditions at the bottom and sides are also noted.

The second step is to note the rate of construction together with the durations of construction stoppage, if any. When necessary the actual rate of construction is modified to enable easy computation on the lines suggested in section 6.3.B.

The most important parameters in calculating excess pore pressures are the coefficient of consolidation c_v and the pore pressure parameter \bar{B} . These values could, however, be varied throughout the construction operation.

The next step is to discretize the core of the dam into a rectangular grid and decide on the time interval so that the space and time steps suit the computer memory requirements.

The input data card reads the space steps in both directions and the time steps.

The READ variables are:

I, J, K

The FORMAT is,

3I5.

OUTPUT INFORMATION

The program computes and prints out the following information:

- (a) reprint of input data;
- (b) pore pressures at nodal points for specified time intervals.

ANALYSIS OF JARI DAM - CORE OF ROLLED SILT
 230 FT. HIGH 40FT. WIDE AT TOP
 200 FT. AT BOTTOM
 U/S SLOPE 1V - 0.2H D/S SLOPE 1V - 0.5H

RATE OF CONSTRUCTION:

50 FT. IN 3 MONTHS
 REST FOR 3 MONTHS
 70 FT. IN 7 MONTHS
 REST FOR 1 1/2 MONTHS
 70 FT. IN 7 1/2 MONTHS
 REST FOR 1 1/2 MONTHS
 40 FT. IN 3 MONTHS
 NEXT 6 MONTHS

COMMON X(24), Y(21), T(38), U(25,22,39), A(39), B(39), R,SA,DH,N,J

READ (5,10) I,J,K

10 FORMAT (3I5)

BOUNCARY CONDITIONS *****

IMPERVIOUS BOTTOM

DO 40 N = 1,K

IF (N.GT.6) GO TO 23

DO 22 L = 1,N

IF (L.LE.3) GO TO 20

M2 = L/4.+0.05

JB = J-2.*M2

GO TO 21

20 JB = J

21 DO 22 M = 1,JB

IF (N.EQ.1 .OR. L.EQ.N .OR. M.EQ.1 .OR. M.EQ.JB) U(L,M,N) = 0.0

22 CONTINUE

GO TO 40

23 CALL KOP

IF (N.GT.8) GO TO 24

GO TO 40

24 IF (N.GT.15) GO TO 27

NA = 6+1

NB = N-2

DO 26 L = NA,NB

M1 = (L-7)/10.+1+0.05

JA = 2.*M1+1

M2 = L/4.+0.05

JB = J-2.*M2

DO 25 M = JA,JB

IF (M.EQ.JA .OR. M.EQ.JB .OR. L.EQ.NB) U(L,M,N) = 0.0

25 CONTINUE

26 CONTINUE

GO TO 40

27 CALL KOPPUL

IF (N.GT.17) GO TO 28


```

      GO TO 40
28  IF (N.GT.24) GO TO 31
      NB = N-4
      NA = 13+1
      DO 30 L = NA,NB
      M1 = (L-7)/10.+1+0.05
      JA = 2.*M1+1
      M2 = L/4.+0.05
      JB = J-2.*M2
      DO 29 M = JA,JB
      IF (M.EQ.JA .OR. M.EQ.JB .OR. L.EQ.NB) U(L,M,N) = 0.0
29  CONTINUE
30  CONTINUE
      GO TO 40
31  CALL KOPPU
      IF (N.GT.28) GO TO 32
      GO TO 40
32  IF (N.GT.32) GO TO 36
      NB = N-8
      NA = 20+1
      DO 34 L = NA,NB
      M1 = (L-7)/10.+1+0.05
      JA = 2.*M1+1
      M2 = L/4.+0.05
      JB = J-2.*M2
      DO 33 M = JA,JB
      IF (M.EQ.JA .OR. M.EQ.JB .OR. L.EQ.NB) U(L,M,N) = 0.0
33  CONTINUE
34  CONTINUE
      GO TO 40
36  CALL NM1
40  CONTINUE

```

```

C
C
C  PHYSICAL CONSTANTS  *****
      CV = 3500./12.
      SA = 1.
      BBAR = 0.6
C  GAMMA = 125. LB/CFT.
      GAMMA = 125.
      WRITE (6,50)(CV, SA, BBAR, GAMMA)
50  FORMAT (////20X, 4F20.5////)

```

```

C
C
C  DO 600 N = 1,K

```

```

C
C
      IF (N.GE.32) GO TO 33
      IF (N.GE.28) GO TO 30
      IF (N.GE.24) GO TO 25
      IF (N.GE.17) GO TO 20
      IF (N.GE.15) GO TO 15
      IF (N.GE. 9) GO TO 10
      IF (N.GE. 6) GO TO 55
      DT = 3./5.

```



```

DX = 10.
R = (CV*DT)/DX**2
DH = GAMMA*BBAR*DX
GO TO 85
55 DT = 3./2.
DX = 10.
CV = 3000./12.
R = (CV*DT)/DX**2
DH = 0.0
GO TO 85
60 DT = 7./7.
DX = 10.
R = (CV*DT)/DX**2
DH = GAMMA*BBAR*DX
GO TO 35
65 DT = 3./4.
DX = 10.
CV = 2750./12.
R = (CV*DT)/DX**2
DH = 0.0
GO TO 85
70 DT = 7.5/7.
DX = 10.
R = (CV*DT)/DX**2
DH = GAMMA*BBAR*DX
GO TO 35
75 DT = 3./3.
DX = 10.
CV = 2500./12.
R = (CV*DT)/DX**2
DH = 0.0
GO TO 85
80 DT = 3./4.
DX = 10.
R = (CV*DT)/DX**2
DH = GAMMA*BBAR*DX
GO TO 85
83 DT = 1.
DX = 10.
CV = 2000./12.
R = (CV*DT)/DX**2
DH = 0.
85 WRITE (6,90) (DT,DX,R,DH)
90 FORMAT (////30X, 4F20.4//)

```

C
C

```

IF (N.GE.6) GO TO 421
KB = N/2.
BB = N/2.
IF (KB.EQ.BB) GO TO 260
M2 = N/4.+0.05
JB = J-2.*M2-1
DO 190 M = 2,JB
A(1) = (2.*R)/(1.+2.*R)
B(1) = ((1.-(2.*R/SA**2))*U(1,M,N)+(R/SA**2)*(U(1,M-1,N)+

```



```

CU(1,M+1,N))+DH)/(1.+2.*R)
  IF (N.EQ.1) GO TO 169
  DO 150 LE=2,N
  A(LE)=R/(1.+2.*R-R*A(LE-1))
  B(LE)=(R/SA**2)*(U(LE,M-1,N)+U(LE,M+1,N))+((1.-((2.*R)/SA**2))*
150  CU(LE,M,N)+DH+R*B(LE-1))/(1.+2.*R-R*A(LE-1))
  CONTINUE
  GO TO 170
169  N = 1
170  U(N,M,N+1) = B(N)
  IF (N.EQ.1) GO TO 190
  LGL = N-1
  DO 180 LGL = 1,LGL
  KG = N-LGL
  U(KG,M,N+1) = B(KG)+A(KG)*U(KG+1,M,N+1)
180  CONTINUE
190  CONTINUE
  JD = J-1
  IF (JB.EQ.JD) GO TO 600
  JC = JB+1
  DO 220 M = JC,JD
  A(1) = (2.*R)/(1.+2.*R)
  B(1) = ((1.-((2.*R)/SA**2))*U(1,M,N)+(R/SA**2)*(U(1,M-1,N)+
CU(1,M+1,N))+DH)/(1.+2.*R)
  DO 210 LE = 2,3
  A(LE)=R/(1.+2.*R-R*A(LE-1))
  B(LE)=(R/SA**2)*(U(LE,M-1,N)+U(LE,M+1,N))+((1.-((2.*R)/SA**2))*
CU(LE,M,N)+DH+R*B(LE-1))/(1.+2.*R-R*A(LE-1))
210  CONTINUE
  U(3,M,N+1) = B(3)
  LGL = 3-1
  DO 215 LGL = 1,LGL
  KG = 3-LGL
  U(KG,M,N+1) = B(KG)+A(KG)*U(KG+1,M,N+1)
215  CONTINUE
220  CONTINUE
  GO TO 600
C
260  DO 420 L = 1,N
  IF (L.EQ.1) GO TO 390
  IF (L.EQ.N) GO TO 401
  A(2) = (2.*(R/SA**2))/(1.+((2.*(R/SA**2))))
  B(2)=(R*(U(L-1,2,N)+U(L+1,2,N))+((1.-2.*R)*U(L,2,N)+DH)/
C((1.+((2.*(R/SA**2))))
  M2 = L/4.+0.05
  JB = J-2.*M2-1
  IF (L.EQ.3) GO TO 411
  DO 350 LA = 3,JB
  A(LA)=(R/SA**2)/(1.+((2.*(R/SA**2)))-(R/SA**2)*A(LA-1))
  B(LA)=(R*(U(L-1,LA,N)+U(L+1,LA,N))+((1.-2.*R)*U(L,LA,N)+DH+
C(R/SA**2)*B(LA-1))/(1.+((2.*(R/SA**2)))-(R/SA**2)*A(LA-1))
350  CONTINUE
  GO TO 405
390  A(2) = (2.*(R/SA**2))/(1.+((2.*(R/SA**2))))
  B(2) = (2.*R*U(L+1,2,N)+((1.-2.*R)*U(L,2,N)+DH)/

```



```

C(1,+(2,*(R/SA**2)))
JB = J-1
DO 400 LA = 3,JB
A(LA)=(R/SA**2)/(1,+(2,*(R/SA**2)))-(R/SA**2)*A(LA-1))
B(LA) = (2,*(R*U(L+1,LA,N)+(1,-2,*(R)*U(L,LA,N)+DH+
C(R/SA**2)*B(LA-1)))/(1,+(2,*(R/SA**2)))-(R/SA**2)*A(LA-1))
400 CONTINUE
GO TO 405
411 JC = JB-1
DO 412 LA = 3,JC
A(LA) = (R/SA**2)/(1,+(2,*(R/SA**2)))-(R/SA**2)*A(LA-1))
B(LA) = (R*(U(L-1,LA,N)+U(L+1,LA,N))+(1,-2,*(R)*U(L,LA,N)+DH+
C(R/SA**2)*B(LA-1)))/(1,+(2,*(R/SA**2)))-(R/SA**2)*A(LA-1))
412 CONTINUE
JB = JC+1
A(JB) = (R/SA**2)/(1,+(2,*(R/SA**2)))-(R/SA**2)*A(JB-1))
B(JB)=(U(L,JB,N)+DH+R*A(JB-1))/(1,+(2,*(R/SA**2)))-(R/SA**2)
C*A(JB-1))
GO TO 405
401 A(2) = (2,*(R/SA**2))/(1,+(2,*(R/SA**2)))
B(2)=(U(L,2,N)+DH)/(1,+(2,*(R/SA**2)))
M2 = L/4,+0.05
JB = J-2,*M2-1
DO 402 LA = 3,JB
A(LA)=(R/SA**2)/(1,+(2,*(R/SA**2)))-(R/SA**2)*A(LA-1))
B(LA)=(U(L,LA,N)+DH+(R/SA**2)*B(LA-1)))/
C(1,+(2,*(R/SA**2)))-(R/SA**2)*A(LA-1))
402 CONTINUE
405 U(L,JB,N+1) = B(JB)
MD = JB-2
DO 410 MMD = 1,MD
MB = JB - MMD
U(L,MB,N+1) = B(MB)+A(MB)*U(L,MB+1,N+1)
410 CONTINUE
420 CONTINUE
GO TO 600
421 IF (N.GE.9) GO TO 430
CALL DORA
GO TO 600
430 IF (N.GE.15) GO TO 495
KC = N/2.
BC = N/2.
IF (KC.EQ.BC) GO TO 596
CALL SIVA
GO TO 600
596 CALL SIV
GO TO 600
495 IF (N.GE.17) GO TO 535
CALL JOGI
GO TO 600
535 IF (N.GE.24) GO TO 598
KD = N/2.
BD = N/2.
IF (KD.EQ.BD) GO TO 597
CALL KOPI

```



```

      GO TO 600
597  CALL KCP2
      GO TO 600
598  IF (N.GE.28) GO TO 599
      CALL SK
      GO TO 600
599  IF (N.GE.32) GO TO 601
      KE = N/2.
      BE = N/2.
      IF (KE.EQ.BE) GO TO 595
      CALL SK1
      GO TO 600
595  CALL SK2
      GO TO 600
601  CALL MM2
600  CONTINUE

```

C
C

```

      DO 900 N = 1,K
      IF (N.GT.32) GO TO 614
      IF (N.GT.28) GO TO 612
      IF (N.GT.24) GO TO 610
      IF (N.GT.17) GO TO 608
      IF (N.GT.15) GO TO 606
      IF (N.GT. 8) GO TO 604
      IF (N.GT. 6) GO TO 602
      DT = 3./5.
      T(N) = DT*(N-1)
      GO TO 620
602  DT = 3./2.
      T(N) = 3.+DT*(N-6)
      GO TO 620
604  DT = 7./7.
      T(N) = 3.+3.0+DT*(N-8)
      GO TO 620
606  DT = 3./4.
      T(N) = 3.+3.0+7.+DT*(N-15)
      GO TO 620
608  DT = 7.5/7.
      T(N) = 3.+3.0+7.+1.5+DT*(N-17)
      GO TO 620
610  DT = 3./3.
      T(N) = 3.+3.0+7.+1.5+7.5+DT*(N-24)
      GO TO 620
612  DT = 3./4.
      T(N) = 3.+3.0+7.+1.5+7.5+1.5+DT*(N-28)
      GO TO 620
614  DT = 1.
      T(N) = 3.+3.0+7.+1.5+7.5+3.+1.5+DT*(N-32)
620  WRITE (6,625) (T(N))
625  FORMAT ('1', 25X, 'T=', 2X, F6.2, 4X, 'MONTHS'////)
      DO 650 M = 1,J
650  Y(M) = DX*SA*(M-1)
      WRITE (6,675) (Y(M), M=1,J)
675  FORMAT (3X, 'X/Y', 1X, 11F11.3/, 7X, 10F11.3////)

```



```
NA = N
IF (N.GT. 6) NA = 6
IF (N.GT. 8) NA = N-2
IF (N.GT.15) NA = 13
IF (N.GT.17) NA = N-4
IF (N.GT.24) NA = 20
IF (N.GT.28) NA = N-8
IF (N.GT.32) NA = 24
DO 800 L = 1,NA
X(L) = DX*(L-1)
M1 = (L-7)/10.+1+0.05
JA = 2.*M1+1
M2 = L/4.+0.05
JB = J-2.*M2
WRITE (6,700) (X(L), (U(L,M,N), M=JA,JB))
700 FORMAT (2X, F6.2, 4X, 11E11.3/, 11X, 10E11.3)
800 CONTINUE
900 CONTINUE
STOP
END
```


C

```

SUBROUTINE KOP
COMMON X(24), Y(21), T(33), U(25,22,39), A(39), B(39), R,SA,DH,N,J
DO 36 L = 1,6
M1 = (L-7)/10.+1+0.05
JA = 2.*M1+1
M2 = L/4.+0.05
JB = J-2.*M2
DO 35 M = JA,JB
IF (N.GT.9) GO TO 42
IF (L.EQ.6 .OR. M.EQ.JA .OR. M.EQ.JB) U(L,M,N) = 0.0
GO TO 35
42 IF (M.EQ.JA .OR. M.EQ.JB) U(L,M,N) = 0.0
35 CONTINUE
36 CONTINUE
RETURN
END

```

C

```

SUBROUTINE KOPPUL
COMMON X(24), Y(21), T(33), U(25,22,39), A(39), B(39), R,SA,DH,N,J
DO 38 L = 7,13
M1 = (L-7)/10.+1+0.05
JA = 2.*M1+1
M2 = L/4.+0.05
JB = J-2.*M2
DO 37 M = JA,JB
IF (N.GT.17) GO TO 43
IF (L.EQ.13 .OR. M.EQ.JA .OR. M.EQ.JB) U(L,M,N) = 0.0
GO TO 37
43 IF (M.EQ.JA .OR. M.EQ.JB) U(L,M,N) = 0.0
37 CONTINUE
38 CONTINUE
RETURN
END

```


C

```

SUBROUTINE KOPPU
COMMON X(24), Y(21), T(38), U(25,22,39), A(39), B(39), R,SA,DH,N,J
DO 41 L = 14,20
M1 = (L-7)/10.+1+0.05
JA = 2.*M1+1
M2 = L/4.+0.05
JB = J-2.*M2
DO 39 M = JA,JB
IF (N.GT.28) GO TO 44
IF (L.EQ.20 .OR. M.EQ.JA .OR. M.EQ.JB) U(L,M,N) = 0.0
GO TO 39
44 IF (M.EQ.JA .OR. M.EQ.JB) U(L,M,N) = 0.0
39 CONTINUE
41 CONTINUE
RETURN
END

```

C

```

SUBROUTINE NM1
COMMON X(24), Y(21), T(38), U(25,22,39), A(39), B(39), R,SA,DH,N,J
DO 46 L = 21,24
M1 = (L-7)/10.+1+0.05
JA = 2.*M1+1
M2 = L/4.+0.05
JB = J-2.*M2
DO 45 M = JA,JB
IF (L.EQ.24 .OR. M.EQ.JA .OR. M.EQ.JB) U(L,M,N) = 0.
45 CONTINUE
46 CONTINUE
RETURN
END

```



```

SUBROUTINE DDRA
COMMON X(24), Y(21), T(38), U(25,22,39), A(39), B(39), R,SA,DH,N,J
KR = N/2.
BR = N/2.
IF (KB.EQ.BB) GO TO 438
M2 = N/4.+0.05
JB = J-2.*M2-1
DO 429 M = 2,JB
  A(1) = (2.*R)/(1.+2.*R)
  B(1) = ((1.-(2.*R/SA**2))*U(1,M,N)+(R/SA**2)*(U(1,M-1,N)+
CU(1,M+1,N))+DH)/(1.+2.*R)
  DO 422 LE = 2,5
    A(LE)=R/(1.+2.*R-R*A(LE-1))
    B(LE)=((R/SA**2)*(U(LE,M-1,N)+U(LE,M+1,N))+(1.-(2.*R)/SA**2))*
CU(LE,M,N)+DH+R*B(LE-1))/(1.+2.*R-R*A(LE-1))
422 CONTINUE
    U(5,M,N+1) = B(5)
    JG = 5-1
    DO 427 LJ = 1,JG
      KJ = 5-LJ
      U(KJ,M,N+1) = B(KJ)+A(KJ)*U(KJ+1,M,N+1)
427 CONTINUE
429 CONTINUE
    JC = J-1
    IF (JB.EQ.JC) GO TO 447
    JD = JB+1
    DO 437 M = JD,JC
      A(1) = (2.*R)/(1.+2.*R)
      B(1) = ((1.-(2.*R/SA**2))*U(1,M,N)+(R/SA**2)*(U(1,M-1,N)+
CU(1,M+1,N))+DH)/(1.+2.*R)
      DO 433 LE = 2,3
        A(LE)=R/(1.+2.*R-R*A(LE-1))
        B(LE)=((R/SA**2)*(U(LE,M-1,N)+U(LE,M+1,N))+(1.-(2.*R)/SA**2))*
CU(LE,M,N)+DH+R*B(LE-1))/(1.+2.*R-R*A(LE-1))
433 CONTINUE
        U(3,M,N+1) = B(3)
        JG = 3-1
        DO 435 LJ = 1,JG
          KJ = 3-LJ
          U(KJ,M,N+1) = B(KJ)+A(KJ)*U(KJ+1,M,N+1)
435 CONTINUE
437 CONTINUE
      GO TO 447
438 IA = 6-1
      DO 445 L = 1,IA
        IF (L.EQ.1) GO TO 439
        A(2) = (2.*(R/SA**2))/(1.+(2.*(R/SA**2)))
        B(2)=(R*(U(L-1,2,N)+U(L+1,2,N))+(1.-2.*R)*U(L,2,N)+DH)/
C(1.+(2.*(R/SA**2)))
        M2 = L/4.+0.05
        JB = J-2.*M2-1
        IF (L.EQ.3) JB = 19
        DO 441 LA = 3,JB
          A(LA)=(R/SA**2)/(1.+(2.*(R/SA**2))-(R/SA**2)*A(LA-1))

```



```

      B(LA)=(R*(U(L-1,LA,N)+U(L+1,LA,N))+(1.-2.*R)*U(L,LA,N)+DH+
441  C(R/SA**2)*B(LA-1))/(1.+(2.*(R/SA**2))-(R/SA**2)*A(LA-1))
      CONTINUE
      IF (L.EQ.3) GO TO 444
      GO TO 442
444  A(20) = (R/SA**2)/(1.+(2.*(R/SA**2))-(R/SA**2)*A(19))
      B(20)=(U(L,20,N)+DH+R*A(20-1))/(1.+(2.*(R/SA**2))-(R/SA**2)
      C*A(19))
      GO TO 442
439  A(2) = (2.*(R/SA**2))/(1.+(2.*(R/SA**2)))
      B(2) = (2.*R*U(L+1,2,N)+(1.-2.*R)*U(L,2,N)+DH)/
      C(1.+(2.*(R/SA**2)))
      M2 = L/4.+0.05
      JB = J-2.*M2-1
      DO 440 LA = 3,JB
      A(LA)=(R/SA**2)/(1.+(2.*(R/SA**2))-(R/SA**2)*A(LA-1))
      B(LA) = (2.*R*U(L+1,LA,N)+(1.-2.*R)*U(L,LA,N)+DH+
      C(R/SA**2)*B(LA-1))/(1.+(2.*(R/SA**2))-(R/SA**2)*A(LA-1))
440  CONTINUE
442  JB = 20
      U(L,JB,N+1) = B(JB)
      IF (L.EQ.1) JA = 2
      JC = JB - JA
      DO 443 JM = 1,JC
      MB = JB-JM
      U(L,MB,N+1) = B(MB)+A(MB)*U(L,MB+1,N+1)
443  CONTINUE
445  CONTINUE
447  RETURN
      END

```


C

```

SUBROUTINE SIVA
COMMON X(24), Y(21), T(38), U(25,22,39), A(39), B(39), R, SA, DH, N, J
NA = N-2
M2 = NA/4.+0.05
JB = J-2.*M2-1
DO 454 M = 2, JB
  A(1) = (2.*R)/(1.+2.*R)
  B(1) = ((1.-(2.*R/SA**2))*U(1,M,N)+(R/SA**2)*(U(1,M-1,N)+
CU(1,M+1,N))+DH)/(1.+2.*R)
  NC = N-2
  IF (M.LE.3) NC = 6
  DO 442 LE = 2, NC
    A(LE)=R/(1.+2.*R-R*A(LE-1))
    B(LE)=((R/SA**2)*(U(LE,M-1,N)+U(LE,M+1,N))+(1.-((2.*R)/SA**2))*
CU(LE,M,N))+DH+R*B(LE-1))/(1.+2.*R-R*A(LE-1))
442  CONTINUE
    U(NC,M,M+1) = B(NC)
    LL = NC-1
    DO 444 LG = 1, LL
      KG = NC-LG
      U(KG,M,M+1) = B(KG)+A(KG)*U(KG+1,M,N+1)
444  CONTINUE
454  CONTINUE
    JC = J-1
    IF (JB.EQ.JC) GO TO 470
    JD = JB+1
    DO 469 M = JD, JC
      A(1) = (2.*R)/(1.+2.*R)
      B(1) = ((1.-(2.*R/SA**2))*U(1,M,N)+(R/SA**2)*(U(1,M-1,N)+
CU(1,M+1,N))+DH)/(1.+2.*R)
      MN = (M-13)/2.
      NC = J-4.*MN-6
      DO 462 LE = 2, NC
        A(LE)=R/(1.+2.*R-R*A(LE-1))
        B(LE)=((R/SA**2)*(U(LE,M-1,N)+U(LE,M+1,N))+(1.-((2.*R)/SA**2))*
CU(LE,M,N))+DH+R*B(LE-1))/(1.+2.*R-R*A(LE-1))
462  CONTINUE
        U(NC,M,M+1) = B(NC)
        LL = NC-1
        DO 466 LG = 1, LL
          KG = NC-LG
          U(KG,M,M+1) = B(KG)+A(KG)*U(KG+1,M,N+1)
466  CONTINUE
469  CONTINUE
470  RETURN
      END

```


C

```

SUBROUTINE SIV
COMMON X(24), Y(21), T(39), U(25,22,39), A(39), B(39), R,SA,DH,N,J
NA = N-2
DO 490 L = 1,NA
M1 = (L-7)/10.+1+0.05
JA = 2.*M1+2
JD = JA-1
IF (L.EQ.1) GO TO 476
IF (L.EQ.NA) GO TO 430
IF (L.EQ.6) GO TO 475
A(JD) = (2.*(R/SA**2))/(1.+(2.*(R/SA**2)))
B(JD)=(R*(U(L-1,JD,N)+U(L+1,JD,N))+(1.-2.*R)*U(L,JD,N)+DH)/
C(1.+(2.*(R/SA**2)))
M2 = L/4.+0.05
JB = J-2.*M2-1
IF (L.LT.3 .OR. L.EQ.7 .OR. L.EQ.11) GO TO 479
DO 474 LA = JA,JB
A(LA)=(R/SA**2)/(1.+(2.*(R/SA**2))-(R/SA**2)*A(LA-1))
B(LA)=(R*(U(L-1,LA,N)+U(L+1,LA,N))+(1.-2.*R)*U(L,LA,N)+DH+
C(R/SA**2)*B(LA-1))/(1.+(2.*(R/SA**2))-(R/SA**2)*A(LA-1))
474 CONTINUE
GO TO 484
475 A(JD) = (2.*(R/SA**2))/(1.+(2.*(R/SA**2)))
B(JD) = (U(L,JD,N)+DH)/(1.+(2.*(R/SA**2)))
JA = JD+1
A(JA)=(R/SA**2)/(1.+(2.*(R/SA**2))-(R/SA**2)*A(JD))
B(JA) = (U(L,JA,N)+DH+(R/SA**2)*U(L,JD,N))/
C(1.+(2.*(R/SA**2))-(R/SA**2)*A(JD))
M2 = L/4.+0.05
JB = J-2.*M2-1
JE = JA+1
DO 477 LA = JE,JB
A(LA)=(R/SA**2)/(1.+(2.*(R/SA**2))-(R/SA**2)*A(LA-1))
B(LA)=(R*(U(L-1,LA,N)+U(L+1,LA,N))+(1.-2.*R)*U(L,LA,N)+DH+
C(R/SA**2)*B(LA-1))/(1.+(2.*(R/SA**2))-(R/SA**2)*A(LA-1))
477 CONTINUE
GO TO 484
476 A(1) = (2.*(R/SA**2))/(1.+(2.*(R/SA**2)))
B(1) = (2.*R*U(L+1,1,N)+(1.-2.*R)*U(L,1,N)+DH)/
C(1.+(2.*(R/SA**2)))
JB = J-1
DO 478 LA = 2,JB
A(LA)=(R/SA**2)/(1.+(2.*(R/SA**2))-(R/SA**2)*A(LA-1))
B(LA) = (2.*R*U(L+1,LA,N)+(1.-2.*R)*U(L,LA,N)+DH+
C(R/SA**2)*B(LA-1))/(1.+(2.*(R/SA**2))-(R/SA**2)*A(LA-1))
478 CONTINUE
GO TO 484
479 JC = JB-1
DO 481 LA = JA,JC
A(LA) = (R/SA**2)/(1.+(2.*(R/SA**2))-(R/SA**2)*A(LA-1))
B(LA) = (R*(U(L-1,LA,N)+U(L+1,LA,N))+(1.-2.*R)*U(L,LA,N)+DH+
C(R/SA**2)*B(LA-1))/(1.+(2.*(R/SA**2))-(R/SA**2)*A(LA-1))
481 CONTINUE
JB = JC+1

```



```

      A(JB) = (R/SA**2)/(1.+(2.*(R/SA**2))-(R/SA**2)*A(JB-1))
      B(JB)=(U(L,JB,N)+DH+R*A(JB-1))/(1.+(2.*(R/SA**2))-(R/SA**2)
C*A(JB-1))
      GO TO 484
490  A(JD) = (2.*(R/SA**2))/(1.+(2.*(R/SA**2)))
      B(JD)=(U(L,JD,N)+DH)/(1.+(2.*(R/SA**2)))
      JA = JD+1
      M2 = L/4.+0.05
      JB = J-2.*M2-1
      DO 482 LA = JA,JB
      A(LA)=(R/SA**2)/(1.+(2.*(R/SA**2))-(R/SA**2)*A(LA-1))
      B(LA)=(U(L,LA,N)+DH+(R/SA**2)*B(LA-1))/
C(1.+(2.*(R/SA**2))-(R/SA**2)*A(LA-1))
482  CONTINUE
484  U(L,JB,N+1) = B(JB)
      IF (L.EQ.1) JA = 2
      MM = JB-JA
      DO 486 MMM = 1,MM
      MB = JB-MMM
      U(L,MB,N+1) = B(MB)+A(MB)*U(L,MB+1,N+1)
486  CONTINUE
490  CONTINUE
      RETURN
      END

```


C

```

SUBROUTINE JOGI
COMMON X(24), Y(21), T(33), U(25,22,39), A(39), B(39), R,SA,DH,N,J
KB = N/2.
DB = N/2.
IF (KB.EQ.DB) GO TO 503
JB = J-1
DO 506 M = 2,JB
A(1) = (2.*R)/(1.+2.*R)
B(1) = ((1.-(2.*R/SA**2))*U(1,M,N)+(R/SA**2)*(U(1,M-1,N)+
CU(1,M+1,N))+DH)/(1.+2.*R)
IF (M.GT.14) GO TO 498
NC = 12
IF (M.LE.3) NC = 6
DO 496 LE = 2,NC
A(LE)=R/(1.+2.*R-R*A(LE-1))
B(LE)=((R/SA**2)*(U(LE,M-1,N)+U(LE,M+1,N))+(1.-((2.*R)/SA**2))*
CU(LE,M,N)+DH+R*B(LE-1))/(1.+2.*R-R*A(LE-1))
496 CONTINUE
GO TO 502
498 MN = (M-13)/2.
NC = J-4.*MN-6
DO 500 LE = 2,NC
A(LE)=R/(1.+2.*R-R*A(LE-1))
B(LE)=((R/SA**2)*(U(LE,M-1,N)+U(LE,M+1,N))+(1.-((2.*R)/SA**2))*
CU(LE,M,N)+DH+R*B(LE-1))/(1.+2.*R-R*A(LE-1))
500 CONTINUE
502 U(NC,M,N+1) = B(NC)
LL = NC-1
DO 504 LG = 1,LL
KG = NC-LG
U(KG,M,N+1) = B(KG)+A(KG)*U(KG+1,M,N+1)
504 CONTINUE
506 CONTINUE
GO TO 516
508 DO 514 L = 1,12
M1 = (L-7)/10.+1+0.05
JA = 2.*M1+2
M2 = L/4.+0.05
JB = J-2.*M2-1
JD = JA-1
IF (L.EQ.1) GO TO 507
IF (L.EQ.6) GO TO 503
A(JD) = (2.*(R/SA**2))/(1.+(2.*(R/SA**2)))
B(JD)=(R*(U(L-1,JD,N)+U(L-1,JD,N))+(1.-2.*R)*U(L,JD,N)+DH)/
C(1.+(2.*(R/SA**2)))
IF (L.EQ.3 .OR. L.EQ.7 .OR. L.EQ.11) GO TO 507
DO 510 LA = JA,JB
A(LA)=(R/SA**2)/(1.+(2.*(R/SA**2))-(R/SA**2)*A(LA-1))
B(LA)=(R*(U(L-1,LA,N)+U(L+1,LA,N))+(1.-2.*R)*U(L,LA,N)+DH+
C(R/SA**2)*B(LA-1))/(1.+(2.*(R/SA**2))-(R/SA**2)*A(LA-1))
510 CONTINUE
GO TO 513
503 A(JD) = (2.*(R/SA**2))/(1.+(2.*(R/SA**2)))
B(JD) = (U(L,JD,N)+DH)/(1.+(2.*(R/SA**2)))

```



```

JA = JB+1
A(JA)=(R/SA**2)/(1.+(2.*(R/SA**2))-(R/SA**2)*A(JB))
B(JA) = (U(L,JA,N)+DH+(R/SA**2)*U(L,JB,N))/
C(1.+(2.*(R/SA**2))-(R/SA**2)*A(JB))
JF = JA+1
DO 505 LA = JE,JB
A(LA)=(R/SA**2)/(1.+(2.*(R/SA**2))-(R/SA**2)*A(LA-1))
B(LA)=(R*(U(L-1,LA,N)+U(L+1,LA,N))+(1.-2.*R)*U(L,LA,N)+DH+
C(R/SA**2)*B(LA-1))/(1.+(2.*(R/SA**2))-(R/SA**2)*A(LA-1))
505 CONTINUE
GO TO 513
509 A(1) = (2.*(R/SA**2))/(1.+(2.*(R/SA**2)))
B(1) = (2.*R*U(L+1,1,N)+(1.-2.*R)*U(L,1,N)+DH)/
C(1.+(2.*(R/SA**2)))
DO 511 LA = JA,JB
A(LA)=(R/SA**2)/(1.+(2.*(R/SA**2))-(R/SA**2)*A(LA-1))
B(LA) = (2.*R*U(L+1,LA,N)+(1.-2.*R)*U(L,LA,N)+DH+
C(R/SA**2)*B(LA-1))/(1.+(2.*(R/SA**2))-(R/SA**2)*A(LA-1))
511 CONTINUE
GO TO 513
507 JC = JB-1
DO 515 LA = JA,JC
A(LA) = (R/SA**2)/(1.+(2.*(R/SA**2))-(R/SA**2)*A(LA-1))
B(LA) = (R*(U(L-1,LA,N)+U(L+1,LA,N))+(1.-2.*R)*U(L,LA,N)+DH+
C(R/SA**2)*B(LA-1))/(1.+(2.*(R/SA**2))-(R/SA**2)*A(LA-1))
515 CONTINUE
JB = JC+1
A(JB) = (R/SA**2)/(1.+(2.*(R/SA**2))-(R/SA**2)*A(JB-1))
B(JB)=(U(L,JB,N)+DH+R*A(JB-1))/(1.+(2.*(R/SA**2))-(R/SA**2)
C*A(JB-1))
513 U(L,JB,N+1) = B(JB)
IF (L.EQ.1) JA = 2
JC = JB - JA
DO 512 PM = 1,JC
MB = JB-PM
U(L,MB,N+1) = B(MB)+A(MB)*U(L,MB+1,N+1)
512 CONTINUE
514 CONTINUE
516 RETURN
END

```


C

```

SUBROUTINE KOP1
COMMON X(24), Y(21), I(39), U(25,22,39), A(39), B(39), R,SA,DH,N,J
NA = N-4
M2 = NA/4.+0.05
JB = J-2.*M2-1
DO 540 M = 2,JB
  A(1) = (2.*R)/(1.+2.*R)
  B(1) = ((1.-(2.*R/SA**2))*U(1,M,N)+R/SA**2)*(U(1,M-1,N)+
CU(1,M+1,N))+DH/(1.+2.*R)
  NC = M-4
  IF (M.LE.5 .AND. M.GT.19) NC = 16
  IF (M.LE.3) NC = 6
  DO 536 LE = 2,NC
    A(LE)=R/(1.+2.*R-R*A(LE-1))
    B(LE)=((R/SA**2)*(U(LE,M-1,N)+U(LE,M+1,N))+(1.-((2.*R)/SA**2))*
CU(LE,M,N)+DH+R*R(LE-1))/(1.+2.*R-R*A(LE-1))
536  CONTINUE
    U(NC,M,N+1) = B(NC)
    LL = NC-1
    DO 538 LG = 1,LL
      KG = NC-LG
      U(KG,M,N+1) = B(KG)+A(KG)*U(KG+1,M,N+1)
538  CONTINUE
540  CONTINUE
    JC = J-1
    IF (JB.EQ.JC) GO TO 543
    JD = JB+1
    DO 546 M = JD,JC
      A(1) = (2.*R)/(1.+2.*R)
      B(1) = ((1.-(2.*R/SA**2))*U(1,M,N)+R/SA**2)*(U(1,M-1,N)+
CU(1,M+1,N))+DH/(1.+2.*R)
      MN = (M-13)/2.
      NC = J-4.*MN-6
      DO 542 LE = 2,NC
        A(LE)=R/(1.+2.*R-R*A(LE-1))
        B(LE)=((R/SA**2)*(U(LE,M-1,N)+U(LE,M+1,N))+(1.-((2.*R)/SA**2))*
CU(LE,M,N)+DH+R*R(LE-1))/(1.+2.*R-R*A(LE-1))
542  CONTINUE
        U(NC,M,N+1) = B(NC)
        LL = NC-1
        DO 544 LG = 1,LL
          KG = NC-LG
          U(KG,M,N+1) = B(KG)+A(KG)*U(KG+1,M,N+1)
544  CONTINUE
546  CONTINUE
548  RETURN
END

```


C

```

SUBROUTINE KOP2
COMMON X(24), Y(21), T(38), U(25,22,39), A(39), B(39), R,SA,DH,N,J
NA = N-4
DO 566 L = 1,NA
M1 = (L-7)/10.+1+0.05
JA = 2.*M1+2
M2 = L/4.+0.05
JB = J-2.*M2-1
JD = JA-1
IF (L.EQ.1) GO TO 554
IF (L.EQ.NA) GO TO 558
IF (L.EQ.6 .OR. L.EQ.16) GO TO 555
A(JD) = (2.*(R/SA**2))/(1.+(2.*(R/SA**2)))
B(JD)=(R*(U(L-1,JD,N)+U(L+1,JD,N))+(1.-2.*R)*U(L,JD,N)+DH)/
C(1.+(2.*(R/SA**2)))
IF (L.EQ.3 .OR. L.EQ.7 .OR. L.EQ.11 .OR. L.EQ.15 .OR. L.EQ.19)
CGO TO 561
DO 552 LA = JA,JB
A(LA)=(R/SA**2)/(1.+(2.*(R/SA**2))-(R/SA**2)*A(LA-1))
B(LA)=(R*(U(L-1,LA,N)+U(L+1,LA,N))+(1.-2.*R)*U(L,LA,N)+DH+
C(R/SA**2)*P(LA-1))/(1.+(2.*(R/SA**2))-(R/SA**2)*A(LA-1))
552 CONTINUE
GO TO 562
554 A(1) = (2.*(R/SA**2))/(1.+(2.*(R/SA**2)))
B(1) = (2.*R*U(L+1,1,N)+(1.-2.*R)*U(L,1,N)+DH)/
C(1.+(2.*(R/SA**2)))
JB = J-1
DO 556 LA = 3,JB
A(LA)=(R/SA**2)/(1.+(2.*(R/SA**2))-(R/SA**2)*A(LA-1))
B(LA) = (2.*R*U(L+1,LA,N)+(1.-2.*R)*U(L,LA,N)+DH+
C(R/SA**2)*B(LA-1))/(1.+(2.*(R/SA**2))-(R/SA**2)*A(LA-1))
556 CONTINUE
GO TO 562
555 A(JD) = (2.*(R/SA**2))/(1.+(2.*(R/SA**2)))
B(JD) = (U(L,JD,N)+DH)/(1.+(2.*(R/SA**2)))
JA = JD+1
A(JA)=(R/SA**2)/(1.+(2.*(R/SA**2))-(R/SA**2)*A(JD))
B(JA) = (U(L,JA,N)+DH+(R/SA**2)*U(L,JD,N))/
C(1.+(2.*(R/SA**2))-(R/SA**2)*A(JD))
JE = JA+1
DO 559 LA = JE,JB
A(LA)=(R/SA**2)/(1.+(2.*(R/SA**2))-(R/SA**2)*A(LA-1))
B(LA)=(R*(U(L-1,LA,N)+U(L+1,LA,N))+(1.-2.*R)*U(L,LA,N)+DH+
C(R/SA**2)*B(LA-1))/(1.+(2.*(R/SA**2))-(R/SA**2)*A(LA-1))
559 CONTINUE
GO TO 562
561 JC = JB-1
DO 565 LA = JA,JC
A(LA) = (R/SA**2)/(1.+(2.*(R/SA**2))-(R/SA**2)*A(LA-1))
B(LA) = (R*(U(L-1,LA,N)+U(L+1,LA,N))+(1.-2.*R)*U(L,LA,N)+DH+
C(R/SA**2)*B(LA-1))/(1.+(2.*(R/SA**2))-(R/SA**2)*A(LA-1))
565 CONTINUE
JB = JC+1
A(JB) = (R/SA**2)/(1.+(2.*(R/SA**2))-(R/SA**2)*A(JB-1))

```



```

      B(JB)=(U(L,JB,N)+DH+R*A(JP-1))/(1.+(2.*(R/SA**2))-(R/SA**2)
      C*A(JB-1))
      GO TO 562
558  A(JD) = (2.*(R/SA**2))/(1.+(2.*(R/SA**2)))
      B(JD)=(U(L,JD,N)+DH)/(1.+(2.*(R/SA**2)))
      DO 560 LA = JA,JB
      A(LA)=(R/SA**2)/(1.+(2.*(R/SA**2))-(R/SA**2)*A(LA-1))
      B(LA)=(U(L,LA,N)+DH+(R/SA**2)*B(LA-1))/
      C(1.+(2.*(R/SA**2))-(R/SA**2)*A(LA-1))
560  CONTINUE
562  U(L,JB,N+1) = B(JB)
      IF (L.EQ.1) JA = 2
      MM = JB - JA
      DO 564 PMM = 1,MM
      MB = JB-PMM
      U(L,MB,N+1) = B(MB)+A(MB)*U(L,MB+1,N+1)
564  CONTINUE
566  CONTINUE
      RETURN
      END

```


C

```

SUBROUTINE SK
COMMON X(24), Y(21), T(38), U(25,22,39), A(39), B(39), R,SA,DH,N,J
KB = N/2.
PB = N/2.
IF (KB.EQ.PB) GO TO 580
JB = J-1
DO 573 M = 2,JB
A(1) = (2.*R)/(1.+2.*R)
B(1) = ((1.-(2.*R/SA**2))*U(1,M,N)+(R/SA**2)*(U(1,M-1,N)+
CU(1,M+1,N))+DH)/(1.+2.*R)
IF (M.GT.12) GO TO 570
NC = 19
IF (M.LE.5) NC = 15
IF (M.LE.3) NC = 6
DO 568 LE = 2,NC
A(LE)=R/(1.+2.*R-R*A(LE-1))
B(LE)=((R/SA**2)*(U(LE,M-1,N)+U(LE,M+1,N))+(1.-((2.*R)/SA**2))*
CU(LE,M,N)+DH+R*B(LE-1))/(1.+2.*R-R*A(LE-1))
568 CONTINUE
GO TO 574
570 MN = (M-13)/2.
NC = J-4.*MN-6
DO 572 LE = 2,NC
A(LE)=R/(1.+2.*R-R*A(LE-1))
B(LE)=((R/SA**2)*(U(LE,M-1,N)+U(LE,M+1,N))+(1.-((2.*R)/SA**2))*
CU(LE,M,N)+DH+R*B(LE-1))/(1.+2.*R-R*A(LE-1))
572 CONTINUE
574 U(NC,M,M+1) = B(NC)
LL = NC-1
DO 576 LG = 1,LL
KG = NC-LG
U(KG,M,M+1) = B(KG)+A(KG)*U(KG+1,M,M+1)
576 CONTINUE
578 CONTINUE
GO TO 583
580 DO 586 L = 1,19
M1 = (L-7)/10.+1+0.05
JA = 2.*M1+2
M2 = L/4.+0.05
JB = J-2.*M2-1
JD = JA-1
IF (L.EQ.1) GO TO 583
IF (L.EQ.6 .OR. L.EQ.16) GO TO 573
A(JD) = (2.*(R/SA**2))/(1.+(2.*(R/SA**2)))
B(JD)=(R*(U(L-1,JD,N)+U(L-1,JD,N))+(1.-2.*R)*U(L,JD,N)+DH)/
C(1.+(2.*(R/SA**2)))
IF (L.EQ.3 .OR. L.EQ.7 .OR. L.EQ.11 .OR. L.EQ.15 .OR. L.EQ.19)
CGO TO 587
DO 582 LA = JA,JB
A(LA)=(R/SA**2)/(1.+(2.*(R/SA**2))-(R/SA**2)*A(LA-1))
B(LA)=(R*(U(L-1,LA,N)+U(L+1,LA,N))+(1.-2.*R)*U(L,LA,N)+DH+
C(R/SA**2)*B(LA-1))/(1.+(2.*(R/SA**2))-(R/SA**2)*A(LA-1))
582 CONTINUE
GO TO 589

```



```

573  A(JD) = (2.*(R/SA**2))/(1.+(2.*(R/SA**2)))
      B(JD) = (U(L,JD,N)+DH)/(1.+(2.*(R/SA**2)))
      JA = JD+1
      A(JA)=(R/SA**2)/(1.+(2.*(R/SA**2))-(R/SA**2)*A(JD))
      B(JA) = (U(L,JA,N)+DH+(R/SA**2)*U(L,JD,N))/
C(1.+(2.*(R/SA**2))-(R/SA**2)*A(JD))
      JE = JA+1
      DO 579 LA = JE,JB
      A(LA)=(R/SA**2)/(1.+(2.*(R/SA**2))-(R/SA**2)*A(LA-1))
      B(LA)=(R*(U(L-1,LA,N)+U(L+1,LA,N))+(1.-2.*R)*U(L,LA,N)+DH+
C(R/SA**2)*B(LA-1))/(1.+(2.*(R/SA**2))-(R/SA**2)*A(LA-1))
579  CONTINUE
      GO TO 589
587  JC = JB-1
      DO 581 LA = JA,JC
      A(LA) = (R/SA**2)/(1.+(2.*(R/SA**2))-(R/SA**2)*A(LA-1))
      B(LA) = (R*(U(L-1,LA,N)+U(L+1,LA,N))+(1.-2.*R)*U(L,LA,N)+DH+
C(R/SA**2)*B(LA-1))/(1.+(2.*(R/SA**2))-(R/SA**2)*A(LA-1))
581  CONTINUE
      JB = JC+1
      A(JB) = (R/SA**2)/(1.+(2.*(R/SA**2))-(R/SA**2)*A(JB-1))
      B(JB)=(U(L,JB,N)+DH+R*A(JB-1))/(1.+(2.*(R/SA**2))-(R/SA**2)
C*A(JB-1))
      GO TO 589
583  A(1) = (2.*(R/SA**2))/(1.+(2.*(R/SA**2)))
      B(1) = (2.*R*U(L+1,1,N)+(1.-2.*R)*U(L,1,N)+DH)/
C(1.+(2.*(R/SA**2)))
      DO 585 LA = JA,JB
      A(LA)=(R/SA**2)/(1.+(2.*(R/SA**2))-(R/SA**2)*A(LA-1))
      B(LA) = (2.*R*U(L+1,LA,N)+(1.-2.*R)*U(L,LA,N)+DH+
C(R/SA**2)*B(LA-1))/(1.+(2.*(R/SA**2))-(R/SA**2)*A(LA-1))
585  CONTINUE
589  U(L,JB,N+1) = B(JB)
      IF (L.EQ.1) JA = 2
      JC = JB - JA
      DO 584 MP = 1,JC
      MB = JB-MP
      U(L,MB,N+1) = B(MB)+A(MB)*U(L,MB+1,N+1)
584  CONTINUE
586  CONTINUE
588  RETURN
      END

```


C
C

```

SUBROUTINE SK1
COMMON X(24), Y(21), I(38), U(25,22,39), A(39), B(39), R,SA,DH,N,J
NC = N-8
M2 = NC/4.+0.05
JB = J-2.*M2-1
DO 592 M = 2,JB
  A(1) = (2.*R)/(1.+2.*R)
  B(1) = ((1.-(2.*R/SA**2))*U(1,M,N)+(R/SA**2)*(U(1,M-1,N)+
CU(1,M+1,N))+DH)/(1.+2.*R)
  IF (M.LE.5) NC = 16
  IF (M.LE.3) NC = 6
  DO 590 LE = 2,NC
    IF (M.GT.5) NC = N-8
    A(LE)=R/(1.+2.*R-R*A(LE-1))
    B(LE)=((R/SA**2)*(U(LE,M-1,N)+U(LE,M+1,N))+(1.-((2.*R)/SA**2))*
CU(LE,M,N)+DH+R*B(LE-1))/(1.+2.*R-R*A(LE-1))
590  CONTINUE
    U(NC,M,N+1) = B(NC)
    LL = NC-1
    DO 591 LG = 1,LL
      KG = NC-LG
      U(KG,M,N+1) = B(KG)+A(KG)*U(KG+1,M,N+1)
591  CONTINUE
592  CONTINUE
    JC = J-1
    IF (JB.EQ.JC) GO TO 651
    JD = JB+1
    DO 595 M = JD,JC
      A(1) = (2.*R)/(1.+2.*R)
      B(1) = ((1.-(2.*R/SA**2))*U(1,M,N)+(R/SA**2)*(U(1,M-1,N)+
CU(1,M+1,N))+DH)/(1.+2.*R)
      MN = (M-13)/2.
      NC = J-4.*MN-6
      IF (M.LE.12) NC = 19
      DO 593 LE = 2,NC
        A(LE)=R/(1.+2.*R-R*A(LE-1))
        B(LE)=((R/SA**2)*(U(LE,M-1,N)+U(LE,M+1,N))+(1.-((2.*R)/SA**2))*
CU(LE,M,N)+DH+R*B(LE-1))/(1.+2.*R-R*A(LE-1))
593  CONTINUE
        U(NC,M,N+1) = B(NC)
        LL = NC-1
        DO 594 LG = 1,LL
          KG = NC-LG
          U(KG,M,N+1) = B(KG)+A(KG)*U(KG+1,M,N+1)
594  CONTINUE
595  CONTINUE
651  RETURN
      END

```


C

```

SUBROUTINE SK2
COMMON X(24), Y(21), T(39), U(25,22,39), A(39), B(39), R,SA,DH,N,J
NA = N-8
DO 659 L = 1,NA
M1 = (L-7)/10.+1+0.05
JA = 2.*M1+2
M2 = L/4.+0.05
JB = J-2.*M2-1
JD = JA-1
IF (L.EQ.1) GO TO 653
IF (L.EQ.6 .OR. L.EQ.16) GO TO 662
IF (L.EQ.NA) GO TO 655
A(JD) = (2.*(R/SA**2))/(1.+(2.*(R/SA**2)))
B(JD) = (R*(U(L-1,JD,N)+U(L+1,JD,N))+(1.-2.*R)*U(L,JD,N)+DH)/
C(1.+(2.*(R/SA**2)))
IF (L.EQ.3 .OR. L.EQ.7 .OR. L.EQ.11 .OR. L.EQ.15 .OR. L.EQ.19
C.OR. L.EQ.23) GO TO 660
DO 652 LA = JA,JB
A(LA) = (R/SA**2)/(1.+(2.*(R/SA**2))-(R/SA**2)*A(LA-1))
B(LA) = (R*(U(L-1,LA,N)+U(L+1,LA,N))+(1.-2.*R)*U(L,LA,N)+DH+
C(R/SA**2)*B(LA-1))/(1.+(2.*(R/SA**2))-(R/SA**2)*A(LA-1))
652 CONTINUE
GO TO 657
662 A(JD) = (2.*(R/SA**2))/(1.+(2.*(R/SA**2)))
B(JD) = (U(L,JD,N)+DH)/(1.+(2.*(R/SA**2)))
JA = JD+1
A(JA) = (R/SA**2)/(1.+(2.*(R/SA**2))-(R/SA**2)*A(JD))
B(JA) = (U(L,JA,N)+DH+(R/SA**2)*U(L,JD,N))/
C(1.+(2.*(R/SA**2))-(R/SA**2)*A(JD))
JE = JA+1
DO 663 LA = JE,JB
A(LA) = (R/SA**2)/(1.+(2.*(R/SA**2))-(R/SA**2)*A(LA-1))
B(LA) = (R*(U(L-1,LA,N)+U(L+1,LA,N))+(1.-2.*R)*U(L,LA,N)+DH+
C(R/SA**2)*B(LA-1))/(1.+(2.*(R/SA**2))-(R/SA**2)*A(LA-1))
663 CONTINUE
GO TO 657
653 A(1) = (2.*(R/SA**2))/(1.+(2.*(R/SA**2)))
B(1) = (2.*R*U(L+1,1,N)+(1.-2.*R)*U(L,1,N)+DH)/
C(1.+(2.*(R/SA**2)))
JB = J-1
DO 654 LA = 2,JB
A(LA) = (R/SA**2)/(1.+(2.*(R/SA**2))-(R/SA**2)*A(LA-1))
B(LA) = (2.*R*U(L+1,LA,N)+(1.-2.*R)*U(L,LA,N)+DH+
C(R/SA**2)*B(LA-1))/(1.+(2.*(R/SA**2))-(R/SA**2)*A(LA-1))
654 CONTINUE
GO TO 657
660 JC = JB-1
DO 661 LA = JA,JC
A(LA) = (R/SA**2)/(1.+(2.*(R/SA**2))-(R/SA**2)*A(LA-1))
B(LA) = (R*(U(L-1,LA,N)+U(L+1,LA,N))+(1.-2.*R)*U(L,LA,N)+DH+
C(R/SA**2)*B(LA-1))/(1.+(2.*(R/SA**2))-(R/SA**2)*A(LA-1))
661 CONTINUE
JB = JC+1
A(JB) = (R/SA**2)/(1.+(2.*(R/SA**2))-(R/SA**2)*A(JB-1))

```



```

      B(JB)=(U(L,JB,N)+DH+R*A(JB-1))/(1.+(2.*(R/SA**2))-(R/SA**2)
C*A(JB-1))
      GO TO 657
655  A(JD) = (2.*(R/SA**2))/(1.+(2.*(R/SA**2)))
      B(JD)=(U(L,JD,N)+DH)/(1.+(2.*(R/SA**2)))
      DO 656 LA = JA, JB
      A(LA)=(R/SA**2)/(1.+(2.*(R/SA**2))-(R/SA**2)*A(LA-1))
      B(LA)=(U(L,LA,N)+DH+(R/SA**2)*B(LA-1))/
C(1.+(2.*(R/SA**2))-(R/SA**2)*A(LA-1))
656  CONTINUE
657  U(L,JB,N+1) = B(JB)
      IF (L.EQ.1) JA = 2
      MM = JB - JA
      DO 658 MMM = 1, MM
      MB = JB-MMM
      U(L,MB,N+1) = B(MB)+A(MB)*U(L,MB+1,N+1)
658  CONTINUE
659  CONTINUE
      RETURN
      END

```


C.

```

SUBROUTINE NM2
COMMON X(24), Y(21), T(33), U(25,22,39), A(39), B(39), R, SA, DH, N, J
KB = N/2.
BB = N/2.
IF (KB.EQ.0) GO TO 666
JB = J-1
DO 665 M = 2, JB
A(1) = (2.*R)/(1.+2.*R)
B(1) = ((1.-(2.*R/SA**2))*U(1,M,N)+(R/SA**2)*(U(1,M-1,N)+
CU(1,M+1,N))+DH)/(1.+2.*R)
IF (M.GT.10) GO TO 661
NC = 23
IF (M.LE.5) NC = 16
IF (M.LE.3) NC = 6
GO 660 LE = 2, NC
A(LE)=R/(1.+2.*R-R*A(LE-1))
B(LE)=((R/SA**2)*(U(LE,M-1,N)+U(LE,M+1,N))+(1.-((2.*R)/SA**2))*
CU(LE,M,N))+DH+R*B(LE-1))/(1.+2.*R-R*A(LE-1))
660 CONTINUE
GO TO 663
661 IF (M.LT.15) MN = (M-14)/2.
IF (M.GE.15) MN = (M-13)/2.
NC = J-4.*MN-6
DO 662 LE = 2, NC
A(LE)=R/(1.+2.*R-R*A(LE-1))
B(LE)=((R/SA**2)*(U(LE,M-1,N)+U(LE,M+1,N))+(1.-((2.*R)/SA**2))*
CU(LE,M,N))+DH+R*B(LE-1))/(1.+2.*R-R*A(LE-1))
662 CONTINUE
663 U(NC,M,N+1) = B(NC)
LL = NC-1
DO 664 LG = 1, LL
KG = NC-LG
U(KG,M,N+1) = B(KG)+A(KG)*U(KG+1,M,N+1)
664 CONTINUE
665 CONTINUE
GO TO 677
666 DO 676 L = 1, 23
M1 = (L-7)/10.+1+0.05
JA = 2.*M1+2
M2 = L/4.+0.05
JB = J-2.*M2-1
JD = JA-1
IF (L.EQ.1) GO TO 672
IF (L.EQ.6 .OR. L.EQ.16) GO TO 668
A(JD) = (2.*(R/SA**2))/(1.+(2.*(R/SA**2)))
B(JD)=(R*(U(L-1,JD,N)+U(L+1,JD,N))+(1.-2.*R)*U(L,JD,N)+DH)/
C(1.+(2.*(R/SA**2)))
IF (L.EQ.3 .OR. L.EQ.7 .OR. L.EQ.11 .OR. L.EQ.15 .OR. L.EQ.19 .OR.
CL.EQ.23) GO TO 670
DO 667 LA = JA, JB
A(LA)=(R/SA**2)/(1.+(2.*(R/SA**2)))-(R/SA**2)*A(LA-1)
B(LA)=(R*(U(L-1,LA,N)+U(L+1,LA,N))+(1.-2.*R)*U(L,LA,N)+DH+
C(R/SA**2)*B(LA-1))/(1.+(2.*(R/SA**2)))-(R/SA**2)*A(LA-1)
667 CONTINUE

```



```

GO TO 674
668 A(JD) = (2.*(R/SA**2))/(1.+(2.*(R/SA**2)))
      B(JD) = (U(L,JD,N)+DH)/(1.+(2.*(R/SA**2)))
      JA = JD+1
      A(JA)=(R/SA**2)/(1.+(2.*(R/SA**2))-(R/SA**2)*A(JD))
      B(JA) = (U(L,JA,N)+DH+(R/SA**2)*U(L,JD,N))/
C(1.+(2.*(R/SA**2))-(R/SA**2)*A(JD))
      JE = JA+1
      DO 669 LA = JC,JB
      A(LA)=(R/SA**2)/(1.+(2.*(R/SA**2))-(R/SA**2)*A(LA-1))
      B(LA)=(R*(U(L-1,LA,N)+U(L+1,LA,N))+(1.-2.*R)*U(L,LA,N)+DH+
C(R/SA**2)*B(LA-1))/(1.+(2.*(R/SA**2))-(R/SA**2)*A(LA-1))
669 CONTINUE
      GO TO 674
670 JC = JB-1
      DO 671 LA = JA,JC
      A(LA) = (R/SA**2)/(1.+(2.*(R/SA**2))-(R/SA**2)*A(LA-1))
      B(LA) = (R*(U(L-1,LA,N)+U(L+1,LA,N))+(1.-2.*R)*U(L,LA,N)+DH+
C(R/SA**2)*B(LA-1))/(1.+(2.*(R/SA**2))-(R/SA**2)*A(LA-1))
671 CONTINUE
      JB = JC+1
      A(JB) = (R/SA**2)/(1.+(2.*(R/SA**2))-(R/SA**2)*A(JB-1))
      B(JB)=(U(L,JB,N)+DH+R*A(JB-1))/(1.+(2.*(R/SA**2))-(R/SA**2)
C*A(JB-1)))
      GO TO 674
672 A(1) = (2.*(R/SA**2))/(1.+(2.*(R/SA**2)))
      B(1) = (2.*R*U(L+1,1,N)+(1.-2.*R)*U(L,1,N)+DH)/
C(1.+(2.*(R/SA**2)))
      DO 673 LA = JA,JB
      A(LA)=(R/SA**2)/(1.+(2.*(R/SA**2))-(R/SA**2)*A(LA-1))
      B(LA) = (2.*R*U(L+1,LA,N)+(1.-2.*R)*U(L,LA,N)+DH+
C(R/SA**2)*B(LA-1))/(1.+(2.*(R/SA**2))-(R/SA**2)*A(LA-1))
673 CONTINUE
674 U(L,JB,N+1) = B(JB)
      IF (L.EQ.1) JA = 2
      JC = JB - JA
      DO 675 MM = 1,JC
      MB = JB-MM
      U(L,MB,N+1) = B(MB)+A(MB)*U(L,MB+1,N+1)
675 CONTINUE
676 CONTINUE
677 RETURN
      END

```


APPENDIX C

COMPUTER PROGRAM AND USAGE FOR ONE-DIMENSIONAL FINITE STRAIN CONSOLIDATION

APPENDIX C

ORGANIZATION OF COMPUTER PROGRAM

The computer program described in this Appendix is based on the theory presented in Chapter VII of this study. The program is in Fortran IV language and may be used on computers of the type IBM 360/67.

The program deals with the one-dimensional, non-linear consolidation behaviour of a sedimenting soil undergoing finite strains. The program furnishes the excess pore pressure and the void ratio throughout the current depth at chosen intervals for any time step. The program also supplies the current height, the total added height, and the average current density at each time step. Finally the program calculates the average degree of consolidation of the sedimented thickness at the end of the duration of deposition.

The program is for a moving boundary problem where the top boundary is in perpetual motion. The program is applicable for the case of a normally consolidating soil whose compressibility and consolidation characteristics are known. The program is presented for a uniform distribution of the added weight on the top (due to sedimenting soil) throughout the current depth of deposit. However, the algorithm can easily be modified to incorporate a continuous variation of the added weight across the depth.

The equation governing one-dimensional, finite strain

consolidation behaviour of a sedimenting soil is given by 7.20. The average degree of consolidation is defined as the ratio of the difference between the total added weight and the total excess pore pressure to the total added weight.

The main program reads all the input data concerning the sedimenting soil and sets up the initial and boundary conditions. Also it establishes the space and time intervals and the initial effective stress of the very thin layer over which sedimentation takes place.

Subroutine FS1 calculates the relevant quantities depending on the material property values supplied by the main program when there is a steady growth of soil layers. It also calculates the current void ratio for each of the nodal points at a specified time. The calculated quantities are then returned to the main program.

Subroutine FS2 calculates the required quantities when the deposit is at a standstill and there is no input in form of growth of layers. The dissipation is allowed to take place at a constant load. The computed quantities (same as in subroutine FS1) are returned to the main program for further calculation.

The main program makes use of the quantities obtained from the subroutine(s) to calculate the excess pore pressure for each of the existing nodal points at prescribed time intervals. Further the program calculates the current height of the sediment (by trapezoidal rule), the average current density (of the sediment thickness), and the average degree

of consolidation at the end of the deposition period by Simpson's rule. The computed results are printed as per the output format.

COMPUTER PROGRAM USAGE

INPUT DATA

The first step in the analysis of one-dimensional, finite strain consolidation of a sedimenting soil is to determine the rate of mass deposition and its duration. Next, the compressibility and permeability characteristics of the soil are to be determined. A choice is to be made as to the input void ratio and corresponding effective stress at which the soil is being deposited.

The required input data cards are as follows in the order presented.

- (a) First card: The first input data card reads the specific gravity, the input void ratio and the input coefficient of consolidation.

The READ variables are:

GS, EO, CV

The FORMAT is,

3F10.3

- (b) Second card: The next data card reads the numerical values of C and D in the equation

$$e = C - D \log_{10} \sigma'$$

and the value of Q in the equation

$$k \propto (\sigma')^Q .$$

The READ variables are:

C, D, Q

The FORMAT is,

3F10.3

(c) Third card: The third input data card reads the time steps required for the entire deposition and standstill operation and that for only the duration of deposition.

The READ variables are:

$K, K1$

The FORMAT is,

2I5

The space step (DDZ), the time step (DDT), and the unit weight of water (UWW) are built in the main program. The appropriate values are to be substituted for these quantities.

OUTPUT INFORMATION

The following information is printed by the program at prescribed time intervals:

- (a) the initial (input) properties of the sedimenting soil together with the time and space steps, the weight of the added layer thickness and the unit weight of water;
- (b) the current height and total added thickness;
- (c) the average current density;
- (d) the excess pore pressure and void ratio at specified space intervals; and
- (e) the average degree of consolidation of the soil deposit at the end of the deposition period.


```

C
C *****
C PROGRAM FOR THE ANALYSIS OF ONE DIMENSIONAL NONLINEAR CONSOLIDA
C -TION SEDIMENTATION FOR A PERIOD & THEREAFTER DISSIP.
C THE SOIL CONSIDERED IS NORMALLY CONSOLIDATED
C *****

```

```

C COMMON Z(101), T(101), U(102,102), E(102,102), SIGMA(101),XA(102),
C 1SIGM(101), U1(101), R1(101), S(101), AD(101), DFT(101), X1(101),
C 2K, K1, L, N, GS, Q, UWW, DT, DT, R, DH, SIGMO, EO, C, D
C *****

```

```

C READ AND PRINT MATERIAL PROPERTIES
C *****

```

```

C 5 FORMAT (3F10.3)
C READ (5,5) GS, EO, CV
C READ (5,5) C, D, Q
C
C READ (5,10) K, K1
C 10 FORMAT (2I5)
C
C WRITE (6,15) GS, EO, CV, C, D, Q
C 15 FORMAT (25X, 'PROPERTIES OF SEDIMENTING SOIL'///, 25X, 'GS=',
C 1F8.3/, 25X, 'EO=', F8.3/, 25X, 'CV=', F8.3/, 25X, 'C=', F8.3/,
C 225X, 'D=', F8.3/, 25X, 'Q=', F8.3///)
C *****

```

```

C SEDIMENTATION TAKES PLACE FOR A TIME N=K1
C THEREAFTER IT IS DISSIPATION AT CONSTANT LOAD
C THE GROWTH OF THE LAYER IS 122 FT. IN 10000 YEARS
C THEREFORE THE TIME INTERVAL DDT IS 10000/61. YEARS FOR 2FT BUILDUP
C
C LET COEFFICIENT OF CONSOLIDATION TO BEGIN WITH BE CV FT.**2 PER YEAR
C THEREFORE DT = CV*DDT
C *****

```

```

C ***** BOUNDARY AND INITIAL CONDITIONS *****
C

```

```

C DO 40 N=1,K
C NA = N
C IF (N.GT.K1) NA=K1
C DO 30 L=1,NA
C IF (N.EQ.1 .OR. L.EQ.NA) GO TO 20
C GO TO 30
C 20 U(L,N) = 0.
C E(L,N) = EO
C 30 CONTINUE
C 40 CONTINUE

```


***** PHYSICAL PROPERTIES *****

DZ = THICKNESS OF SOLIDS = LAYER THICKNESS/(1.+EO)
 DH = WEIGHT OF SOIL ADDED AT TOP DURING THE TIME INTERVAL DDT
 UWW = UNIT WEIGHT OF WATER = 64. LB/FT**3

THE VOID RATIO - LOG(SIGMA) RELATIONSHIP IS OF THE FORM

$$\text{VOID RATIO} = C - D * \text{LOG}_{10}(\text{SIGMA})$$

 THIS RELATIONSHIP IS GENERALLY ACKNOWLEDGED FOR A
 NORMALLY CONSOLIDATED SOIL
 THEREFORE $\text{SIGMA} = \text{EXP}((C - \text{VOID RATIO}) / (0.434 * D))$

DDT = 10000./61.
 DDZ = 2.
 DZ = DDZ/(1.+EO)
 DT = CV*DDT
 UWW = 64./2000.
 R = DT/DZ**2
 DH = 4.685*DDZ/122.
 SIGMO = EXP((C-EO)/(0.434*D))

WRITE (6,45) DDT, DZ, DT, UWW, DH, SIGMO
 45 FORMAT (25X, 'DDT =', F8.3/, 25X, 'DZ =', F8.3/, 25X, 'DT =',
 1F8.3/, 25X, 'UWW =', F8.3/, 25X, 'DH =', F8.3/, 25X, 'SIGMO =',
 2F8.3//)

THIS PART OF THE PROGRAM CALCULATES THE EXCESS PORE PRESSURE
 AT NODAL POINTS AT EVERY TIME INTERVAL DDT

DO 200 N=1,K
 IF (N.GE.K1) GO TO 94
 CALL FS1
 GO TO 96
 94 CALL FS2
 96 P1(1) = 2.*U1(1)/(1.+2.*U1(1))
 S(1) = AD(1)/(1.+2.*U1(1))
 IF (N.EQ.1) GO TO 125
 NA = N
 K2 = K1-1
 IF (N.GE.K1) NA=K2
 DO 100 L=2,NA
 R1(L) = U1(L)/(1.+2.*U1(L)-U1(L)*R1(L-1))
 S(L) = (AD(L)+U1(L)*S(L-1))/(1.+2.*U1(L)-U1(L)*P1(L-1))
 100 CONTINUE
 U(NA,N+1) = S(NA)
 NB = NA-1
 DO 120 NC = 1,NB
 KB = NA-NC


```

      U(KB,N+1) = S(KB)+R1(KB)*U(KB+1,N+1)
120  CONTINUE
      GO TO 200
125  U(1,2) = S(1)
200  CONTINUE
      WRITE (6,97) (SIGM(L),SIGMA(L),U(L,K),E(L,K),DET(L),UI(L),AD(L),
1L=1,K)
97  FORMAT(3X, 7F16.9)
C      THIS PART OF THE PROGRAM CALCULATES THE CURRENT HEIGHT
C      OF THE SEDIMENT      BY TRAPEZOIDAL RULE
C
      DO 240 N=1,K
      IF (N.EQ.1) GO TO 220
      NA = N
      IF (N.GT.K1) NA = K1
      NB = NA-1
      X2 = 1.+E(1,N)+I.+E(NA,N)
      IF (N.EQ.2) GO TO 230
      X3 = 0.
      DO 210 L = 2,NB
      X3 = X3+2.*(1.+E(L,N))
210  CONTINUE
      X1(N) = (X2+X3)*DZ/2.
      GO TO 240
220  X1(N) = 0.
      GO TO 240
230  X1(N) = X2*DZ/2.
240  CONTINUE
C
      WRITE (6,250)
250  FORMAT ('1', 45X, 'TIME STEPS', 2X, 'CURRENT HEIGHT',
16X, 'TOTAL ADDED THICKNESS'//)
      DO 270 N=1,K
      NA = N
      IF (N.GT.K1) NA = K1
      Z1 = DZ*(NA-1)*(1.+EO)
      WRITE (6,260) N, X1(N), Z1
260  FORMAT (47X, 15, F17.7, 6X, F17.7/)
270  CONTINUE
C      THIS PART OF THE PROGRAM CALCULATES THE AVERAGE CURRENT DENSITY
C
      WRITE (6,277)
277  FORMAT ('1', 10X, 'TIME', 25X, 'AV. DENSITY'//)
      DO 279 N = 1,K,5
      T(N) = DDT*(N-1)
      NA = N
      IF (N.GT.K1) NA = K1
      DO 271 L = 1,NA
271  X1(L) = (E(L,N)+GS)*UWW/(1.+E(L,N))
      IF (N.EQ.1) GO TO 273
      NB = NA-1
      X4 = X1(1)+X1(NA)
      IF (N.EQ.2) GO TO 274
      X5 = 0.

```



```

      DO 272 L = 2, NB
272  X5 = X5+X1(L)
      XA(N) = (X4+X5)/N
      GO TO 276
273  XA(N) = X1(1)
      GO TO 276
274  XA(N) = X4/N
276  WRITE (6,278) T(N), XA(N)
278  FORMAT (4X, F10.2, 25X, F8.3/)
279  CONTINUE
C
C   THIS PART OF THE PROGRAM CALCULATES THE AVERAGE DEGREE OF
C   CONSOLIDATION BY SIMPSON'S RULE AT THE END OF DEPOSITION PERIOD
C
      AX = K1/2.
      NX = K1/2.
      K2 = K1
      IF (AX.EQ.NX) K2 = K1-1
      AA = 0.
      DO 275 L = 2,K2,2
275  AA = U(L,K1) + AA
      KA = K2-1
      AB = 0.
      DO 280 L = 3,KA,2
280  AB = AB + U(L,K1)
C
C   AC - INTEGRATION OF PORE PRESSURE VALUES
C   ACC - INTEGRATION OF TOTAL ADDED WEIGHT = 0.5*GAMMA*HEIGHT**2
C   ADA - AVERAGE DEGREE OF CONSOLIDATION
C
      AC = (U(1,K1)+U(K1,K1))+4.*AA+2.*AB)*DDZ/3.
      IF (K1.EQ.K2) GO TO 285
      AC = AC+(U(K1,K1)+U(K2,K1))*0.5*DDZ
285  ACC = ((K1-1)*DH)*((K1-1)*DZ)*0.5*(1.+EO)
      ADA = (ACC-AC)/ACC
C
      DO 600 N=1,K,10
C
      T(N) = DDT*(N-1)
      NA = N
      IF (N.GT.K1) NA=K1
      DET(1) = 0.
      DO 300 L=1,NA
      IF(L.EQ.1) GO TO 290
      DET(L) = DET(L-1)+F(L,N)-EO
290  Z(L) = DZ*(1.+EO)*(L-1)+DET(L)*DZ
300  CONTINUE
      WRITE (6,400) T(N)
400  FORMAT (///20X, 'TIME ELAPSED=', 2X, F10.2/)
      WRITE (6,450)
450  FORMAT (/63X, 'Z', 12X, 'U', 15X, 'E'/)
      WRITE (6,500) (Z(L), U(L,N), E(L,N), L=1,NA)
500  FORMAT (50X, F15.1, F15.7, F15.3)
600  CONTINUE
C

```



```

DET(1) = 0.
DO 610 L=1,K1
  IF(L.EQ.1) GO TO 605
  DET(L) = DET(L-1)+E(L,K1)-FO
605 Z(L) = DZ*(1.+FO)*(L-1)+DET(L)*DZ
610 CONTINUE
  T(K1) = DDT*(K1-1)
  WRITE (6,620) T(K1)
620 FORMAT (///20X, 'TIME ELAPSED=', 2X, F10.2/)
  WRITE (6,630)
630 FORMAT (/63X, 'Z', 12X, 'U', 15X, 'E'/)
  WRITE (6,640) (Z(L), U(L,K1), E(L,K1), L=1,K1)
640 FORMAT (50X, F15.1, F15.7, F15.3)
C
  T(K1) = DDT*(K1-1)
  WRITE (6,650) ADA, T(K1)
650 FORMAT ('1', 5X, 'AVERAGE DEGREE OF CONSOLIDATION =', F8.3,
15X, 'AT THE END OF ', F12.4, 1X, 'YEARS')
C
C   THIS PART OF THE PROGRAM CALCULATES THE AVERAGE DEGREE OF
C   CONSOLIDATION BY SIMPSON'S RULE AT THE END OF PERIOD N=K
C
  AY = K/2.
  NY = K/2.
  K3 = K
  IF (AY.EQ.NY) K3 = K-1
  AA = 0.
  DO 660 L=2,K3,2
660 AA = AA+U(L,K)
  KA = K3-1
  AB = 0.
  DO 670 L=3,KA,2
670 AB = AB+ U(L,K)
  AC = (U(1,K)+U(K,K)+4.*AA+2.*AB)*DDZ/3.
  IF (K.EQ.K3) GO TO 680
  AC = AC+(U(K,K)+U(K3,K))*0.5*DDZ
680 ACC= ((K1-1)*DH)*((K1-1)*DZ)*0.5*(1.+FO)
  ADA = (ACC-AC)/ACC
  T(K) = DDT*(K-1)
  WRITE (6,690) ADA, T(K)
690 FORMAT (///10X, 'AV. DEG. OF CONS.', F8.3, 15X, 'AT', F12.4, 'YRS')
  STOP
  END

```

THIS SUBROUTINE CALCULATES THE RELEVANT QUANTITIES
WHEN THERE IS A STEADY GROWTH OF THE LAYERS

SUBROUTINE FS1

```

COMMON Z(101), T(101), U(102,102), F(102,102), SIGMA(101),XA(102),
1SIGM(101), U1(101), R1(101), S(101), AD(101), DET(101), X1(101),
2K, K1, L, N, GS, Q, UWW, DZ, DT, R, DH, SIGMO, EO, C, D
DO 90 L=1,N
  IF (N.EQ.1) GO TO 70
  IF (L.EQ.N) GO TO 50
  SIGM(L) = (N-L)*DH
  SIGMA(L) = SIGM(L)-U(L,N)+SIGMO
  E(L,N) = C-0.434*D*ALOG(SIGMA(L))
  DET(L) = (F(L,N)-E(L,N-1))*DZ*UWW/DZ
  IF (L.EQ.1) GO TO 60
  DET(L) = DET(L)+DET(L-1)
  GO TO 60
50  E(L,N) = EO
  U1(L) = P/(1.+EO)**2
  SIGMA(L) = SIGMO
  DET(N) = DET(N-1)
  AD(L) = U(L,N)+DH-Q*U1(L)*((U(L,N)-U(L-1,N))**2/SIGMA(L))
1-Q*U1(L)*DZ*UWW*(GS-1.)*((U(L,N)-U(L-1,N))/SIGMA(L))
2+DET(L)*DT
  GO TO 95
60  U1(L) = R*(SIGMA(L)/SIGMO)**(Q+1.)/(1.+EO)**2
  IF (L.EQ.1) GO TO 80
  AD(L) = U(L,N)+DH-Q*U1(L)*((U(L+1,N)-U(L-1,N))**2/(4.*SIGMA(L))-
10*DZ*U1(L)*UWW*(GS-1.)*((U(L+1,N)-U(L-1,N))/(2.*SIGMA(L))
2+DET(L)*DT
  GO TO 90
70  U1(1) = P/(1.+EO)**2
80  IF (N.EQ.1) DET(1) = 0.
  AD(1) = U(1,N)+DH+DET(1)*DT
90  CONTINUE
95  RETURN
END

```

THIS SUBROUTINE CALCULATES THE REQUIRED QUANTITIES
WHEN THERE IS NO INPUT IN FORM OF GROWTH OF LAYERS
THAT IS, THE PORE PRESSURE GENERATION TERM IS ABSENT
THIS IS ACHIEVED BY PUTTING $DH = 0$.
THE DISSIPATION IS ALLOWED TO TAKE PLACE AT A CONSTANT LOAD
AFTER THE PRESCRIBED TIME LIMIT OF LAYER GROWTH

SUBROUTINE FS2

```

COMMON Z(101), T(101), U(102,102), E(102,102), SIGMA(101), XA(102),
1SIGM(101), U1(101), R1(101), S(101), AD(101), DET(101), X1(101),
2K, K1, L, N, GS, Q, UWW, CZ, DT, R, DH, SIGMO, EO, C, D
K2 = K1-1
DO 165 L=1,K2
SIGM(L) = (K1-L)*DH
SIGMA(L) = SIGM(L)-U(L,N)+SIGMO
E(L,N) = C-0.434*D*ALOG(SIGMA(L))
DET(L) = (E(L,N)-E(L,N-1))*D7*UWW/DT
IF (L.EQ.1) GO TO 155
DET(L) = DET(L)+DET(L-1)
155 U1(L) = R*(SIGMA(L)/SIGMO)**(Q+1.)/(1.+EO)**2
IF (L.EQ.1) GO TO 160
AD(L) = U(L,N)-Q*U1(L)*(U(L+1,N)-U(L-1,N))**2/(4.*SIGMA(L))-
1Q*D7*U1(L)*UWW*(GS-1.)*(U(L+1,N)-U(L-1,N))/(2.*SIGMA(L))
2+DET(L)*DT
GO TO 165
160 AD(1) = U(1,N)+DET(1)*DT
165 CONTINUE
RETURN
END

```


APPENDIX D

COMPUTER PROGRAM AND USAGE FOR
EROSION AND SWELLING IN VALLEY FORMATION

APPENDIX D

ORGANIZATION OF THE COMPUTER PROGRAM

The computer program presented in the Appendix is based on the theory offered in Chapter VIII of this thesis. The program is in Fortran IV language and may be used directly on computers of the type IBM 360/67.

The program determines the deficient pore pressures for a low swelling deposit eroded at a constant rate over a period of time and for an assumed standstill thereafter. Essentially the program is based on Gibson's (1958) theory for consolidation of sedimenting layers. The deposit is assumed to extend to infinity in its depth. The top of the deposit is eroded to a depth of 250 feet. For all practical purposes the infinite depth is achieved at about 2000 feet from the uneroded surface. The algorithm developed is for a constant rate of erosion and for an uniform distribution of load (removed) throughout the depth. However both these assumptions can be altered and the program modified for any sort of erosion schedule (which can be later approximated into a suitable number of linear rates of erosion) and to include a continuous variation of the load removed across the depth.

The governing equation for the dissipation of deficient pore pressures for an eroding sediment is given by 8.1. The analysis can be carried out for any value of the coefficient of consolidation and for several rates of erosion (for 250

feet depth of erosion) and subsequent swelling (same duration for all rates of erosion).

The program has all the input data built in and sets up the boundary and initial conditions. It establishes the rate of erosion and the space interval for the finite difference grid. It then determines the time interval for the above space interval and the same time interval is used for the duration of subsequent swelling. Thus the total space steps, time steps for erosion and subsequent standstill are established. Depending on the governing material parameters, the program calculates the deficient pore pressure at each nodal point at prescribed time intervals. The calculated results are printed out as per the output formats.

The program also plots the deficient pore pressures against the depth. This is carried out by the Calcomp plotter which operates on the principle that digital commands from a tape activate step motors to produce a plot. Further for various nodal points, the program calculates the hydrostatic pressure of the eroded sediment and the existing pore water pressure at the end of erosion and at subsequent times. The existing pore water pressure is the sum of the deficient pore pressure and hydrostatic pressure. The program plots both these quantities against depth at prescribed time intervals.

OUTPUT INFORMATION

The following information is computed and printed by the program:

- (1) reprint of input data;
- (2) pore pressures (deficient at nodal points at specified time intervals;
- (3) plots the deficient pore pressure isochrones and existing water pressures at the end of erosion and subsequent time intervals and the hydrostatic pressure of the eroded sediment.


```

C
C
C      *****
C THIS PROGRAM DETERMINES THE DEFICIENT PORE PRESSURE ISOCHRONES
C FOR A LOW SWELLING FULLY SATURATED DEPOSIT WHICH WAS ERODED
C AND IT PLOTS THE DEFICIENT PORE PRESSURE ISOCHRONES
C AT SPECIFIED INTERVALS OF TIME
C GIVEN LENGTH OF TIME AND THEN IT IS ASSUMED TO STANDSTILL
C FOR THE SUBSEQUENT PERIOD OF TIME
C THE PARAMETERS THAT GO INTO THE CALCULATIONS ARE:
C     1. THE COEFFICIENT OF SWELLING FOR THE MATERIAL
C     2. THE DEPTH OF FLUVIAL EROSION (DEPTH OF THE VALLEY)
C     3. THE DURATION OF EROSION
C     4. THE DURATION OF STANDSTILL

```

```

C THE BOTTOM BOUNDARY IS NOT FIXED AS IT EXTENDS THEORETICALLY
C TO INFINITE DEPTH. AS SUCH ARBITRARY DEPTH OF SAY
C 1000. FT. OR 5000. FT. MAY BE CHOSEN, AT WHICH DEPTH THERE IS
C NO PERCEPTIBLE VARIATION IN PORE PRESSURE DEFICIT
C CONSIDER 2000. FT. OF DEPOSIT

```

```

C THE PROPERTIES OF THE VALLEY *****
C     DEPTH OF VALLEY                250 FT.
C     DURATION OF EROSION            10000 YEARS
C     SUBSEQUENT DURATION OF STANDSTILL 10000 YEARS
C     THE COEFFICIENT OF SWELLING    10.0 FT. SQ. / YEAR

```

```

C SPACE STEP RE 5 FT.          DX = 5. FT.
C THEREFORE TIME STEP FOR EROSION = 10000*5/250 = 200 YPS.
C SAME TIME STEP MAY BE USED FOR DURATION OF STANDSTILL
C THEREFORE SPACE STEPS = (2000/5)+1 = 401
C AND TIME STEPS INCLUDING STANDSTILL = (10000+10000)/200+1
C                                     = 101
C AND TIME STEPS FOR DURATION OF EROSION ONLY = 10000/200+1
C                                     = 51

```

```

C *****
C *****
C *****

```

```

C DIMENSION X(201), T(151), U(202,152), A(202), B(202),
C 1BUF(2048), XX(205), YY(205), AX(205)
C CALL PLOTS(BUF,8192)
C CALL XLIMIT (100.0)
C I = 201
C K = 101
C K1 = 51
C CV = 10.
C DX = 5.
C DT = 200.
C R = CV*DT/DX**2

```

```

C
C     DH = THE AMOUNT OF SOIL BEING ERODED OUT
C DH = 10. UNITS
C
C DH = 10.

```



```

C          BOUNDARY CONDITIONS          *****
C
DO 20 M=1,K1
DO 10 L=1,I
IF (M.EQ.1 .OR. L.EQ.M) U(L,M) = 0.
10 CONTINUE
20 CONTINUE

C
C      THIS PART OF THE PROGRAM CALCULATES THE PORE PRESSURE DEFICIENCY
C      DURING EROSION
C
IA = I-1
DO 50 M=1,K1
MA = M+1
A(M) = R/(1.+2.*R)
B(M) = (U(M,M)-DH)/(1.+2.*R)
DO 30 L=MA,IA
A(L) = R/(1.+2.*R-R*A(L-1))
B(L) = (U(L,M)-DH+R*B(L-1))/(1.+2.*R-R*A(L-1))
30 CONTINUE
B(I) = (U(I,M)-DH+2.*R*B(I-1))/(1.+2.*R-2.*R*A(I-1))

C
U(I,M+1) = B(I)
LLA = I-M-2
DO 40 LLL = 1,LLA
KA = I-LLL
U(KA,M+1) = B(KA)+A(KA)*U(KA+1,M+1)
40 CONTINUE
50 CONTINUE

C
C      THIS PART OF THE PROGRAM DEALS WITH THE STANDSTILL SITUATION
C
DO 80 M=K1,K

C          BOUNDARY CONDITION AT TOP
C
U(K1,M) = 0.
A(K1) = R/(1.+2.*R)
B(K1) = U(K1,M)/(1.+2.*R)
K2 = K1+1
DO 60 L=K2,IA
A(L) = R/(1.+2.*R-R*A(L-1))
B(L) = (U(L,M)+R*B(L-1))/(1.+2.*R-R*A(L-1))
60 CONTINUE
B(I) = (U(I,M)+2.*R*B(IA))/(1.+2.*R-2.*R*A(IA))

C
U(I,M+1) = 0(I)
LLC = I-K1-1
DO 70 LCL=1,LLC
KD = I-LCL
U(KD,M+1) = B(KD)+A(KD)*U(KD+1,M+1)
70 CONTINUE
80 CONTINUE

C
C

```



```

C      THIS PART OF THE PROGRAM PRINTS OUT THE OUTPUT
C      FOR DEFICIENT PORE PRESSURE VALUES AT VARIOUS DEPTHS
C
C      WRITE (6,100)
100    FORMAT ('1', ///25X, 'PORE PRESSURE VALUES DURING EROSION'////)
      DO 125 M = 1,K1, 5
125    T(M) = DT*(M-1)
      WRITE (6,150) (T(M), M=1,K1,5)
150    FORMAT (8X, 'X / T', 11F11.4//)
      DO 250 L = 1,I
      X(L) = DX*(L-1)
      J = K1
      IF (L-K1) 175, 200, 200
175    J = L
200    WRITE (6,225) (X(L), (U(L,JJ), JJ=1,J,5))
225    FORMAT (1X, F6.1, 4X, 11E11.3)
250    CONTINUE
C
      J = K1
      DO 400 M1 = 1,2
      K2 = J
      J = J+25
      WRITE (6,275)
275    FORMAT ('1', ///25X, 'PORE PRESSURE VALUES DURING STANDSTILL'////)
      DO 300 M=K2,J,5
300    T(M) = DT*(M-1)
      WRITE (6,325) (T(M), M=K2,J,5)
325    FORMAT (8X, 'X / T', 6F16.4//)
      DO 375 L=K1,I
      X(L) = DX*(L-1)
      WRITE (6,350) (X(L), (U(L,JJ), JJ=K2,J,5))
350    FORMAT (6X, F6.1, 4X, 6E16.4//)
375    CONTINUE
400    CONTINUE
C
C      CALL PLOT(0.0,0.0,3)
      CALL PLOT (0.0,20.0,-3)
      XX(152) = -500.
      XX(153) = 500./2.
      CALL AXIS (0.0,0.0,'DEFICIENT PORE PR',17,32.0,0.0,XX(152),XX(153)
1,10.0)
      CALL PLOT (2.0,0.0,-3)
      YY(152) = 0.
      YY(153) = 2000./10.
      CALL AXIS(0.0,0.0,'DEPTH IN FEET',13,10.0,270.0,YY(152),YY(153),
C10.0)
      CALL PLOT(0.0,0.0,-3)
C
C      DH = 10. UNITS = BULK UNIT WEIGHT * DX = 130. * 5.
C      THEREFORE UNIT WEIGHT OF WATER = 10*62.4/(130*5) = 0.961538 UNITS
C
      DO 2 N=K1,K,25
      IA = I

```



```

DO 1 L=K1,IA
  Y(L) = DX*(L-1)
  XX(L-50) = Y(L,K)-500.
  YY(L-50) = -X(L)
  AX(L-50) = 0.961538*DX*(L-51)
1  CONTINUE
  IF (N.GT,K1) GO TO 82
  CALL FLINF (XX,YY,151,1,0,0)
  DO 82 L = K1,IA
82  XX(L-50) = XX(L-50)+AX(L-50)
  CALL FLINF (XX,YY,151,1,0,0)
  GO TO 2
83  KB = K1+25
  IF (N.GT,KB) GO TO 85
  CALL FLINF (XX,YY,151,1,0,0)
  DO 84 L = K1,IA
84  XX(L-50) = XX(L-50)+AX(L-50)
  CALL FLINF (XX,YY,151,1,0,0)
  GO TO 2
85  CALL FLINF (XX,YY,151,1,0,0)
  DO 86 L = K1,IA
86  XX(L-50) = XX(L-50)+AX(L-50)
  CALL FLINF (XX,YY,151,1,0,0)
  DO 81 L = K1,IA
  XX(L-50) = 0.961538*DX*(L-51)-500.
  YY(L-50) = -X(L)
81  CONTINUE
  CALL FLINF (XX,YY,151,1,0,0)
2  CONTINUE
  CALL SYMBOL (4,0,-1.5,0.10,'CV=      FT**2/YEAR',0.0,19)
  CALL PLOT (32.0,32.0,-3)
  CALL PLOT (0,0,0.0,999)
  STOP
  END

```


B29967